

March 3, 2016

Cynthia A. Eck
Document Control Officer
USDA APHIS BRS Policy Coordination Program
4700 River Road, Unit 146
Riverdale, MD 20737

Dear Ms. Eck,

Please find attached a petition for extension of 14-093-01p submitted by the J.R. Simplot Company entitled "Petition for Extension of Nonregulated Status for X17 Ranger Russet and Y9 Atlantic Potatoes with Late Blight Resistance, Low Acrylamide Potential, Lowered Reducing Sugars, and Reduced Black Spot".

The submission includes:

- 2 hard copies,
- 1 CD containing Microsoft Word 2013 and PDF versions of the document, and
- 1 CD with PDF references.

No Confidential Business Information is being submitted.

Thank you for your careful review of the petition.

Sincerely,



Matthew Pence
Regulatory Manager
J.R. Simplot Company
5369 West Irving Street
Boise, ID 83706
Tel.: (208) 780-6040
matthew.pence@simplot.com



Petition for Extension of Nonregulated Status for X17 Ranger Russet and Y9 Atlantic Potatoes with Late Blight Resistance, Low Acrylamide Potential, Lowered Reducing Sugars, and Reduced Black Spot

The J.R. Simplot Company submits this petition under 7 CFR 340.6 to request that the Administrator make a determination that the articles should not be regulated under 7 CFR Part 340.

The petition is for extension of 14-093-01p deregulating W8 Russet Burbank.

Prepared by Matthew Pence Ph.D.*, Raina Spence, Tracy Rood, Jeff Habig Ph.D., and Susan Collinge Ph.D.

Contributors: Sathya Adimulam, Juan Pablo Burzaco, Jeff Hein, Steve Hystad, Rebecca Kirkpatrick, Janet Layne, Deborah Newby, Eric Rosenbaum, Megan Tribble, Troy Weeks Ph.D., and Jingsong Ye Ph.D.

J.R. Simplot Company

OECD unique identifiers: SPS-~~00~~X17-5 and SPS-~~000~~Y9-7

March 3, 2016

***Corresponding Author:**

Matthew Pence Ph.D.
J.R. Simplot Company
5369 West Irving Street
Boise, ID 83706
Tel.: (208) 780-6040
matthew.pence@simplot.com

This Document (Including Appendices) Does Not Contain Confidential Business Information

Certification

The undersigned certifies that, to the best knowledge and belief of the undersigned, this petition includes all information and views on which to base a determination, and that it includes all relevant data and information known to the petitioner which are unfavorable to the petition.



Matthew Pence Ph.D.
Regulatory Manager
J.R. Simplot Company
5369 West Irving Street
Boise, ID 83706

Table of Contents

Table of Contents	3
Table of Figures	5
List of Tables	7
List of Abbreviations, Acronyms, Definitions, and Commonly Used Terms	8
Summary	10
1.0 Rationale for X17 and Y9 Potato Varieties	12
1.1 Basis for Determination of Nonregulated Status under 7 CFR §340.6	15
1.2 Rationale for Using the Extension Process	15
1.3 Submissions to Other U.S. Regulatory Agencies	17
1.4 Prior Environment Release of X17 and Y9	17
2.0 Development of X17 and Y9 Potato Varieties	18
2.1 Characterization of the Recipient Varieties	18
2.2 Description of DNA Used for Transformation	20
2.3 Activity and Function of the Genes in X17 and Y9	23
2.4 Description of Marker-Free Transformation	25
3.0 Genetic Characterization of X17 and Y9	27
3.1 Single Genomic Insertion Loci in X17 and Y9	27
3.1.1 Single Insertion Locus in X17 Associated with pSIM1278	27
3.1.2 Single Insertion Locus in X17 Associated with pSIM1678	31
3.1.3 Single Insertion Locus in Y9 Associated with pSIM1278	34
3.1.4 Single Insertion Locus in Y9 Associated with pSIM1678	36
3.2 Structures of the pSIM1278 and pSIM1678 Inserts in X17 and Y9	38
3.2.1 pSIM1278 Insert Structure in X17	38
3.2.2 pSIM1678 Insert Structure in X17	44
3.2.3 pSIM1278 Insert Structure in Y9	51
3.2.4 pSIM1678 Insert Structure in Y9	64
3.2.5 Analysis of Potential Fusion Proteins in Y9	71
3.3 Absence of pSIM1278 and pSIM1678 Backbone Sequence in X17 and Y9	72
3.4 Stability of the Inserts across Clonal Cycles	79
3.4.1 X17 Genetic Stability	79
3.4.2 Y9 Genetic Stability	84
3.5 Summary of the Genetic Characterization of X17 and Y9	87
4.0 Gene Down-Regulation in X17 and Y9	88
4.1 Down-Regulation in X17 Tuber and Leaf Tissues	88
4.2 Down-Regulation in Y9 Tuber and Leaf Tissues	90
5.0 The VNT1 Protein in X17 and Y9	92
5.1 VNT1 Protein Identity	92
5.2 Mode of Action	93
5.3 Levels of the VNT1 Protein in X17 and Y9 Tissues	93
5.4 Levels of Rpi-vnt1 Transcript in X17 and Y9 Tissues	93
5.5 Efficacy of the Rpi-vnt1 Gene in Field Trials	95
5.6 Safety Assessment of VNT1	95
6.0 Comparative Assessment of X17 and Y9	96
7.0 Phenotypic Performance and Field Observations for X17 and Y9	97
7.1 Field Trial Details	97
7.2 X17 and Y9 Phenotypic and Tuber Assessment Results	99

7.3	Insect, Disease, and Abiotic Stressor Assessments.....	103
7.4	Conclusions for Agronomic Performance and Field Observations	106
8.0	Compositional Assessment for X17 and Y9.....	107
8.1	Compositional Nutrient Analysis.....	107
8.1.1	Proximates, Vitamins, and Minerals	107
8.1.2	Total Amino Acids	109
8.1.3	Glycoalkaloids	111
8.2	Composition Efficacy Assessment of X17 and Y9.....	112
8.2.1	Free Amino Acids	112
8.2.2	Reducing Sugars	114
8.2.3	Acrylamide	116
8.3	Compositional Assessment Conclusions.....	118
9.0	Environmental Safety Assessment for X17 and Y9	119
10.0	Stewardship of X17 and Y9 Potatoes	120
10.1	Stewardship for Commercial Products	120
10.2	Regulatory Clearances in Foreign Markets and Plan for U.S. Commercialization	120
11.0	Summary of Environmental Assessment Considerations	121
12.0	Conclusion: Extension of Nonregulated Status for X17 and Y9	123
13.0	References	124
14.0	Appendix A: X17 and Y9 USDA Notifications	129
15.0	Appendix B: Molecular Methods and Materials	131
16.0	Appendix C: VNT1 Expression Methods and Materials	134
17.0	Appendix D: Comparative Assessment Methods and Materials	143

Table of Figures

Figure 1-1. 2014 Certified Seed Potato Acres, By Variety.....	14
Figure 2-1. Clonal Cycle Nomenclature.....	19
Figure 2-2. Map of pSIM1678 Construct.....	21
Figure 2-3. T-DNA of pSIM1678	21
Figure 2-4. Starch Breakdown.....	24
Figure 2-5. Development and Selection of F10 and J3 Events.....	25
Figure 2-6. Development and Selection of X17 and Y9 Events	26
Figure 3-1. pSIM1278 Insert Number Characterization.....	29
Figure 3-2. Single Insertion Locus for the pSIM1278 Insert in X17	30
Figure 3-3. pSIM1678 Insert Number Characterization.....	32
Figure 3-4. Single Insertion Locus for the pSIM1678 Insert in X17	33
Figure 3-5. Single pSIM1278 Insertion Locus in Y9	35
Figure 3-6. Single pSIM1678 Insertion Locus in Y9	37
Figure 3-7. Structure of the pSIM1278 Insert in X17	39
Figure 3-8. Southern Hybridization of Ranger Russet, F10, and X17 Genomic DNA with ASN.....	40
Figure 3-9. Southern Hybridization of Ranger Russet, F10, and X17 Genomic DNA with AGP	41
Figure 3-10. Southern Hybridization of Ranger Russet, F10, and X17 Genomic DNA with GBS.....	42
Figure 3-11. Southern Hybridization of Ranger Russet, F10, and X17 Genomic DNA with R1	43
Figure 3-12. Structure of the pSIM1678 Insert in X17 With Digestion Patterns and Probe Binding Sites .	45
Figure 3-13. Southern Hybridization of Ranger Russet Genomic DNA with INV	46
Figure 3-14. Southern Hybridization of Ranger Russet Genomic DNA MfeI and SphI Digest with INV.....	47
Figure 3-15. Southern Hybridization of Ranger Russet Genomic DNA with VNT	49
Figure 3-16. Southern Analysis of EcoRI/EcoRV Digested Genomic DNA with VNT	50
Figure 3-17. Structure of the pSIM1278 Insert in Y9.	52
Figure 3-18. Southern Hybridization of Atlantic, J3, and Y9 Genomic DNA with ASN	55
Figure 3-19. Southern Hybridization of Atlantic, J3, and Y9 Genomic DNA with GBS1	56
Figure 3-20. Southern Hybridization of Atlantic, J3, and Y9 Genomic DNA with AGP	57
Figure 3-21. Southern Hybridization of Atlantic, J3, and Y9 Genomic DNA with R1	58
Figure 3-22. Southern Hybridization of Atlantic, J3, and Y9 Genomic DNA after PacI Digest with AGP	59
Figure 3-23. Southern of Atlantic, J3, and Y9 SacI/XbaI Digested Genomic DNA with AGP	60
Figure 3-24. Southern Hybridization of Atlantic, J3, and Y9 Genomic DNA after PacI Digest with GBS1...	61
Figure 3-25. Southern of Atlantic, J3, and Y9 SacI/XbaI Digested Genomic DNA with GBS1	62
Figure 3-26. Southern Hybridization of Atlantic, J3, and Y9 Genomic DNA with GBS2	63
Figure 3-27. Structure of the pSIM1678 Insert in Y9 with Digestion Patterns and Probe Binding Sites	65
Figure 3-28. Southern Hybridization of Atlantic, J3, and Y9 Genomic DNA with VNT.....	66
Figure 3-29. Southern of Atlantic, J3, and Y9 SacI/XbaI Digested Genomic DNA with VNT	67
Figure 3-30. Southern Hybridization of Atlantic, J3, and Y9 Genomic DNA with INV.....	68
Figure 3-31. Southern Hybridization of Atlantic, J3, and Y9 Genomic DNA after PacI Digest with INV	69
Figure 3-32. Southern of Atlantic, J3, and Y9 Genomic DNA after SacI/XbaI Digest with INV.....	70
Figure 3-33. No Fusion Proteins Produced from the Right Side of the pSIM1678 Insert	72
Figure 3-34. Structure of the pSIM1278/pSIM1678 Backbone with pSIM1278 Insert in X17	74
Figure 3-35. Structure of the pSIM1278/pSIM1678 Backbone with pSIM1278 Insert in Y9	74
Figure 3-36. Southern Blots Probed With BB1-4 Show No Evidence of Backbone DNA in X17.....	75
Figure 3-37. No Evidence of Backbone DNA Corresponding to Probes BB5-BB8 in X17	76
Figure 3-38. Southern Blots Probed With BB1-4 Show No Evidence of Backbone DNA in Y9.....	77
Figure 3-39. No Evidence of Backbone DNA Corresponding to Probes BB5-BB8 in Y9	78

Figure 3-40. Structure of the pSIM1278 and pSIM1678 Insert in X17	80
Figure 3-41. Structure of the pSIM1278 and pSIM1678 Insert in Y9	80
Figure 3-42. X17 Insert Stability in G0 and G2 clonal Cycles as Visualized with AGP and GBS Probes.....	81
Figure 3-43. X17 Insert Stability in G0 and G2 Clonal Cycles as Visualized with ASN and R1 Probes.....	82
Figure 3-44. X17 Insert Stability in G0 and G2 Clonal Cycles as Visualized with INV and VNT Probes	83
Figure 3-45. Y9 Insert Stability in G0 and G2 Clonal Cycles as Visualized with AGP and GBS Probes	85
Figure 3-46. Y9 Insert Stability in G0 and G2 Clonal Cycles as Visualized with ASN and R1 Probes	86
Figure 3-47. Y9 Insert Stability in G0 and G2 Clonal Cycles as Visualized with INV and VNT Probes	87
Figure 4-1. All RNAi-Targets Down-Regulated in X17 Tubers	89
Figure 4-2. Minor Changes in Asn1 Gene Expression in X17 Leaves.....	89
Figure 4-3. RNAi Target Gene Down-Regulation in Y9 Tubers.....	90
Figure 4-4. RNAi Target Gene Down-Regulation in Y9 Leaf.....	91
Figure 5-1. Amino Acid Sequence of VNT1	92
Figure 5-2. Rpi-vnt1 Transcript Levels in X17 Measured by RT-qPCR.....	94
Figure 5-3. Rpi-vnt1 Transcript Levels in Y9 Measured by RT-qPCR.....	95
Figure 16-1. Melt Curve Analysis of the Rpi-vnt1 Amplicon in X17	137
Figure 16-2. Coomassie Stained SDS-PAGE Gel of Ranger Russet and X17 Tissue Protein Extracts.....	138
Figure 16-3. VNT1 Limit of Quantitation in X17	139
Figure 16-4. Melt Curve Analysis of the Rpi-vnt1 Amplicon in Y9	140
Figure 16-5. Coomassie Stained SDS-PAGE Gel of Atlantic and Y9 Tissue Protein Extracts	141
Figure 16-6. VNT1 Limit of Quantitation in Y9	142

List of Tables

Table 1-1. Summary of X17 and Y9 Genes and Intended Traits	12
Table 1-2. Regulatory Status of Simplot Events	15
Table 1-3. Comparison between Previously Deregulated W8 and X17 and Y9	16
Table 1-4. EPA Submissions	17
Table 2-1. Genetic Elements of pSIM1678 T-DNA	22
Table 7-1. Characteristics Evaluated for X17	97
Table 7-2. Characteristics Evaluated for Y9	97
Table 7-3. X17 Field Trial Locations.....	98
Table 7-4. Y9 Field Trial Locations.....	99
Table 7-5. Phenotypic, Yield, and Grading Characteristics of X17	100
Table 7-6. Phenotypic, Yield, and Grading Characteristics of Y9	102
Table 7-7. X17 Abiotic and Biotic Stressor Observations.....	104
Table 7-8. Y9 Abiotic and Biotic Stressor Observations	105
Table 8-1. Proximates, Vitamins, and Minerals in X17 and Ranger Russet	108
Table 8-2. Proximates, Vitamins, and Minerals in Y9 and Atlantic	109
Table 8-3. Total Amino Acids in X17 and Ranger Russet.....	110
Table 8-4. Total Amino Acids in Y9 and Atlantic	111
Table 8-5. Glycoalkaloids in X17 and Ranger Russet.....	112
Table 8-6. Glycoalkaloids in Y9 and Atlantic	112
Table 8-7. Free Amino Acids in Tubers at Harvest in X17	113
Table 8-8. Free Amino Acids in Tubers at Harvest in Y9	113
Table 8-9. Sugars in X17 and Ranger Russet Tubers at Harvest and after Storage at 7.7 °C.....	114
Table 8-10. Sugars in X17 and Ranger Russet Tubers after Cold Storage at 3.3 °C	115
Table 8-11. Sugars in Y9 and Ranger Russet Tubers at Harvest and after Storage at 10 °C	115
Table 8-12. Sugars in Y9 and Atlantic Tubers after Storage at 3.3 °C	116
Table 8-13. Acrylamide in Fries from X17 and Ranger Russet at Harvest and after Storage at 7.7 °C.....	117
Table 8-14. Acrylamide in Fries from X17 and Ranger Russet Stored after Storage at 3.3 °C.....	117
Table 8-15. Acrylamide in Chips from Y9 and Atlantic at Harvest and after Storage at 10 °C.....	117
Table 8-16. Acrylamide in Chips from Y9 and Atlantic after Storage at 3.3 °C	118
Table 11-1. Summary of Environmental Assessment Considerations for X17 and Y9.....	121
Table 14-1. X17 USDA Release Notifications and Planted Acreage Details	129
Table 14-2. Y9 USDA Release Notifications and Planted Acreage Details	130
Table 16-1. X17 Plant Material Collection Locations	134
Table 16-2. Y9 Plant Material Collection Locations	134
Table 16-3. Primers Used for qPCR.....	136
Table 16-4. Cycling Parameters	136
Table 17-1. Common Potato Insect and Disease Symptoms	146
Table 17-2. Reference Variety Sites and Sample Size	148

List of Abbreviations, Acronyms, Definitions, and Commonly Used Terms

Abbreviation	Definition
ADP	Adenosine diphosphate
AGP	Probe used to detect <i>Agp</i> promoter sequence
<i>Agp</i>	ADP-glucose pyrophosphorylase gene
<i>A. tumefaciens</i>	<i>Agrobacterium tumefaciens</i>
AP1	Adapter primer 1
AP2	Adapter primer 2
ASN	Probe used to detect <i>Asn1</i> sequence
ASN1	<i>Asn1</i> gene-derived probe used in DNA gel blot hybridization
<i>Asn1</i>	Asparagine synthetase-1 gene
ATP	Adenosine triphosphate
Backbone DNA	DNA associated with construct backbone
BB1-BB8	Probes that detect pSIM1278/pSIM1678 backbone regions
bp	Base pair
CC	Coiled-coil domain
CFR	Code of Federal Regulations
CVR	Conventional variety range
cwt/A	Unit of measure equal to 100 lbs/acre or weight (lbs) of tubers harvested/acre divided by 100
DIGII	Molecular weight markers
DIGVII	Molecular weight markers
DNA insert	DNA sequence from pSIM1278 or pSIM1678 integrated into the potato genome
dNTP	Dideoxy nucleotide triphosphate
dsRNA	Double-stranded RNA
EPA	Environmental Protection Agency
ETS	Excellence Through Stewardship
FDA	Food and Drug Administration
FG, FG1, FG2	Field grown year
G0	First clonal cycle of plants and tuber seed
G1	Plants and tubers resulting from G0 seed
G2	Plants and tubers resulting from G1 seed
GBS, GBS1	Probe used to detect one region of the <i>Gbs</i> promoter sequence
GBS2	Probe used to detect second region of the <i>Gbs</i> promoter sequence
<i>Gbss</i>	Granule-bound starch synthase gene
IB	Internal band
Innate®	A branded biotechnology approach that uses plant genes to enhance desired traits
INV	Probe used to detect <i>VInv</i> sequence
IPM	Integrated pest management
<i>ipt</i>	Isopentenyltransferase gene—produces cytokinin hormones associated with plant growth and development
JB	Junction band
kb	Kilobase
LB	Left border (25-base pair) is similar to <i>A. tumefaciens</i> T-DNA border
LRR	Leucine-rich repeat domain

MOPS	3-(N-morpholino)propanesulfonic acid
NB	Nucleotide-binding
NBY	Nutrient broth-yeast extract
NGS	Next generation sequencing
<i>nptII</i>	Neomycin phosphotransferase II gene – used as/for marker for plant transformation, gene expression, and regulation studies
OECD	Organization for Economic Cooperation and Development
ORF	Open reading frame
<i>P. infestans</i>	<i>Phytophthora infestans</i>
pAGP	Truncated sequence that is not a functional promoter
<i>pAgp</i>	Promoter of the ADP glucose pyrophosphorylase gene
pBR322	Backbone element
PCR	Polymerase chain reaction
pGbss	Promoter of the granule-bound starch synthase gene
pGEM-T	Cloning vector
<i>PhL</i>	Phosphorylase-L gene
PPO	Polyphenol oxidase enzyme
<i>Ppo5</i>	Polyphenol oxidase-5 gene
qPCR	Quantitative PCR
pVS1	Backbone element
R-protein	Resistance protein
R1	Southern blot probe used to detect the R1 cassette
<i>R1</i>	Water dikinase R1 gene
RB	Right border
<i>Rpi-vnt1</i> gene	Resistance against <i>P. infestans</i> from <i>S. venturii</i>
RT-qPCR	Reverse transcription-qualitative polymerase chain reaction
<i>S. tuberosum</i>	<i>Solanum tuberosum</i>
<i>S. venturii</i>	<i>Solanum venturii</i>
SDS	Sodium dodecyl sulfate
Somaclonal variation	Genetic and/or phenotypic variation among clonally propagated plants of a single donor clone; generated by tissue culture and other forms of vegetative propagation
SPS-ØØX17-5	OECD identifier for X17
SPS-ØØØY9-7	OECD identifier for Y9
SSC	Saline sodium citrate
<i>Ubi7</i>	Polyubiquitin 7 promoter
<i>Ubi3</i>	Polyubiquitin 3 terminator
USDA-APHIS	United States Department of Agriculture-Animal and Plant Health Inspection
<i>VInv</i>	Vacuolar invertase
VNT	Probe used to detect <i>Rpi-vnt1</i> sequence
VNT1	VNT1 protein
WT	Wild-type

Summary

The J.R. Simplot Company has developed the Ranger Russet SPS-ØØX17-5 (X17) and Atlantic SPS-ØØØY9-7 (Y9) potato events as retransformations of previously deregulated events F10 and J3, respectively. The retransformation introduces late blight resistance and invertase down-regulation in addition to the quality traits of reduced black spot and lower reducing sugars, and the benefit of lower acrylamide potential. The trait additions would be difficult to achieve through traditional breeding as potato is tetraploid, highly heterozygous, and sensitive to inbreeding depression. Incorporation of the traits is most efficiently accomplished through transformation of each potato variety of interest. Ranger Russet and Atlantic are important commercial varieties for the processing and chipping industries, respectively.

X17 and Y9 were developed using the same construct and transformation method as W8, a previously deregulated event. Simplot is submitting data for X17 Ranger Russet and Y9 Atlantic as an extension of W8 Russet Burbank, the antecedent organism, demonstrating similarity for trait mechanism-of-action in the same crop. Simplot requests a determination from the United States Department of Agriculture-Animal and Plant Health Inspection Service (USDA-APHIS) that events SPS-ØØX17-5 and SPS-ØØØY9-7 and their progeny no longer be considered regulated articles under 7 CFR 340.

Late blight is a devastating disease among cultivated *Solanaceae* species. In potato, late blight affects foliage and tubers causing rapid necrosis and crop loss if left untreated. The Irish Potato Famine was the result of late blight and demonstrates the aggressiveness of the disease. Simplot's late blight resistant potato varieties X17 and Y9, combined with current IPM practices, have the potential to provide long-term benefits.

Reducing black spot, the black or greyish color found in damaged or cut potatoes, reduces waste and improves quality. Decreasing the amount of reducing sugars in potato helps maintain the quality and color of many potato products, including fries and chips. Decreased amounts of reducing sugars may enable modified storage conditions with lower temperatures and increased storage lengths. These modifications may decrease storage losses due to high tuber respiration rates occurring under typical storage conditions.

Molecular characterizations, agronomic, phenotypic, and compositional assessments demonstrate that X17 and Y9 are similar to W8, have low plant pest potential, and provide valuable traits to the potato industry and consumers.

X17 and Y9 were generated, similar to W8, by *Agrobacterium*-mediated transformation with pSIM1278 and retransformation with pSIM1678. The T-DNA from pSIM1278, maintained in X17 and Y9, was intended to down-regulate four potato genes through RNA interference (RNAi):

- *Asn1* (asparagine synthetase) for reduced free asparagine contributing to low acrylamide potential;
- *R1* (water dikinase) for lower reducing sugars contributing to low acrylamide potential;
- *PhL* (phosphorylase-L) for lower reducing sugars contributing to low acrylamide potential; and
- *Ppo5* (polyphenol oxidase-5) for reduced black spot.

The pSIM1678 T-DNA was designed to down-regulate the potato vacuolar invertase gene (*VInv*) through RNAi and express the *Rpi-vnt1* gene:

- *VInv* (vacuolar invertase) for lower reducing sugars contributing to low acrylamide potential and modified storage conditions;
- *Rpi-vnt1* (resistance against *Phytophthora infestans* from *Solanum venturii*) for late blight resistance.

The VNT1 protein has a non-toxic mode of action against the target pest and signals the programmed death of pathogen-infected plant cells limiting spread of the disease. The VNT1 protein is expressed at levels less than 100 ppb in tuber and leaf tissue. Human exposure to VNT1 is expected to be negligible due to the low expression level of the protein, which also limits exposure to non-target organisms and the environment.

Molecular analyses demonstrate that X17 and Y9 maintain the pSIM1278 insertion as shown with F10 and J3, and contain a single copy of the pSIM1678 insert. Also, backbone sequences were not introduced, and the inserts are stable through multiple cycles of potato clonal propagation.

Agronomic and phenotypic analyses demonstrate that X17 and Y9 are equivalent to their respective controls, Ranger Russet and Atlantic varieties, and other conventional potatoes. The data support an unlikely increase in plant pest or volunteer potential for X17 and Y9 compared to controls.

Compositional analyses of X17 and Y9 were conducted to evaluate key nutrient (proximates, vitamins, amino acids, and minerals) and glycoalkaloid levels compared to controls. In addition, concentrations of free amino acids, sugars, and acrylamide were measured to evaluate trait efficacy. The Food and Drug Administration (FDA) will review details of the compositional analyses as a component of the food and feed safety assessment of X17 and Y9 potatoes.

The traits introduced into X17 and Y9 enhance disease resistance and potato quality without enhancing weediness, impacting agronomic characteristics, insects and other non-target organisms, weed or disease susceptibility, endangered species, or biodiversity. Planting, cultivation, management, and harvest processes are not affected other than potential reduction in fungicide use. Based on these data and analyses, Simplot requests that USDA-APHIS grant an extension of nonregulated status for the X17 and Y9 events and their progeny.

1.0 Rationale for X17 and Y9 Potato Varieties

SPS-ØØX17-5 (X17) and SPS-ØØØY9-7 (Y9) are new potato events developed by the J.R. Simplot Company. The rationale for developing X17 Ranger Russet and Y9 Atlantic potatoes is the same as for developing the antecedent organism, W8 Russet Burbank, deregulated on September 2, 2015 (14-093-01p). It provides additional potato varieties having late blight resistance, low acrylamide potential, lowered reducing sugars, and reduced black spot. The introduced traits provide increased value by potentially lowering costs associated with disease management, handling and processing, and storage.

The development of these traits in potato is accomplished by introducing partial or full-length potato gene sequences through transformation. A summary of the target genes and their intended functions appears in Table 1-1. The addition of multiple traits into potato is difficult to achieve through traditional breeding because potato is tetraploid, highly heterozygous, and sensitive to inbreeding depression. Incorporating these traits is accomplished through transformation of each potato variety of interest.

Table 1-1. Summary of X17 and Y9 Genes and Intended Traits

Construct	Gene Target	Mechanism	Intended Trait	Intended Benefit
pSIM1278	<i>Asn1</i> : asparagine synthetase-1 ^{1,2}	RNAi down-regulation	Reduces free asparagine	Contributes to low acrylamide potential ³
	<i>R1</i> : water dikinase ^{1,2}	RNAi down-regulation	Lowers reducing sugars	Contributes to low acrylamide potential ³
	<i>PhL</i> : phosphorylase-L ^{1,2}	RNAi down-regulation	Lowers reducing sugars	Contributes to low acrylamide potential ³
	<i>Ppo5</i> : polyphenol oxidase-5 ^{1,2}	RNAi down-regulation	Reduces enzymatic darkening	Reduced black spot
pSIM1678	<i>VInv</i> : vacuolar invertase ²	RNAi down-regulation	Lowers reducing sugars	Prevents excess darkening during frying and contributes to low acrylamide potential ³
	<i>Rpi-vnt1</i> : R-gene ²	Protein overexpression	Confers resistance to <i>P. infestans</i>	Late blight resistance

¹ Previously deregulated trait in Simplot petition 13-022-01p and 15-140-01p.

² Previously deregulated trait in Simplot petition 14-093-01p.

³ Acrylamide is formed primarily from asparagine and reducing sugars heated at temperatures above 120 °C, as occurs during frying.

Late blight is caused by the oomycete *P. infestans* and resulted in the Irish Potato Famine in the mid-1800s. Fungicides are used to prevent disease, however, over-reliance can drive adaptation of the pathogen and lead to fungicide-resistant strains of *P. infestans* (Daayf and Platt, 2003; Deahl et al., 1993; Fry et al., 2015). As disease pressure increases and frequent fungicide applications are needed, reliance on fungicides may become unsustainable. Concern over cost and human risk, as well as environmental impacts, and evolution of fungicide-resistant strains of late blight, is leading to the development of new strategies for disease control (Kessel et al., 2014). The X17 and Y9 varieties will provide growers with another tool to use in conjunction with fungicides and crop rotation as part of an integrated pest management strategy.

The presence of acrylamide in various food products has garnered public interest in the last decade. Although acrylamide is not present in fresh potatoes, it is formed when the amino acid asparagine and the reducing sugars glucose and fructose in carbohydrate-rich foods are heated at temperatures above 120 °C (248 °F). FDA's Draft Guidance for Industry on Acrylamide in Foods states that "reducing acrylamide in foods may mitigate potential human health risks from exposure to acrylamide," which is particularly relevant in light of recent toxicology studies (Eck, 2013; FDA, 2013). An extensive list of potential mitigation techniques summarized in FDA's guidance document focused primarily on lowering the reducing sugar levels in potatoes. Decreased levels of both reducing sugars and asparagine contribute to lowering the amount of acrylamide formed in cooked potato products (Shepherd et al., 2010). Reduced asparagine and sugar levels in X17 and Y9 resulted in approximately 70% reductions in the amount of acrylamide formed in fries and chips compared to control varieties.

Sugar content contributes to the quality of processed potato by affecting the color of finished products. Color is important for rating the quality of fries and chips, with darker colors being undesirable. Lowering the levels of reducing sugars in potato not only contributes to low acrylamide potential, but also improves quality by limiting the coloration of potato during processing. Sugar levels in tubers fluctuate as starch is metabolized. Cold-induced sweetening occurs at cooler storage temperatures, thus warmer storage temperatures are recommended for potato in order to minimize sugar metabolism and preserve quality. Lower reducing sugars may enable lower temperatures during tuber storage without sacrificing quality that can also lead to reductions in yield losses from respiration and disease. This benefit is particularly valuable in chipping varieties such as Atlantic, a variety usually processed directly out of the field. With the addition of lower reducing sugars, Y9 may offer storage possibilities not previously available for this variety.

When tubers are exposed to impact or pressure, black spot is the resulting defect. Black spot is a post-harvest physiological phenomenon primarily resulting from the handling of potato tubers during harvest, transport, and processing, and refers to the black or grayish color that may form in the interior of damaged potatoes (Eck, 2013). The darkening and discoloration of damaged or impacted (pressure bruised) potatoes is associated with the enzyme polyphenol oxidase (PPO). Enzymatic darkening occurs when PPO leaks from damaged cells and reacts with phenolic compounds to form colored pigments.

Simplot has transformed Ranger Russet and Atlantic varieties because the conventional untransformed varieties are popular and have proven merit in commercial production (Figure 1-1). The Ranger Russet variety stores well, offers generally good yields, and although is used in fresh and dehydrated markets, predominantly goes to the making of fries (Woodell et al., 1991). Atlantic produces high-quality chips, and off-grade tubers may be used in dehydrated potato products (PAA, 2015a).

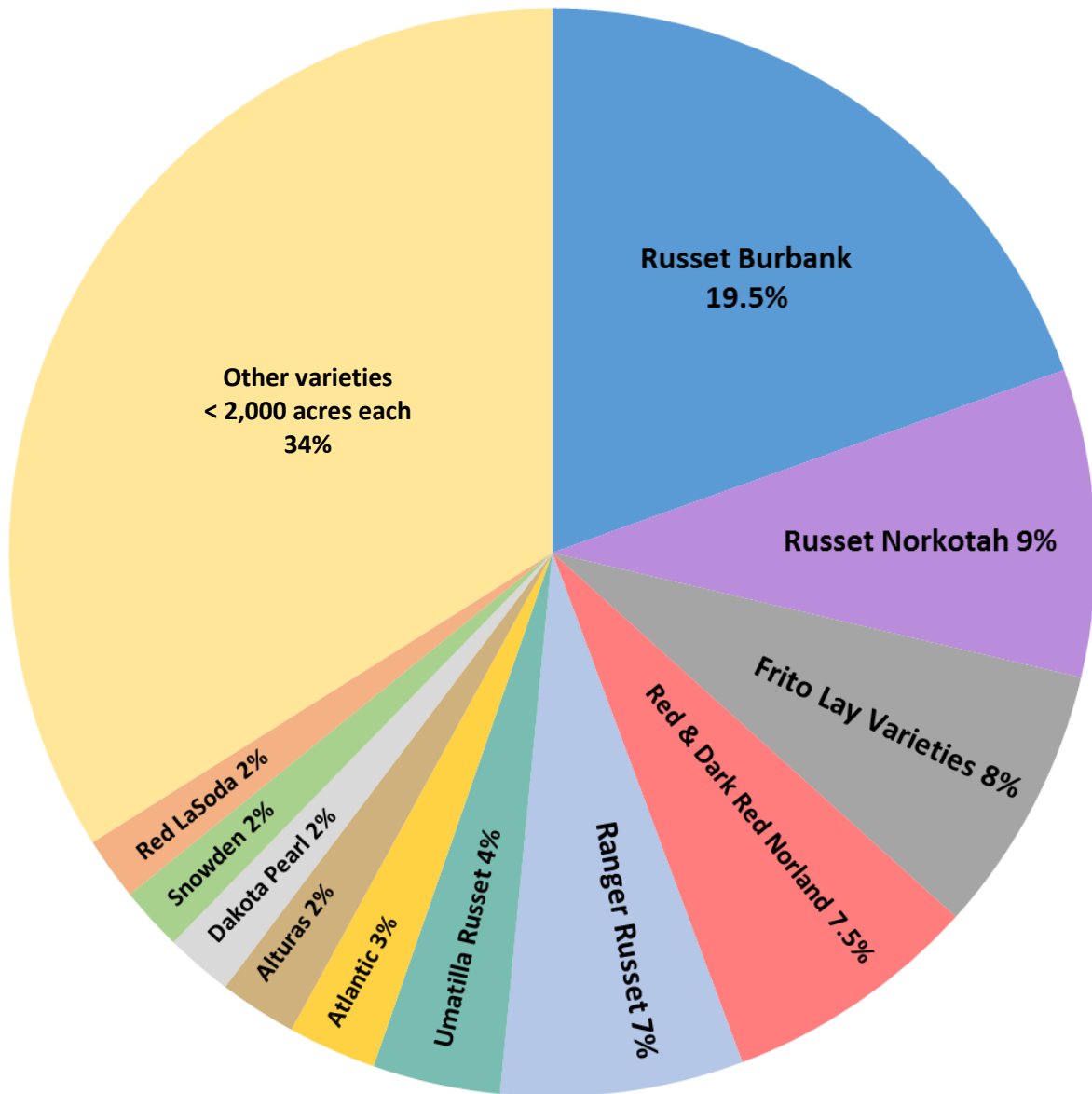


Figure 1-1. 2014 Certified Seed Potato Acres, By Variety

The graph shows the top potato varieties, grown for seed in the US, during 2014. Forty-one total different varieties were grown on more than 300 acres. Potatoes grown on less than 2000 acres are combined as other varieties which account for 34% of all potatoes planted. Source: National Potato Council, 2015

1.1 Basis for Determination of Nonregulated Status under 7 CFR §340.6

The Animal and Plant Health Inspection Service (APHIS) and the U.S. Department of Agriculture (USDA) have responsibility under the Plant Protection Act (7 U.S.C. 7701-7772) to prevent the introduction or dissemination of plant pests into or within the U.S. Part 340 regulates the introduction of organisms produced or altered through genetic engineering that are or may be considered plant pests.

The USDA-APHIS regulation 7 CFR §340.6(e) provides for an applicant to petition APHIS for evaluation of data submitted for a determination, based on similarity to an antecedent organism, that a regulated article, the genetically modified crop, does not pose a potential for plant pest risk and therefore, should not be regulated as such. A finding for deregulation would be made based on the similarity of the additional regulated article to an antecedent organism, i.e., an organism that has already been the subject of a determination of nonregulated status by USDA-APHIS under 7 CFR 340.6. The antecedent organism is used as a reference for comparison to the regulated article under consideration, as provided by the regulations.

Simplot is submitting data for X17 and Y9 as an extension of W8, the antecedent organism, demonstrating similarity for trait mechanism-of-action in the same crop, and requests a determination from USDA-APHIS that events SPS-ØØX17-5 and SPS-ØØØY9-7, and their progeny, be no longer considered regulated articles under 7 CFR 340.

1.2 Rationale for Using the Extension Process

X17 and Y9 are re-transformations of the F10 and J3 events, respectively, that were deregulated on November 10, 2014 in petition 13-022-01p (Table 1-2).

Table 1-2. Regulatory Status of Simplot Events

Variety	pSIM1278		pSIM1678	
	Event	Status	Event	Status
Russet Burbank	E56	Not deregulated	W8	Deregulated 9/2/15; 14-093-01p
Ranger Russet	F10	Deregulated 11/10/14 13-022-01p	X17	Subject of this extension
Atlantic	J3	Deregulated 11/10/14 13-022-01p	Y9	Subject of this extension

Events X17 and Y9, which were transformed with the same constructs—pSIM1278 and pSIM1678—using the same transformation method as W8, a previously deregulated event, are good candidates for the extension process. X17 and Y9 are new varieties of the same species with the same incorporated T-DNA as W8 (Table 1-3). The observed phenotype, introduced traits, and conclusions from molecular, agronomic, phenotypic, and compositional assessments are the same for X17, Y9, and W8. X17 and Y9 do not exhibit additional traits beyond what was expressed in W8.

Table 1-3. Comparison between Previously Deregulated W8 and X17 and Y9

	Deregulated W8	X17	Y9
USDA Number	14-093-01p	Not yet issued	
Date of Deregulation	September 2015	Not yet deregulated	
Date of Environmental Assessment	July 2015	Not yet assessed	
Recipient Organism	Potato (<i>S. tuberosum</i> subsp. <i>tuberosum</i>)	Same	Same
Variety	Russet Burbank	Ranger Russet	Atlantic
Fertility	Male Sterile	Male Fertile	Male Fertile
Transformation Method	<i>A. tumefaciens</i>	Same	Same
Constructs	pSIM1278 and pSIM1678	Same	Same
Benefits	Late blight resistance, low acrylamide potential, lowered reducing sugars, and reduced black spot	Same	Same
Traits and Gene Functions	<i>Rpi-vnt1</i> : late blight resistance <i>Asn1</i> : down-regulated, reduced free asparagine <i>R1</i> : down-regulated, lower reducing sugars <i>PhL</i> : down-regulated, lower reducing sugars <i>VInv</i> : down-regulated, lower reducing sugars <i>Ppo5</i> : down-regulated, reduced enzymatic darkening	Same	Same
Molecular	Well characterized and contains stable inserts	Same	Same
Agronomic	Agronomically and phenotypically similar to conventional parent variety, other than the intended late blight resistance	Same	Same
Composition	Compositionally similar to conventional parent variety, other than intended changes to free asparagine and reducing sugars	Same	Same
Plant Pest	Similar to parent variety in terms of reproductive fitness, gene flow, and other plant pest characteristics	Same	Same

1.3 Submissions to Other U.S. Regulatory Agencies

As new transformed events, X17 and Y9 are regulated by USDA-APHIS Biotechnology Regulatory Services.

As food products, X17 and Y9 are within the scope of the FDA policy statement concerning regulation of food products derived from new plant varieties, including those developed by recombinant DNA techniques. A voluntary safety and nutritional assessment of X17 and Y9 will be submitted to the FDA Center for Food Safety and Applied Nutrition.

As plant-incorporated protectants, X17 and Y9 are subject to regulation by the EPA under the Federal Insecticide, Fungicide and Rodenticide Act. Applications submitted to the EPA for X17 and Y9 are summarized in Table 1-4. Section 3 registration applications for X17 and Y9 together with a request for a permanent exemption from the requirement of a tolerance for the VNT1 protein (pursuant to the Federal Food Drug and Cosmetic Act) have been submitted to EPA.

Table 1-4. EPA Submissions

Simplot EPA Submissions	Purpose	Application Date	Date Issued	Expiration Date
8917-EUP-1	Crop destruct EUP for field testing	January 2014	May 2014	February 2015
8917-EUP-2	EUP with temporary tolerance exemption for field testing	February 2014	February 2015	December 2015
Extension of 8917-EUP-2	EUP with extension of temporary tolerance exemption for field testing	July 2015	December 2015	April 2017
8917-R, 8917-E, and 8917-G	Registration for commercial planting and request for permanent tolerance exemption for VNT1	November 2015	pending	To be determined by EPA

1.4 Prior Environment Release of X17 and Y9

X17 and Y9 have been field tested in the U.S. since 2012. X17 has been grown in eight states and Y9 has been grown in 12 states, as authorized by the USDA-APHIS notifications listed in Appendix A.

2.0 Development of X17 and Y9 Potato Varieties

SPS-ØØX17-5 (X17) and SPS-ØØØY9-7 (Y9) are new potato events developed by the J.R. Simplot Company. X17 was developed from the Ranger Russet variety. Y9 was developed from the Atlantic variety.

2.1 Characterization of the Recipient Varieties

The Ranger Russet variety was jointly released in 1991 by the USDA and Idaho, Oregon, Washington, and Colorado state agricultural experiment stations. Ranger Russet is a full-season variety grown in the Northwest U.S. and is well suited for frozen processing and fresh market. Ranger Russet tubers display white flesh, plentiful, moderately shallow eyes, and store for medium-length (around 4-6 months). Plants are large with thick stems with upright or spreading foliage. Flowers have red-purple corolla and yellow fertile anthers. Ranger Russet displays some resistance to *Verticillium* wilt, Potato Virus X, Potato Virus Y, leafroll net necrosis, and *Fusarium* dry rot. The variety is resistant to hollow heart (PAA, 2015b).

The Atlantic variety was released by the USDA potato breeding program at Beltsville, Maryland in 1978. It is a standard variety for chipping (chip processing) and is typically used directly from the field. Atlantic is widely grown in the U.S. and is a mid-season potato. Tubers are oval to round with white flesh and shallow eyes. Tuber dormancy is medium-long. Plants are moderately large with thick, upright stems. Flower corolla are pale lavender and anthers are orange with abundant pollen. Atlantic is tolerant to scab and *Verticillium* wilt; resistant to pinkeye, and highly resistant to Race A of golden nematode, Potato Virus X, and tuber net necrosis (PAA, 2015a; Webb et al., 1978).

Although Ranger Russet and Atlantic varieties are male fertile, the probability of outcrossing remains low due to the lack of pollinators and geographic overlap between cultivated and wild potato species. Pollination of fertile potato varieties is mostly by bumblebee (*Bombus impatiens*), which has a relatively short flight range (less than three kilometers) (OECD, 1997). Pollen dispersal by nectar seeking pollinators is limited because potato flowers lack nectar limiting their attractiveness to honeybee *Apis mellifera* and *Bombus fervidus* species. Wind was shown to play an insignificant role in pollen dispersal (OECD, 1997).

For fertile potato varieties, 80-100% of true seed is derived from self-pollination (Plaisted, 1980). A potential source of volunteers is true potato seed, produced via pollination, which develops inside small fruiting bodies formed on the potato vine. However, true potato seed is highly heterozygous, leading to longer establishment times and tubers sets, resulting in lower yield than what is typical with cloned potato tubers (Pallais et al., 1988). Plants produced from true seed are no weedier than volunteer plants produced from overwintered tubers and are relatively easy to control in rotational crops.

While there appears to be minimal, if any, overlap geographically between cultivated and wild potatoes in the U.S., there is a possibility that a few wild potato plants may be growing near potato fields (Love, 1994). However, the potential for hybridization between wild and domesticated potatoes is extremely unlikely. Although approximately 200 species of wild potatoes are known, only two species grow within U.S. borders, including the tetraploid species *Solanum fendleri* (recently reclassified as *Solanum stoloniferum*) and the diploid species *Solanum jamesii* (Bamberg and Rio, 2011; Bamberg et al., 2003; Hijmans and Spooner, 2001). In addition to geographic separation, other biological barriers to gene transfer include multiple ploidy levels and endosperm imbalances. Hybridization between native and

cultivated potatoes has never been reported in the U.S., although gene transfer has been accomplished using special laboratory techniques (Love, 1994).

Potatoes are clonally propagated and differ from genetically propagated or seed grown crops. Maize and soybean, for example, produce seed through sexual recombination (meiosis) resulting in progeny that are genetically and phenotypically unique. Potato tubers are not true seed of potato plants, but instead are clonal tissue. Potato plants arising from clonal propagation are genetically identical having not undergone meiotic recombination. Clonal propagation is not sexual reproduction, and the cloned material is considered genetically and phenotypically stable. Nomenclature used throughout for potato clonal cycles is shown in Figure 2-1.

Somaclonal variation occurs when genetically dissimilar individuals are derived from vegetative propagation. It is especially common during tissue culture in which a callus stage is included. *S. tuberosum* varieties are prone to somaclonal variation during tissue culture and may exhibit a degree of heterogeneity (OECD, 1997). Several steps were taken during event selection to mitigate somaclonal variation. Initially, a number of transformed plants of both X17 and Y9 were produced. A late blight assay was used to screen for plants expressing the VNT1 protein. Plants exhibiting partial resistance to late blight were discarded. Asymptomatic plants were selected and advanced for field testing. Anomalous phenotypes due to somaclonal variation were addressed in replicated field trials grown in several geographic regions that were carefully monitored for undesirable or off phenotypes. Any plants with off-types were removed. The selection process was conducted by experienced agronomists observing the growth characteristics of the transformed events compared to controls. Further studies confirming that somaclonal variation did not occur in X17 and Y9, including phenotypic evaluations, are discussed in Section 7.

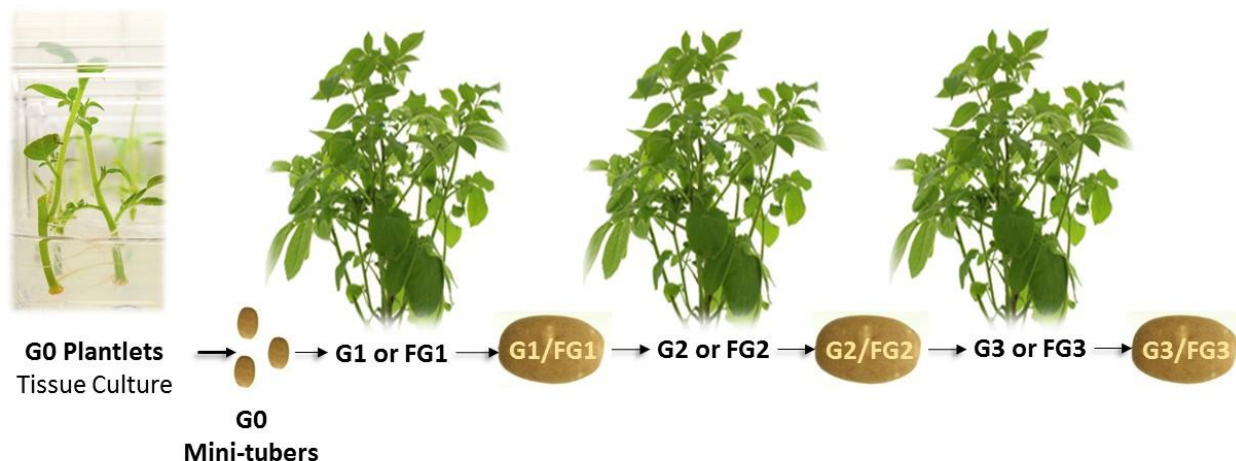


Figure 2-1. Clonal Cycle Nomenclature

Plantlets, propagated from cuttings of G0 tissue, are grown typically in soil, by Nutrient Film Technique, or using hydroponics. Tubers from G0 plantlets are mini-tubers. An entire mini-tuber is planted in the greenhouse (G = greenhouse) or field (FG = field) to produce a G1/FG1 plant. Tubers from G1/FG1 plants may be cut (2-4 oz. (55-115 g) pieces) or used whole as “seed pieces” to produce G2/FG2 plants. This process is repeated for increasing clonal plants and “seed”.

2.2 Description of DNA Used for Transformation

The pSIM1278 and pSIM1678 constructs, used to transform Ranger Russet and Atlantic to generate X17 and Y9, consist of two parts: backbone DNA and T-DNA.

Both constructs were developed with identical backbone sequences containing bacterial and potato DNA intended to support maintenance of the constructs prior to plant transformation. The backbone contains well-characterized bacterial origins of replication from plasmids pVS1 and pBR322, the *nptII* gene for bacterial resistance to kanamycin, and the *Agrobacterium ipt* gene flanked by the potato polyubiquitin (*Ubi7*) promoter and polyubiquitin (*Ubi3*) terminator. The *ipt* gene was introduced as a 2.6-kb *SacII* fragment into the vector backbone and is used for screening transformed plants (Garbarino and Belknap, 1994).

The T-DNA regions are intended for stable integration into the plant genome. The pSIM1278 T-DNA contains cassettes intended to down-regulate levels of asparagine (*Asn1*), reducing sugars (*R1* and *PhL*), and polyphenol oxidase (*Ppo5*). The pSIM1278 construct map and genetic elements table are the same as was provided for events F10, J3, V11, and W8 and are not shown.

The pSIM1678 T-DNA consists of the *Rpi-vnt1* expression cassette, which consists of the VNT1 protein coding region regulated by the native *Rpi-vnt1* promoter and terminator sequences, and a down-regulation cassette for the plant vacuolar invertase gene, *VInv*, consisting of sequence from the potato *VInv* gene arranged as an inverted repeat and flanked by opposing plant promoters, *pGbss* and *pAgp*. The pSIM1678 construct map and genetic elements table are the same as was provided for event W8. The pSIM1678 construct map and genetic elements table are shown for reference (Figure 2-2, Figure 2-3 and Table 2-1).

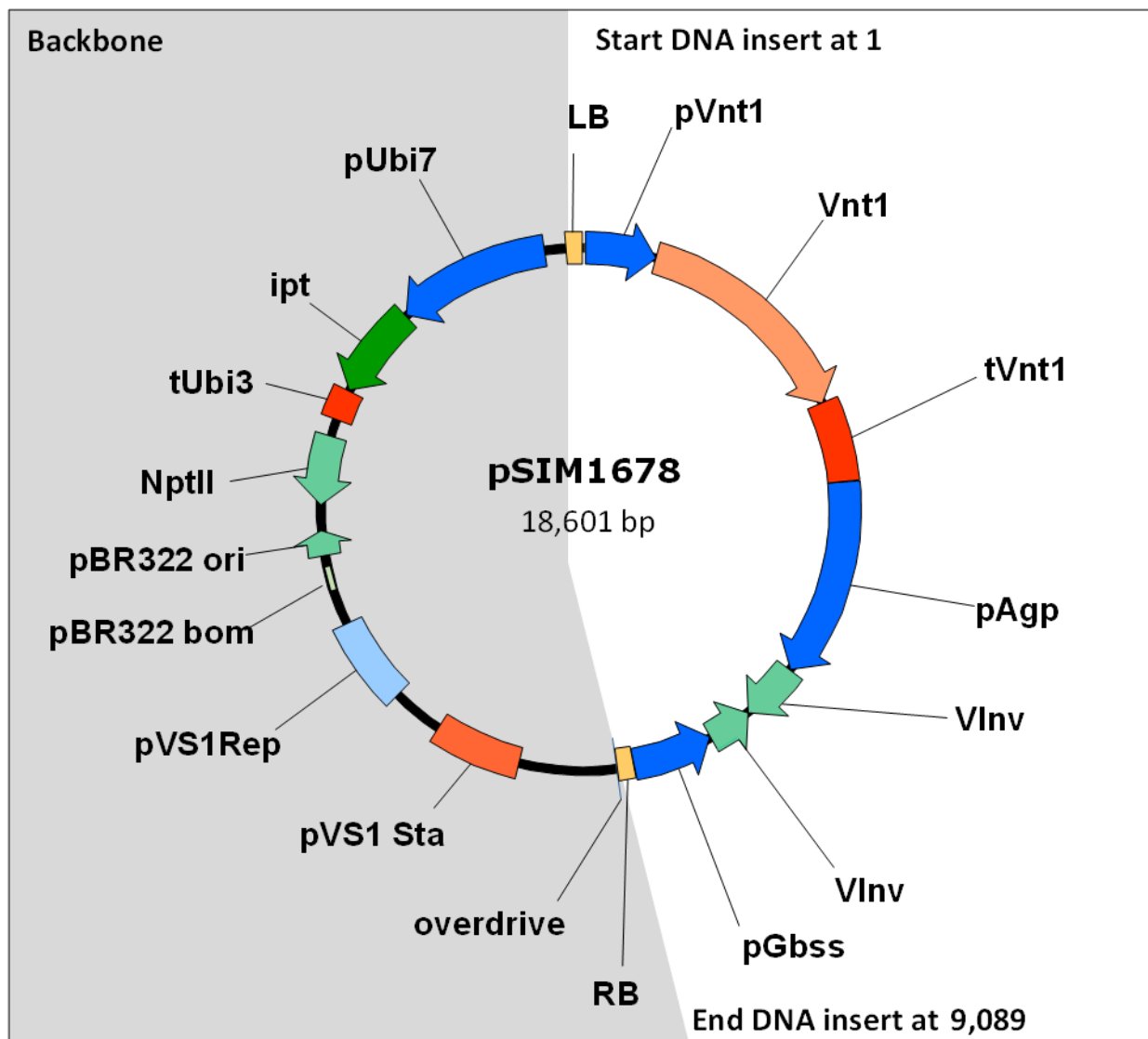


Figure 2-2. Map of pSIM1678 Construct

Map showing the backbone (shaded) and T-DNA elements of the pSIM1678 construct.



Figure 2-3. T-DNA of pSIM1678

Linear diagram of the T-DNA intended for insertion in X17 and Y9 potato events.

Table 2-1. Genetic Elements of pSIM1678 T-DNA

Genetic Element	Origin	Accession Number	Position (pSIM1678)	Size (bp)	Intended Function
1. Left Border (LB) site ¹	Synthetic	AY566555 ² (bases 1-25)	1 - 25	25	Secondary cleavage site releases ssDNA insert from pSIM1678
2. LB Region	<i>S. tuberosum</i> var. Ranger Russet.	AY566555 ² (bases 1-187)	26 - 187	162	Supports secondary cleavage at LB
3. Intervening Sequence	<i>S. tuberosum</i>	AF393847	188 - 193	6	Sequence used for DNA cloning
4. Native <i>Rpi-vnt1</i> gene promoter	<i>S. venturii</i>	FJ423044	194 - 902	709	Drives expression of the <i>Rpi-vnt1</i> gene
5. <i>Rpi-vnt1</i> gene coding sequence	<i>S. venturii</i>	FJ423044	903 - 3,578	2676	Expresses the VNT1 protein
6. Native <i>Rpi-vnt1</i> gene terminator	<i>S. venturii</i>	FJ423044	3,579 - 4,503	925	Terminates transcription of <i>Rpi-vnt1</i>
7. Intervening Sequence	<i>S. tuberosum</i>	HM363755	4,504 - 4,510	7	Sequence used for DNA cloning
8. ADP glucose pyrophosphorylase gene promoter (<i>pAgp</i>)	<i>S. tuberosum</i> var. Ranger Russet	HM363752	4,511 - 6,770	2260	Drives expression of the <i>Vlnv</i> inverted repeat, especially in tubers
9. Intervening Sequence	<i>S. tuberosum</i> var. Ranger Russet	DQ206630	6,771 - 6,776	6	Sequence used for DNA cloning
10. <i>Vlnv</i> gene fragment (sense orientation)	<i>S. tuberosum</i> var. Ranger Russet	DQ478950	6,777 - 7,274	498	Generates a dsRNA to down regulate <i>Vlnv</i> transcripts
11. <i>Vlnv</i> gene fragment extension (sense orientation)	<i>S. tuberosum</i> var. Ranger Russet	DQ478950	7,275 - 7,455	181	Loop sequence of the <i>Vlnv</i> inverted repeat
12. Intervening Sequence	<i>S. tuberosum</i> var. Ranger Russet	X73477	7,456 - 7,461	6	Sequence used for DNA cloning
13. <i>Vlnv</i> gene fragment (anti-sense orientation)	<i>S. tuberosum</i> var. Ranger Russet	DQ478950	7,462 - 7,965	504	Generates a dsRNA to down regulate <i>Vlnv</i> transcripts
14. Intervening Sequence	<i>S. tuberosum</i> var. Ranger Russet	X95996	7,966 - 7,971	6	Sequence used for DNA cloning
15. Granule-bound starch synthase gene promoter (<i>pGbss</i>) (opposite orientation from <i>pAgp</i>)	<i>S. tuberosum</i> var. Ranger Russet	X83220 ²	7,972 - 8,894	923	Drives expression of the <i>Vlnv</i> inverted repeat, especially in tubers
16. Intervening Sequence	<i>S. tuberosum</i>	AF143202	8,895 - 8,903	9	Sequence used for DNA cloning
17. Right Border (RB) region	<i>S. tuberosum</i> var. Ranger Russet	AY566555 ³ (bases 231-416)	8,904 - 9,064	161	Supports primary cleavage at RB
18. RB sequence ¹	Synthetic	AY566555 ³ (bases 392-416)	9,065 - 9,089	25	Primary cleavage site releases ssDNA insert from pSIM1678 (VanHaaren et al., 1989)

¹The LB and RB sequences (25-bp each) were synthetically designed to be similar to and function like T-DNA borders from *A. tumefaciens*.

²GenBank Accession HM363755 is replaced with a citation to GenBank Accession X83220 to properly include the full *pGbss* (2nd copy) DNA insert sequence present in the pSIM1278 construct.

³GenBank Accession AY566555 was revised to clarify the sources of DNA for the border regions.

2.3 Activity and Function of the Genes in X17 and Y9

The activity and function of the down-regulated and expressed genes in X17 and Y9 are identical to those in W8. Down-regulation is not the result of any expressed protein. Instead, the produced double stranded RNA (dsRNA) is recognized by the plant's RNA interference pathway, cut into short pieces, and processed to capture and degrade the mRNA of the targeted genes. Briefly, the down-regulated potato genes in X17 and Y9 and the endogenous functions of their proteins are:

- Asparagine synthetase 1 (*Asn1*)—ASN1 converts glutamine to asparagine by transferring the side-chain amine from glutamine to aspartate to form asparagine;
- Water dikinase R1 (*R1*)—R1 binds starch and phosphorylates glucose at the carbon-6 position, opening the compact starch molecule (Ritte et al., 2000, 2006);
- Phosphorylase-L (*PhL*)—Phosphorylase L (PhL) degrades starch by release of glucose-1-phosphate from the free non-reducing end of the starch molecule (Hanes, 1940);
- Vacuolar invertase (*VInv*)—Invertase converts sucrose into glucose and fructose; and
- Polyphenol oxidase (*Ppo5*)—PPO catalyzes the oxidation of *o*-diphenols to *o*-quinones, which auto-polymerize to form dark, insoluble melanin polymers, responsible for the coloration of oxidized plant tissues.

The only expressed gene in X17 and Y9 is *Rpi-vnt1* and the endogenous function of the protein is:

- Resistance against *P. infestans* (*Rpi-vnt1*)—VNT1 is an R-protein from the wild *Solanum* species, *S. venturii*, which functions in the recognition of *P. infestans* and elicits a hypersensitive response in potato, conferring resistance to late blight disease.

The activity and function of VNT1 are discussed further in Section 5.

R1, PhL, and invertase function in starch metabolism in tubers (Figure 2-4). Starch, the major carbohydrate reserve in potato tubers, is broken down and converted to sugars to provide energy in support of cellular functions. Water dikinase (R1), also known as glucan water dikinase, binds to starch and phosphorylates glucose at the carbon-6 position (Ritte et al., 2000, 2006). Phosphorylation opens up the compact starch polymer, making it accessible to other degrading enzymes, and influences the rate of starch breakdown (Edner et al., 2007; Lorberth et al., 1998). Down-regulating the expression of the *R1* gene results in a reduction of phosphorylated starch which contributes to the stability of the starch polymer and lower concentrations of available reducing sugars (Lorberth et al., 1998).

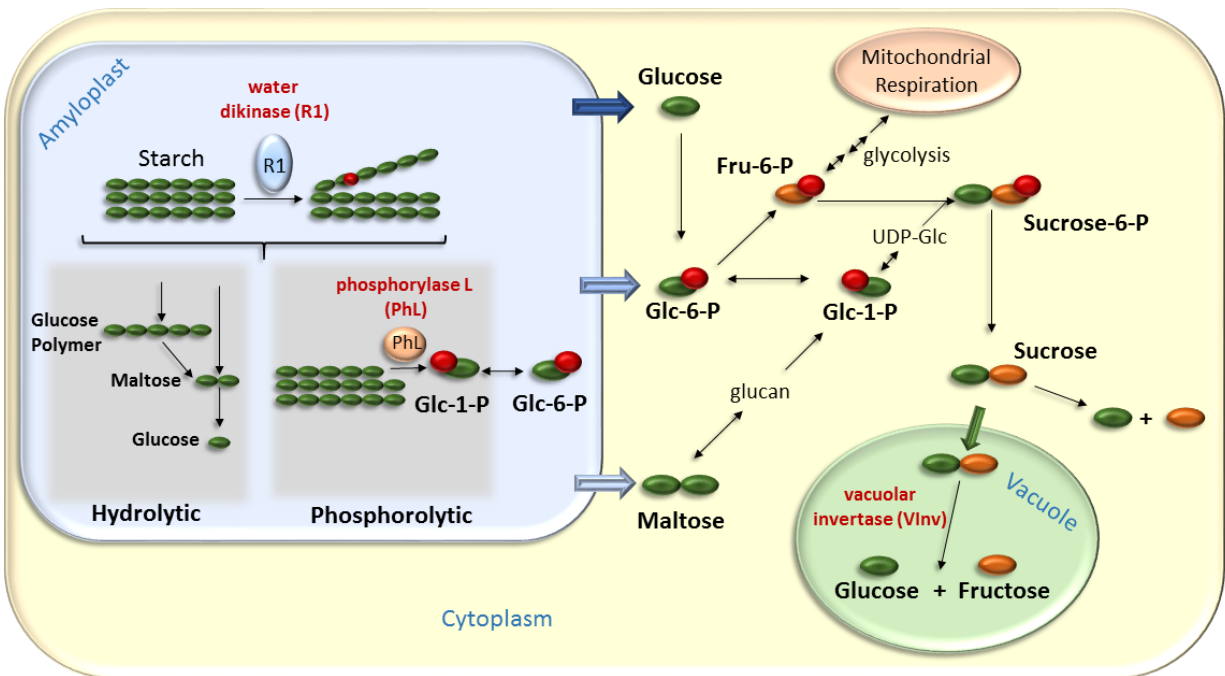


Figure 2-4. Starch Breakdown

Starch polymers stored in the amyloplast are broken down to glucose monomers (green ovals) through a series of enzymatic reactions (black arrow). R1, PhL, and VInv are shown in their respective roles in starch degradation. R1 phosphorylates (red circles) glucose disrupting the compact structure of starch. PhL degrades starch by converting glucose to glucose-1-phosphate. VInv hydrolyzes sucrose to glucose and fructose (orange oval). The figure represents a simplified model of starch metabolism to highlight the roles of R1, PhL, and VInv and is based on (Malone et al., 2006; Sowokinos, 2001).

Starch degrading enzymes include hydrolases (e.g. amylases) and phosphorylases. Hydrolytic degradation of starch by amylases converts starch into glucose polymers and maltose and glucose monomers. Phosphorolytic degradation of starch by phosphorylases, including PhL, releases glucose-1-phosphate from starch which is converted to glucose (Hanes, 1940). Down-regulation of *PhL* lowers the concentration of reducing sugars (glucose and fructose) by inhibiting the breakdown of starch during tuber storage (Kamrani et al., 2011). The down-regulation of *R1* and *PhL* combines to reduce starch degradation leading to lower levels of reducing sugars.

Following starch breakdown in the amyloplast, resulting glucose, glucose-6-phosphate, and maltose monomers are transported to the cytoplasm where they are shuttled into the glycolysis pathway providing energy for mitochondrial respiration or are metabolized into sucrose (Malone et al., 2006; Sowokinos, 2001). Invertases, including *VInv*, also known as acid invertase, hydrolyze sucrose to release glucose and fructose monomers. Down-regulation of *VInv* inhibits the breakdown of sucrose, limiting the concentrations of free glucose and fructose in stored tubers (Ye et al., 2010; Zrenner et al., 1996).

2.4 Description of Marker-Free Transformation

Events X17 and Y9 were developed through transformation using protocols identical to W8. X17 and Y9 are retransformations of deregulated F10 and J3 events, respectively. The process for transformation and selection of F10 and J3 events is shown in Figure 2-5. The process for X17 and Y9 is shown in Figure 2-6.

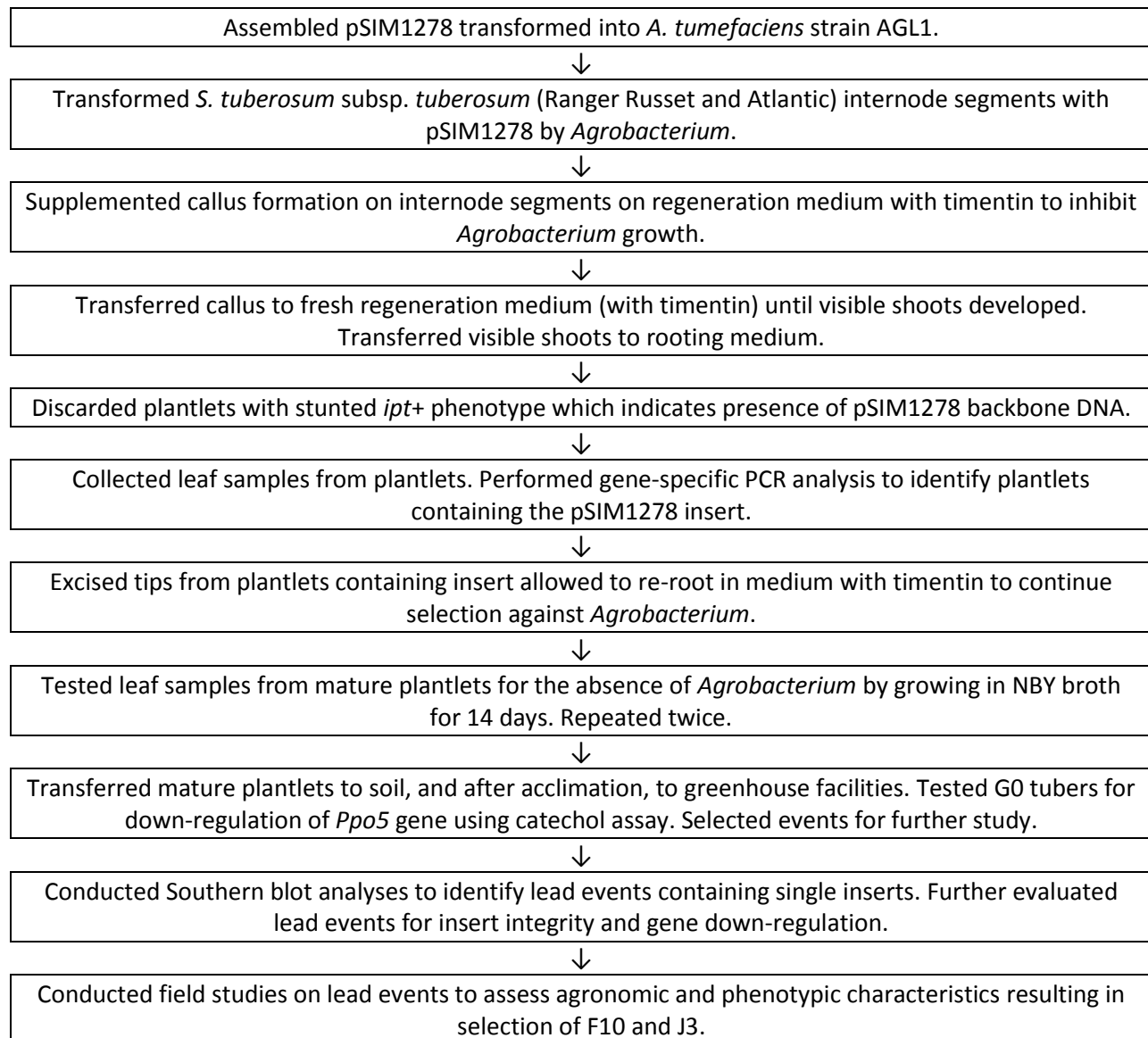


Figure 2-5. Development and Selection of F10 and J3 Events

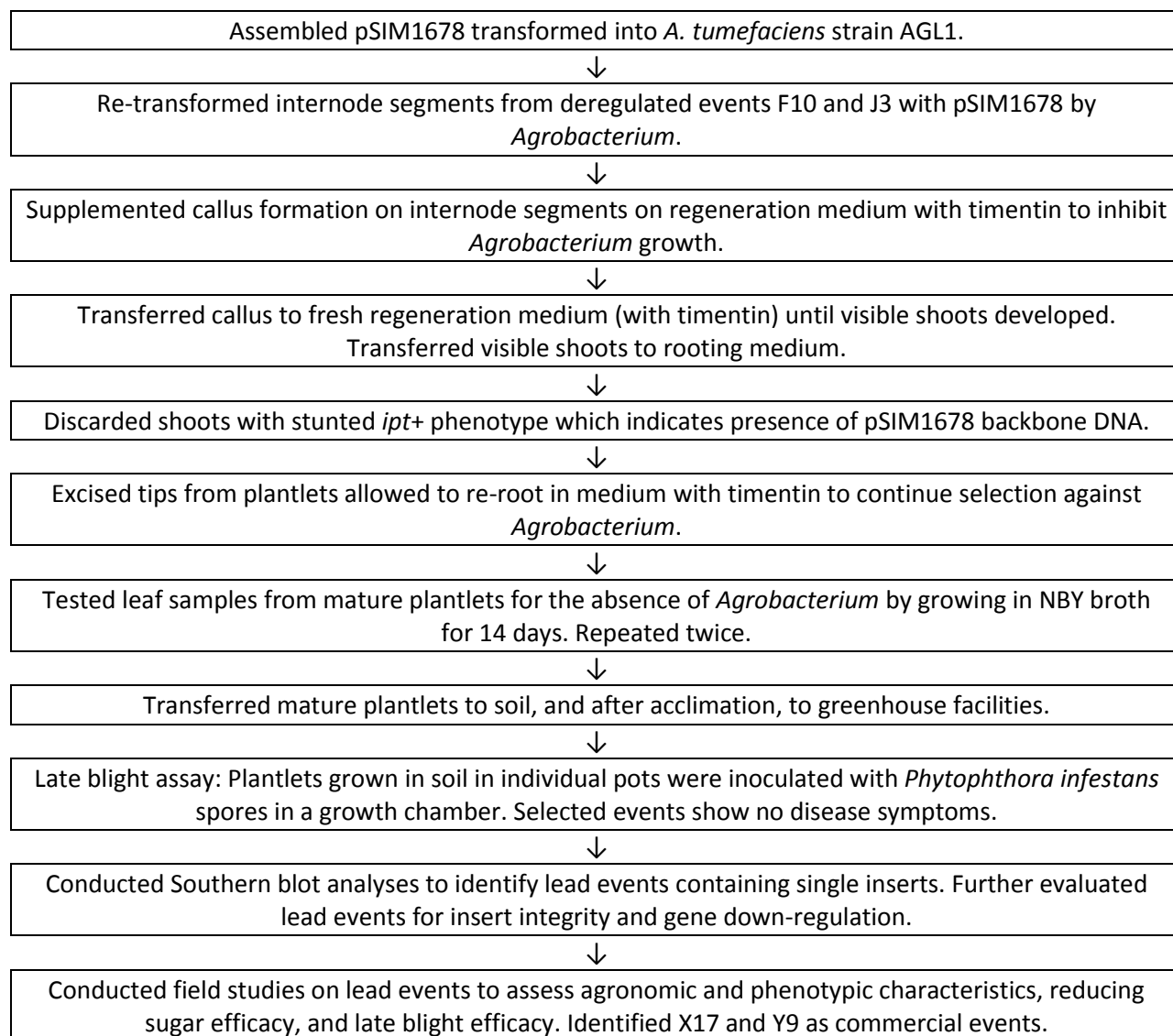


Figure 2-6. Development and Selection of X17 and Y9 Events

3.0 Genetic Characterization of X17 and Y9

X17 and Y9 were successfully transformed with pSIM1278 and pSIM1678, as expected. Molecular analyses demonstrated that the pSIM1678 insert in X17 was integrated at a single locus in the Ranger Russet genome and that the pSIM1678 insert in Y9 was integrated at a single locus in the Atlantic genome (Section 3.1). The characterization of the inserts in X17 show that both inserts, pSIM1278 and pSIM1678, consist of nearly full-length T-DNA (Section 3.2). The characterization of the inserts in Y9 show that the pSIM1278 insert consists of a nearly full-length T-DNA flanked by an additional *Asn1/Ppo5* and partial *PhL/R1* cassette, and the pSIM1678 insert consists of a nearly full-length T-DNA flanked by an additional, partial *VInv* cassette (Section 3.2). Further characterization demonstrated that backbone sequences were not introduced and that the inserts are genetically stable across clonal cycles (Section 3.3 and Section 3.4).

The molecular characterization of X17 and Y9 was performed using:

- Southern analysis showing pSIM1278 and pSIM1678 inserts integrate into single genomic loci (see Section 3.1);
- Southern, PCR, and sequencing analyses showing the structure of the inserts (see Section 3.2);
- Southern analysis demonstrating backbone sequences were not introduced (see Section 3.3); and
- Southern analysis confirming stability of the inserts through clonal cycles (see Section 3.4).

3.1 Single Genomic Insertion Locus in X17 and Y9

DNA samples from X17 and Y9 and controls were digested with the *BbsI* restriction enzyme and detected using multiple probes spanning the length of the pSIM1278 and pSIM1678 T-DNA. The pSIM1278 and pSIM1678 T-DNA share some identical sequences, including left and right border regions and *Agp* and *Gbss* promoters. In the Southern analysis, probes hybridizing to these regions detect both pSIM1278 and pSIM1678 inserts. Blots made with these probes are expected to contain two bands, one from pSIM1278 and the other from pSIM1678. F10 or J3 samples (which contain only pSIM1278) were used to distinguish between pSIM1278 and pSIM1678 bands observed in X17 or Y9 samples on blots where probes recognize both inserts.

The *BbsI* restriction enzyme cuts frequently within the potato genome, but not within either of the T-DNA, resulting in a distinct band that, regardless of the probes used, is the same size for each insertion event. Observation of more than one band indicates the presence of more than one insertion locus. Because *BbsI* cuts frequently in the potato genome, it is unlikely that two inserts would give rise to the same size band following digestion.

Wild-type (WT) genomic DNA was spiked with purified construct DNA (either pSIM1278 or pSIM1678) at a concentration of one copy per genome equivalent to ensure that the sensitivity of the probe was sufficient to detect a single copy of the insert in the genome.

3.1.1 Single Insertion Locus in X17 Associated with pSIM1278

The pSIM1278 insert in X17 is the same as in F10. The number of pSIM1278 insertion loci were reevaluated in X17 by Southern analysis, using F10 and Ranger Russet (WT) as controls. Samples were digested with the *BbsI* restriction enzyme and hybridized with probes spanning the entire pSIM1278 T-

DNA (see Figure 3-1). The results confirm that X17 maintains a single pSIM1278 insertion locus (Figure 3-2).

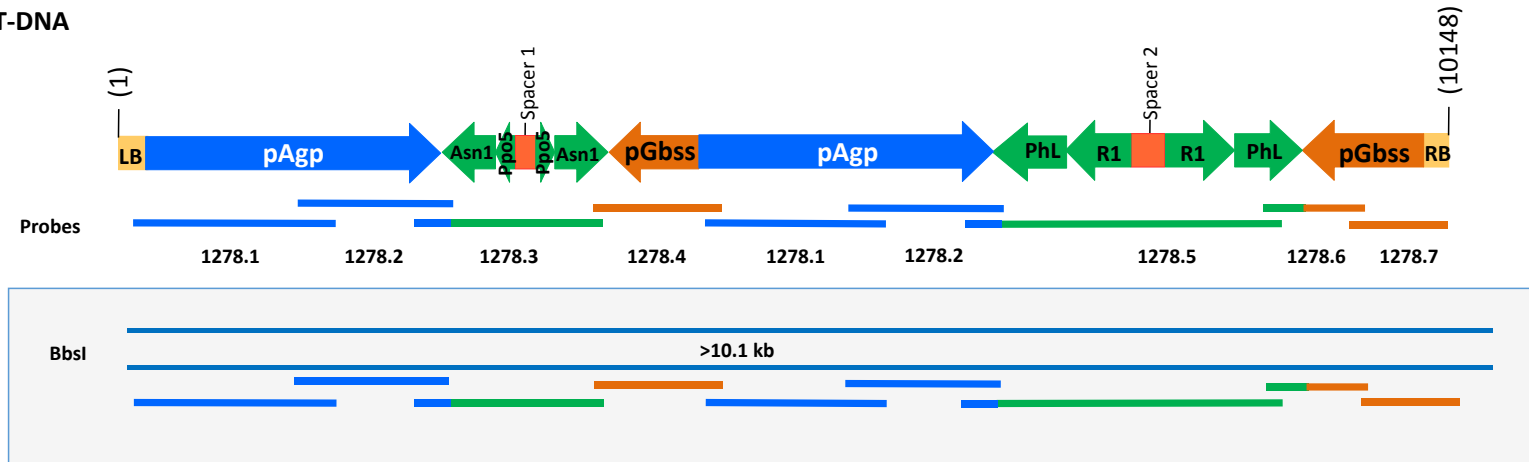
Digestion of X17 genomic DNA with BbsI and hybridization with the seven 1278 probes identified two, unique high molecular weight bands in X17 samples originating from pSIM1278 (red arrow) and pSIM1678 (blue arrow) insertions (Figure 3-2). The pSIM1278 insertion locus was distinguished from the pSIM1678 locus by comparing WT and F10 samples to X17. Bands present in F10, but not WT, are uniquely associated with the pSIM1278 transformation. Bands unique to X17 are associated with the pSIM1678 transformation.

The pSIM1278 transformation resulted in a single pSIM1278 insertion locus in F10 that was maintained in X17. A single band was observed in both F10 and X17 samples that was not present in WT (Figure 3-2, red arrows). This pSIM1278 insert band migrated faster than the pSIM1278 construct control (black arrows), indicating that the size of the insert was smaller than 10.8 kb following digestion with BbsI. This was confirmed by the molecular characterization of the structure of the pSIM1278 insert summarized in Section 3.2.

The higher molecular weight band (Figure 3-2, blue arrows) observed in X17, but not F10, corresponds to the pSIM1678 insert. The pSIM1678 insert was detected by the 1278 probe set as all seven probes have some complementarity with either *pAgp* or *pGbss* sequences present in pSIM1678 (see Figure 3-1).

Detection of the construct control (black arrows) indicated that all probes had sufficient sensitivity to detect a single insert in the genome. Only one fragment was identified unique to F10 and X17 by any of the seven probes.

(A) pSIM1278 T-DNA



(B) pSIM1678 T-DNA

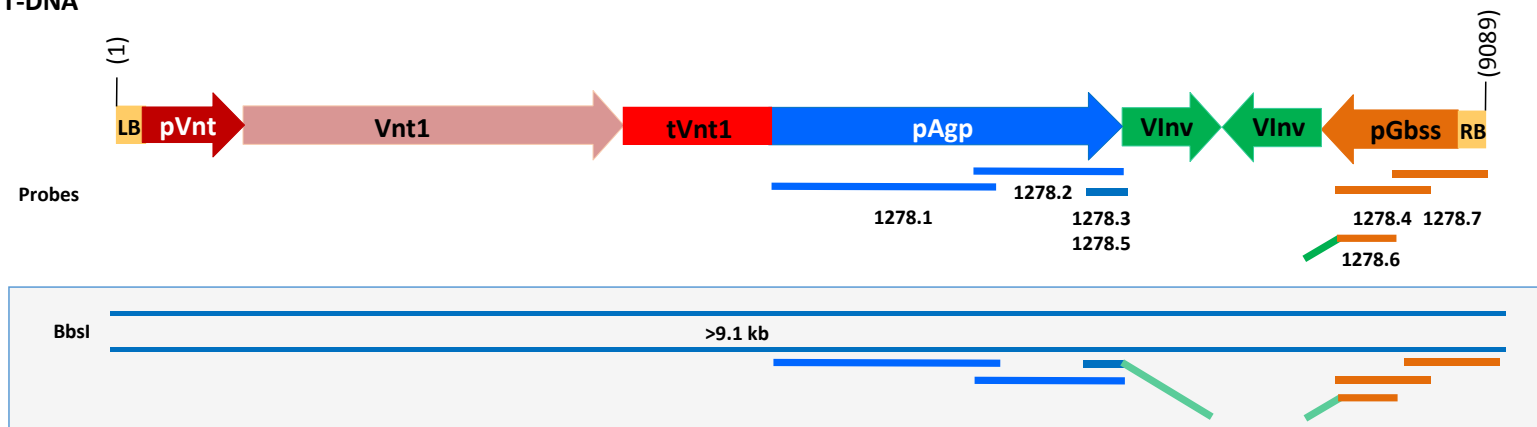


Figure 3-1. pSIM1278 Insert Number Characterization

(A) Seven probes designed to hybridize the pSIM1278 T-DNA were used to determine the number of pSIM1278 insertion events in X17 and Y9. Probes that hybridize to more than one site within the T-DNA are shown (i.e. 1278.1 binds to the two copies of the *Agp* promoter). Probes 1278.3, 1278.5, and 1278.6 overlap multiple elements (indicated using two colors). (B) 1278 probes will also hybridize to the pSIM1678 T-DNA. The expected digestion products and probe binding sites are shown.

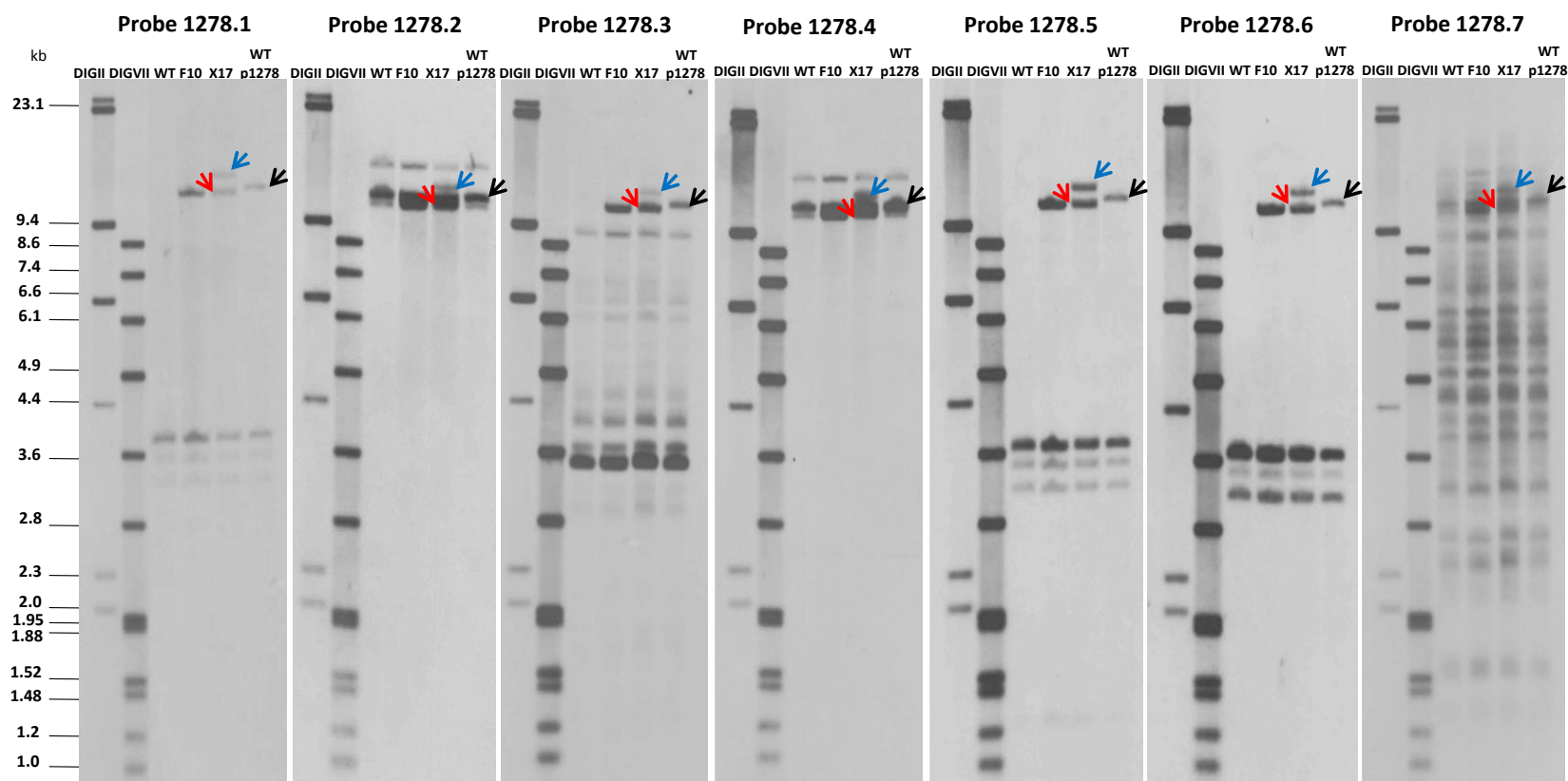


Figure 3-2. Single Insertion Locus for the pSIM1278 Insert in X17

BbsI digested genomic DNA from X17, F10, Ranger Russet (WT), and WT spiked with pSIM1278 construct DNA (WT p1278) was hybridized with the indicated probe (1278.1-1278.7). Three types of bands were observed in addition to endogenous bands common to all samples: 1) unique to F10 and X17 (not found in WT) corresponding to pSIM1278 (**red**), 2) unique to X17 corresponding to pSIM1678 (**blue**), and 3) associated with spiked pSIM1278 DNA (**black**) in WT samples. Molecular weight markers, DIGII and DIGVII, were included on each gel. Sizes are in kilobases (kb).

3.1.2 Single Insertion Locus in X17 Associated with pSIM1678

The number of pSIM1678 insertion loci in X17 was evaluated by Southern analysis, using F10 and Ranger Russet (WT) as controls. Samples were digested with BbsI and hybridized with multiple probes spanning the entire pSIM1678 T-DNA (Figure 3-3). The results confirm that X17 contains a single pSIM1678 insertion locus (Figure 3-4).

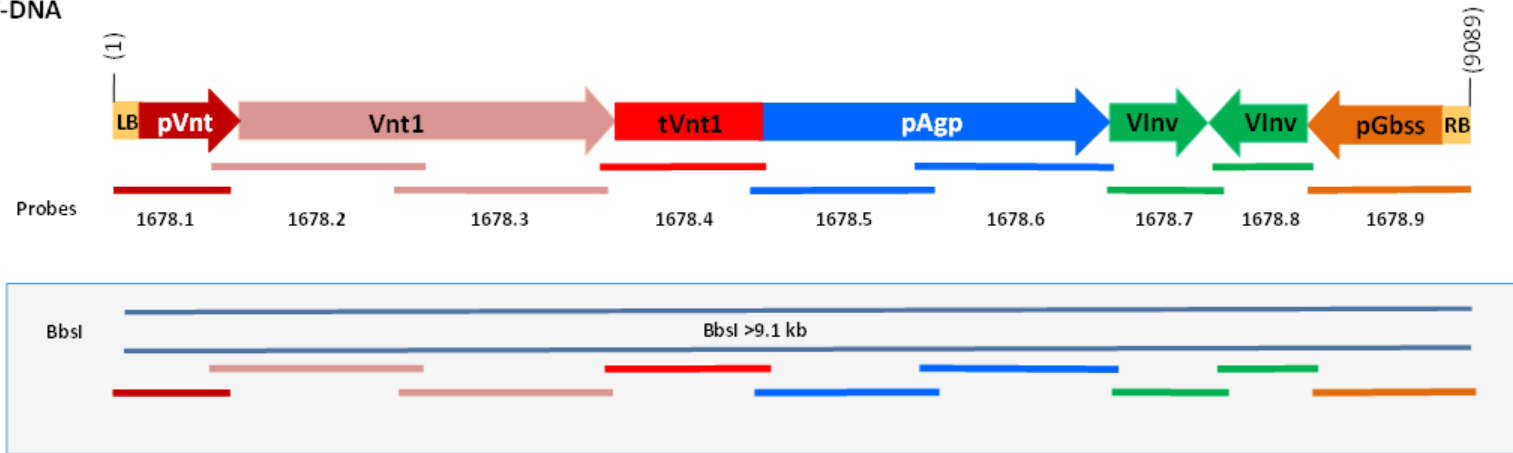
Digestion of X17 genomic DNA with BbsI and hybridization with the nine 1678 probes identified unique high molecular weight bands in X17 samples. Using probes specific to pSIM1678, Southern analysis resulted in a single band indicating a single pSIM1678 locus (Figure 3-4, blue arrows). With probes also hybridizing to sequences from pSIM1278, an additional band was observed (Figure 3-4; red arrows).

The pSIM1678 retransformation of F10 resulted in a single pSIM1678 insertion locus in the X17 genome. A single band was observed in X17 that was not present in WT or F10 (Figure 3-4; blue arrows). The pSIM1678 insert band was larger than 9.8 kb and migrated slower than the pSIM1678 construct control digestion product (p1678, black arrows). The same size pSIM1678 insert band was detected by the 1278 and 1678 probes (compare Figure 3-2 and Figure 3-4).

Detection of the construct control (black arrows) indicated that the probes had sufficient sensitivity to detect a single insert. Only one band was identified unique to X17 by any of the probes that hybridize to the pSIM1678 T-DNA indicating that transformation with pSIM1678 resulted in a single insert in the genome.

Due to complementarity with *pAgp*, *pGbss*, or border regions, several of the 1678 probes detected the pSIM1278 insert. The pSIM1278 insert was detected by probes 1678.1, 1678.5, 1678.6, and 1678.9 (Figure 3-4, red arrows). The size of the BbsI digestion fragment containing the pSIM1278 insert was the same (10.6 kb) size as the fragment detected using the 1278 probes (compare Figure 3-2 and Figure 3-4).

(A) pSIM1678 T-DNA



(B) pSIM1278 T-DNA

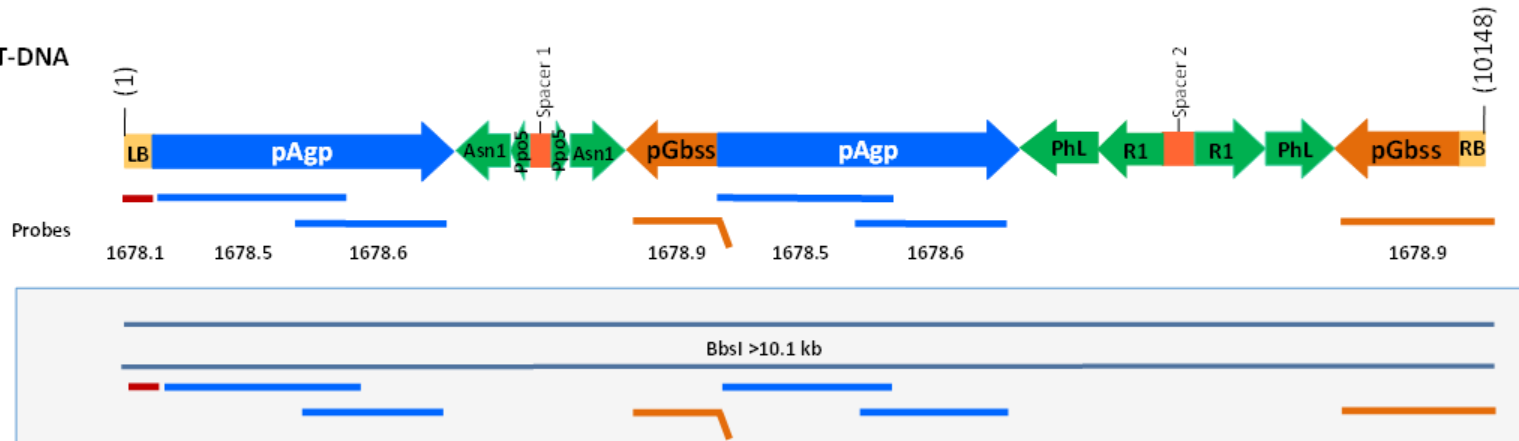


Figure 3-3. pSIM1678 Insert Number Characterization

(A) A series of nine probes were designed to cover the entire pSIM1678 T-DNA. (B) Because of identical sequence, the pSIM1278 T-DNA structure is shown to indicate where hybridization occurs with the 1678 probes. The expected digestion products are shown in boxes, with probe binding sites indicated.

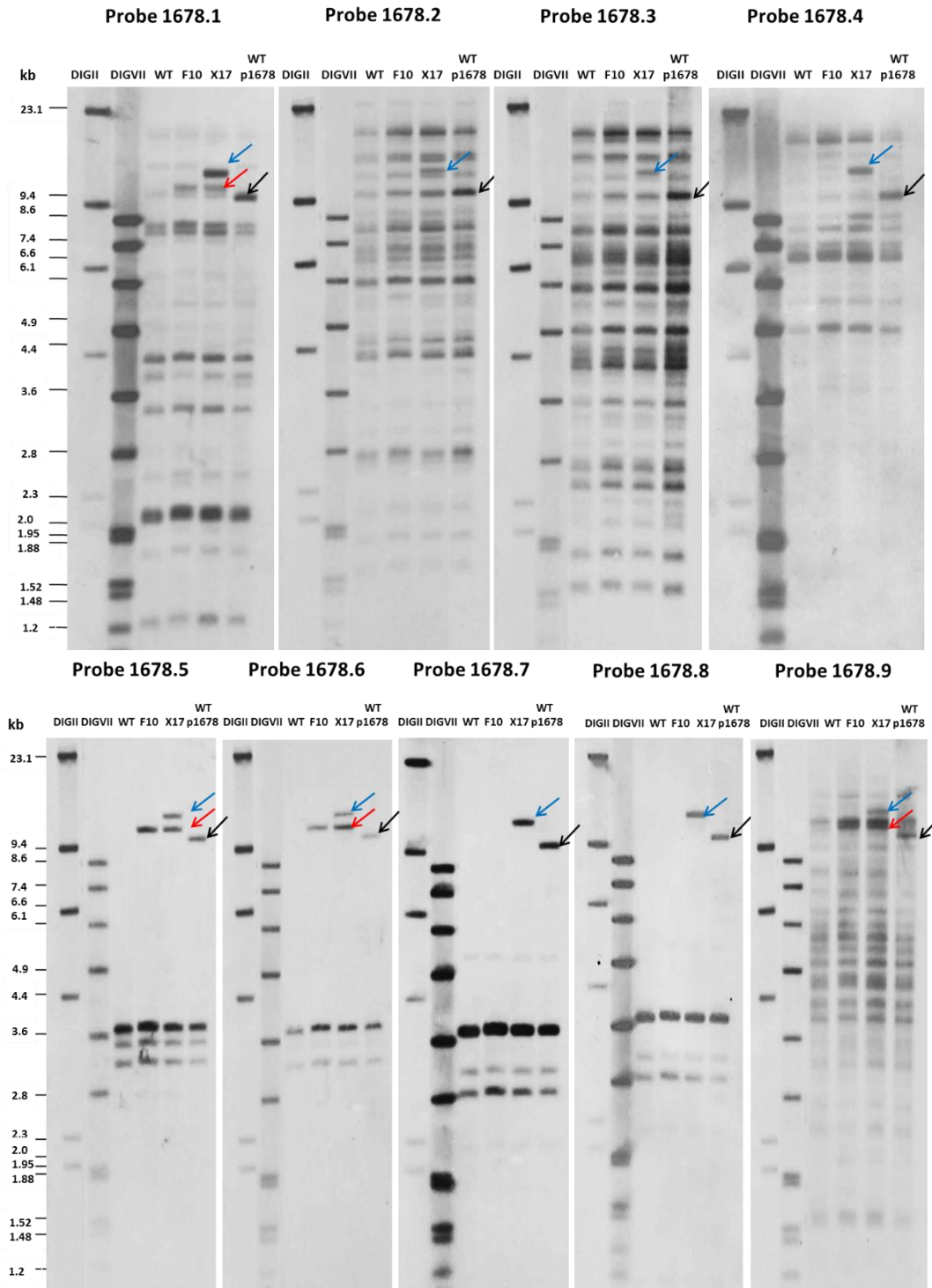


Figure 3-4. Single Insertion Locus for the pSIM1678 Insert in X17

BbsI digested genomic DNA from X17, F10, Ranger Russet (WT), and WT spiked with pSIM1678 construct DNA (WT p1678) was hybridized with the indicated probe (1678.1-1678.9). Three types of bands were observed in addition to endogenous bands common to all samples: 1) unique to F10 and X17 corresponding to pSIM1278 (**red**), 2) unique to X17 corresponding to pSIM1678 (**blue**), and 3) associated with spiked pSIM1678 DNA (**black**) into WT samples. Molecular weight markers, DIGII and DIGVII, are on each gel, labeled in kilobases (kb).

3.1.3 Single Insertion Locus in Y9 Associated with pSIM1278

The pSIM1278 insert in Y9 is the same as in J3. The number of insertion loci of the pSIM1278 insert was reevaluated in Y9 by Southern analysis, using J3 and Atlantic (WT) as controls. Samples were digested with the BbsI restriction enzyme and hybridized with probes spanning the entire pSIM1278 T-DNA (see Figure 3-1). The results confirm that Y9 maintains a single pSIM1278 insert (Figure 3-5).

Digestion of Y9 genomic DNA with BbsI and hybridization with the seven 1278 probes identified two, unique high molecular weight bands in Y9 samples (Figure 3-5). The pSIM1278 insert was distinguished from the pSIM1678 insert by comparing Y9 to WT and J3 samples. Bands present in J3, but not WT, are uniquely associated with the pSIM1278 transformation. Bands unique to Y9 are associated with the pSIM1678 transformation.

A single band was observed in J3 and Y9 samples that was not present in WT (Figure 3-5, red arrows). This band (about 20 kb) corresponds to the pSIM1278 insert and about 4 kb of flanking DNA on either side. As expected, the size of the pSIM1278 insert was the same in each blot and distinct from the pSIM1278 construct control digestion product (WT p1278, black arrows).

Detection of the construct control indicated the probes had sufficient sensitivity to detect a single insert in the genome. The pSIM1278 transformation resulted in a single insert in the Atlantic genome indicated by a single observed band in the J3 and Y9 samples.

Due to complementarity with *pAgp*, *pGbss*, or border regions, several of the 1278 probes detected the pSIM1678 insert (see Figure 3-3). The pSIM1678 fragment unique to the Y9 sample (Figure 3-5, blue arrow) migrated faster than the 10.8 kb band from the construct control (Figure 3-5, black arrow) indicating it was smaller than 10.8 kb.

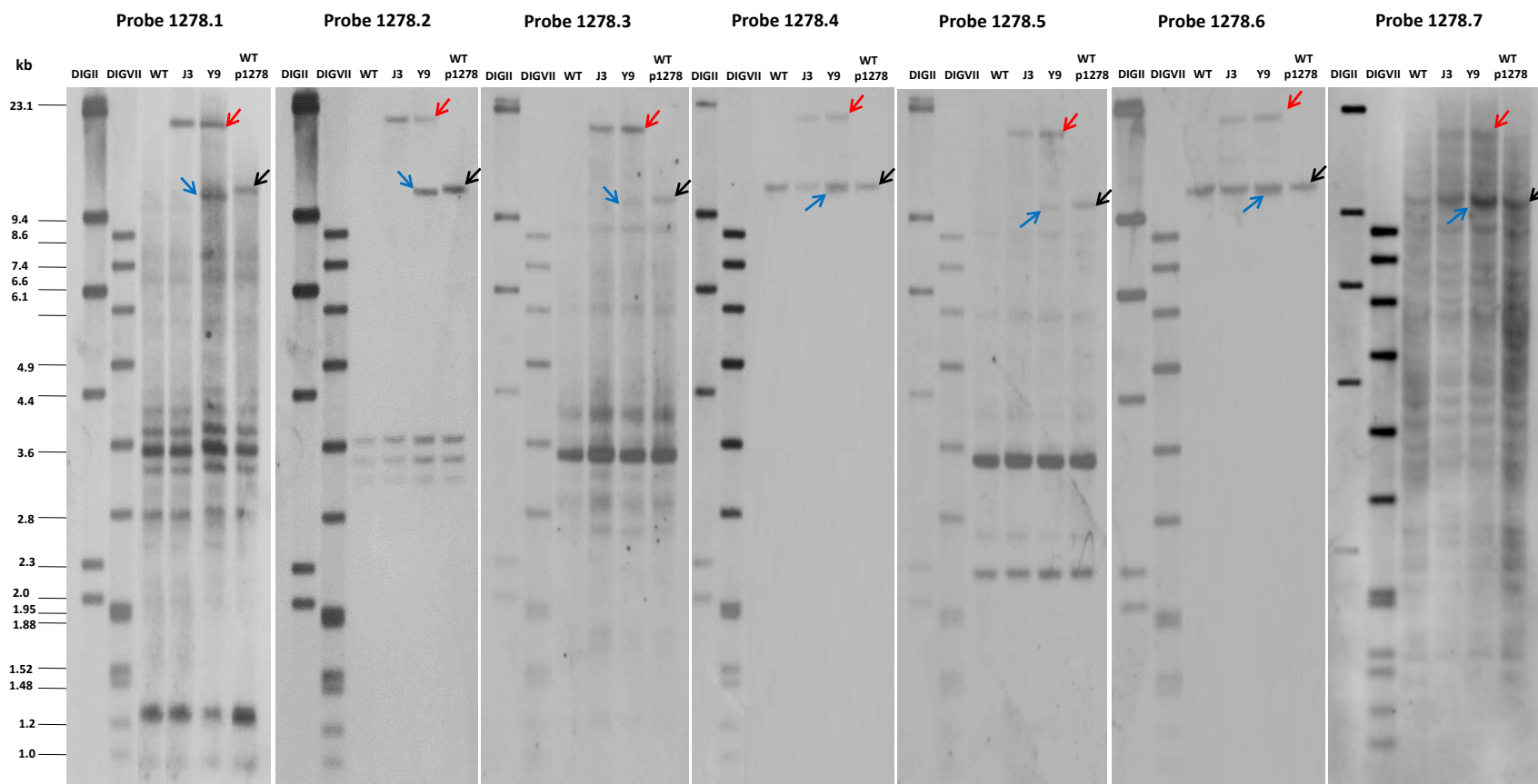


Figure 3-5. Single pSIM1278 Insertion Locus in Y9

BbsI digested genomic DNA from Y9, J3, Atlantic (WT), and WT spiked with pSIM1278 construct DNA (WT p1278) was hybridized with the indicated probe (1278.1–1278.7). Three types of bands were observed in addition to endogenous bands common to all samples: 1) unique to F10 and X17 corresponding to pSIM1278 (**red**), 2) unique to X17 corresponding to pSIM1678 (**blue**), and 3) associated with spiked pSIM1678 DNA (**black**) into WT samples. Molecular weight markers, DIGII and DIGVII, are shown.

3.1.4 Single Insertion Locus in Y9 Associated with pSIM1678

Digestion of Y9 genomic DNA with BbsI and hybridization with the nine 1678 probes identified unique high molecular weight bands in the Y9 samples. With probes specific to pSIM1678 only a single band was observed (Figure 3-6; blue arrows). With probes also hybridizing to sequences from pSIM1278, an additional band was observed (Figure 3-6, red arrows).

The pSIM1678 retransformation of J3 resulted in a single pSIM1678 insert locus in the Y9 Atlantic genome. A single band was observed in Y9 samples that was not present in WT or J3 (Figure 3-6, blue arrows). This pSIM1678 insert fragment was 10.6 kb and migrated slower than the pSIM1678 construct control digestion product (p1678, black arrows). The same size pSIM1678 insert band was detected by the 1278 and 1678 probes (compare Figure 3-5 and Figure 3-6).

Detection of the construct control (black arrows) indicated that the probes had sufficient sensitivity to detect a single insert in the genome. Only one band was identified unique to Y9 by any of the probes that hybridize to the pSIM1678 T-DNA indicating that transformation with pSIM1678 resulted in a single insert in the Atlantic genome.

Due to complementarity with *pAgp*, *pGbss*, or border regions several of the 1678 probes detected the pSIM1278 insert. A second band (about 20 kb) corresponding to the locus containing the pSIM1278 insert was observed in the J3 and Y9 samples by probes 1678.5, 1678.6, and 1678.9 (Figure 3-6, red arrows). The 1678.1 probe which hybridizes to the LB region of the T-DNA did not detect the pSIM1278 insert due to the absence of this region in the pSIM1278 insert (see Section 3.2). There were no additional bands detected by the 1678 probe set.

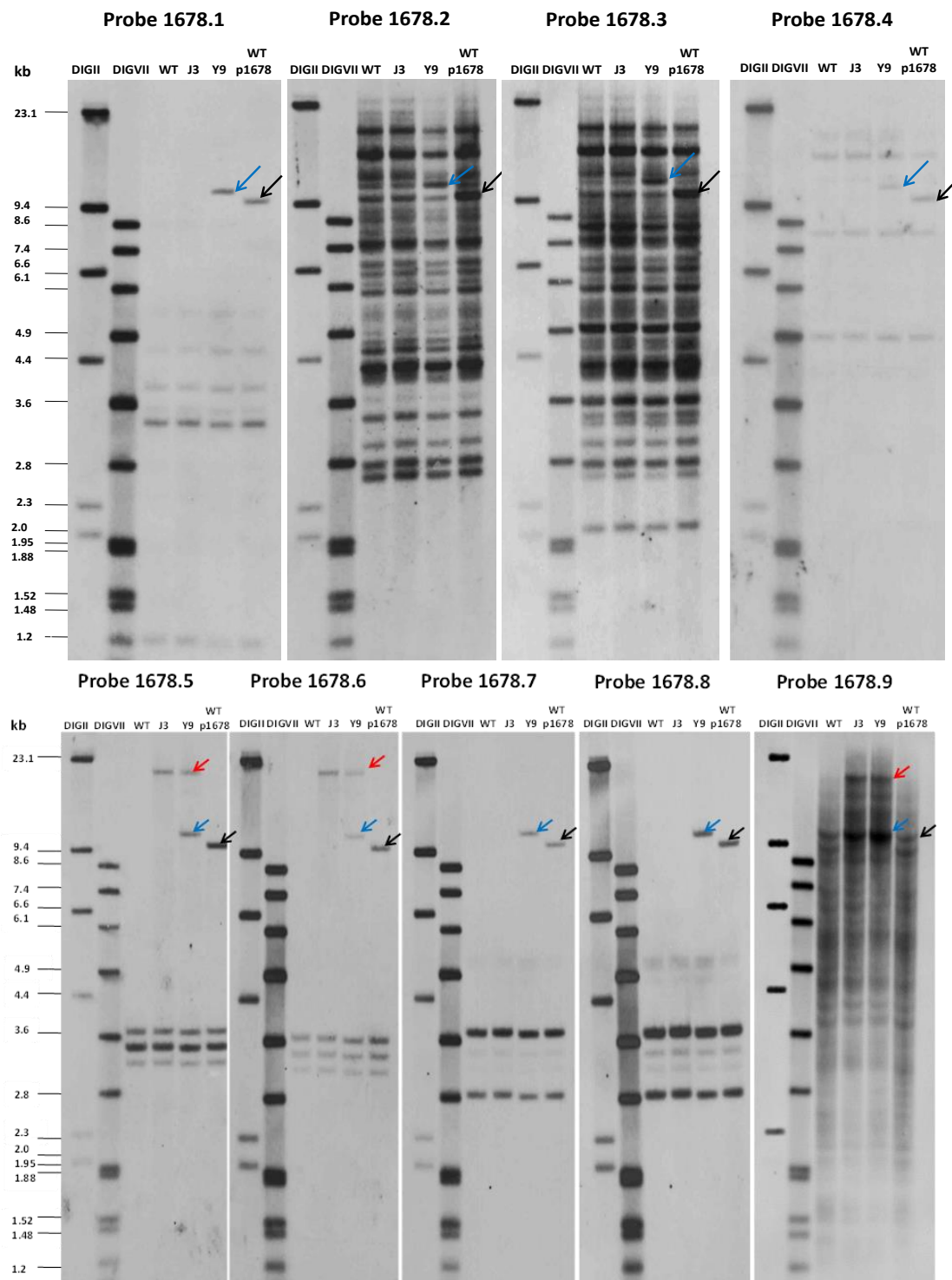


Figure 3-6. Single pSIM1678 Insertion Locus in Y9

BbsI digested genomic DNA from Y9, J3, Atlantic (WT), and WT spiked with pSIM1678 construct DNA (WT p1678) was hybridized with the indicated probe (1678.1-1678.9). Three types of bands were observed in addition to endogenous bands common to all samples: 1) unique to J3 and Y9 corresponding to pSIM1278 (**red**), 2) unique to Y9 corresponding to pSIM1678 (**blue**), and 3) associated with spiked pSIM1678 DNA (**black**) into WT samples. Molecular weight markers, DIGII and DIGVII, are shown.

3.2 Structures of the pSIM1278 and pSIM1678 Inserts in X17 and Y9

The structures of the pSIM1278 and pSIM1678 inserts in X17 are shown in Figure 3-7 and Figure 3-12. Both pSIM1278 and pSIM1678 inserts consist of a nearly full-length T-DNA.

The structures of the pSIM1278 and pSIM1678 inserts in Y9 are shown in Figure 3-17 and Figure 3-27. The pSIM1278 insert consists of a nearly full-length T-DNA flanked by an additional Asn1/Ppo5 cassette on the left side, and a partial PhL/R1 cassette on the right side. The pSIM1678 insert consists of a nearly full-length T-DNA with an additional, partial VInv cassette on the right side.

Southern blot analyses supporting the insert structures in X17 are provided in Section 3.2.1 and Section 3.2.2, and for Y9 in Section 3.2.3 and Section 3.2.4

3.2.1 pSIM1278 Insert Structure in X17

The insertion site analysis in Section 3.1 indicated that the pSIM1278 insert in X17 is contained within the 10.6 kb fragment resulting from digestion with BbsI. The size of the fragment detected by Southern analysis suggests that the insert consists of a single, full-length copy of the T-DNA. The sequences of the left and right regions joining the pSIM1278 insert to the genomic DNA were determined by DNA sequencing (Layne et al., 2015a). The left junction sequence indicated a 2 bp deletion of the pSIM1278 T-DNA LB region with an addition of 6 bp not found in either the genome or the insert. The right junction sequence indicated a 55 bp deletion of the RB region. Adjacent plant genome sequence (out to 1 kb) was determined by DNA sequencing. BbsI restriction sites were identified near the right and left junctions. The locations of the BbsI restriction sites were consistent with the 10.6 kb fragment observed empirically in Section 3.1. The data indicate that the pSIM1278 insert is a nearly full-length T-DNA (see Figure 3-7).

Southern analysis was used to determine the structure of the pSIM1278 insert. X17 genomic DNA was digested with EcoRV, HindIII, XbaI, or with both EcoRI/ScaI and hybridized with AGP, ASN, GBS, and R1 probes. As controls, a Ranger Russet (WT) sample with or without spiked pSIM1278 construct (p1278) was also analyzed. The spiked construct was at a concentration of one copy per genome equivalent prior to digestion. The spiked control was used to confirm that the probes were sensitive enough to detect a single pSIM1278 fragment in the genome. The spike also served as a size marker to confirm the size of internal bands. Bands observed in F10 and X17 samples are from pSIM1278. Bands found only in X17 are from pSIM1678.

The presence of an intact Asn1/Ppo5 inverted repeat was evidenced by the observation of 0.7 and 2.3 kb EcoRV bands, a 4.2 kb HindIII band, and a 4.0 kb EcoRI/ScaI band using the ASN probe (Figure 3-8). The 2.3 EcoRV and 4.2 HindIII fragments were detected by the AGP and GBS probes (Figure 3-9 and Figure 3-10) as expected. The 3.8 kb EcoRI/ScaI band was detected using the AGP, GBS, and R1 probes (Figure 3-9, Figure 3-10, and Figure 3-11). The 1.3 kb HindIII and 0.8 kb EcoRI/ScaI fragments were detected by the R1 probe (Figure 3-11). All expected internal bands were observed in both F10 and X17 samples.

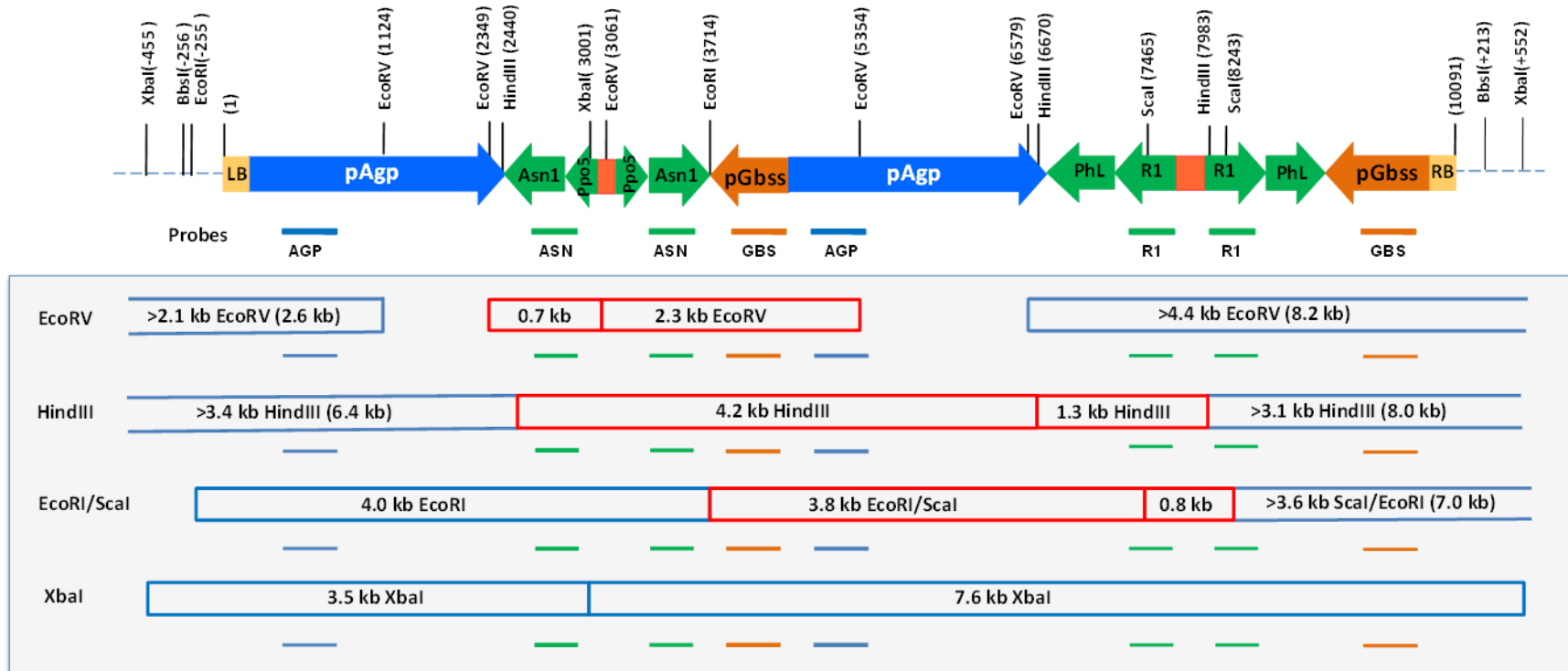


Figure 3-7. Structure of the pSIM1278 Insert in X17

The structure of the pSIM1278 insert in X17 is shown with restriction sites. Product bands resulting from digestion with selected enzymes are shown as colored boxes with fragment sizes indicated. Probe hybridizations are indicated with colored lines. Red boxes are internal bands, blue closed boxes are junction bands with known sizes, and open-ended blue boxes indicate junction bands of unknown size (restriction sites were not identified within the 1 kb of flanking genomic sequence). Estimated junction band sizes based on migration of identified bands on Southern blots is indicated in parenthesis.

ASN Probe

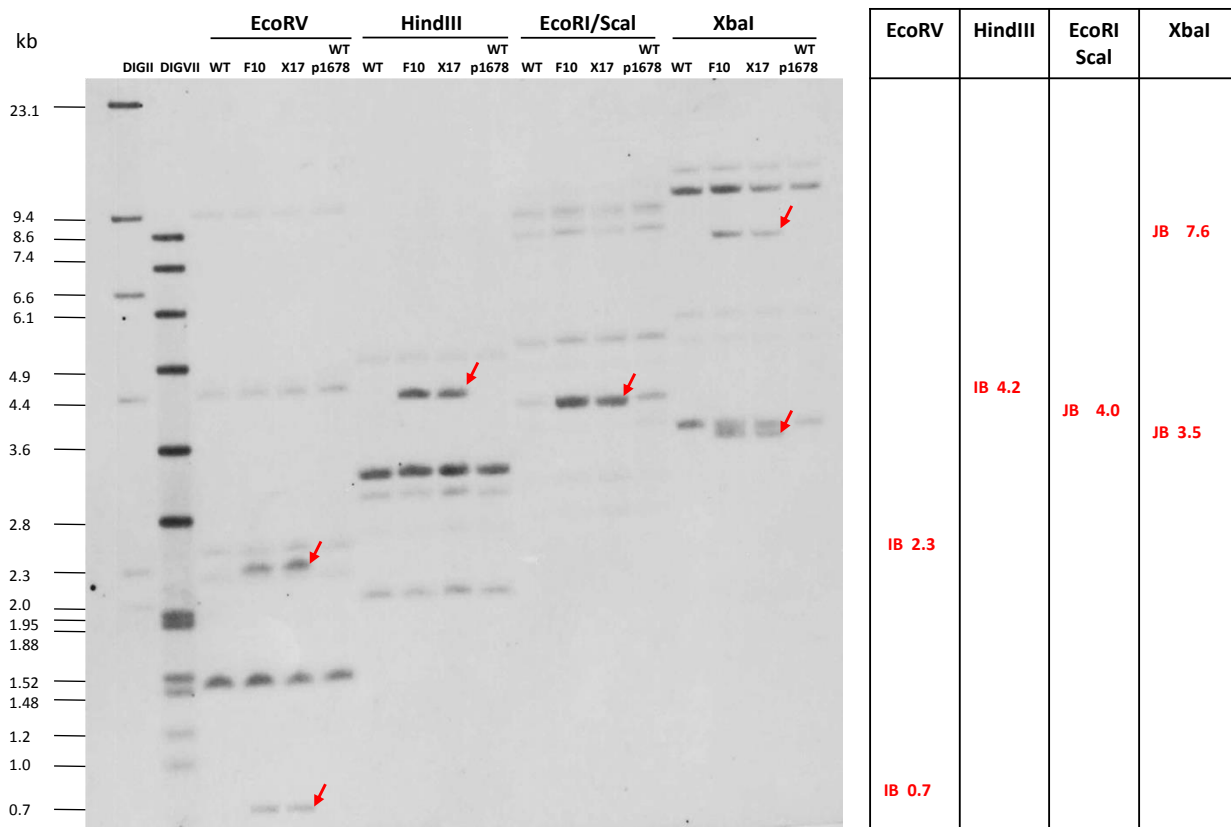


Figure 3-8. Southern Hybridization of Ranger Russet, F10, and X17 Genomic DNA with ASN

Genomic DNA of Ranger Russet control (WT), F10, X17, and WT spiked with pSIM1678 construct DNA was digested with EcoRV, HindIII, EcoRI/Scal, and XbaI and hybridized with the ASN probe. Size of the DIGII and DIGVII molecular weight markers are indicated adjacent to the blot image. Colored arrows were used to distinguish between any bands associated with the pSIM1278 insert (**red**). Estimated sizes of insert-specific bands are indicated in the table. (JB) junction bands, (IB) internal bands.

AGP Probe

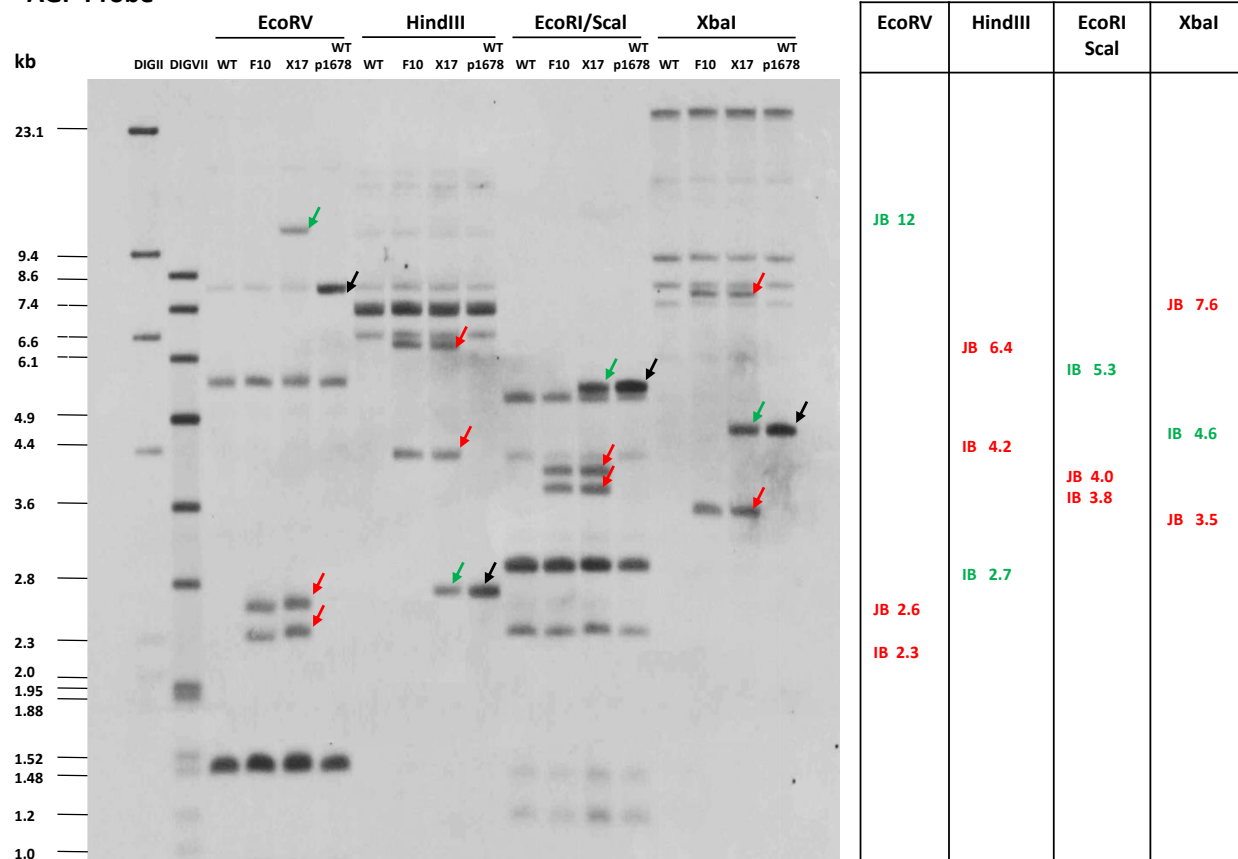


Figure 3-9. Southern Hybridization of Ranger Russet, F10, and X17 Genomic DNA with AGP

Genomic DNA of Ranger Russet control (WT), F10, X17, and WT spiked with pSIM1678 construct DNA was digested with EcoRV, HindIII, EcoRI/Scal, and XbaI and hybridized with the AGP probe. Size of the DIGII and DIGVII molecular weight markers are indicated adjacent to the blot image. Colored arrows were used to distinguish between any bands associated with the pSIM1278 insert (**red**), the pSIM1678 insert (**green**) and the spiked pSIM1678 (**black**). Estimated sizes of insert-specific bands are indicated in the table. (JB) junction bands, (IB) internal bands.

GBS Probe

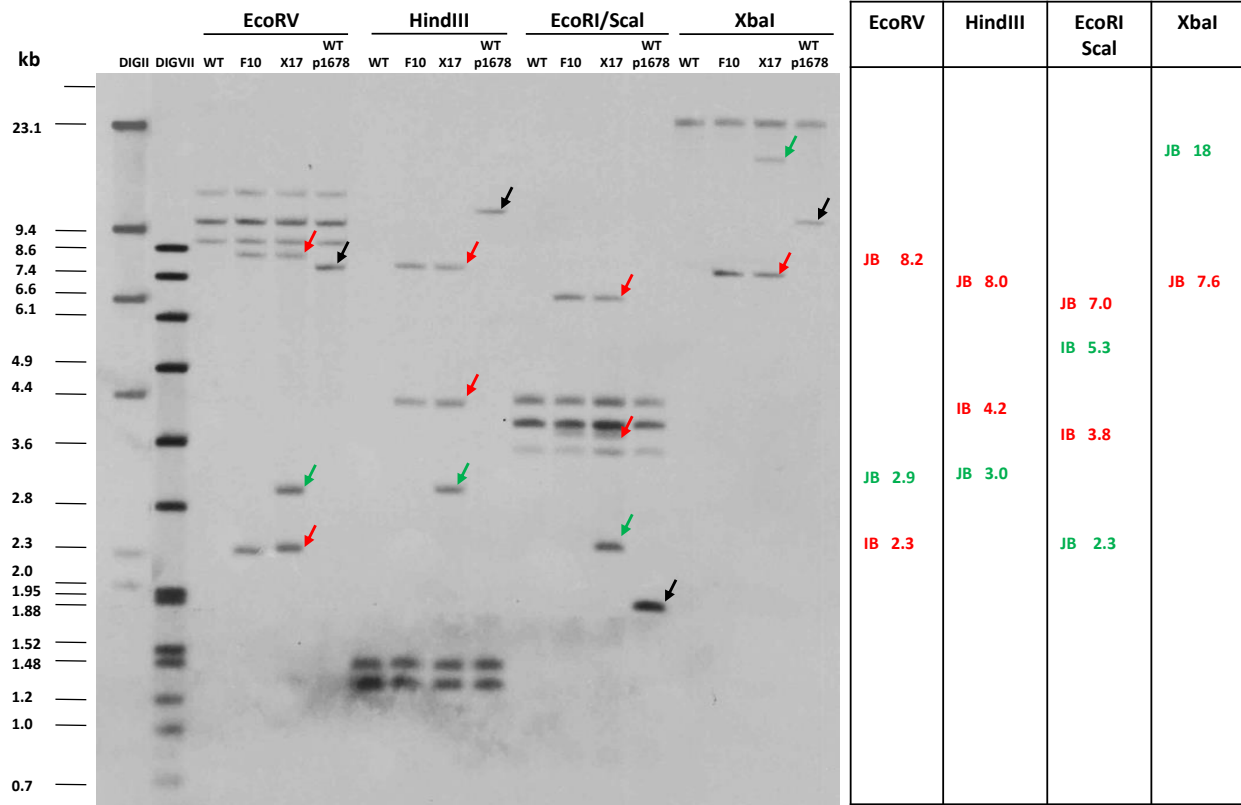


Figure 3-10. Southern Hybridization of Ranger Russet, F10, and X17 Genomic DNA with GBS
Ranger Russet control (WT), F10, X17, and WT spiked with pSIM1678 construct DNA was digested with EcoRV, HindIII, EcoRI/Scal, and XbaI and hybridized with the GBS probe. Size of the DIGII and DIGVII molecular weight markers are indicated adjacent to the blot image. Colored arrows were used to distinguish between any bands associated with the pSIM1278 insert (**red**), the pSIM1678 insert (**green**) and the spiked pSIM1678 (**black**). Estimated sizes of insert-specific bands are indicated in the table. (JB) junction bands, (IB) internal bands.

Probe R1

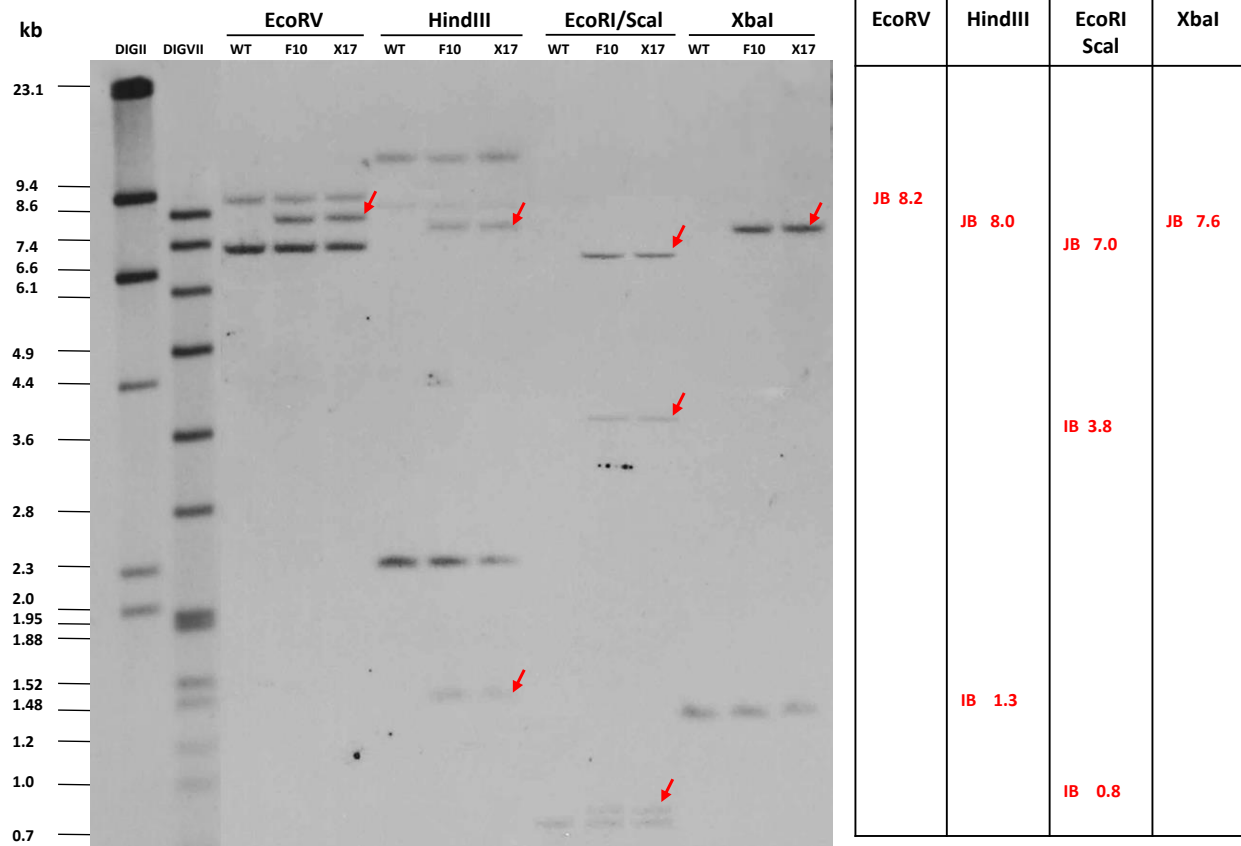


Figure 3-11. Southern Hybridization of Ranger Russet, F10, and X17 Genomic DNA with R1
Ranger Russet control (WT), F10, X17, and WT spiked with pSIM1678 construct DNA was digested with EcoRV, HindIII, EcoRI/Scal, and XbaI and hybridized with the R1 probe. Size of the DIGII and DIGVII molecular weight markers are indicated adjacent to the blot image. Colored arrows were used to distinguish between any bands associated with the pSIM1278 insert (**red**). Estimated sizes of insert-specific bands are indicated in the table. (JB) junction bands, (IB) internal bands.

Because each integration site is unique for each insert, the analysis of junction fragments provides structural information as well as confirmation of a single insertion event. Multiple inserts would result in unexpected numbers of junction bands. EcoRI and XbaI sites in the left flanking region were used to determine the size of the junction bands arising from EcoRI/Scal and XbaI digests (4.0 kb and 3.5 kb, respectively). Both fragments were specifically detected in blots hybridized with ASN and AGP probes (Figure 3-8 and Figure 3-9). Similarly, the right flanking region contained an XbaI restriction site used to predict a 7.6 kb band, which was detected by the four probes as expected (Figure 3-8, Figure 3-9, Figure 3-10, and Figure 3-11). The observation of predicted junction bands provided support for the structure of the pSIM1278 insert as shown in Figure 3-7.

EcoRV, HindIII, EcoRI, and Scal sites were not found in the 1 kb of flanking genomic sequence making the exact size of junction bands from EcoRV, HindIII, or EcoRI/Scal digests unpredictable. Minimum sizes based on known sequence were calculated for these junction bands and corresponding bands were identified by Southern analysis. The two left junction bands associated with EcoRV and HindIII digests were identified by the AGP probe. The measured size of each band (2.6 kb EcoRV and 6.4 kb HindIII) was consistent with expectations (Figure 3-9). Similarly, three fragments associated with the right junction (8.2 kb EcoRV, 8.0 kb HindIII, and 7.0 kb EcoRI/Scal) were detected by the GBS and R1 probes consistent with estimated sizes (Figure 3-10 and Figure 3-11). No unexpected bands were identified that would have indicated additional insertion events. The data indicate that X17 maintains a single, nearly full-length pSIM1278 insert.

3.2.2 pSIM1678 Insert Structure in X17

The structure of the pSIM1678 insert in X17 was determined using the AGP and GBS probes (see green arrows in Figure 3-9 and Figure 3-10), and by analysis of MfeI and SphI digests probed with the pSIM1678 specific probes, VNT and INV. AGP and GBS probes identify pSIM1278 and pSIM1678 inserts containing *Agp* and *Gbss* promoter sequences. The structure of the insert is shown in Figure 3-12.

The junction sequences and 1 kb of flanking genomic DNA was determined by DNA sequencing. The sequences indicated a 7 bp deletion in the pSIM1678 T-DNA LB region and a 23 bp deletion in the RB region. BbsI restriction sites were not identified within the 1 kb of determined sequence.

The structure of the pSIM1678 insert in X17 was determined by Southern analysis to look for internal bands that were predicted from the T-DNA sequence. Bands detected in X17, but not WT or F10, are associated with the pSIM1678 insert. The 2.7 kb HindIII, 5.3 kb EcoRI/Scal, and 4.6 kb XbaI bands were detected using the AGP probe (Figure 3-9). The 4.6 kb XbaI and 5.3 kb EcoRI/Scal bands were detected using the INV probe as expected (Figure 3-13). The INV probe hybridizes to pSIM1678, but not pSIM1278.

The VNT probe was designed to hybridize with the promoter region of *Rpi-vnt1* rather than the coding sequence because the high number of R-gene homologs in potato complicate Southern analysis (see results with probes 1678.2, 1678.3, and 1678.4 in Figure 3-5). The VNT probe binds near the left border making it ideal for detecting left junction bands.

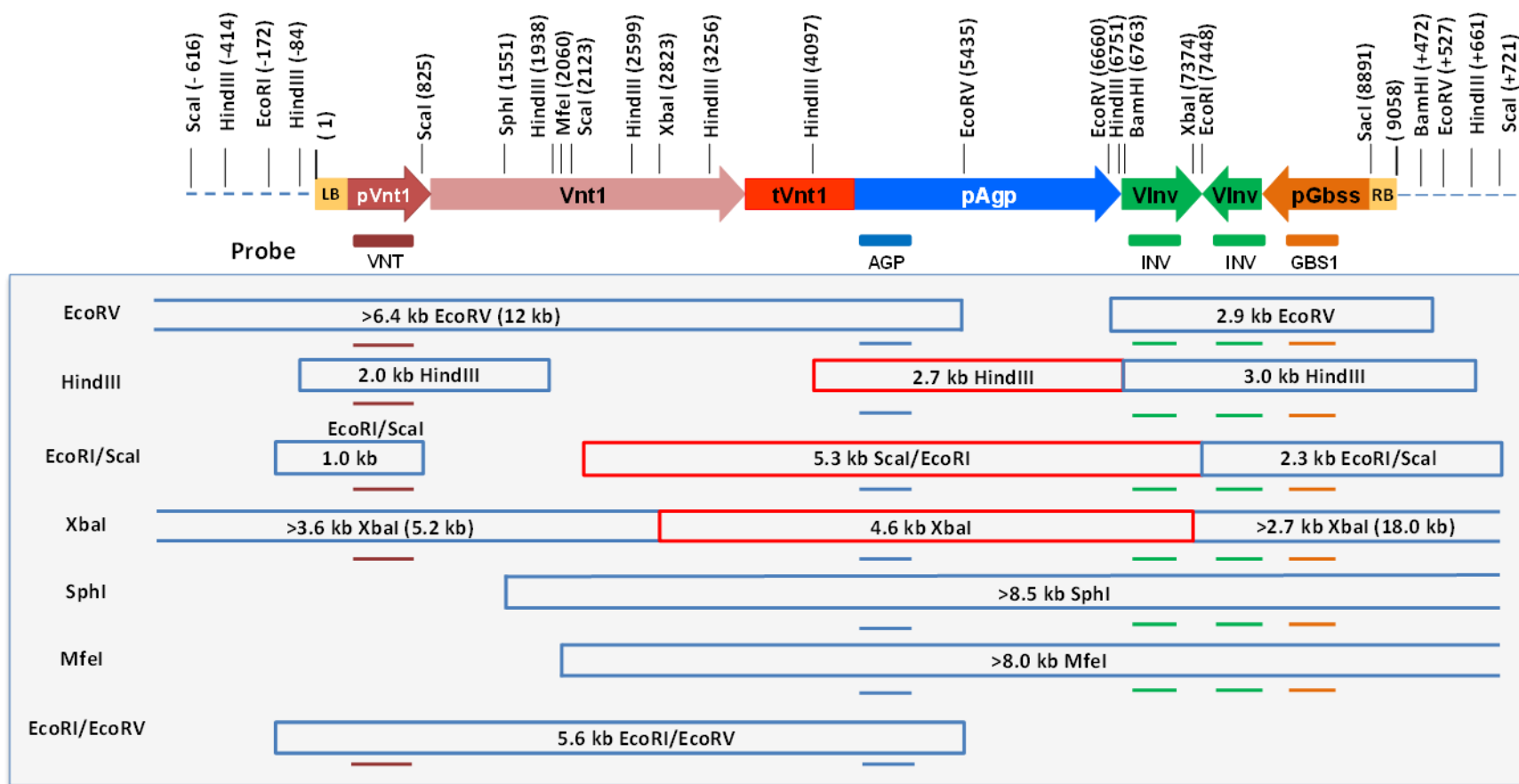


Figure 3-12. Structure of the pSIM1678 Insert in X17 With Digestion Patterns and Probe Binding Sites

The expected digestion products for each restriction enzyme digest are shown as colored boxes with the expected fragment size. Probes are indicated below each fragment with colored lines. Only digest/probe combinations necessary to support the model are shown. All expected probe binding sites are indicated. Red boxes are internal bands (IB) associated with pSIM1678. Blue boxes are junction bands. In some cases, restriction sites in the flanking region were identified and band sizes are predictable, while in other cases, the location of restriction sites and band sizes are unknown. The estimated size of identified junction bands is indicated in parenthesis.

INV Probe

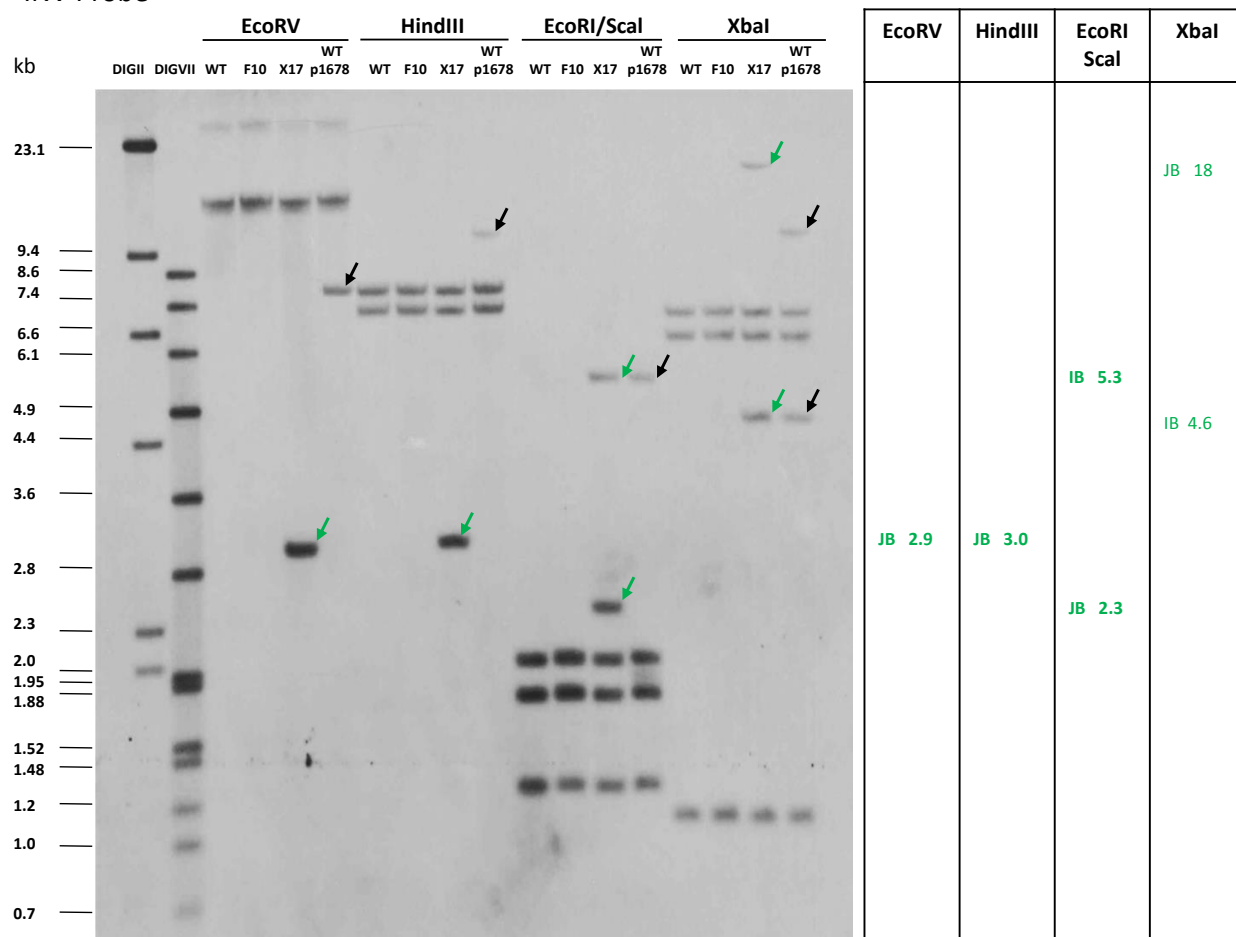


Figure 3-13. Southern Hybridization of Ranger Russet Genomic DNA with INV

Genomic DNA of Ranger Russet control (WT), F10, X17, and WT spiked with pSIM1678 construct DNA was digested with EcoRV, HindIII, EcoRI/Scal, and XbaI and hybridized with the INV probe. Size of the DIGII and DIGVII molecular weight markers are indicated adjacent to the blot image. Colored arrows were used to distinguish between any bands associated with the pSIM1678 insert (**green**) and the spiked pSIM1678 (**black**). Estimated sizes of insert-specific bands are indicated in the table. (JB) junction bands, (IB) internal bands.

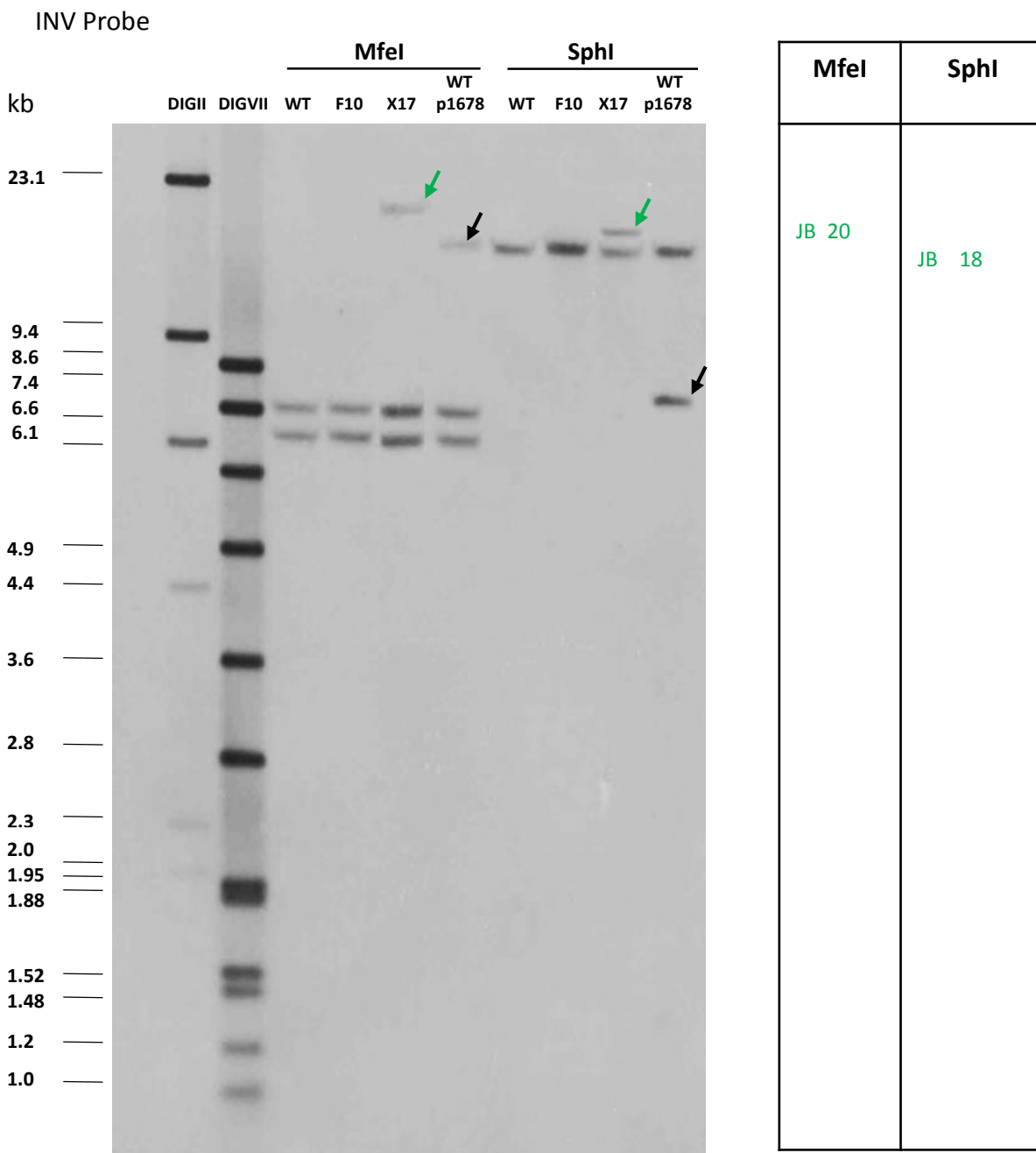


Figure 3-14. Southern Hybridization of Ranger Russet Genomic DNA MfeI and SphI Digest with INV
 Genomic DNA of Ranger Russet control (WT), F10, X17, and WT spiked with pSIM1678 construct DNA was digested with MfeI and SphI and hybridized with the INV probe. Size of the DIGII and DIGVII molecular weight markers are indicated adjacent to the blot image. Colored arrows were used to distinguish between any bands associated with the pSIM1678 insert (**green**) and the spiked pSIM1678 (**black**). Estimated sizes of insert-specific bands are indicated in the table. (JB) junction bands, (IB) internal bands.

The HindIII (2.0 kb) and EcoRI/Scal (1 kb) junction bands, detected by the VNT probe, link the left side of the pSIM1678 insert with flanking sequence, as does the junction bands from EcoRV and XbaI digestion (Figure 3-12). The EcoRV junction band extends into the pSIM1678 insert overlapping all three internal bands (red boxes in Figure 3-12). This EcoRV band was detected by both the AGP and VNT probes (Figure 3-9 and Figure 3-15). DNA sequencing identified an EcoRI site in the flanking region adjacent to the left border. A combined EcoRI/EcoRV digest, probed with VNT, produced a 5.6 kb junction band connecting the insert to a known location in the flanking region (Figure 3-16). The overlap of this 5.6 kb junction band with the pSIM1678 internal bands provide further support for the structure of the left side of the insert.

DNA sequencing identified a number of restriction sites used to characterize the right side of the insert with the INV and GBS probes. Unlike the GBS probe, the INV probe is specific to the pSIM1678 insert. Bands of the expected sizes, 2.9 kb EcoRV and 3.0 kb HindIII, were observed in blots probed with INV (Figure 3-13). The XbaI and EcoRI/Scal digests bisect the VInv cassette resulting in an internal band and a junction band for each digest. The observed 5.3 kb IB and 2.3 kb JB EcoRI/Scal and 4.6 kb IB and 18 kb JB XbaI bands confirm the presence of a complete copy of the VInv inverted repeat at the right side of the insert (Figure 3-13). These junction bands were also detected using the GBS probe (Figure 3-10). Additional digests with SphI and MfeI provide support for the structure of the right side of the insert. The expected bands extending from the *Rpi-vnt1* gene to the right flanking region were detected by the INV probe (Figure 3-14). The absence of unexpected bands indicates that pSIM1678 was inserted at a single site in the genome. The data indicate that X17 consists of a single, nearly full-length insert from pSIM1678.

VNT Probe

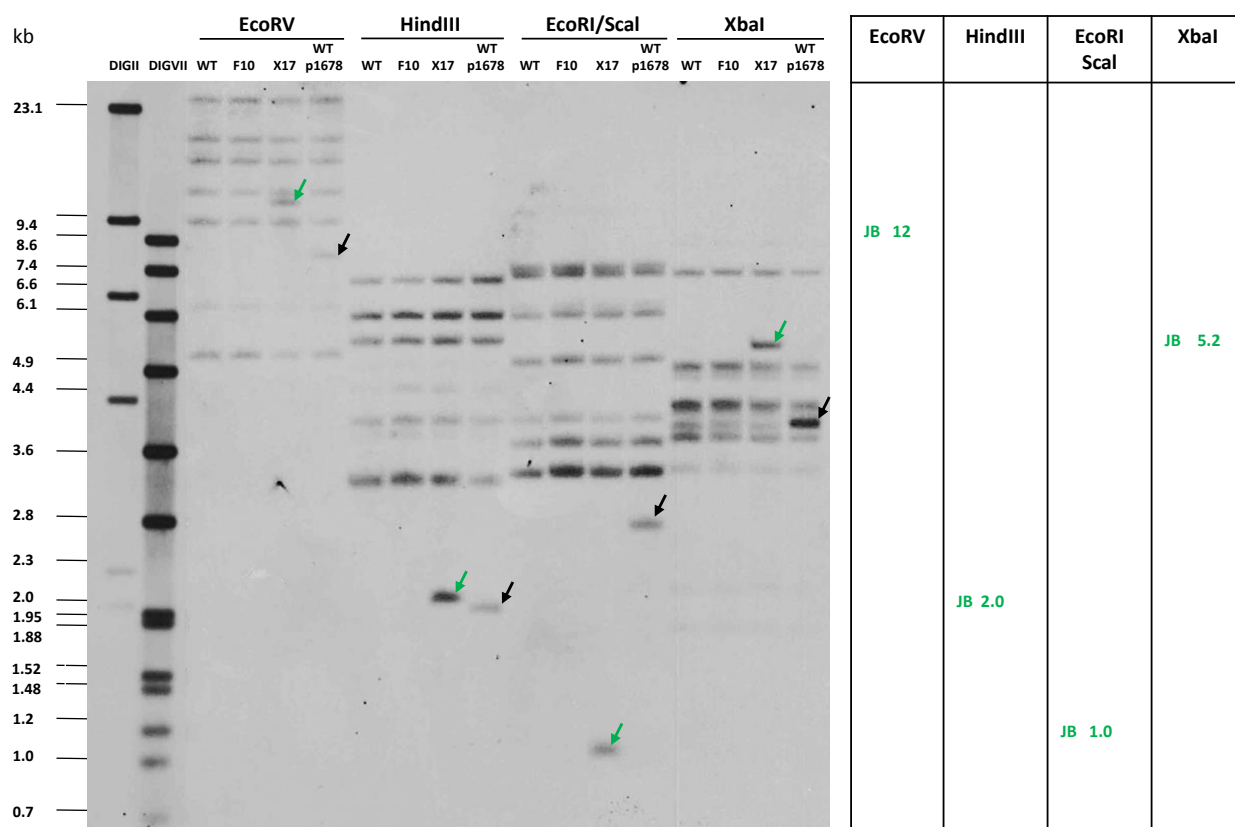


Figure 3-15. Southern Hybridization of Ranger Russet Genomic DNA with VNT

Genomic DNA of Ranger Russet control (WT), F10, X17, and WT spiked with pSIM1678 construct DNA was digested with EcoRV, HindIII, EcoRI/Scal, and XbaI and hybridized with the VNT probe. Size of the DIGII and DIGVII molecular weight markers are indicated adjacent to the blot image. Colored arrows were used to distinguish between any bands associated with the pSIM1678 insert (**green**) and the spiked pSIM1678 (**black**). Estimated sizes of insert-specific bands are indicated in the table. (JB) junction bands, (IB) internal bands.

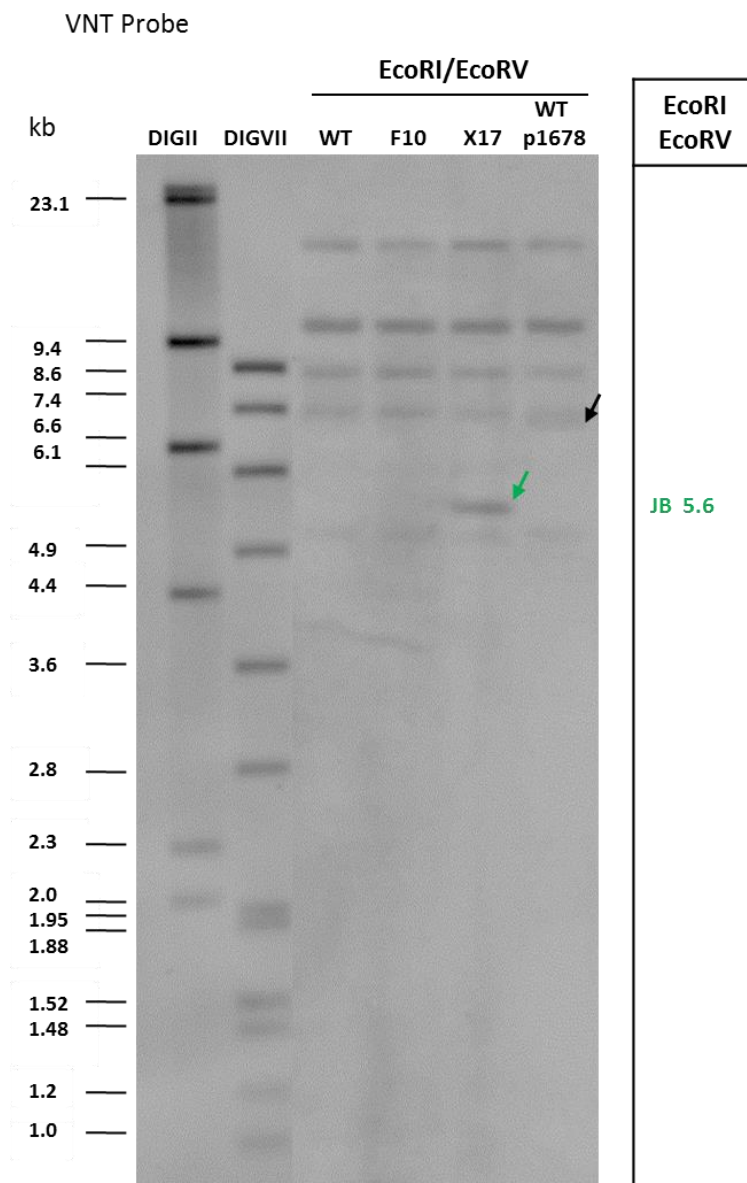


Figure 3-16. Southern Analysis of EcoRI/EcoRV Digested Genomic DNA with VNT

Genomic DNA of Ranger Russet control (WT), F10, X17, and WT spiked with pSIM1678 construct DNA was digested with EcoRI/EcoRV and hybridized with the VNT probe. Size of the DIGII and DIGVII molecular weight markers are indicated adjacent to the blot image. Colored arrows were used to distinguish between any bands associated with the pSIM1678 insert (**green**) and the spiked pSIM1678 (**black**). Estimated sizes of insert-specific bands are indicated in the table. (JB) junction bands, (IB) internal bands.

3.2.3 pSIM1278 Insert Structure in Y9

Insertion analysis (Section 3.1) demonstrated that the pSIM1278 insert was contained within an approximately 20 kb BbsI digestion fragment. Junction sequences were determined by DNA sequencing using a combination of Sanger and Illumina Hi-Seq Next Generation Sequencing (NGS) (Layne et al., 2015b). The left side of the insert consists of pAGP sequence joining the plant genome as indicated in Figure 3-17. The pAGP sequence is truncated and not a functional promoter (Layne et al., 2015b). The right side of the insert consists of a partial PhL/R1 cassette (see Figure 3-17). Several restriction sites identified in the 1 kb of flanking sequence were used in the Southern analyses of the insert structure.

Y9 genomic DNA was digested with several restriction enzymes including: (1) EcoRV, (2) EcoRI/Scal, (3) HindIII, (4) XbaI, (5) EcoRI/SacI, (6) HindIII/SacI, (7) XbaI/SacI, (8) PaeI, (9) EcoRI/PaeI, (10) HindIII/PaeI, (11) XbaI/PaeI, and (12) SacI and probed with AGP, ASN, GBS1, GBS2, and R1 probes. Figure 3-17 shows the structure of the Y9 pSIM1278 insert and highlights the expected internal and junction bands that were observed in the Southern analysis. The structure of the pSIM1278 insert is described separately as left, middle, and right sections.

WT samples were spiked with pSIM1678, prior to digestion, at a concentration of a single copy per genome equivalent and were used as a control to show that the probes were sensitive enough to detect a single insert copy in the genome. J3 samples contain only the pSIM1278 insert and were used as a control in the characterization of Y9 to distinguish between bands arising from pSIM1278 or pSIM1678 sequences. Bands in common between J3 and Y9 are related to the pSIM1278 insert, and bands unique to Y9 are from pSIM1678.

Structure of the Middle Section

The middle section of the insert is shown in Figure 3-17 and consists of a nearly full-length pSIM1278 T-DNA comprised of Asn1/Ppo5 and PhL/R1 cassettes flanked by the *pAgp* and *pGbss* promoters. Observations of all expected internal bands from the middle section of the insert confirm the presence of a nearly full-length T-DNA. Several different digestions were performed in generating the internal bands including: EcoRV (0.7 kb and 2.3 kb), EcoRI/Scal (3.8 kb and 0.8 kb), EcoRI/SacI (6.2 kb), HindIII/SacI (2.0 kb), HindIII (4.2 kb and 1.3 kb), and XbaI/SacI (6.9 kb).

The 0.7 kb and 2.3 kb EcoRV bands were observed in blots probed with ASN (Figure 3-18). The 2.3 kb EcoRV band was also detected using the GBS1 and AGP probes (Figure 3-19 and Figure 3-20). The 3.8 kb EcoRI/Scal band was detected by the GBS1, AGP, and R1 probes (Figure 3-19, Figure 3-20, and Figure 3-21). A high band intensity observed for the 3.8 kb EcoRI/Scal band in the GBS1 and R1 blots suggests that an additional 3.8 kb band, which was identified in the right section of the insert, resulted from Scal digestions. The 0.8 kb Scal band was detected using the R1 probe only (Figure 3-21).

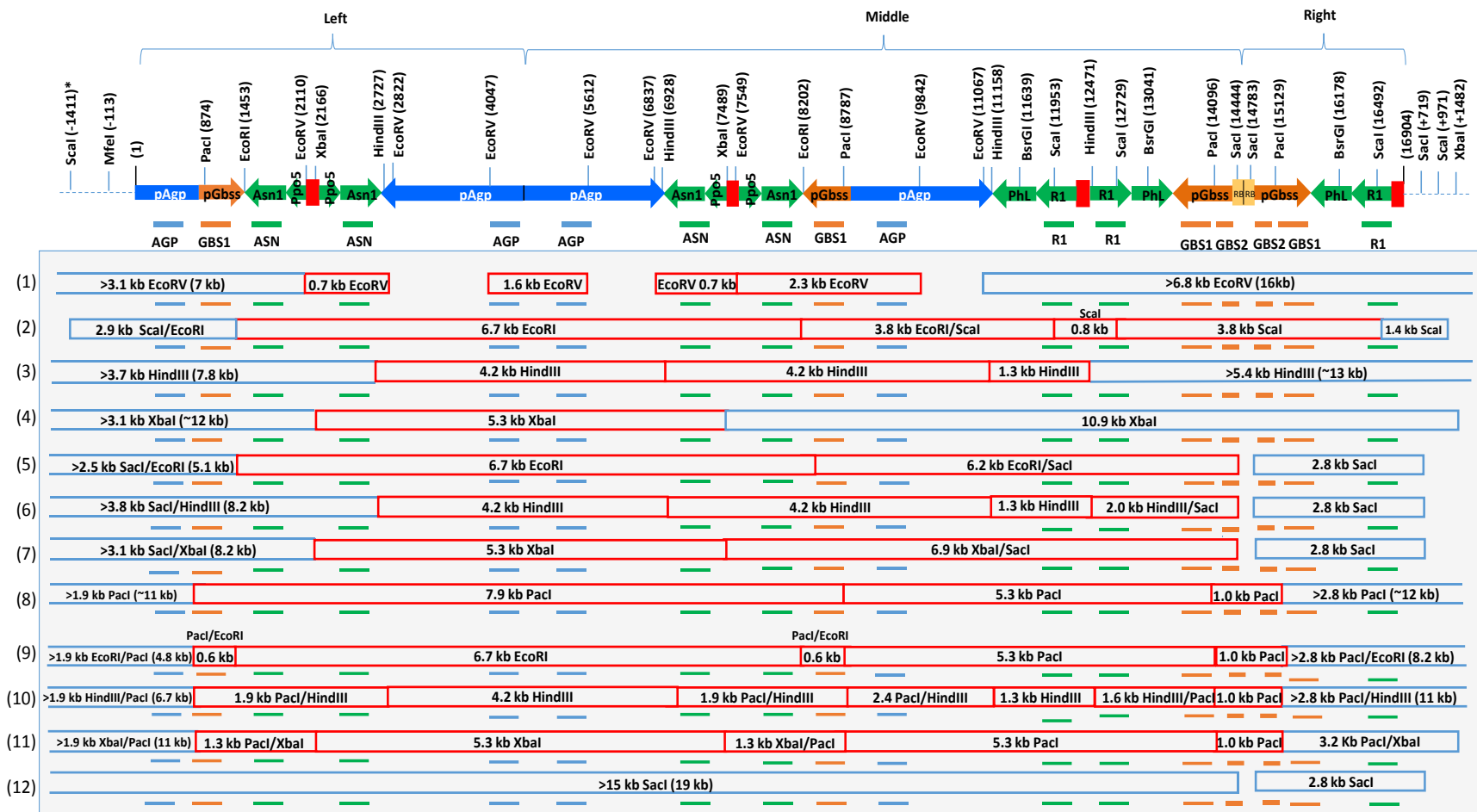


Figure 3-17. Structure of the pSIM1278 Insert in Y9.

The digestion products and sizes are shown. Red boxes are internal bands. Blue boxes are junction bands of known or unknown size. Probes detecting each digestion product are indicated with colored lines. Only digest/probe combinations necessary to support the model are shown. Restriction digests: 1) EcoRV, (2) EcoRI/Scal, (3) HindIII, (4) XbaI, (5) EcoRI/SacI, (6) HindIII/SacI, (7) XbaI/SacI, (8) PacI, (9) EcoRI/PacI, (10) HindIII/PacI, (11) XbaI/PacI, and (12) SacI. *The location of the Scal site in the flanking sequence was determined from the reference genome available at MSU (<http://potato.plantbiology.msu.edu>).

The 6.2 kb EcoRI/SacI band was observed in AGP probed blots and extends from the Asn1/Ppo5 inverted repeat/pGbss junction on the left into the RB region (compare Figure 3-17 and Figure 3-22). The 6.9 kb XbaI/SacI band was observed in AGP and GBS1 blots (Figure 3-23 and Figure 3-25). As expected, this 6.9 kb band had high intensity when probed with GBS1 due to two binding sites (compare Figure 3-17 and Figure 3-35). The 2.0 kb HindIII/SacI band that overlaps with the EcoRI/SacI digestion products was observed using the GBS1 probe (Figure 3-24). The 4.2 kb HindIII band was observed on ASN, GBS1, and AGP probed blots (Figure 3-18, Figure 3-19, and Figure 3-20). The high intensity of the 4.2 kb HindIII band indicated the presence of additional HindIII digestion products and suggested that additional pAGP elements existed in the insert. The 1.3 kb HindIII band was only observed using the R1 probe (Figure 3-21).

The observation of expected internal bands in the middle section of the insert establish the presence of a nearly full-length pSIM1278 T-DNA. As mentioned, the presence of high intensity bands indicated the insert contained additional copies of pSIM1278 elements. The location and direction of these elements were elucidated using a combination of enzyme digests and Southern blot and DNA sequencing analyses. The following sections describing the analysis of the left and right junction bands provides empirical support for the structure presented in Figure 3-17, with a second Asn1/Ppo5 cassette on the left side and a partial PhL/R1 cassette on the right side.

Structure of the Left Section

The increased band intensity observed for the 4.2 kb HindIII band hybridized with the AGP probe indicated a second fragment of similar size was contained within the insert. The fragment was shown to connect the left and middle sections of the insert. The two inverted copies of the pAGP promoter that make up the fragment were confirmed by DNA sequencing (Layne et al., 2015b). The sequencing analysis also predicted a 1.6 kb EcoRV band detectable using the AGP probe (Figure 3-20). The 4.2 kb HindIII and 1.6 kb EcoRV bands covering the left/middle internal junction were confirmed by a number of larger digestion products. The 5.3 kb XbaI and 6.7 kb EcoRI bands were detected when hybridized with the AGP probe (Figure 3-20), and the 7.9 kb PaeI band was detected on AGP and GBS1 probed blots (Figure 3-22 and Figure 3-24).

The band intensity of the 7.9 kb PaeI band observed with the GBS1 probe indicated a second copy of the *Gbss* promoter. Similarly, increased band intensity observed for the 0.6 kb PaeI/EcoRI band corresponds to the *Gbss* promoter adjacent to the Asn1/Ppo5 inverted repeat (Figure 3-25). DNA sequencing confirmed the structure of the left side, including a second Asn1/Ppo5 cassette connected to the plant genome through a truncated, nonfunctional pAGP element (Layne et al., 2015b). A single junction band was detected in all Southern blots hybridized with the AGP probe supporting the conclusion from Section 3.1 of a single pSIM1278 insertion locus (compare Figure 3-17 to Figure 3-20, Figure 3-22, and Figure 3-23). Importantly, the 2.9 kb EcoRI/Scal band observed with the GBS1 and AGP probes connected the insert to a predicted location in the plant genome (Figure 3-19 and Figure 3-20).

Structure of the Right Section

The presence of a partial copy of the PhL/R1 inverted repeat in the right section was suggested by the EcoRI/Scal digest hybridized with the R1 probe (Figure 3-21). A single copy of the inverted repeat should have resulted in three fragments. Two internal bands (3.8 and 0.8 kb) plus a single junction band were observed, however, the high intensity of the 3.8 kb band indicated the presence of a fourth fragment (Figure 3-21). High intensity was also seen with the 16 kb EcoRV junction band suggesting the presence of more than one copy of the PhL/R1 inverted repeat (Figure 3-21). Because the 0.8 kb Scal band was not observed to have high intensity, the second copy of the PhL/R1 inverted repeat appeared to be truncated (Figure 3-21). This hypothesis was confirmed by sequencing of the right section (Layne et al., 2015b). The right section consists of a partial PhL/R1 inverted repeat with a junction between a truncated Spacer 2 element and the plant genome (Figure 3-17). A number of restriction sites (i.e. SacI, Scal, and XbaI) were identified in the right flanking region and used to confirm the structure of the right section of the pSIM1278 insert.

The Scal restriction site located in the right flanking region was used to demonstrate that the 1.4 kb EcoRI/Scal band was the right junction band (Figure 3-17). This observation confirmed the presence of a partial PhL/R1 cassette on the right side. Illumina Hi-Seq Next Generation Sequencing (NGS) confirmed that an inverted repeat of the RB region made up the junction between the middle and right sections (Layne et al., 2015b). The 2.8 kb SacI and 3.2 kb PacI/XbaI bands detected by the GBS1 probe connected the right section to the flanking region together with different digests that generated single junction bands detected by the GBS1 probe (compare Figure 3-17 to Figure 3-19, Figure 3-24, and Figure 3-25).

A 1.0 kb PacI band covering the junction between the middle and right sections was observed (Figure 3-26). The GBS1 probe does not hybridize to this region of the long form of the *pGbss* element and a second probe, called GBS2, was designed to be specific to this region. As shown in Figure 5-26, a 1.0 kb PacI band (red arrows) was observed as expected.

[illegible]

Genomic DNA of Atlantic control (WT), J3, and Y9 was digested with EcoRV, HindIII, and EcoRI/ScaI and hybridized with the ASN probe. Size of the DIGII and DIGVII molecular weight markers are indicated adjacent to the blot image. Colored arrows were used to distinguish between any bands associated with the pSIM1278 insert (**red**). Estimated sizes of insert-specific bands are indicated in the table. *Indicates fragment with multiple binding probe hybridization sites. **Indicates multiple fragments of the same size. (JB) junction bands, (IB) internal bands.

Probe GBS1

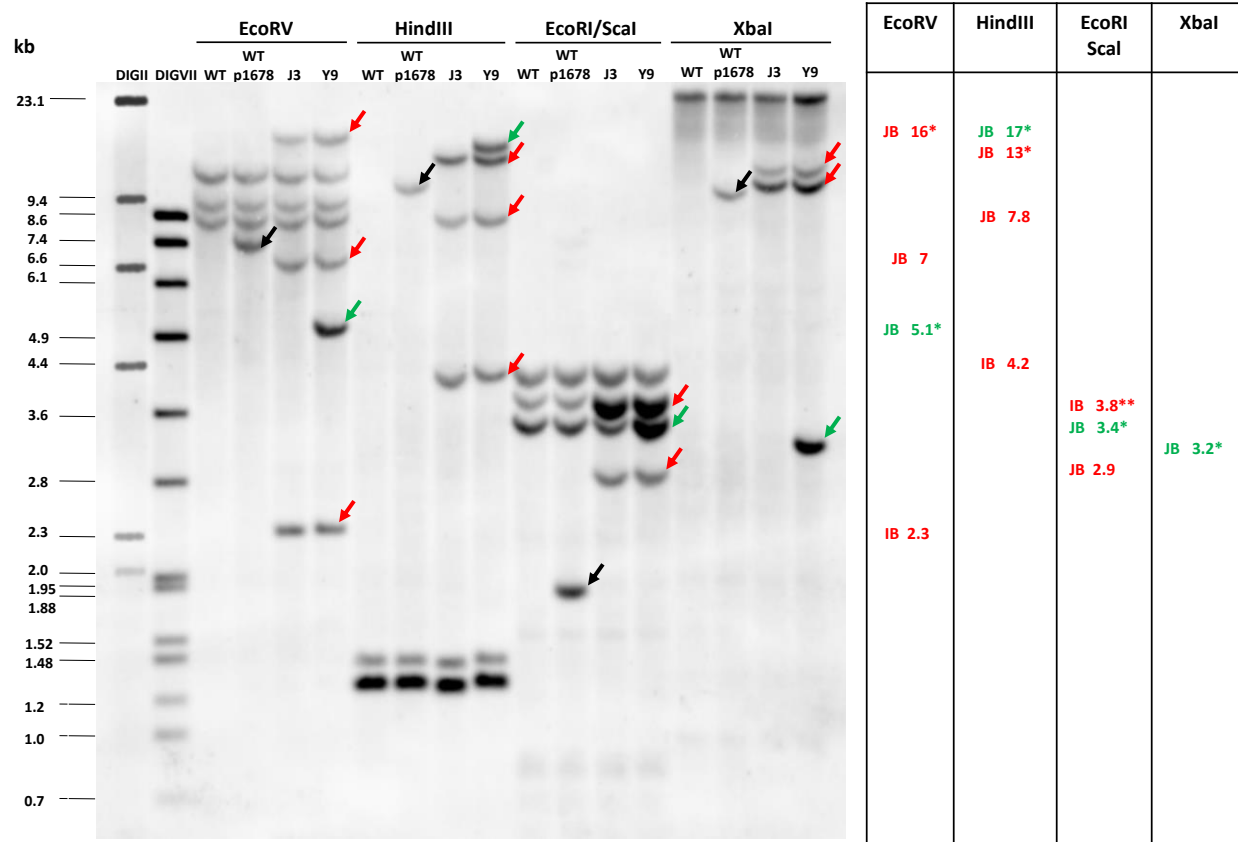


Figure 3-19. Southern Hybridization of Atlantic, J3, and Y9 Genomic DNA with GBS1

Genomic DNA of Atlantic control (WT), J3, Y9, and WT spiked with pSIM1678 construct DNA was digested with EcoRV, HindIII, EcoRI/Scal, and XbaI and hybridized with the GBS1 probe. Size of the DIGII and DIGVII molecular weight markers are indicated adjacent to the blot image. Colored arrows were used to distinguish between any bands associated with the pSIM1278 insert (**red**), the pSIM1678 insert (**green**) and the spiked pSIM1678 (**black**). Estimated sizes of insert-specific bands are indicated in the table. The construct bands are used to show that probes can detect a single insert in the genome and provide a size comparison for internal bands contained within the boundary of the T-DNA. *Indicates fragment with multiple binding probe hybridization sites. **Indicates multiple fragments of the same size. (JB) junction bands, (IB) internal bands.

Probe AGP

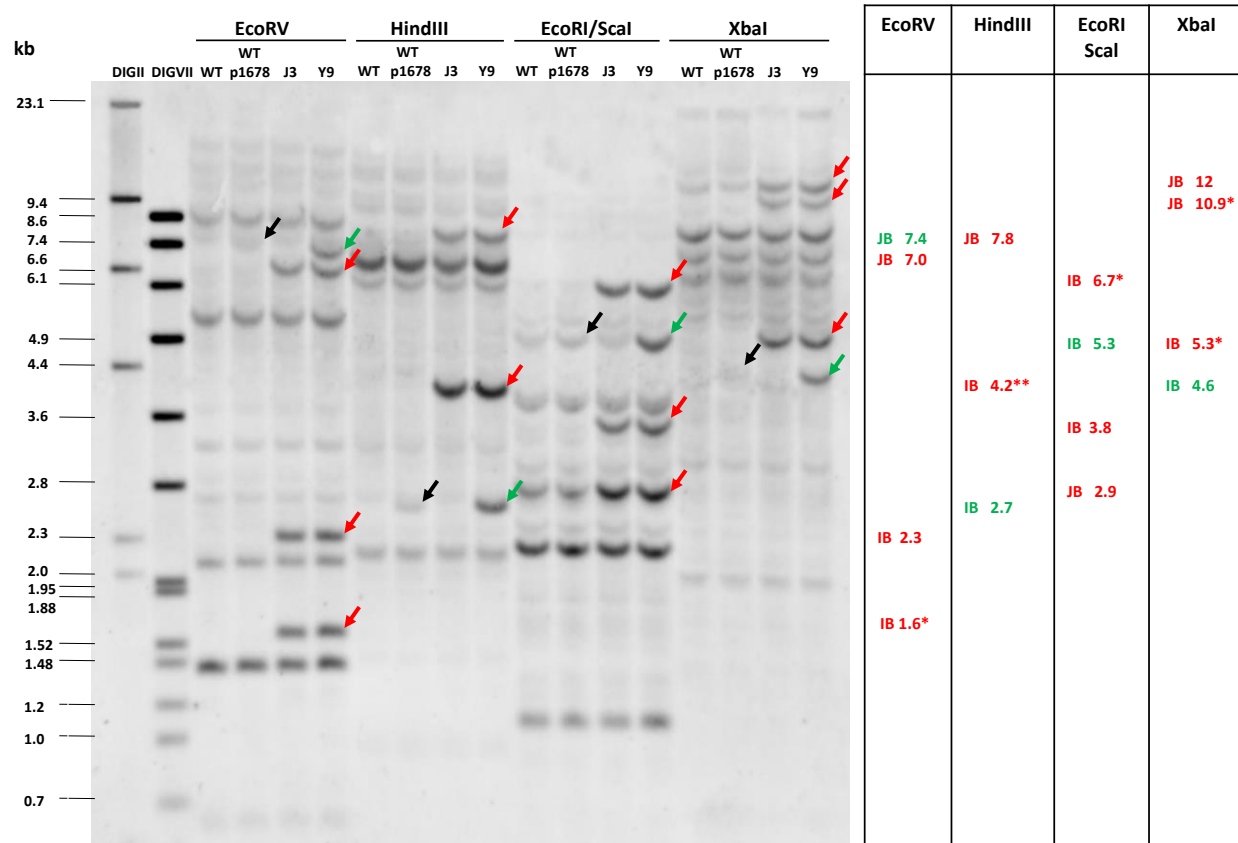


Figure 3-20. Southern Hybridization of Atlantic, J3, and Y9 Genomic DNA with AGP

Genomic DNA of Atlantic control (WT), J3, Y9, and WT spiked with pSIM1678 construct DNA was digested with EcoRV, HindIII, EcoRI/Scal, and XbaI and hybridized with the AGP probe. Size of the DIGII and DIGVII molecular weight markers are indicated adjacent to the blot image. Colored arrows were used to distinguish between any bands associated with the pSIM1278 insert (**red**), the pSIM1678 insert (**green**) and the spiked pSIM1678 (**black**). Estimated sizes of insert-specific bands are indicated in the table. The construct bands are used to show that probes can detect a single insert in the genome and provide a size comparison for internal bands contained within the boundary of the T-DNA. *Indicates fragment with multiple binding probe hybridization sites. **Indicates multiple fragments of the same size. (JB) junction bands, (IB) internal bands.

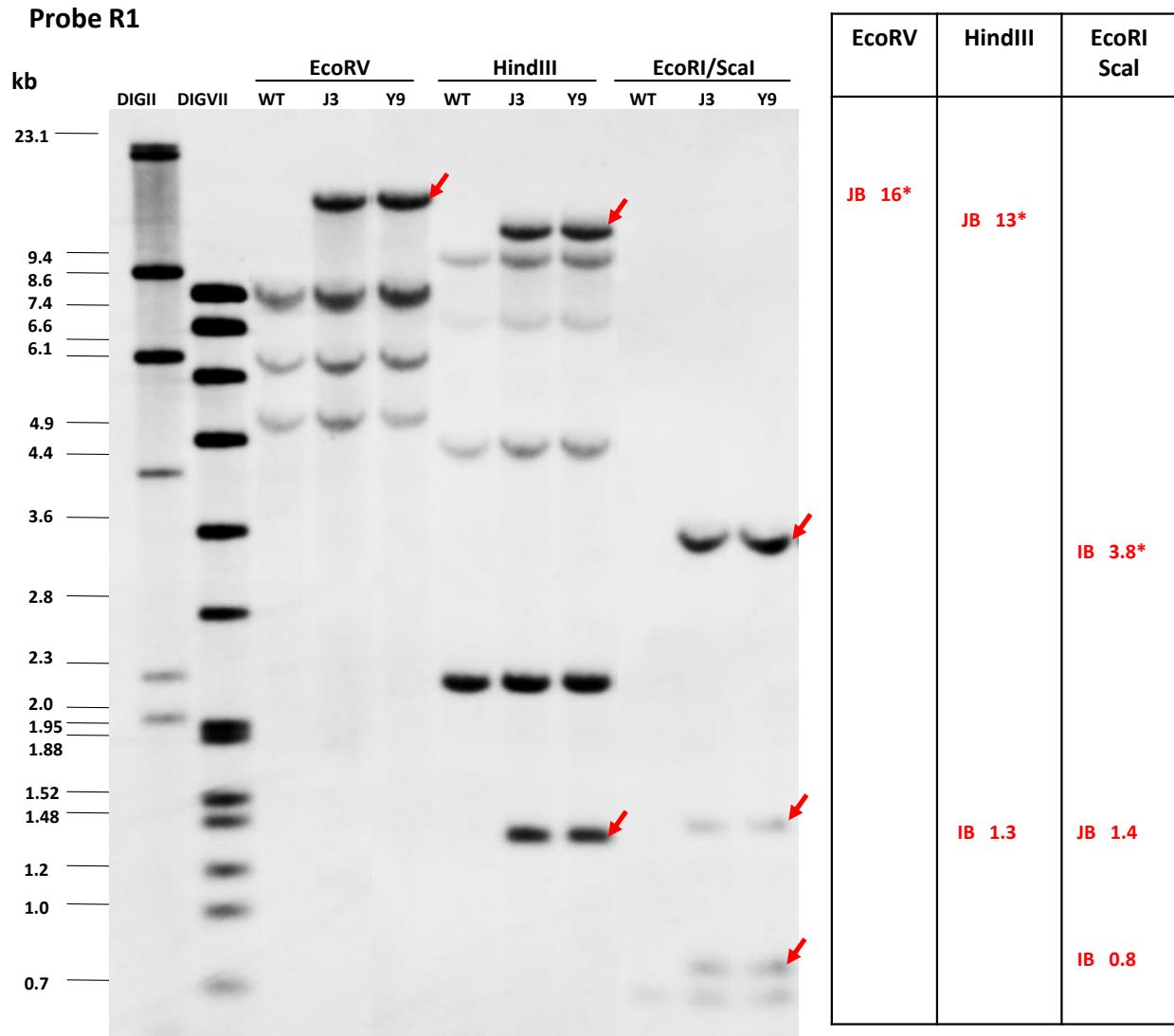


Figure 3-21. Southern Hybridization of Atlantic, J3, and Y9 Genomic DNA with R1

Genomic DNA of Atlantic control (WT), J3, and Y9 was digested with EcoRV, HindIII, and EcoRI/Scal and hybridized with the R1 probe. Size of the DIGII and DIGVII molecular weight markers are indicated adjacent to the blot image. Colored arrows were used to distinguish between any bands associated with the pSIM1278 insert (**red**). Estimated sizes of insert-specific bands are indicated in the table. *Indicates fragment with multiple binding probe hybridization sites. (JB) junction bands, (IB) internal bands.

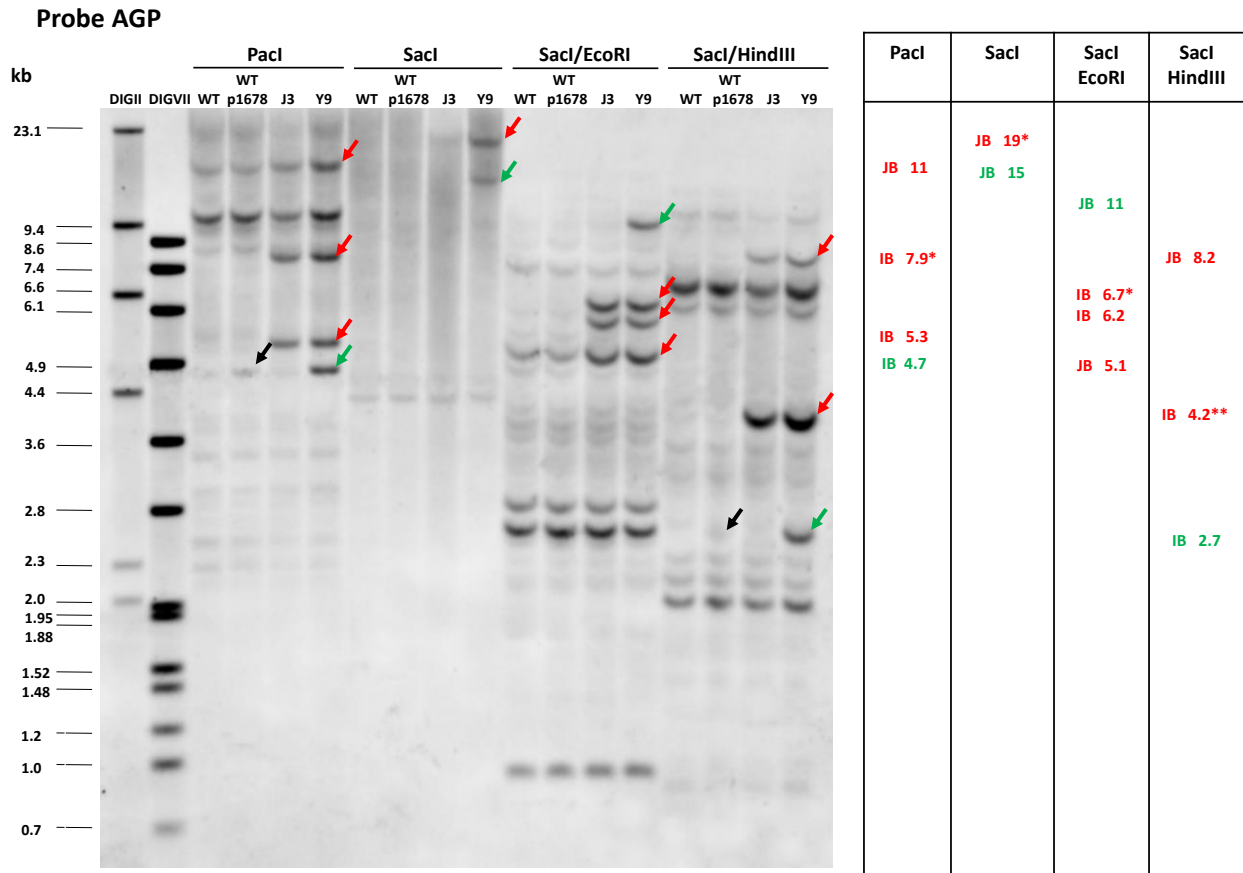


Figure 3-22. Southern Hybridization of Atlantic, J3, and Y9 Genomic DNA after PacI Digest with AGP
 Genomic DNA of Atlantic control (WT), J3, Y9, and WT spiked with pSIM1678 construct DNA was digested with PacI, SacI, SacI/EcoRI and SacI/HindIII and hybridized with the AGP probe. Size of the DIGII and DIGVII molecular weight markers are indicated adjacent to the blot image. Colored arrows were used to distinguish between any bands associated with the pSIM1278 insert (**red**), the pSIM1678 insert (**green**) and the spiked pSIM1678 (**black**). Estimated sizes of insert-specific bands are indicated in the table. The construct bands are used to show that probes can detect a single insert in the genome and provide a size comparison for internal bands contained within the boundary of the T-DNA. *Indicates fragment with multiple binding probe hybridization sites. **Indicates multiple fragments of the same size. (JB) junction bands, (IB) internal bands.

Probe AGP

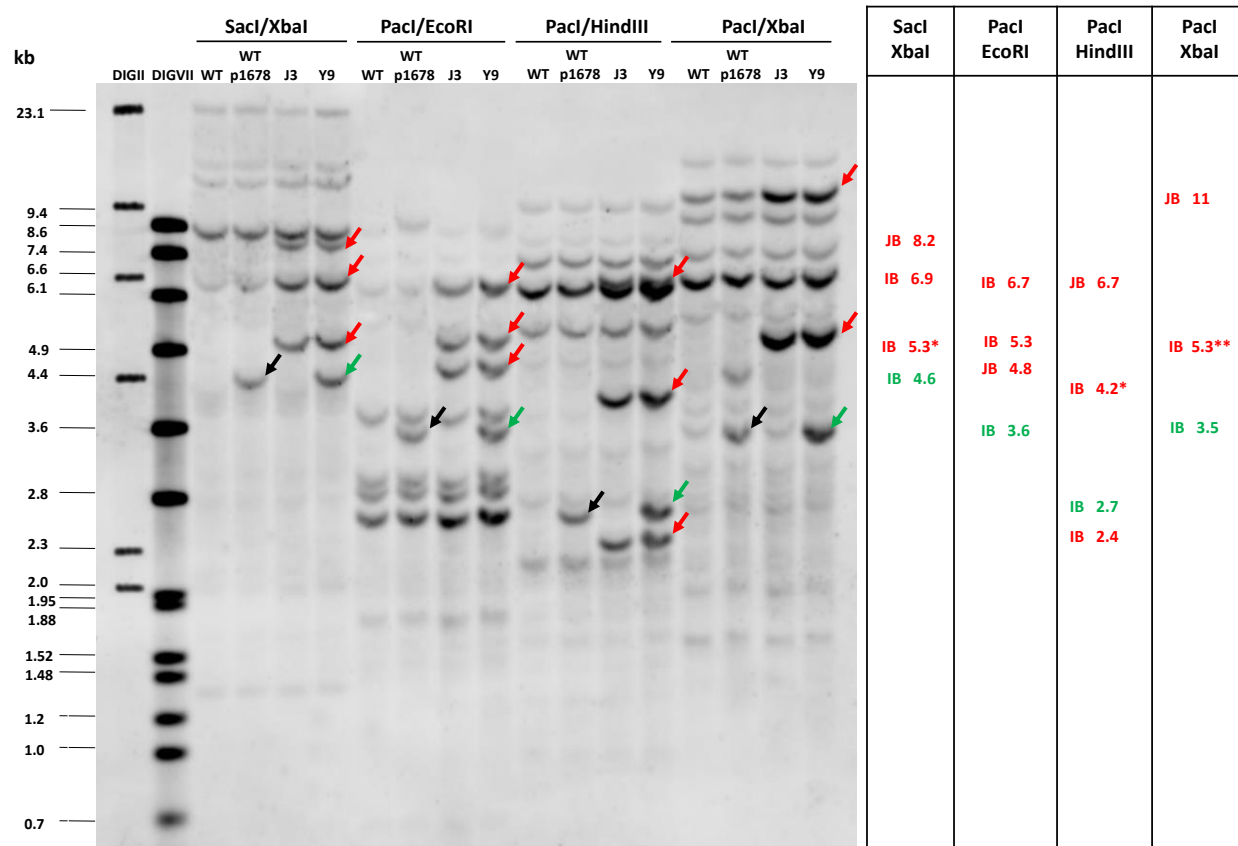


Figure 3-23. Southern of Atlantic, J3, and Y9 SacI/XbaI Digested Genomic DNA with AGP

Genomic DNA of Atlantic control (WT), J3, Y9, and WT spiked with pSIM1678 construct DNA was digested with SacI/XbaI, PacI/EcoRI, PacI/HindIII, and PacI/XbaI and hybridized with the AGP probe. Size of the DIGII and DIGVII molecular weight markers are indicated adjacent to the blot image. Colored arrows were used to distinguish between any bands associated with the pSIM1278 insert (**red**), the pSIM1678 insert (**green**) and the spiked pSIM1678 (**black**). Estimated sizes of insert-specific bands are indicated in the table. The construct bands are used to show that probes can detect a single insert in the genome and provide a size comparison for internal bands contained within the boundary of the T-DNA. *Indicates fragment with multiple binding probe hybridization sites. **Indicates multiple fragments of the same size. (JB) junction bands, (IB) internal bands.

Probe GBS1

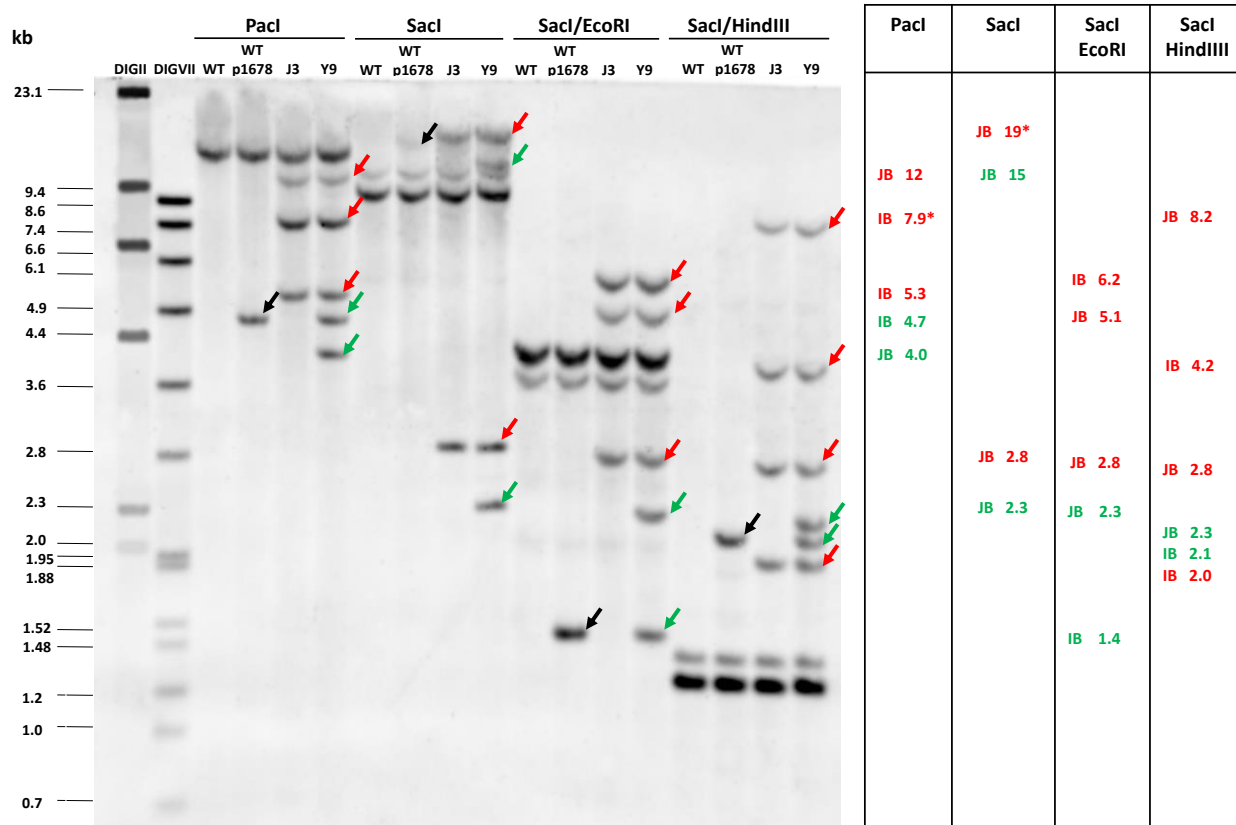


Figure 3-24. Southern Hybridization of Atlantic, J3, and Y9 Genomic DNA after PacI Digest with GBS1
 Genomic DNA of Atlantic control (WT), J3, Y9, and WT spiked with pSIM1678 construct DNA was digested with PacI, SacI, SacI/EcoRI and SacI/HindIII and hybridized with the GBS1 probe. Size of the DIGII and DIGVII molecular weight markers are indicated adjacent to the blot image. Colored arrows were used to distinguish between any bands associated with the pSIM1278 insert (**red**), the pSIM1678 insert (**green**) and the spiked pSIM1678 (**black**). Estimated sizes of insert-specific bands are indicated in the table. The construct bands are used to show that probes can detect a single insert in the genome and provide a size comparison for internal bands contained within the boundary of the T-DNA. *Indicates fragment with multiple binding probe hybridization sites. (JB) junction bands, (IB) internal bands.

Probe GBS1

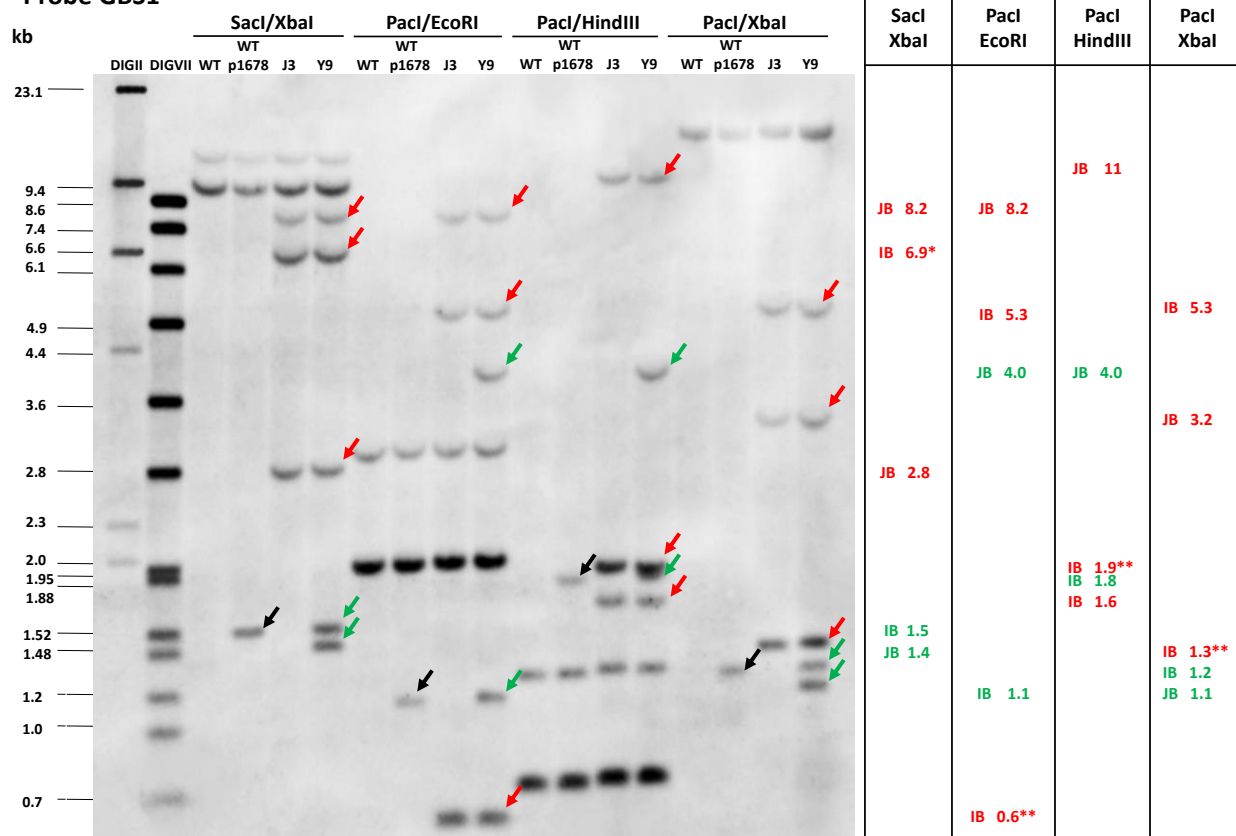


Figure 3-25. Southern of Atlantic, J3, and Y9 SacI/XbaI Digested Genomic DNA with GBS1

Genomic DNA of Atlantic control (WT), J3, Y9, and WT spiked with pSIM1678 construct DNA was digested with SacI/XbaI, PacI/EcoRI, PacI/HindIII, and PacI/XbaI and hybridized with the GBS1 probe. Size of the DIGII and DIGVII molecular weight markers are indicated adjacent to the blot image. Colored arrows were used to distinguish between any bands associated with the pSIM1278 insert (**red**), the pSIM1678 insert (**green**) and the spiked pSIM1678 (**black**). Estimated sizes of insert-specific bands are indicated in the table. The construct bands are used to show that probes can detect a single insert in the genome and provide a size comparison for internal bands contained within the boundary of the T-DNA. *Indicates fragment with multiple binding probe hybridization sites. **Indicates multiple fragments of the same size. (JB) junction bands, (IB) internal bands.

[illegible]

Genomic DNA of Atlantic control (WT), J3, and Y9 was digested with PacI/EcoRI, PacI/HindIII, and PacI/XbaI and hybridized with the GBS2 probe. Size of the DIGII and DIGVII molecular weight markers are indicated adjacent to the blot image. Colored arrows were used to distinguish between any bands associated with the pSIM1278 insert (red), the pSIM1678 insert (green). Estimated sizes of insert-specific bands are indicated in the table. *Indicates fragment with multiple binding probe hybridization sites. (JB) junction bands, (IB) internal bands.

3.2.4 pSIM1678 Insert Structure in Y9

The pSIM1678 insert consists of a nearly full-length T-DNA flanked by a partial VInv cassette on the right side (Figure 3-27). The junctions between the pSIM1678 insert and the plant genome were determined through a combination of Sanger and Illumina Hi-Seq NGS (Layne et al., 2015b). The left junction of the insert connected a truncated *Rpi-vnt1* promoter (pVnt1) with the genome and the right junction connected sequence from the VInv cassette to the plant genome. From the sequence, several restriction sites were identified and used in the structural analysis.

Southern analysis was used to characterize the pSIM1678 insert structure. Two new probes (i.e. VNT and INV), in addition to the GBS1, GBS2, and AGP probes used for pSIM1278, allowed detection of the pSIM1678 insert. The VNT probe hybridizes to the *Rpi-vnt1* promoter located near the left border of the pSIM1678 T-DNA. Probes hybridizing to the Vnt1 coding sequence were not used in structural analysis as a high number of homologous potato genes make data interpretation difficult.

Y9 genomic DNA was digested with several different restriction enzymes including: HindIII (2.7 kb), EcoRI/Scal (5.3 kb), PaeI (4.7 kb), and XbaI/SacI (4.6 kb and 1.5 kb) and probed for internal fragments within the boundaries of the T-DNA for confirmation of the insert structure.

Southern analysis of the pSIM1678 insert confirmed the presence and size of each of the internal bands. All four digests produced fragments unique to the Y9 sample that were detected by the AGP probe. As expected, the 2.7 kb HindIII band was only detected by the AGP probe (Figure 3-20, Figure 3-22, and Figure 3-23). The 5.3 kb EcoRI/Scal, 4.7 kb PaeI, and 4.6 kb XbaI bands were detected by both the AGP probe (Figure 3-20, Figure 3-22, and Figure 3-23) and the INV probe (Figure 3-30, Figure 3-31, and Figure 3-32). In addition, the 1.5 kb XbaI/SacI fragment corresponding to the right side of the T-DNA was detected by the GBS1 and INV probes (Figure 3-25 and Figure 3-32). These overlapping internal bands cover the length of the T-DNA except for the left end containing the pVnt1 element. The 4.4 kb PaeI/XbaI and the 5.4 kb PaeI/EcoRI fragments detected by the VNT probe (Figure 3-29) overlap the 5.3 kb EcoRI/Scal internal band and extend into the flanking region to a predicted PaeI site as shown in Figure 3-27. The Southern and DNA sequencing analysis indicate the pSIM1678 insert contains a nearly full-length T-DNA with a deletion of the LB region and a small region at the 5' end of the *Rpi-vnt1* promoter.

The presence of an inverted partial VInv cassette on the right side of the insert was identified by Southern analysis and confirmed by DNA sequencing. The 2.3 kb SacI fragment (SacI/EcoRI, SacI/HindIII, and SacI) on the right side was detected by the GBS1 and INV probes (Figure 3-24 and Figure 3-31). These fragments extend from the RB region into the flanking region. A slightly smaller 1.4 kb fragment with the same probe specificity was observed when SacI was combined with XbaI due to an XbaI restriction site in the flanking region. Similarly, a 1.1 kb PaeI/XbaI fragment connected the PaeI site in the pGbss element with the flanking region. As expected, the band was not detected by GBS2, but was detected by GBS1 and INV (Figure 3-25, Figure 3-26, and Figure 3-32). Note the truncated INV element was indicated by decreased signal intensity associated with bands for the region hybridized with the INV probe (Figure 3-31 and Figure 3-32).

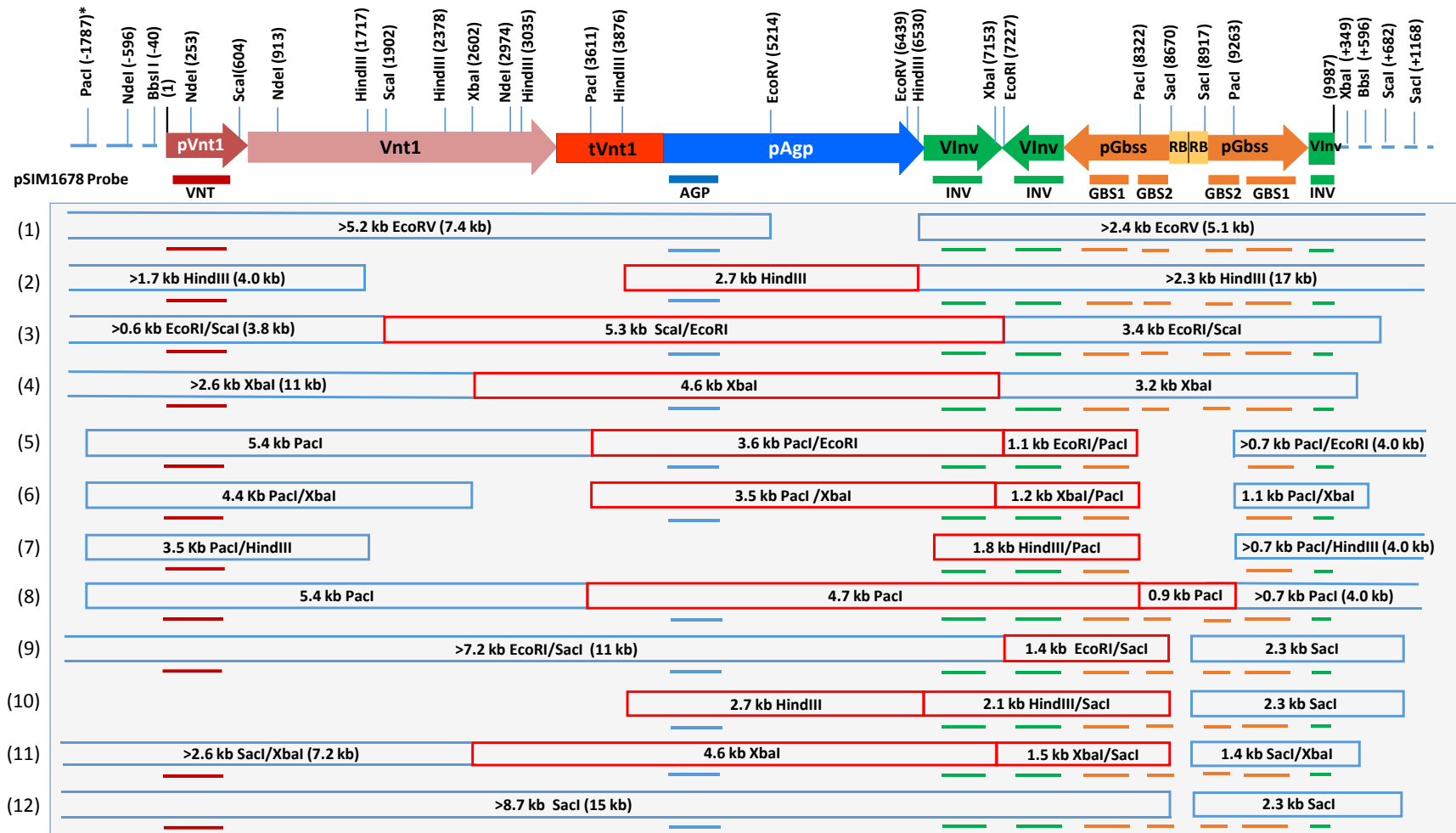


Figure 3-27. Structure of the pSIM1678 Insert in Y9 with Digestion Patterns and Probe Binding Sites

The digestion products are shown as colored boxes with sizes indicated. Red boxes represent internal bands. Blue-closed boxes are junction bands of known sizes. Open-ended blue boxes are junction bands of unknown size. The probes detecting each digestion product are indicated with colored lines. Only digest/probe combinations necessary to support the model are shown. Restriction digests: (1) EcoRV, (2) HindIII, (3) EcoRI/SacI, (4) XbaI, (5) EcoRI/PacI, (6) XbaI/PacI, (7) HindIII/PacI, (8) PacI, (9) EcoRI/SacI, (10) HindIII/SacI, (11) XbaI/SacI, and (12) SacI. *Location of PacI site was determined using the reference genome available from MSU (<http://potato.plantbiology.msu.edu>).

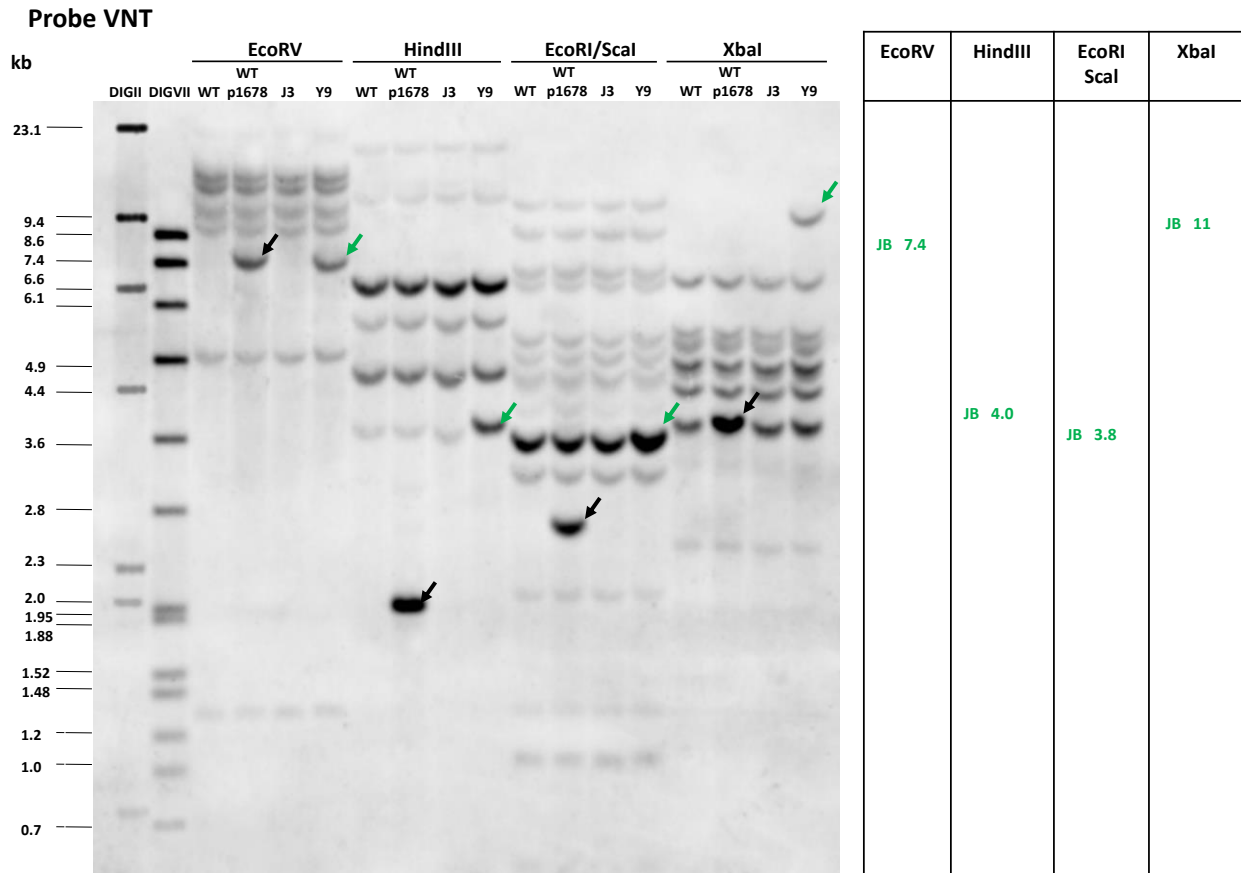


Figure 3-28. Southern Hybridization of Atlantic, J3, and Y9 Genomic DNA with VNT

Genomic DNA of Atlantic control (WT), J3, Y9, and WT spiked with pSIM1678 construct DNA was digested with EcoRV, HindIII, EcoRI/Scal, and XbaI and hybridized with the pSIM1678-specific VNT probe. Size of the DIGII and DIGVII molecular weight markers are indicated adjacent to the blot image. Colored arrows were used to distinguish between any bands associated with the pSIM1678 insert (**green**) and the spiked pSIM1678 (**black**). Estimated sizes of insert-specific bands are indicated in the table. The construct bands are used to show that probes can detect a single insert in the genome and provide a size comparison for internal bands contained within the boundary of the T-DNA. (JB) junction bands, (IB) internal bands.

Probe VNT

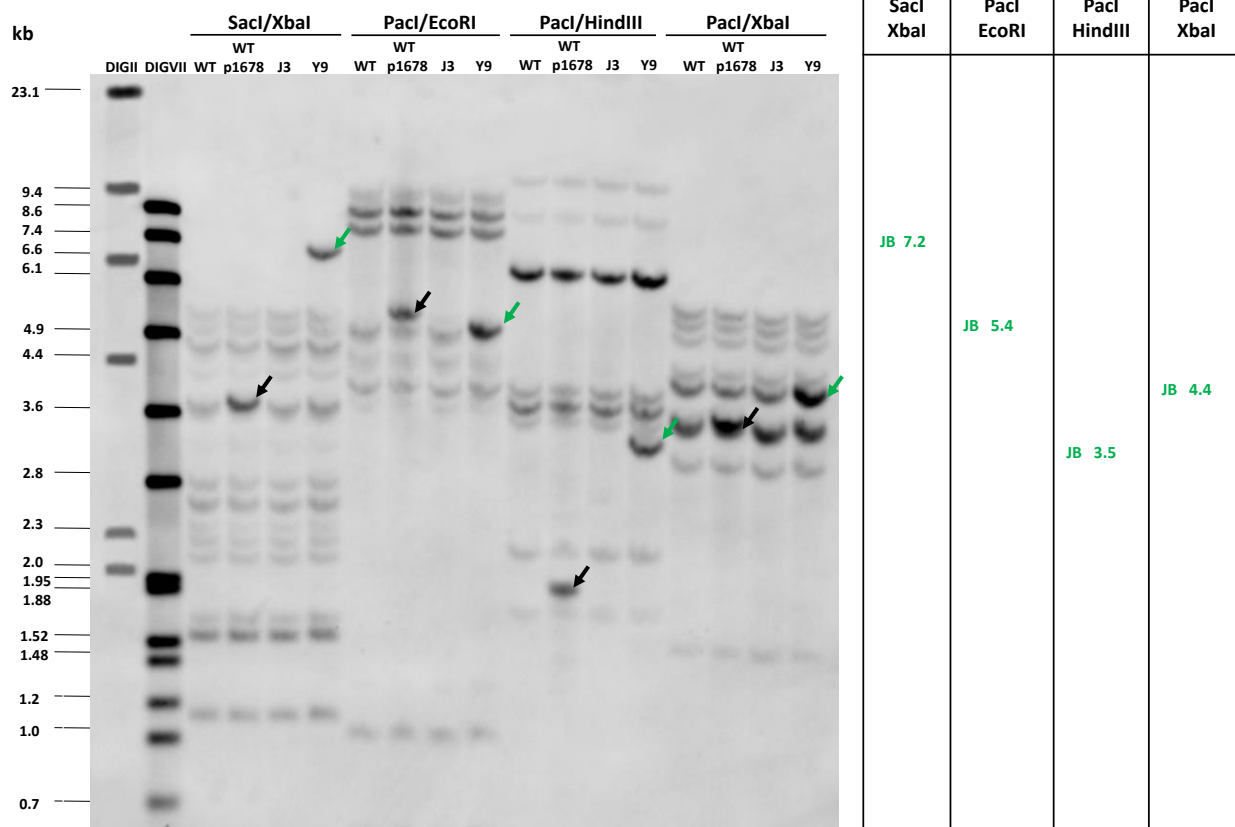


Figure 3-29. Southern of Atlantic, J3, and Y9 SacI/XbaI Digested Genomic DNA with VNT

Genomic DNA of Atlantic control (WT), J3, Y9, and WT spiked with pSIM1678 construct DNA was digested with SacI/XbaI, PacI/EcoRI, PacI/HindIII, and PacI/XbaI and hybridized with the pSIM1678-specific VNT probe. Size of the DIGII and DIGVII molecular weight markers are indicated adjacent to the blot image. Colored arrows were used to distinguish between any bands associated with the pSIM1678 insert (**green**) and the spiked pSIM1678 (**black**). Estimated sizes of insert-specific bands are indicated in the table. The construct bands are used to show that probes can detect a single insert in the genome and provide a size comparison for internal bands contained within the boundary of the T-DNA. (JB) junction bands, (IB) internal bands.

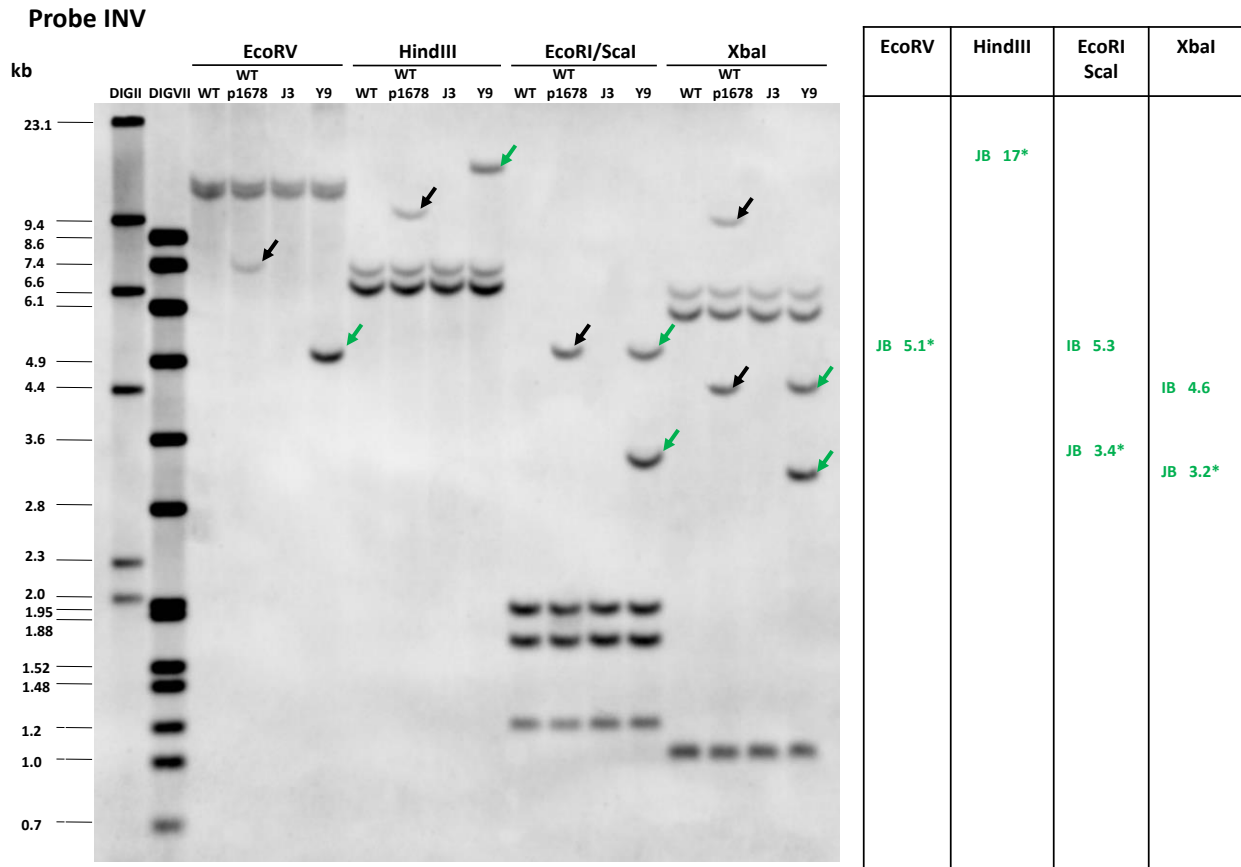


Figure 3-30. Southern Hybridization of Atlantic, J3, and Y9 Genomic DNA with INV

Genomic DNA of Atlantic control (WT), J3, Y9, and WT spiked with pSIM1678 construct DNA was digested with EcoRV, HindIII, EcoRI/Scal, and XbaI and hybridized with the pSIM1678-specific INV probe. Size of the DIGII and DIGVII molecular weight markers are indicated adjacent to the blot image. Colored arrows were used to distinguish between any bands associated with the pSIM1678 insert (**green**) and the spiked pSIM1678 (**black**). Estimated sizes of insert-specific bands are indicated in the table. The construct bands are used to show that probes can detect a single insert in the genome and provide a size comparison for internal bands contained within the boundary of the T-DNA. *Indicates fragment with multiple binding probe hybridization sites. (JB) junction bands, (IB) internal bands.

Probe INV

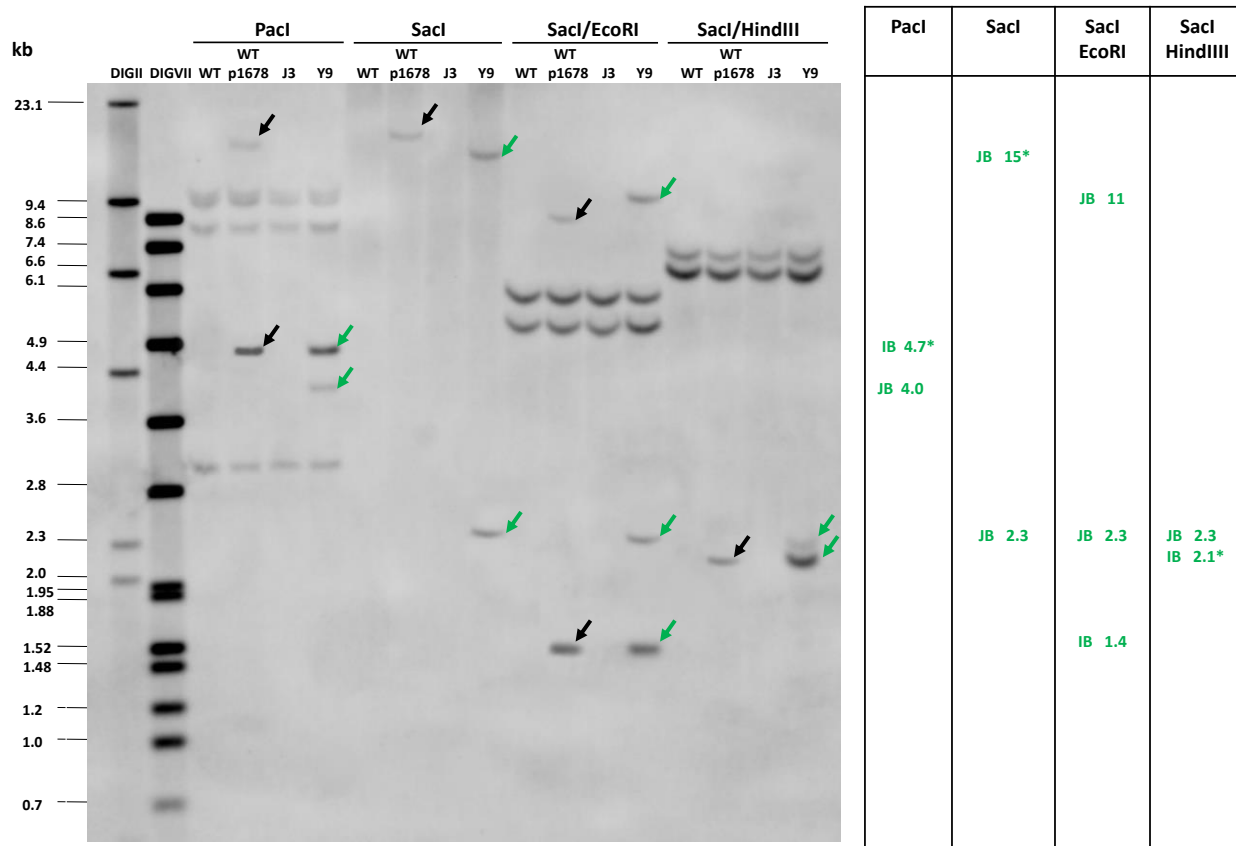


Figure 3-31. Southern Hybridization of Atlantic, J3, and Y9 Genomic DNA after Pacl Digest with INV
 Genomic DNA of Atlantic control (WT), J3, Y9, and WT spiked with pSIM1678 construct DNA was digested with Pacl, SacI, SacI/EcoRI and SacI/HindIII and hybridized with the pSIM1678-specific INV probe. Size of the DIGII and DIGVII molecular weight markers are indicated adjacent to the blot image. Colored arrows were used to distinguish between any bands associated with the pSIM1678 insert (**green**) and the spiked pSIM1678 (**black**). Estimated sizes of insert-specific bands are indicated in the table. The construct bands are used to show that probes can detect a single insert in the genome and provide a size comparison for internal bands contained within the boundary of the T-DNA. *Indicates fragment with multiple binding probe hybridization sites. (JB) junction bands, (IB) internal bands.

Probe INV

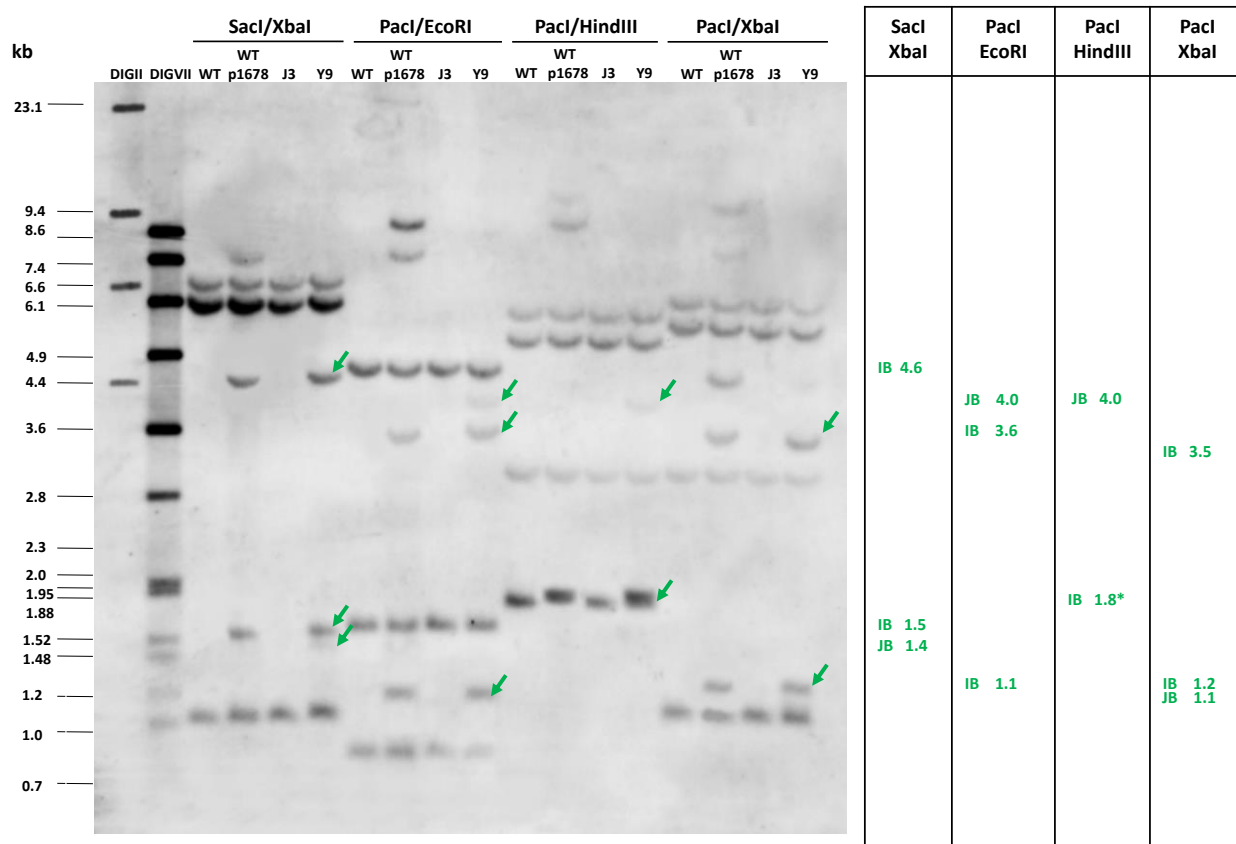


Figure 3-32. Southern of Atlantic, J3, and Y9 Genomic DNA after SacI/XbaI Digest with INV

Genomic DNA of Atlantic control (WT), J3, Y9, and WT spiked with pSIM1678 construct DNA was digested with *SacI*/*XbaI*, *PacI*/*EcoRI*, *PacI*/*HindIII*, and *PacI*/*XbaI* and hybridized with the pSIM1678-specific INV probe. Size of the DIGII and DIGVII molecular weight markers are indicated adjacent to the blot image. Colored arrows were used to distinguish between any bands associated with the pSIM1678 insert (**green**) and the spiked pSIM1678 (**black**). Estimated sizes of insert-specific bands are indicated in the table. The construct bands are used to show that probes can detect a single insert in the genome and provide a size comparison for internal bands contained within the boundary of the T-DNA. *Indicates fragment with multiple binding probe hybridization sites. (JB) junction bands, (IB) internal bands.

Based upon NGS reads, a 0.9 kb *PacI* fragment was expected to cover the junction between the two inverted RB regions. The GBS1 probe only hybridizes to the region downstream of the *PacI* site in *pGbss* so a second probe, GBS2, specific to this upstream region was used to confirm the structure at this junction. As shown in Figure 3-26, a 0.9 kb *PacI* band (green arrows) was observed as expected. Due to a similar duplication in the pSIM1278 and pSIM1678 inserts, small but distinct *PacI* fragments were detected for both inserts.

The sequencing and Southern data showed that transformation with pSIM1678 resulted in a single insert consisting of a nearly full-length T-DNA flanked by a partial duplication of the *VInv* cassette. There are additional digests shown in Figure 3-27 that were not described in detail, but offer further support for the structure presented. The pSIM1678 insert contains a copy of the *Rpi-vnt1* gene expression cassette and an intact copy of the *VInv* down-regulation cassette.

3.2.5 Analysis of Potential Fusion Proteins in Y9

The right side of the pSIM1678 insert contains an intact *Gbss* promoter oriented towards adjacent flanking genome sequence (Figure 3-33). The potential for producing novel proteins from this *Gbss* promoter was determined by identifying a putative RNA transcript and any open reading frames (ORF) greater than 30 codons.

The transcriptional initiation site of the *Gbss* promoter was determined by mapping the 5' end of the endogenous transcript (PGSC0003DMT400031568, MSU database). The data indicate likely transcription initiation within the *Gbss* promoter at a location 303 base pairs upstream of the *pGbss/VInv* junction. A diagram of the putative RNA transcript derived from the *Gbss* promoter is shown in Figure 3-33.

An ORF analysis was performed to determine if any fusion proteins could potentially be generated from the putative RNA transcript, if it were transcribed and properly processed into messenger RNA (mRNA). Start and stop codons were mapped for each of the three reading frames, but only a single reading frame was identified. The ORF was unlikely to result in a fusion protein as it was entirely contained within the *Gbss* promoter (Figure 3-33). Because the *Gbss* promoter is present in the conventional potato genome, the ORF identified within the promoter, is not novel to Y9. No ORFs spanning the junctions between insert elements or the potato genome were identified. These results show no evidence supporting a fusion protein being generated from the transcript. Downstream open reading frames are unlikely to be translated into protein as the ribosome generally initiates at the first initiation site (AUG) relative to the 5' end of an mRNA.

The pSIM1678 insert contains a complete copy of the *VInv* cassette for the production of siRNAs complementary to the *VInv* sequence. The RNAi pathway is expected to actively target all *VInv* transcripts for destruction preventing protein translation, even the one from the partial *VInv* cassette at the right border.

In summary, a transcript generated from the *Gbss* promoter at the right border of the pSIM1678 insert:

- Is unlikely to include the necessary cis-elements to be processed into a functional mRNA;
- Will not produce a fusion protein between the insert and the genome sequence;
- Will not produce a fusion protein between elements within the DNA insert; and
- Will be targeted for destruction by the RNA interference pathway in the cell due to complementarity with siRNAs derived from the complete *VInv* cassette.

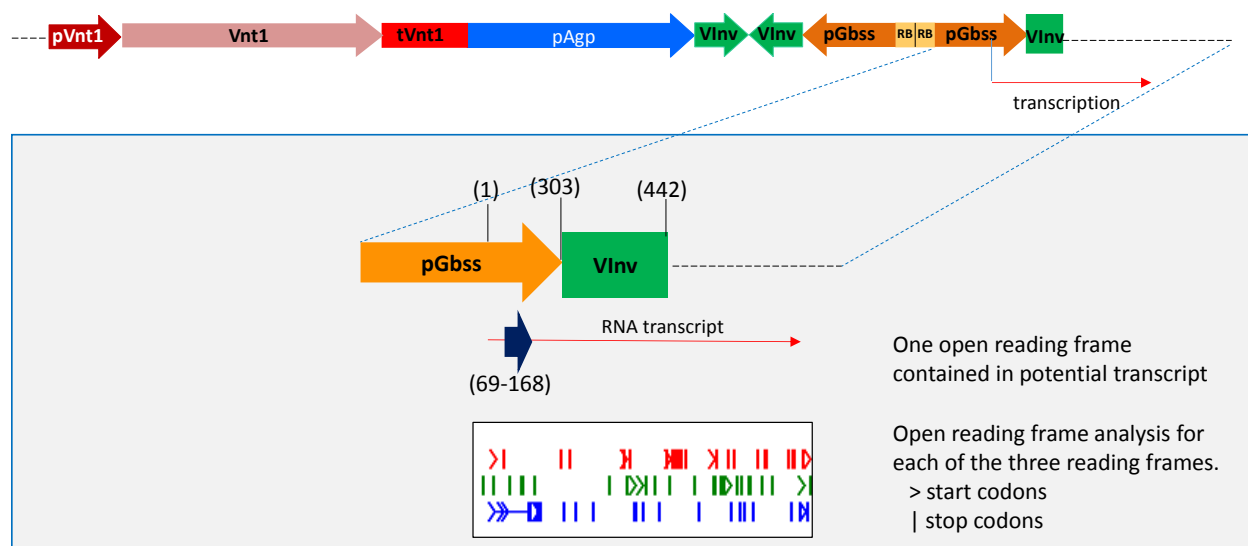


Figure 3-33. No Fusion Proteins Produced from the Right Side of the pSIM1678 Insert

A single transcript was predicted to be generated from the *Gbss* promoter (red arrow). Transcription starts at (1), 303 bp upstream of the pGbss/VInv junction. A single ORF was identified (blue arrow) with translational start and stop sites. Start and stop codons for each reading frame (red, blue, and green) over the potential transcript are shown. The ORF output was generated using the web-based application (<http://www0.nih.gov/~jun/cgi-bin/frameplot.pl>) with a required ORF size of 30 or more codons.

3.3 Absence of pSIM1278 and pSIM1678 Backbone Sequence in X17 and Y9

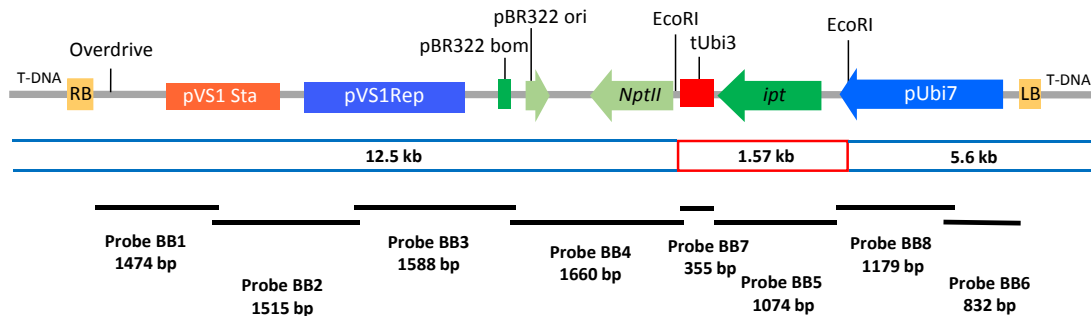
X17 and Y9 were evaluated for the presence of backbone DNA. Genomic DNA isolated from Ranger Russet (WT), X17, Atlantic (WT), and Y9 plants was digested with restriction enzymes and fragments detected by Southern using eight probes spanning the identical pSIM1278 and pSIM1678 backbone. The DNA concentration was normalized following digestion and equivalent gel loading of samples was verified by ethidium bromide staining of agarose gels. No backbone sequences were detected in X17 or Y9.

Genomic DNA, isolated from Ranger Russet (WT), X17, Atlantic (WT) and Y9, was digested with *EcoRI* or *EcoRI/Scal*. The pSIM1278 construct (1278) spiked into WT genomic DNA, at a concentration of one copy per genome equivalent, was used as a control to ensure sufficient probe sensitivity in detecting a single copy of any inserted backbone. A representation of the backbone, with expected band sizes, is shown for X17 (see Figure 3-34) and Y9 (see Figure 3-35).

EcoRI digestion of backbone DNA is expected to produce three bands (12.5 kb, 1.57 kb, and 5.6 kb) detectable by the BB1-BB8 probes (see Figure 3-34A and Figure 3-35A). Because of issues with cross reactivity between backbone probes BB7 and BB8 with pSIM1278 T-DNA sequences, a double digest with *EcoRI/Scal* was used to identify false positive results. The sequence of the spacer 2 element within the PhL/R1 inverted repeat is derived from the *Ubi7* promoter and is detected by the BB8 probe in both the pSIM1278 construct control and the pSIM1278 insert in X17 and Y9 (see Figures 3-34B and 3-35B). Digestion of pSIM1278 construct, or X17 and Y9 sample DNA, with *EcoRI/Scal* produces a 0.8 kb band (see Figure 3-37 and Figure 3-39). A 1.4 kb band in Y9 samples is due to an additional partial PhL/R1 cassette on the right side of the insert (Figure 3-39).

Backbone DNA was not detected by Southern analysis in X17 or Y9 genomic DNA using backbone probes BB1-BB8 (Figure 3-36, Figure 3-37, Figure 3-38, and Figure 3-39). An expected 12.5 kb band was observed in control samples (Figure 3-36 and Figure 3-38). Also, 1.57 and 5.6 kb bands were observed in control samples with BB5-BB8 (Figure 3-37 and Figure 3-39). The expected 0.8 kb band for X17, and 0.8 and 1.4 kb bands for Y9 were observed together with an expected 0.8 kb band in control samples using probe BB8 (Figure 3-37 and Figure 3-39). These bands correspond to the spacer 2 region in both backbone and T-DNA sequences. Endogenous bands not related to the transformations were observed in all samples in the blots hybridized with probes BB3, BB6, BB7, and BB8. The Southern analysis of X17 and Y9 demonstrated that no backbone sequence was incorporated into the genome during transformation.

A pSIM1278 and pSIM1678 Backbone



B pSIM1278 insert in X17

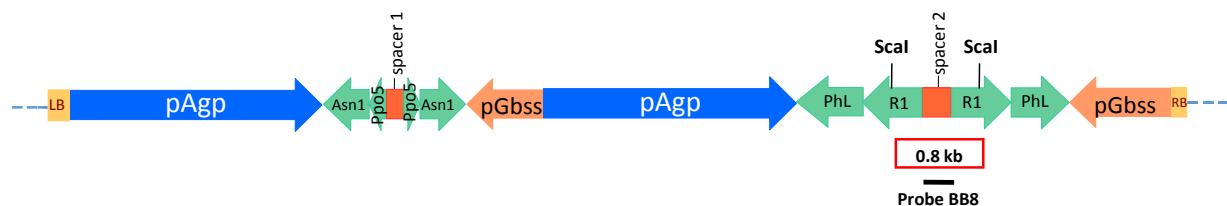
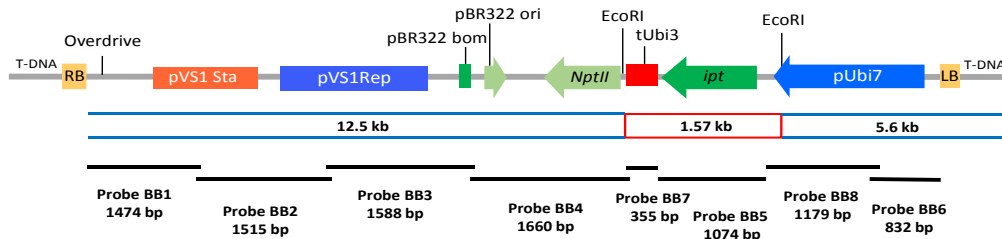


Figure 3-34. Structure of the pSIM1278/pSIM1678 Backbone with pSIM1278 Insert in X17

(A) The pSIM1278/pSIM1678 backbone is complementary to eight probes (BB1-BB8) that span the sequence. Probe sizes are indicated. EcoRI restriction sites, with band sizes, are shown as colored boxes. (B) Structure of the pSIM1278 insert in X17. The BB8 probe detects the spacer 2 region within a 0.8 kb band resulting from *Scal* digestion.

A pSIM1278 and pSIM1678 Backbone



B pSIM1278 Insert in Y9

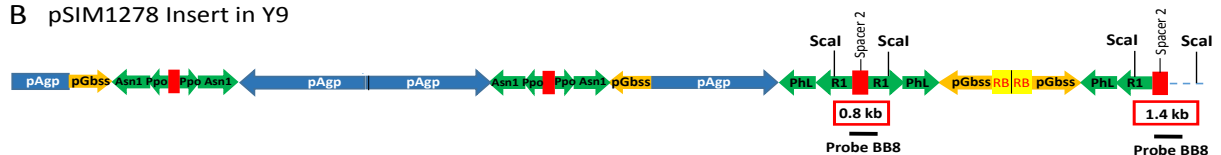


Figure 3-35. Structure of the pSIM1278/pSIM1678 Backbone with pSIM1278 Insert in Y9

(A) The pSIM1278/pSIM1678 backbone is complementary to eight probes (BB1-BB8) that span the sequence. Probe sizes are indicated. EcoRI restriction sites, with band sizes, are shown as colored boxes. (B) Structure of the pSIM1278 insert in Y9. The BB8 probe detects spacer 2 regions within 0.8 and 1.4 kb bands resulting from *Scal* digestion.

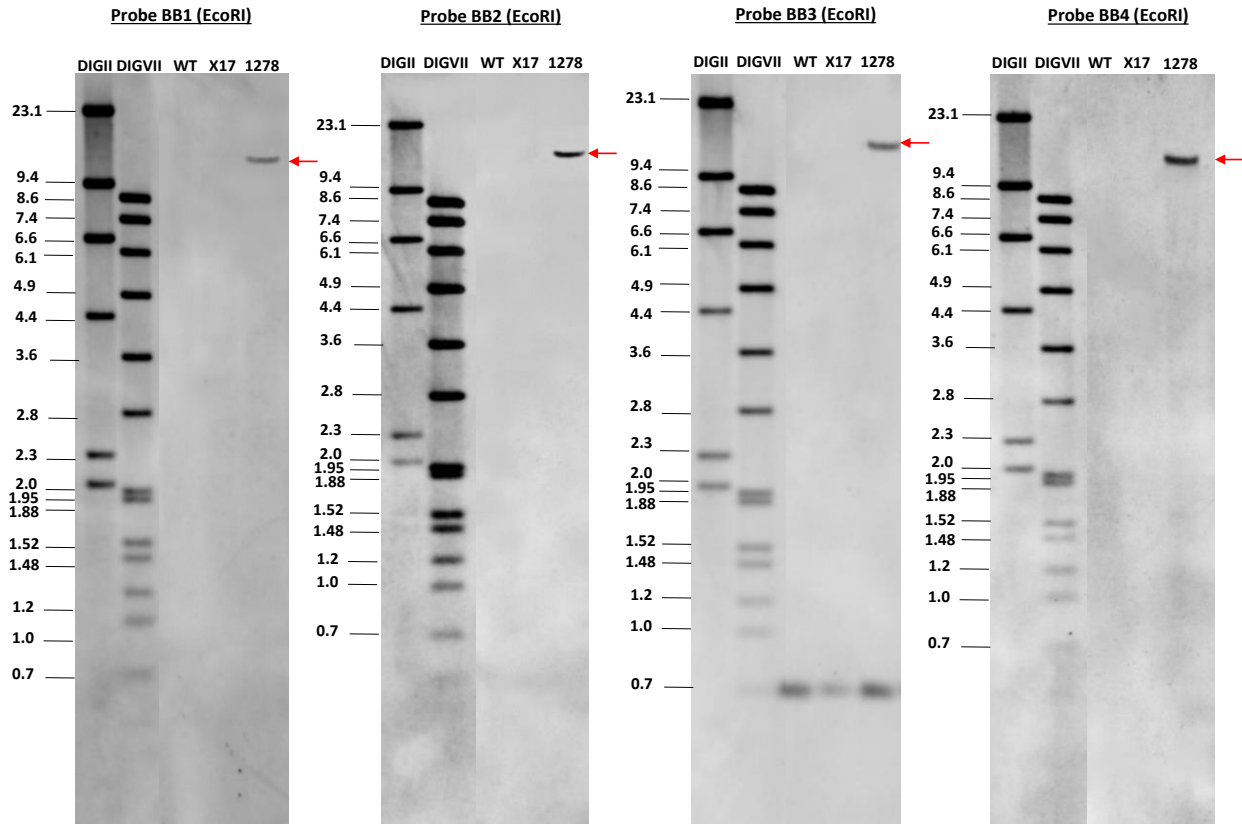


Figure 3-36. Southern Blots Probed With BB1-4 Show No Evidence of Backbone DNA in X17

Southern blots of genomic DNA isolated from Ranger Russet (WT), X17, and WT spiked with pSIM1278 (1278). Molecular weight markers, DIGII and DIGVII, are labeled in kilobases (kb). Red arrows indicate expected 12.5 kb bands unique to pSIM1278.

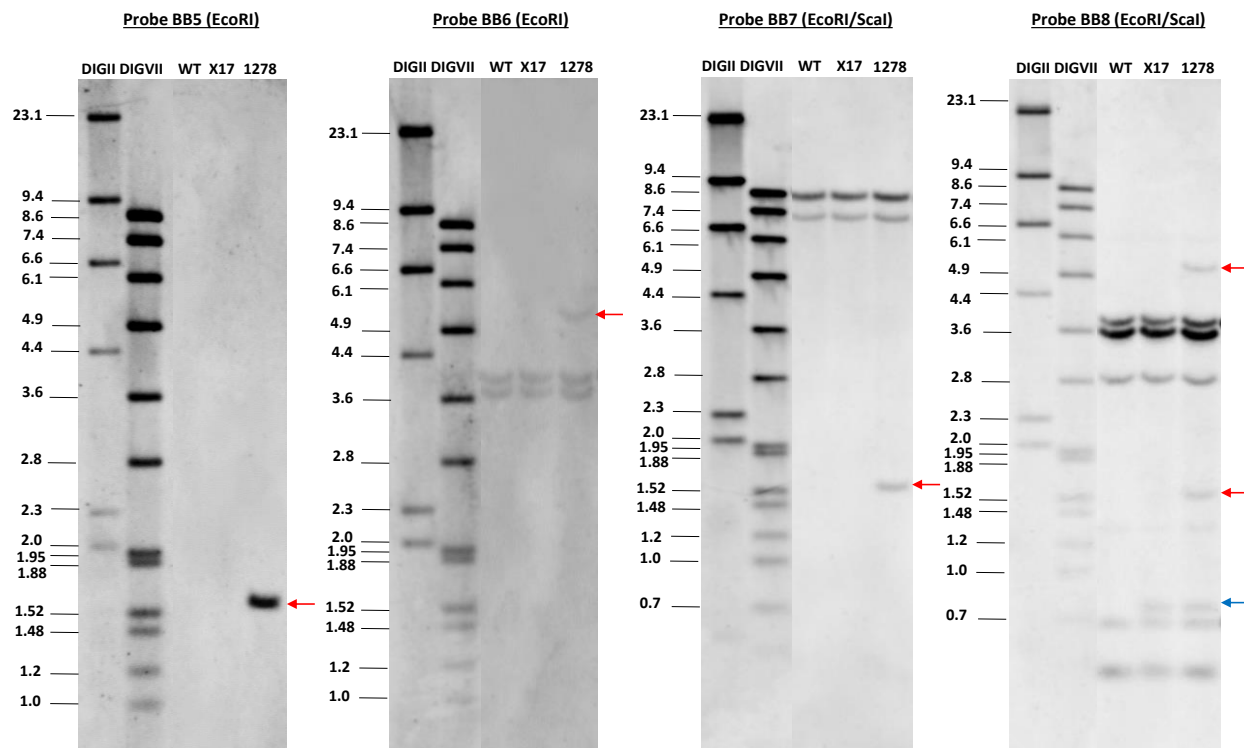


Figure 3-37. No Evidence of Backbone DNA Corresponding to Probes BB5-BB8 in X17

Southern blots of genomic DNA isolated from Ranger Russet (WT), X17, and WT spiked with pSIM1278 (1278). Molecular weight markers, DIGII and DIGVII, are labeled in kilobases (kb). Red arrows indicate expected bands (1.57 kb and 5.6 kb) unique to pSIM1278. Blue arrow indicates 0.8 kb band associated with the spacer 2 element of the pSIM1278 insert in X17.

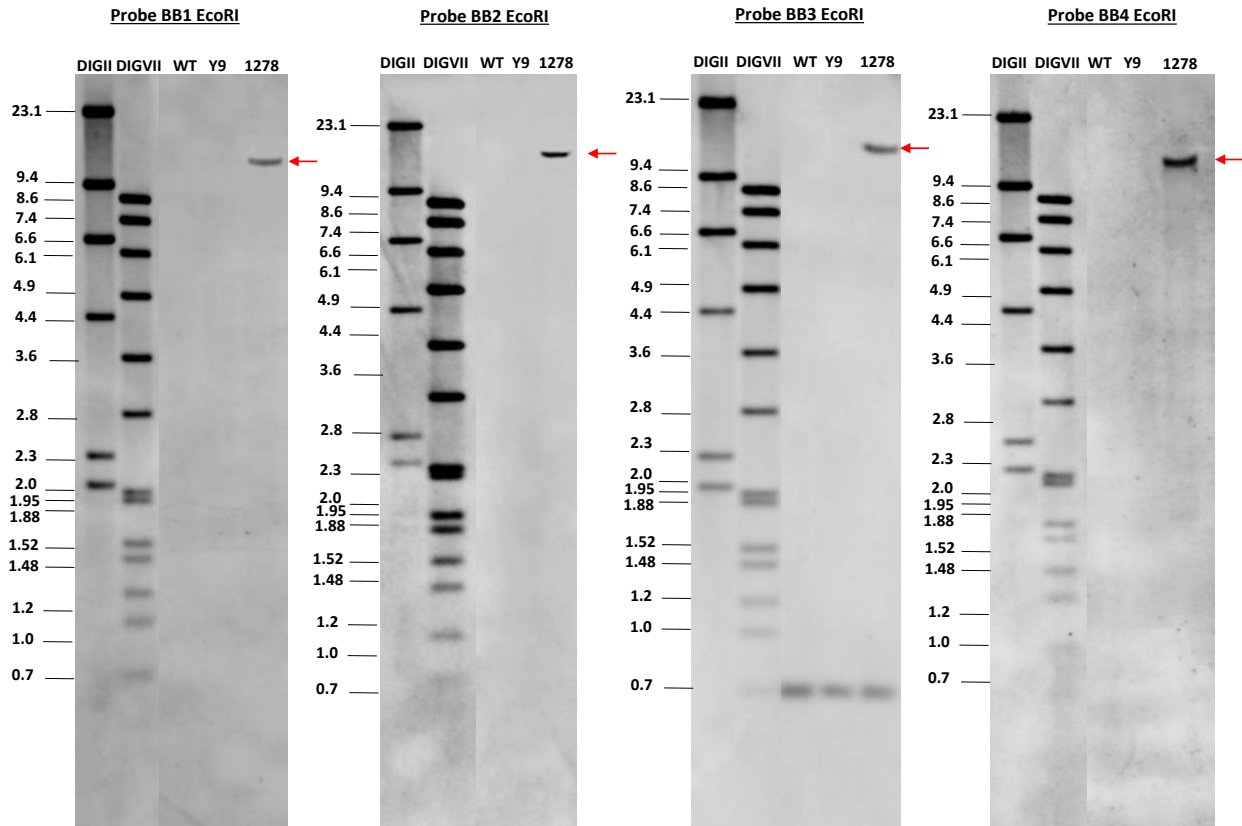


Figure 3-38. Southern Blots Probed With BB1-4 Show No Evidence of Backbone DNA in Y9

Southern blots of genomic DNA isolated from Atlantic (WT), Y9, and WT spiked with pSIM1278 (1278). Molecular weight markers, DIGII and DIGVII, are labeled in kilobases (kb). Red arrows indicate expected 12.5 kb bands unique to pSIM1278.

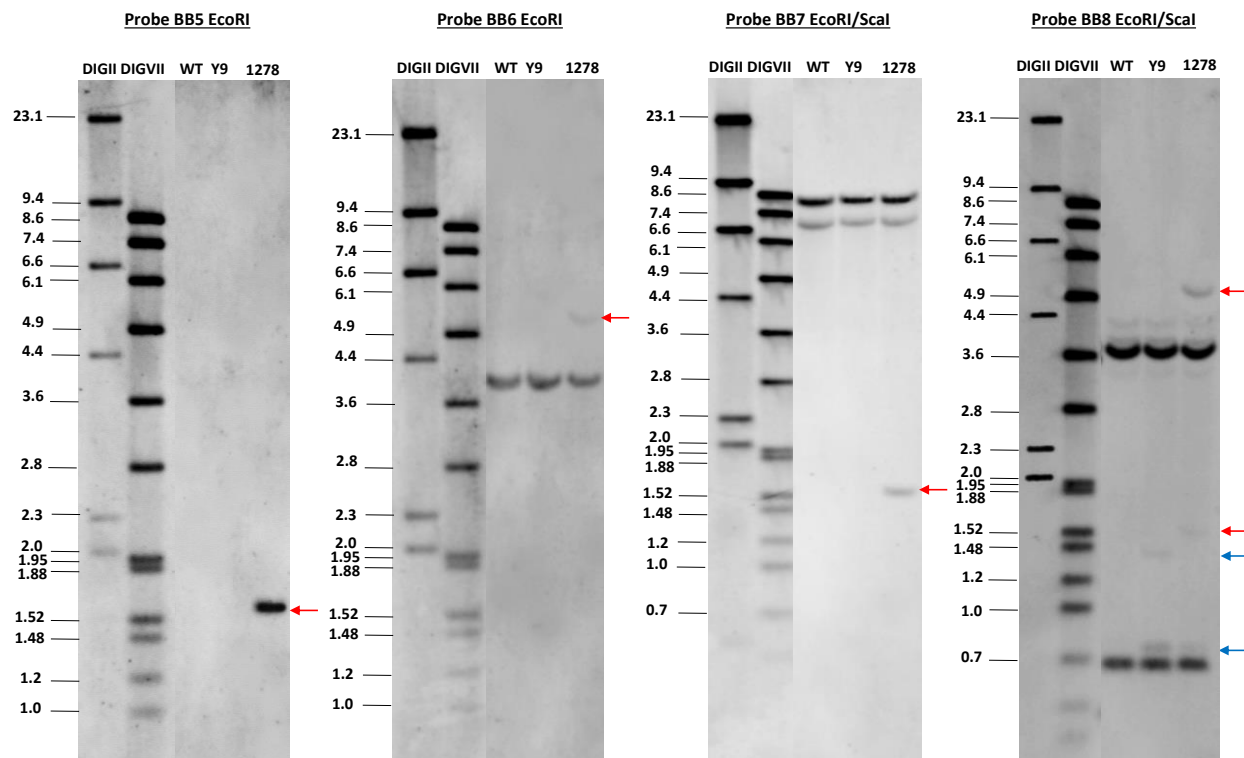


Figure 3-39. No Evidence of Backbone DNA Corresponding to Probes BB5-BB8 in Y9

Southern blots of genomic DNA isolated from Atlantic (WT), Y9, and WT spiked with pSIM1278 (1278). Molecular weight markers, DIGII and DIGVII, are labeled in kilobases (kb). Red arrows indicate expected bands (1.57 kb and 5.6 kb) unique to pSIM1278. Blue arrows indicates 0.8 and 1.4 kb bands associated with the spacer 2 element of the pSIM1278 insert in Y9.

3.4 Stability of the Inserts across Clonal Cycles

Potatoes are propagated asexually. The progeny plants have not recombined meiotically and are, therefore, genetically and phenotypically identical to the mother plant and to each other. Stability of the inserts in X17 and Y9 events was assessed, however, to show that DNA introduced into potato through transformation is stable over several clonal cycles.

Genetic stability of the inserts in X17 and Y9 were assessed by determining the presence or absence of the insert in G0 and G2 plants. Six probes that hybridize to the inserts (AGP, ASN, GBS, R1, INV, and VNT) were used in Southern analysis. The GBS and AGP probes hybridize elements contained in both pSIM1278 and pSIM1678, while ASN and R1 are specific to pSIM1278, and VNT and INV are specific to pSIM1678. Evidence for genetic stability would be observation of a consistent banding pattern among X17 and Y9 progeny from multiple clonal cycles. Ranger Russet (WT), X17, Atlantic (WT), and Y9 genomic DNA was digested with EcoRV resulting in multiple bands distinguishable by size and probe specificity (see Figure 3-40 and Figure 3-41).

3.4.1 X17 Genetic Stability

For X17, the EcoRV digest is expected to produce a total of six bands (sizes are 2.6 kb, 0.7 kb, 2.3 kb, and 8.2 kb for pSIM1278 and 12 kb and 2.9 kb for pSIM1678; see Figure 3-40). Southern blots hybridized separately with the AGP, GBS, ASN, and R1 probes confirmed the presence of the pSIM1278 associated bands (Figure 3-42 and Figure 3-43). Southern blots hybridized separately with the AGP, GBS, INV, and VNT probes confirmed the presence of the pSIM1678 associated bands (Figure 3-42 and Figure 3-44).

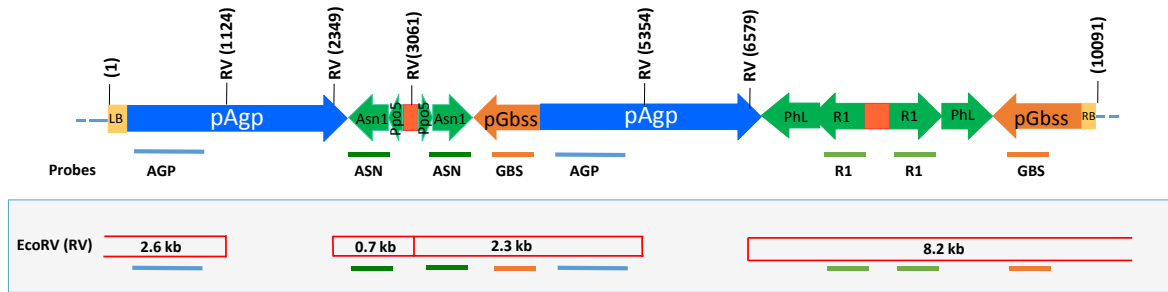
The AGP and GBS probes hybridize to both inserts, which have identical *Agp* and *Gbss* promoter sequences. The AGP probe hybridized to two bands (2.3 kb and 2.6 kb) associated with the pSIM1278 insert and the 12 kb band corresponding to the pSIM1678 insert (Figure 3-42A). The GBS probe hybridized to two bands (2.3 kb and 8.2 kb) associated with the pSIM1278 insert and the 2.9 kb band associated with the pSIM1678 insert (Figure 3-42B). These bands were consistently detected in both G0 and G2 X17 samples indicative of a stable insertion.

The ASN and R1 probes hybridize to genetic elements only within the pSIM1278 insert. Two bands were detected using the ASN probe (0.7 kb and 2.3 kb; Figure 3-45A). The R1 probe detected an 8.2 kb band associated with the pSIM1278 insert (Figure 3-43B).

The INV and VNT probes hybridize only within the pSIM1678 insert. The INV probe detected a 2.9 kb band, while the VNT probe detected a 12 kb band as expected (Figure 3-44). The bands were consistently detected in both G0 and G2 X17 samples indicative of a stable insertion.

Other bands observed in the blots are due to endogenous potato genes that are identical to elements of the pSIM1278 and pSIM1678 T-DNA. The endogenous bands also remained constant over the tested clonal cycles.

A) pSIM1278 Insert



B) pSIM1678 Insert

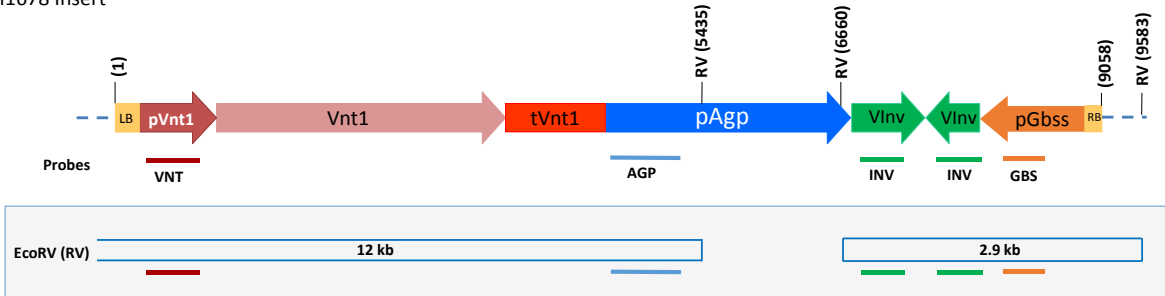
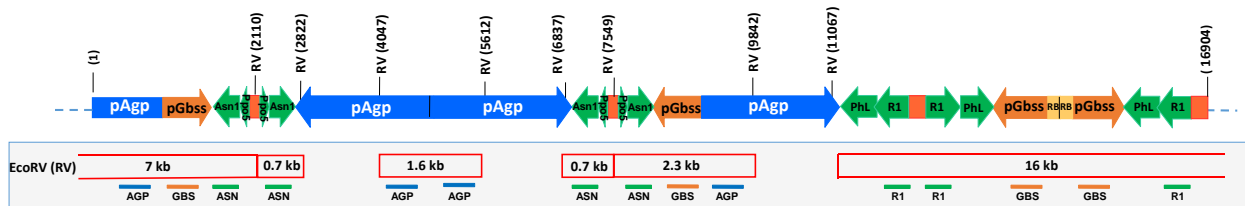


Figure 3-40. Structure of the pSIM1278 and pSIM1678 Insert in X17

(A) pSIM1278 insert and (B) pSIM1678 insert in X17 with EcoRV digestion product sizes and probe complementarity. The expected bands following EcoRV digestion are shown. Red boxes indicate bands associated with pSIM1278. Blue boxes are bands associated with pSIM1678. The colored indicator below corresponds to the complementary probe.

A) pSIM1278 Insert



B) pSIM1678 Insert

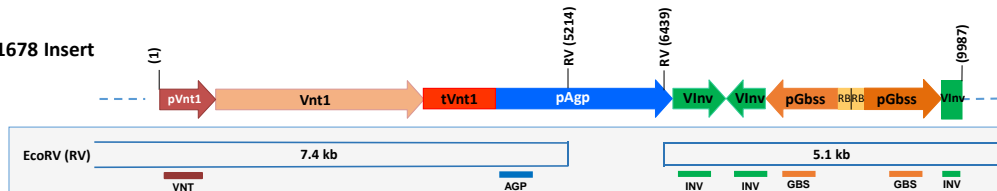


Figure 3-41. Structure of the pSIM1278 and pSIM1678 Insert in Y9

(A) pSIM1278 insert and (B) pSIM1678 insert in Y9 with EcoRV digestion product sizes and probe complementarity. The expected bands following EcoRV digestion are shown. Red boxes indicate bands associated with pSIM1278. Blue boxes are bands associated with pSIM1678. The colored indicator below corresponds to the complementary probe.

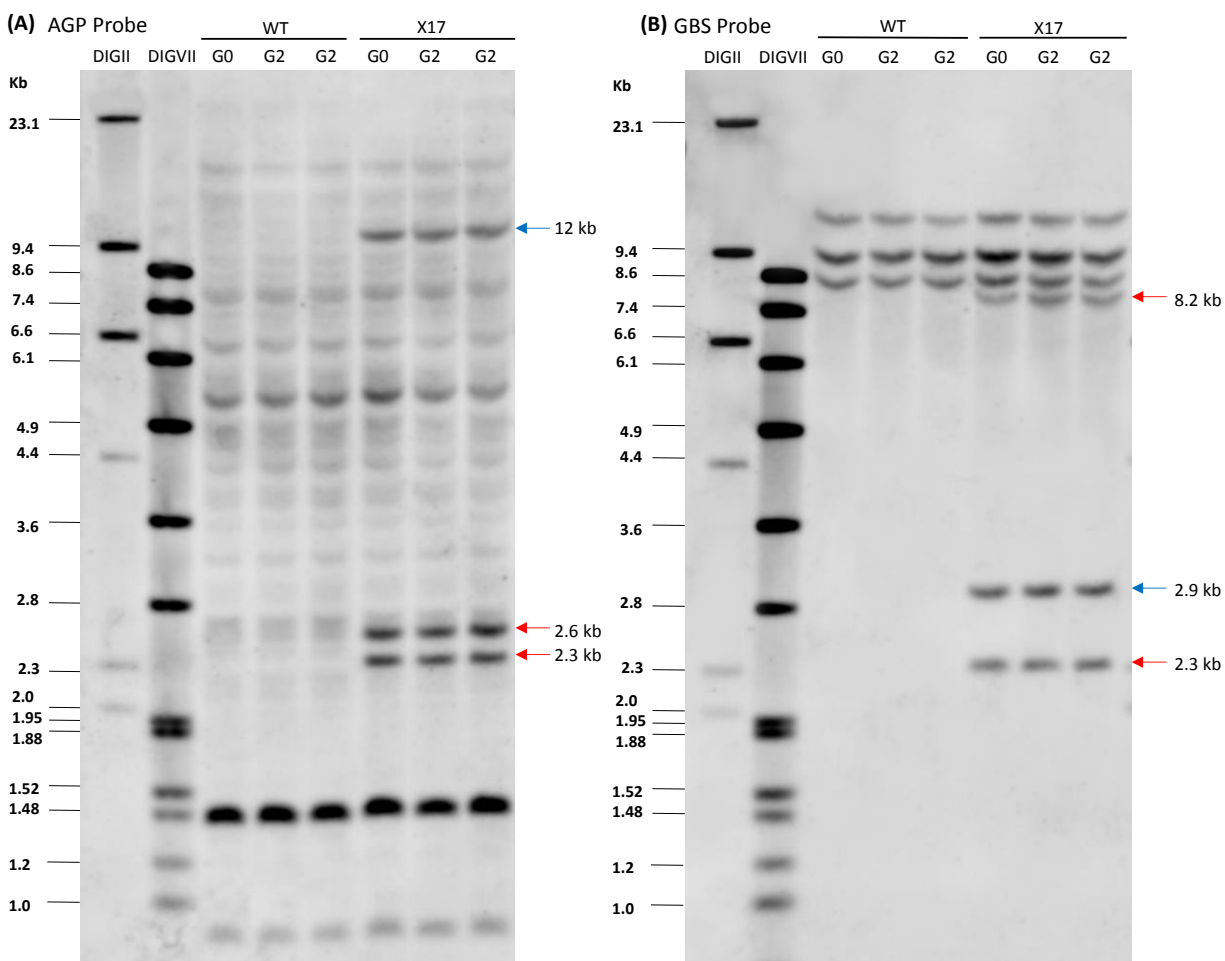


Figure 3-42. X17 Insert Stability in G0 and G2 clonal Cycles as Visualized with AGP and GBS Probes

Southern blots of genomic DNA isolated from G0 and G2 plants of Ranger Russet control (WT) and X17 hybridized with (A) AGP probe or (B) GBS probe. Four μ g of each sample was digested with EcoRV and separated by electrophoresis prior to transfer and hybridization with the indicated probe. Red arrows indicate pSIM1278 insert bands and blue arrows indicate pSIM1678 insert bands. Molecular weight markers (DIGII and DIGVII) were included with band sizes indicated in kilobase pairs (kb).

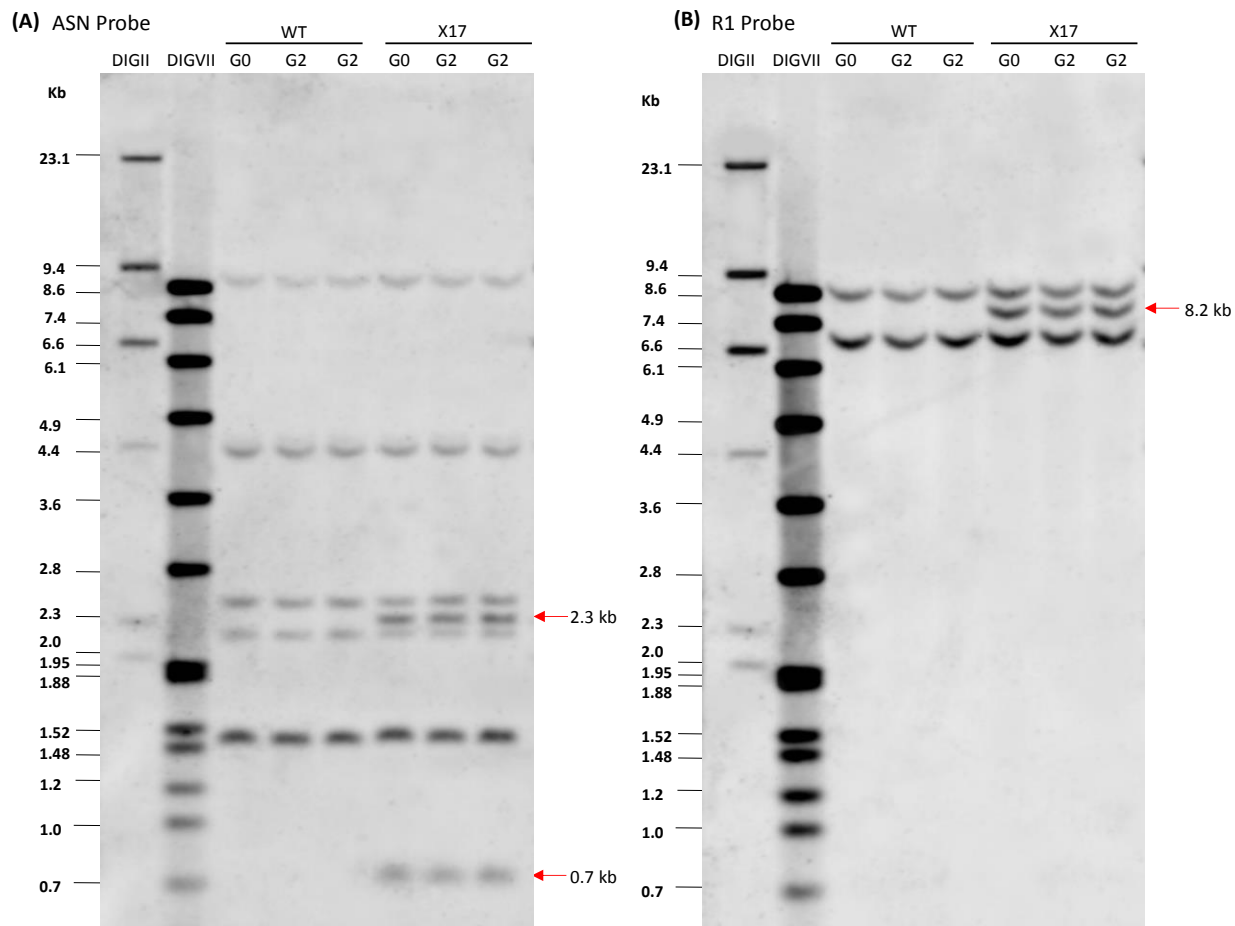


Figure 3-43. X17 Insert Stability in G0 and G2 Clonal Cycles as Visualized with ASN and R1 Probes

Southern blots of genomic DNA isolated from G0 and G2 plants of Ranger Russet control (WT) and X17 hybridized with (A) ASN probe or (B) R1 probe. Four μ g of each sample was digested with EcoRV and separated by electrophoresis prior to transfer and hybridization with the indicated probe. Red arrows indicate pSIM1278 insert bands. Molecular weight markers (DIGII and DIGVII) were included with band sizes indicated in kilobase pairs (kb).

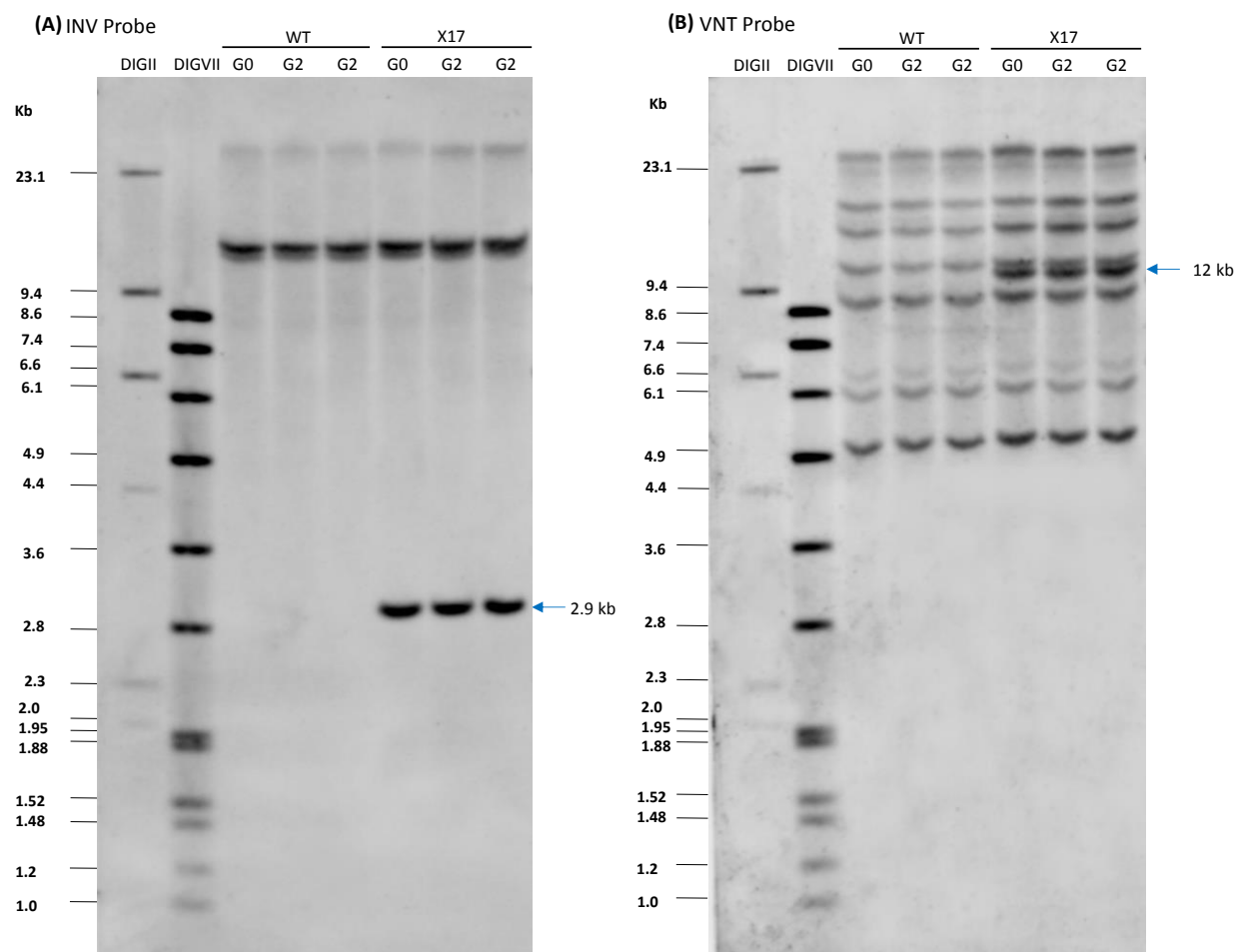


Figure 3-44. X17 Insert Stability in G0 and G2 Clonal Cycles as Visualized with INV and VNT Probes
 Southern blots of genomic DNA isolated from G0 and G2 plants of Ranger Russet control (WT) and X17 hybridized with (A) INV probe or (B) VNT probe. Four μ g of each sample was digested with EcoRV and separated by electrophoresis prior to transfer and hybridization with the indicated probe. Blue arrows indicate pSIM1678 insert bands. Molecular weight markers (DIGII and DIGVII) were included with band sizes indicated in kilobase pairs (kb).

3.4.2 Y9 Genetic Stability

For Y9, the EcoRV digest is expected to produce a total of eight bands (sizes are 7 kb, 0.7 kb, 1.6 kb, 0.7 kb, 2.3 kb, and 16 kb from pSIM1278 and 7.4 kb and 5.1 kb from pSIM1678; see Figure 3-41). Southern blots hybridized separately with the AGP, GBS, ASN, and R1 probes confirmed the presence of the pSIM1278 associated bands (Figure 3-45 and Figure 3-46). Southern blots hybridized separately with the AGP, GBS, INV, and VNT probes confirmed the presence of the pSIM1678 associated bands (Figure 3-45 and Figure 3-47).

The AGP and GBS probes hybridize to both inserts, which have identical *Agp* and *Gbss* promoter sequences. The AGP probe hybridized to three bands (7 kb, 2.3 kb and 1.6 kb) associated with the pSIM1278 insert and the 7.4 kb band corresponding to the pSIM1678 insert (Figure 3-45A). The GBS probe hybridized to three bands (7 kb, 2.3 kb and 16 kb) associated with the pSIM1278 insert and the 5.1 kb band associated with the pSIM1678 insert (Figure 3-45B). These bands were consistently detected in both G0 and G2 X17 samples indicative of a stable insertion.

The ASN and R1 probes hybridize to genetic elements only within the pSIM1278 insert. Three bands were detected using the ASN probe (7 kb, 0.7 kb and 2.3 kb; Figure 3-46A). The R1 probe detected a 16 kb band associated with the pSIM1278 insert (Figure 3-46B).

The INV and VNT probes hybridize only within the pSIM1678 insert. The INV probe detected a 5.1 kb band, while the VNT probe detected a 7.4 kb band as expected (Figure 3-47). The bands were consistently detected in both G0 and G2 X17 samples indicative of a stable insertion.

Other bands observed in the blots are due to endogenous potato genes that are identical to elements of the pSIM1278 and pSIM1678 T-DNA. The endogenous bands also remained constant over the tested clonal cycles.

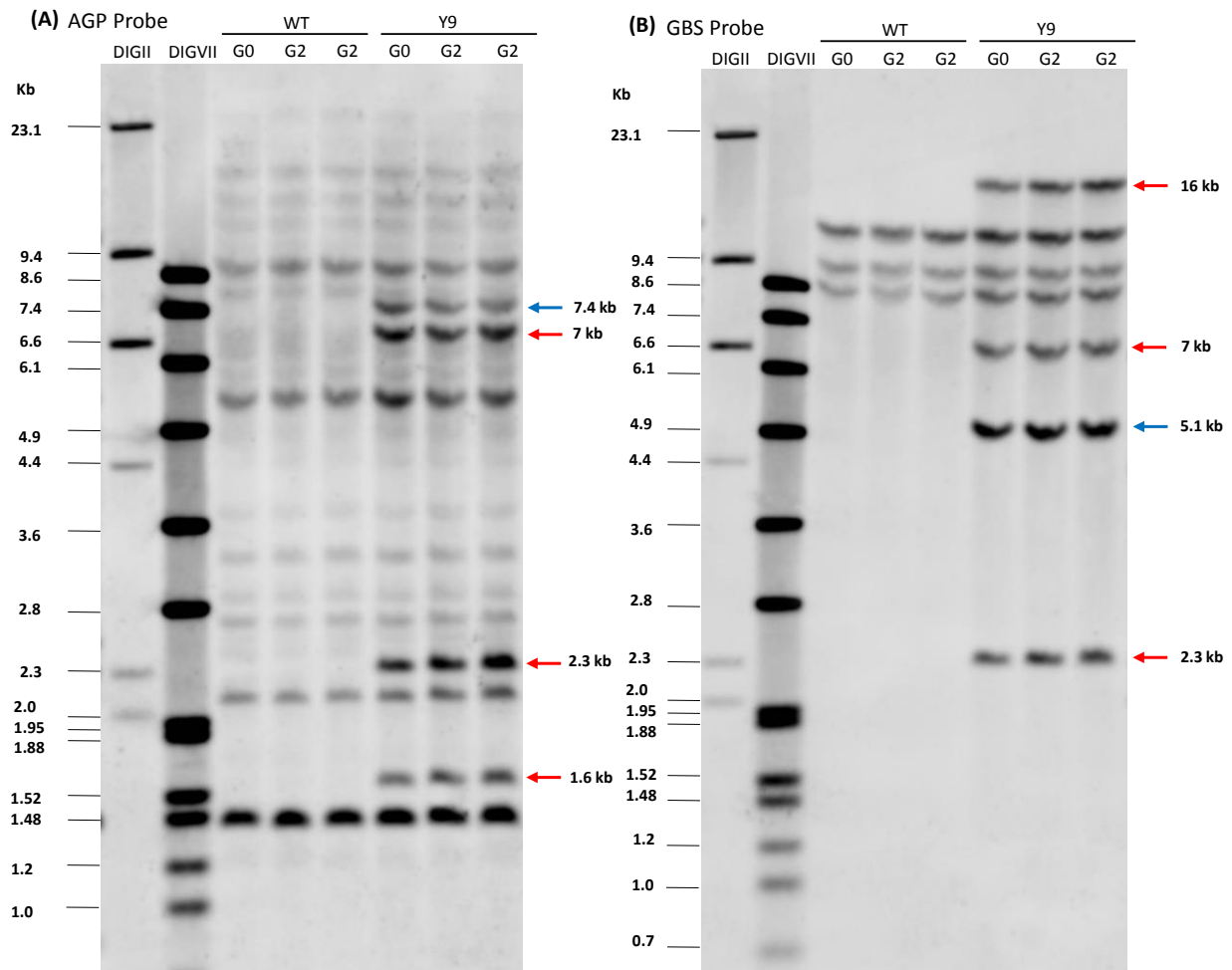


Figure 3-45. Y9 Insert Stability in G0 and G2 Clonal Cycles as Visualized with AGP and GBS Probes
 Southern blots of genomic DNA isolated from G0 and G2 plants of Atlantic control (WT) and Y9 hybridized with (A) AGP probe or (B) GBS probe. Four μg of each sample were digested with EcoRV and separated by electrophoresis prior to transfer and hybridization with the indicated probe. Red arrows indicate pSIM1278 insert bands and blue arrows indicate pSIM1678 insert bands. Molecular weight markers (DIGII and DIGVII) were included with band sizes indicated in kilobase pairs (kb).

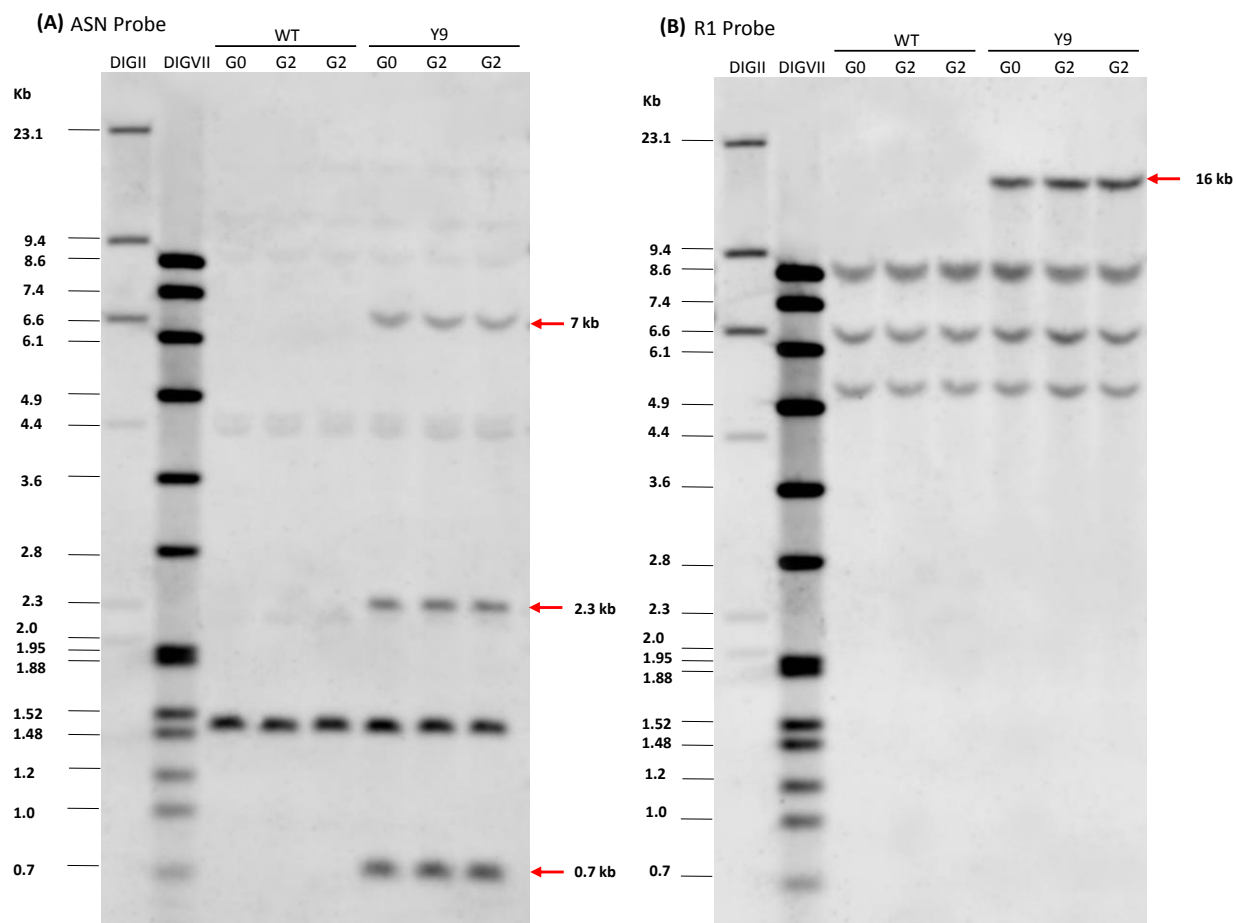


Figure 3-46. Y9 Insert Stability in G0 and G2 Clonal Cycles as Visualized with ASN and R1 Probes

Southern blots of genomic DNA isolated from G0 and G2 plants of Atlantic control (WT) and Y9 hybridized with (A) ASN probe or (B) R1 probe. Four μ g of each sample were digested with EcoRV and separated by electrophoresis prior to transfer and hybridization with the indicated probe. Red arrows indicate pSIM1278 insert bands. Molecular weight markers (DIGII and DIGVII) were included with band sizes indicated in kilobase pairs (kb).

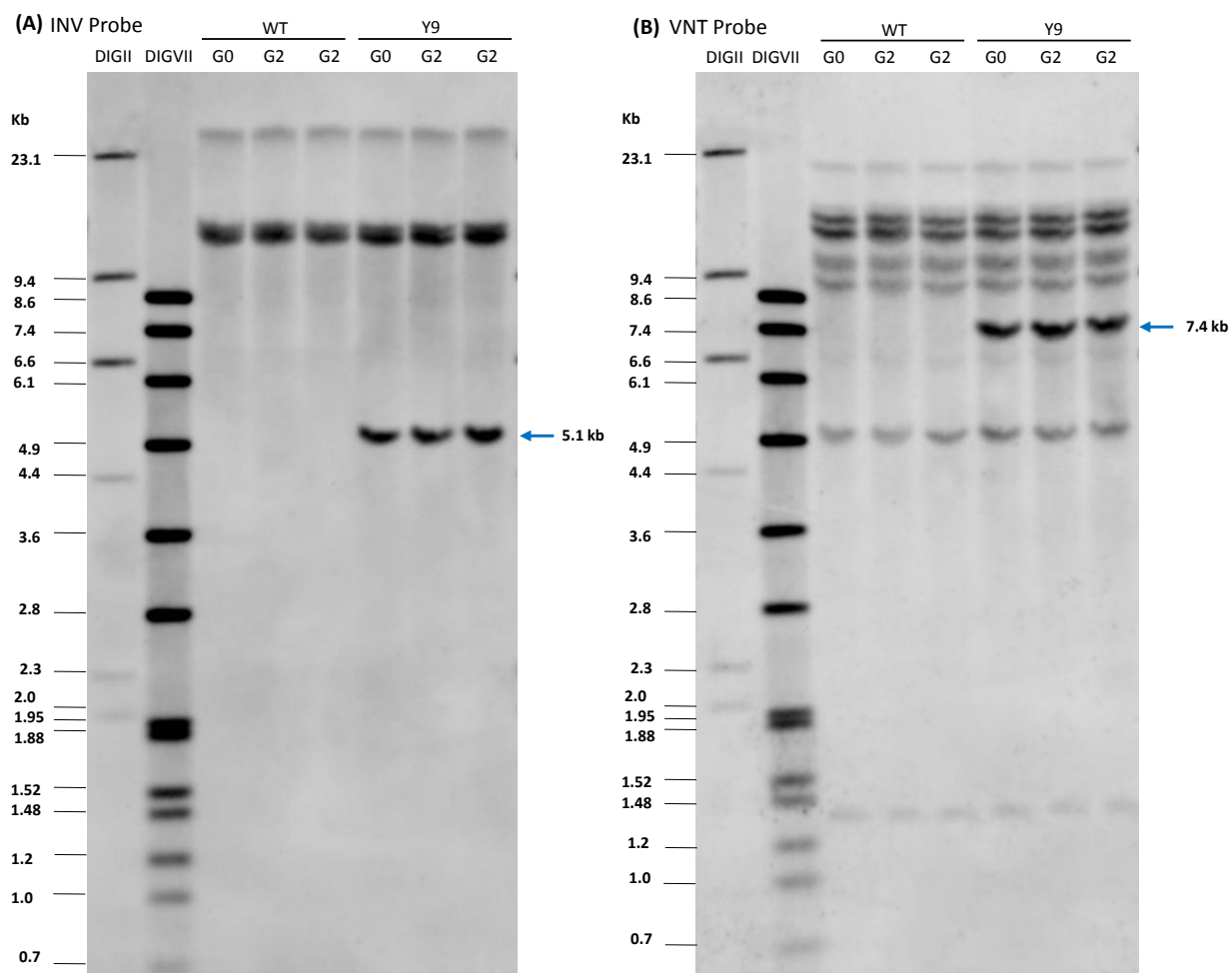


Figure 3-47. Y9 Insert Stability in G0 and G2 Clonal Cycles as Visualized with INV and VNT Probes
 Southern blots of genomic DNA isolated from G0 and G2 plants of Atlantic control (WT) and Y9 hybridized with (A) INV probe or (B) VNT probe. Four μg of each sample were digested with EcoRV and separated by electrophoresis prior to transfer and hybridization with the indicated probe. Blue arrows indicate pSIM1678 insert bands. Molecular weight markers (DIGII and DIGVII) were included with band sizes indicated in kilobase pairs (kb).

3.5 Summary of the Genetic Characterization of X17 and Y9

Molecular characterization showed that X17 contains a single insertion locus for each of the pSIM1278 and pSIM1678 inserts. For X17, the structure of the pSIM1278 and pSIM1678 inserts consist of a nearly full-length T-DNA. Molecular characterization showed that Y9 contains a single insertion locus for each of the pSIM1278 and pSIM1678 inserts. The single insert from pSIM1278 consists of a nearly full-length T-DNA flanked by an additional Asn1/Ppo5 down-regulation cassette on one side and a partial PhL/R1 cassette on the other side. The single insert from pSIM1678 consists of a nearly full-length T-DNA flanked by an additional partial VInv cassette. No backbone sequences were introduced into X17 or Y9 during transformation, and the insertions in X17 and Y9 are stable over multiple potato clonal cycles.

4.0 Gene Down-Regulation in X17 and Y9

X17 and Y9 were developed by transforming Ranger Russet and Atlantic varieties with pSIM1278 and then retransforming with pSIM1678. The pSIM1278 construct introduced two cassettes intended to down-regulate expression of the *Asn1*, *Ppo5*, *PhL*, and *R1* genes. The retransformation with pSIM1678 introduced a cassette to down-regulate the *Vlnv* gene.

Each cassette is driven by promoters primarily active in tubers to facilitate tissue-specific down-regulation. The effectiveness of target gene down-regulation and tissue-specificity was evaluated by northern blot analysis in potato tuber and leaf tissues.

4.1 Down-Regulation in X17 Tuber and Leaf Tissues

RNA was isolated from field-grown X17 and Ranger Russet control plants (WT) and analyzed by northern blot to determine the extent of down-regulation of the target genes. Tissue specificity was determined by comparing gene expression levels between tuber and leaf tissues.

The results showed that *Asn1*, *Ppo5*, and *Vlnv* genes were down-regulated in tubers (Figure 4-1). Partial down-regulation of *Asn1* was observed in leaf tissue. The 18S RNA and total RNA levels were consistent across samples allowing direct comparison of *Asn1*, *Ppo5*, *PhL*, *R1*, and *Vlnv* transcripts between samples in a given tissue.

The absence or decreased intensity of bands in X17 tuber samples probed for the target genes indicated down-regulation of these genes in X17 tubers compared to the WT controls (Figure 4-1). The extent of down-regulation varied, *Ppo5* and *Vlnv* down-regulation was particularly strong as nearly complete absence of the target RNA signal was observed. Decreased gene expression was not observed for the *PhL* and *R1* genes in X17 tubers.

A minor decrease in *Asn1* gene expression was observed in X17 leaf samples (Figure 4-2). There was no observable down-regulation of the other genes in X17 leaf samples compared to the WT control, consistent with tuber-specific gene silencing (Figure 4-2).

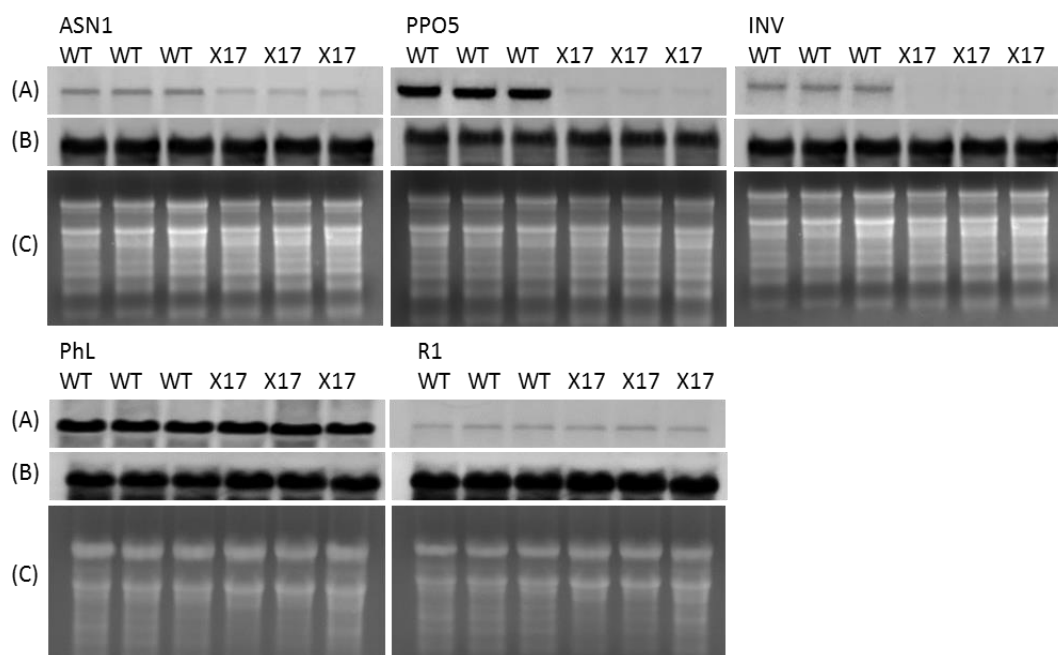


Figure 4-1. All RNAi-Targets Down-Regulated in X17 Tubers

Northern blots were probed for the RNAi target genes: *Asn1*, *Ppo5*, *PhL*, *R1*, and *VInv*. (A) Samples analyzed with the indicated probe. (B) 18S RNA as a gel loading control. (C) Total RNA is shown stained with ethidium bromide. Three biological replicates were evaluated in each gel.

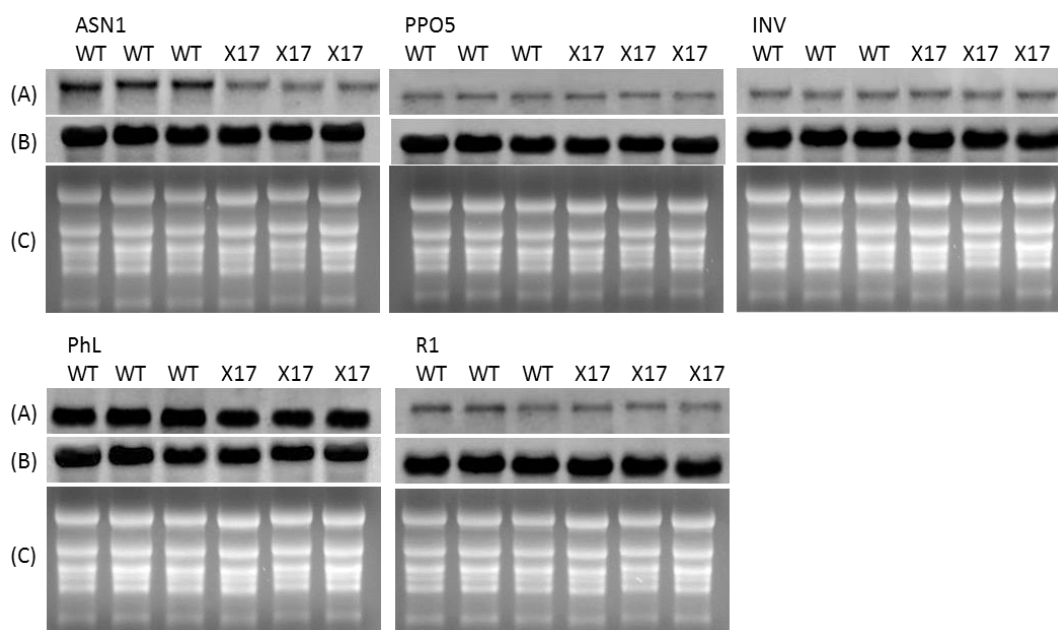


Figure 4-2. Minor Changes in *Asn1* Gene Expression in X17 Leaves

Northern blots were probed for the RNAi target genes: *Asn1*, *Ppo5*, *PhL*, *R1*, and *VInv*. (A) Samples analyzed with the indicated probe. (B) 18S RNA as a gel loading control. (C) Total RNA is shown stained with ethidium bromide. Three biological replicates were evaluated in each gel.

4.2 Down-Regulation in Y9 Tuber and Leaf Tissues

RNA was isolated from field-grown Y9 and Atlantic control plants (WT) and analyzed by northern blot to determine the extent of down-regulation of the target genes. Tissue specificity was determined by comparing gene expression levels between tuber and leaf tissues.

The results showed that *Asn1*, *Ppo5*, *PhL*, and *Vlnv* genes were down-regulated in tubers (Figure 4-3). Partial down-regulation of *Asn1* was observed in leaf tissue. The 18S RNA and total RNA levels were consistent across samples allowing direct comparison of *Asn1*, *Ppo5*, *PhL*, *R1*, and *Vlnv* transcripts between samples in a given tissue.

The absence or decreased intensity of bands in Y9 tuber samples probed for *Asn1*, *Ppo5*, *PhL*, and *Vlnv* indicated down-regulation of these genes in Y9 tubers compared to the Atlantic controls (WT) (Figure 4-3). The down-regulation of *Asn1*, *Ppo5*, and *Vlnv* was particularly strong as indicated by the nearly complete absence of target RNA signal. The down-regulation of *PhL* was not to the same extent, but did show decreased expression compared to the Atlantic control. The *R1* gene did not show any down-regulation.

A minor decrease in *Asn1* gene expression was observed in Y9 leaf samples (Figure 4-4). There was no observable down-regulation of the other genes in Y9 leaf samples compared to the WT control consistent with tuber-specific gene silencing (Figure 4-4).

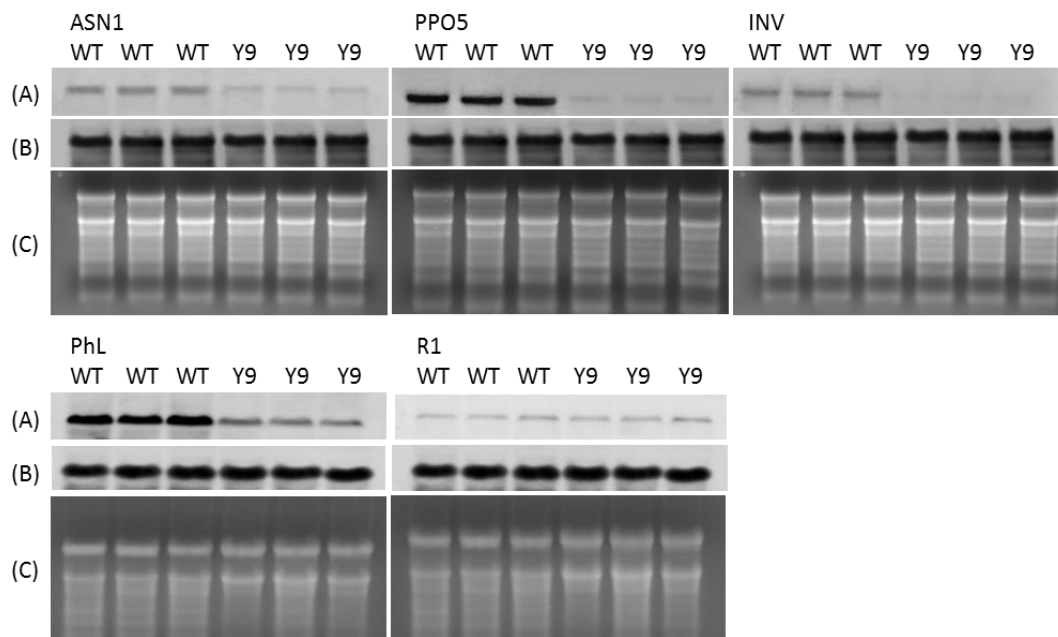


Figure 4-3. RNAi Target Gene Down-Regulation in Y9 Tubers

Northern blots were probed for the RNAi target genes: *Asn1*, *Ppo5*, *PhL*, *R1*, and *Vlnv*. (A) Samples analyzed with the indicated probe. (B) 18S RNA as a gel loading control. (C) Total RNA is shown stained with ethidium bromide. Three biological replicates were evaluated in each gel.

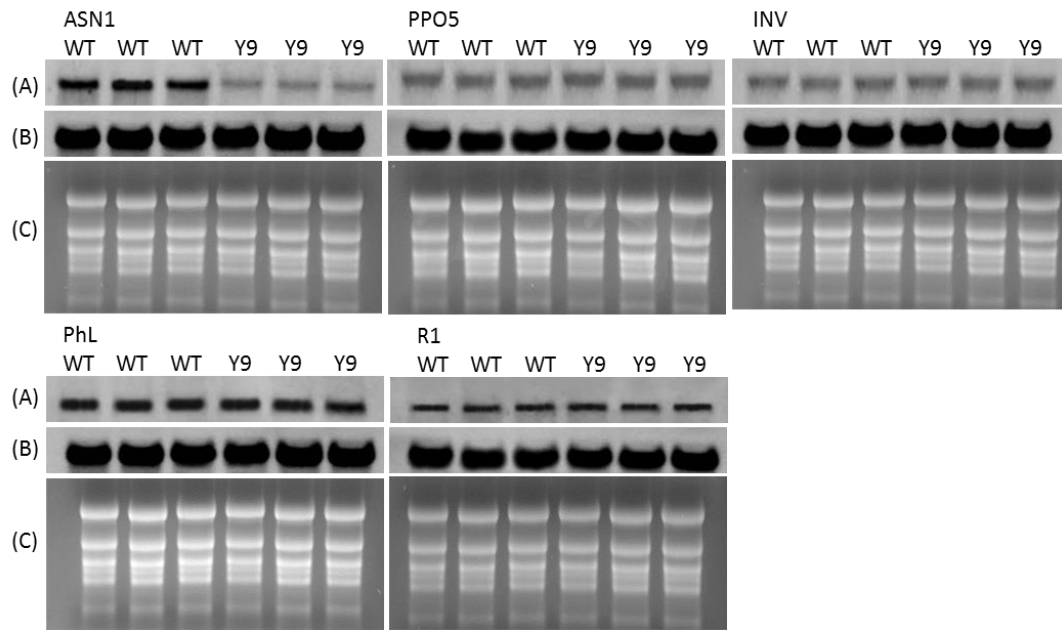


Figure 4-4. RNAi Target Gene Down-Regulation in Y9 Leaf

Northern blots were probed for the RNAi target genes: *Asn1*, *Ppo5*, *PhL*, *R1*, and *VInv*. (A) Samples analyzed with the indicated probe. (B) 18S RNA as a gel loading control. (C) Total RNA is shown stained with ethidium bromide. Three biological replicates were evaluated in each gel.

5.0 The VNT1 Protein in X17 and Y9

VNT1 is the only introduced protein in X17 and Y9 as the intended result of transforming with pSIM1278 and pSIM1678. Information about the identity of the VNT1 protein, its mode of action in potato, the levels of VNT1 protein and *Rpi-vnt1* transcript in X17 and Y9 leaf and tuber tissue, late blight efficacy, and a safety assessment for the VNT1 protein are summarized briefly below. These data are being reviewed by EPA as part of a Section 3 registration application and petition for a permanent exemption from the requirement of a tolerance for the VNT1 protein and the genetic material necessary for its production in potatoes.

5.1 VNT1 Protein Identity

Resistance proteins (R-proteins), such as VNT1, are found in animals and plants and function as signal transduction ATPases, playing an important role in pathogen recognition and signaling of immune responses (Leipe et al., 2004). The structure of R-proteins is highly conserved and consists of a central nucleotide-binding (NB) domain flanked on either side by an N-terminal toll-like/interleukin-1 or coiled-coil (CC) domain and a C-terminal leucine-rich repeat (LRR) domain (Takken and Govers, 2012). The LRR is the least conserved and has been hypothesized to function in effector recognition.

The *Rpi-vnt1.1* gene (accession: FJ423044.1) is one of three R-genes identified in the wild species *S. venturii* and is identical to the *Rpi-phu1* gene from the related species, *S. phureja* (Śliwka et al., 2013). The gene produces an 891 amino acid CC-NB-LRR R-protein (see Figure 5-1), which is a homolog of the Tm-2² tomato mosaic virus disease resistance protein (Foster et al., 2009).

```
001 MNYCVYKTWA VDSYFPFLIL TFRKKKFNEK LKEMAEIILLT AVINKSIEIA
051 GNVLFQEGTR LYWLKEDIDW LQREMRHIRS YVDNAKAKEV GGDSRVKNLL
101 KDIQQLAGDV EDLLDEFLPK IQQSNKFICC LKTVSFADEF AMEIEKIKRR
151 VADIDRVRTT YSITDTSNNN DDCIPLDRRR LFLHADETEV IGLEDDFNTL
201 QAKLLDHDLP YGVVSIVGMP GLGKTTLAKK LYRHVCHQFE CSGLVYVSQQ
251 PRAGEILHDI AKQVGLTEEE RKENLENNLR SLLKIKRYVI LLDDIWDVEI
301 WDDLKLVLP E CDSKIGSRII ITSRSNSVGR YIGGDFSIVH LQPLDSEKSF
351 ELFTKKIFNF VNDNWNANASP DLVNIGRCIV ERCGGIPLAI VVTAGMLRAR
401 GRTEHAWN RV LESMAHKIQD GCGKVLALSY NDLPIALRPC FLYFGLYPED
451 HEIRAFDLTN MWIAEKLIVV NTGNGREAES LADDVLNDLV SRNLIQVAKR
501 TYDGRISSCR IHDLLHSLCV DLAKESNFFH TEHNAFGDPS NVARVRRITF
551 YSDDNAMNEF FHLNPKPMKL RSLFCFTKDR CIFSQMAHLN FKLLQVLVVV
601 MSQKG YQHVT FPKKIGNMSC LRYVRLEGAI RVKLPNSIVK LKCLETL DIF
651 HSSSKLPFGV WESKILRHLC YTEECYCVSF ASPFCRIMPP NNLQTLMWVD
701 DKFCEPRL LH RLINLRTL CI MDVSGSTIKI LSALSPVPRA LEVLKLRFFK
751 NTSEQINLSS HPNIVELGLV GFSAMLLNIE AFPPNLVKLN LVGLMVDGHL
801 LAVLKKLPKL RILILLWCRH DAEKMDLSGD SFPQLEVLVI EDAQGLSEVT
851 CMDDMSMPKL KKLFLVQGNP ISPISLRVSE RLAKLRISQV L
```

Figure 5-1. Amino Acid Sequence of VNT1

5.2 Mode of Action

The expression of *Rpi-vnt1* confers broad-spectrum, late blight resistance in wild and cultivated potato. The VNT1 protein, as part of the plant immune system, recognizes the Avr-vnt1 effector protein secreted by *P. infestans* and signals a hypersensitive response that destroys infected tissue through programmed cell death, restricting growth and spread of the pathogen to other parts of the plant (Moffett et al., 2002; Morel and Dangl, 1997; Pel, 2010; Rairdan et al., 2008).

R-protein expression and signal transduction are tightly regulated in the cell by maintaining low protein levels, which are kept in an inactive state through intramolecular protein interactions that block signaling until conformational changes due to specific cognate ligand (effector) binding activate signal transduction (Spoel and Dong, 2012). Importantly, unlike Bt proteins, R-proteins do not confer pest resistance by directly targeting the pest or acting as toxins. Instead, they activate a hypersensitive response within the host plant that restricts spread of the pathogen.

5.3 Levels of the VNT1 Protein in X17 and Y9 Tissues

Expression of the *Rpi-vnt1* gene in X17 and Y9 is driven by the native VNT1 promoter. In general, R-proteins are expressed at low levels in plants—in some cases estimated to be as low as 18 ppt (Bushey et al., 2014). Numerous homologs of *Rpi-vnt1* are present in potato varieties and other wild *Solanum* species (Jupe et al., 2012). In order to distinguish the VNT1 protein in X17 and Y9 from endogenous homologs in potato, a western immunoblot assay was developed. A VNT1 polyclonal antibody was generated using a VNT1-specific peptide, FHSSSKLPFGVWESKIL, which is part of the LRR domain. R-protein homologs made development of a VNT1-specific antibody challenging. Despite the high sensitivity of the antibody, cross-reactivity was high in tuber and leaf samples.

VNT1 protein levels were assessed in field-grown X17 and Y9 leaf and tuber tissues. The limit of detection of VNT1 in the assay was 9 pg. The limits of quantitation for VNT1 in the assay were 30-60 ppb for tuber tissue and 60-70 ppb for leaf tissue, and were dependent on potato variety. Collectively, the data demonstrated that expression levels of the VNT1 protein were not above background levels and were conservatively estimated to be <100 ppb (Appendix C).

5.4 Levels of *Rpi-vnt1* Transcript in X17 and Y9 Tissues

Quantitative reverse-transcriptase polymerase chain reaction (RT-qPCR) was used to verify expression of the *Rpi-vnt1* transcript in X17 and Y9 leaf and tuber tissue. Total RNA was isolated from tissues of X17, Y9, and their respective controls and subjected to RT-qPCR using *Rpi-vnt1*-specific primers (see Appendix C for methods). Expression of *Rpi-vnt1* was normalized to a set of endogenous housekeeping genes, α -tubulin and elongation factor 1 α , within each sample.

Rpi-vnt1 mRNA transcript levels in X17, Y9, and respective control leaf tissues were compared to levels in the native *S. venturii* leaf (Figures 5-2 and 5-3). Expression of the *Rpi-vnt1* gene was similar between the two events, X17 and Y9, and *S. venturii* leaf tissue. Expression of *Rpi-vnt1* in Ranger Russet and Atlantic leaf was not detected. Significantly lower levels of *Rpi-vnt1* transcript were measured in X17 and Y9 tubers compared to X17 and Y9 leaf. High R-gene expression in leaf tissue, but not in tuber tissue, is consistent with other work on the expression levels of R-genes (Pel, 2010). The data indicate that, like W8, the *Rpi-vnt1* gene is transcribed in X17 and Y9 leaf and tuber tissues, and are consistent with low levels of gene expression and protein accumulation in the plants.

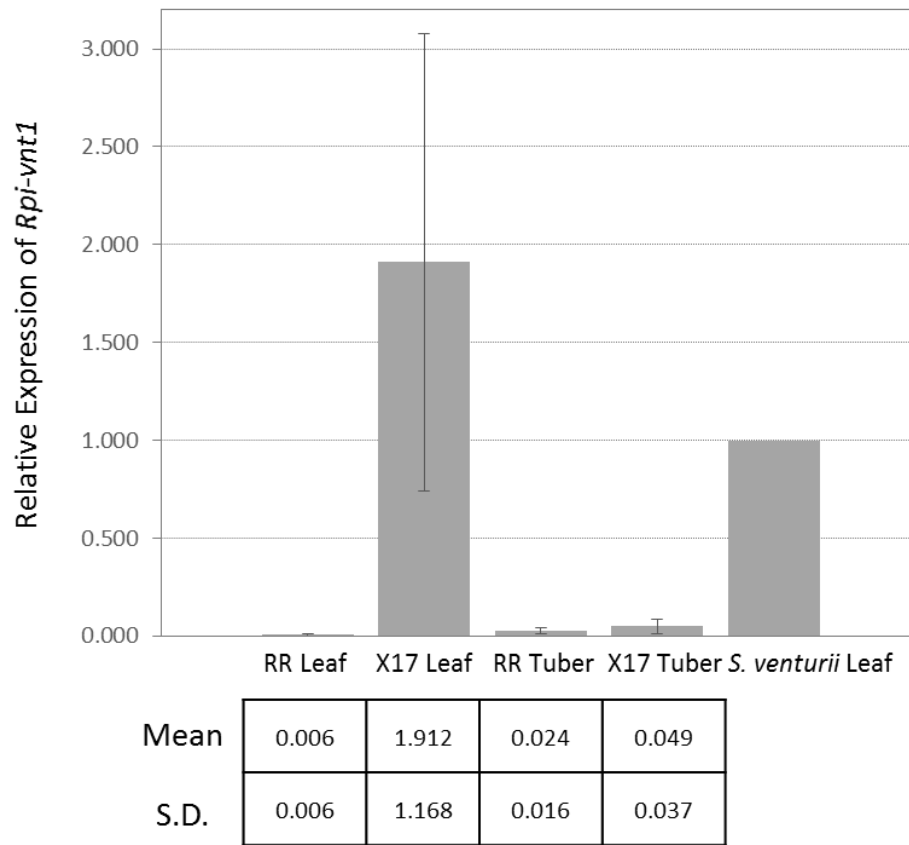


Figure 5-2. *Rpi-vnt1* Transcript Levels in X17 Measured by RT-qPCR

Transcript levels in X17 and Ranger Russet (RR) tuber and leaf tissue were analyzed as three biological replicates performed in triplicate. Data are shown relative to *S. venturii*.

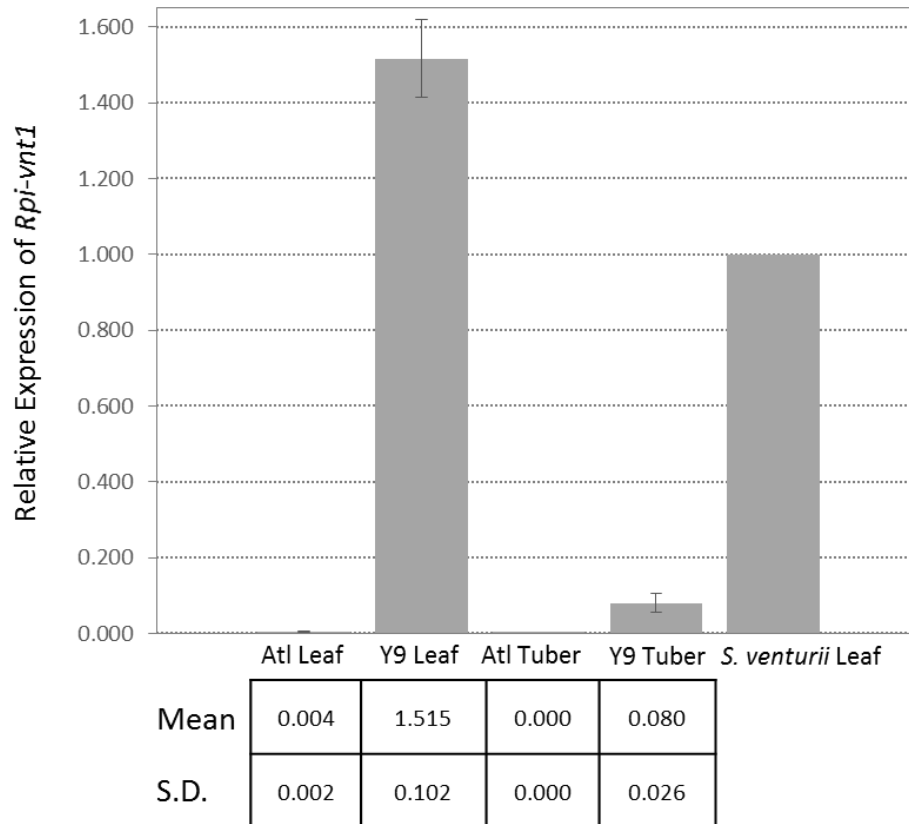


Figure 5-3. *Rpi-vnt1* Transcript Levels in Y9 Measured by RT-qPCR

Transcript levels in Y9 and Atlantic tuber and leaf tissue were analyzed as three biological replicates performed in triplicate. Data are shown relative to *S. venturii*.

5.5 Efficacy of the *Rpi-vnt1* Gene in Field Trials

Field trials to evaluate the foliar efficacy of the *Rpi-vnt1* gene in X17 and Y9 against *P. infestans* were conducted at a total of five sites during the 2013 and 2014 growing seasons. Plots were inoculated with strains US-8, US-22, or US-23. The degree of foliar infection was rated throughout the season. Similar to W8, a significant reduction in disease progression of late blight was observed in X17 and Y9 compared to controls, demonstrating late blight efficacy.

5.6 Safety Assessment of VNT1

The food and feed safety assessment of the VNT1 protein expressed in X17 and Y9 considered several factors, including safety of the donor organism, history of safe use, allergenic and toxic potential, and dietary exposure. Information and data related to these topics are being evaluated by EPA. Using bioinformatics, a comprehensive analysis of possible homology between toxins and allergens with the VNT1 protein sequence was conducted. The analyses demonstrated that the VNT1 protein does not have amino acid sequence similarities with known allergens or protein toxins that could have adverse effects to human or animal health.

6.0 Comparative Assessment of X17 and Y9

As was done for W8, phenotypic and compositional comparative assessments were conducted to determine the comparability of X17 and Y9 to conventional potatoes that have a long history of safe use in the environment and as food and feed.

To ensure accurate evaluations of X17 and Y9, proper selection of comparator varieties was important. For X17 and Y9, the most relevant comparators are their non-transformed parental varieties, Ranger Russet and Atlantic, respectively. The only difference between transformed events and their respective parental varieties is that X17 and Y9 underwent transformation and contain the pSIM1278 and pSIM1678 inserts. Statistical analysis was used to determine whether X17 and Y9 were different from controls.

Other important comparators include additional varieties of conventional potatoes that are grown in typical potato-growing regions. These represent potato varieties that are planted commercially and are used to assess the normal range of phenotypic and compositional variation. For agronomic and phenotypic studies, commercial potato varieties were used to generate a conventional variety range for all parameters. For composition, data obtained from conventional varieties grown in Simplot studies in 2012, 2013, and 2014 was used to generate a statistical tolerance interval (see Appendix D for details). This tolerance interval predicts, with 95% confidence, 99% of the expected values for a given analyte. It uses the variability in the existing data set to calculate the predicted range for each analyte, given a larger dataset. This provides helpful context to understand the expected range of composition in conventional potato varieties using the same analytical methods as were used for X17 and Y9. Scientific literature was also assessed to provide a combined range of analyte values for conventional potatoes, giving further context to results.

Simplot has submitted conventional potato composition data for inclusion in the ILSI Crop Composition Database. These data will be available for viewing upon publication of an updated database (<https://www.cropcomposition.org/query/cite.html>).

Comparative assessment data were interpreted, after statistical analysis, as follows:

- When p-values were available and the p-value indicated no statistical significance, it was unlikely that there was a difference that was meaningful, and the assessment was considered complete; and
- If the p-value indicated statistical significance or if a p-value was not present, the mean value for the event was compared to a tolerance interval, conventional variety range (CVR), or combined literature range. Mean X17 and Y9 values within these ranges were considered within the natural variation for potatoes and any difference was unlikely to be meaningful.

The phenotype and compositional comparative assessments for X17 and Y9 are provided in Section 7.0 and Section 8.0, respectively. The analyses indicate that X17 and Y9 are comparable to their corresponding parental varieties and other conventional potatoes with respect to the characteristics measured. Overall, these analyses indicate that X17 and Y9 are not materially different from conventional potatoes, pose no more risk than conventional potato varieties in food, feed, and the environment, and are as safe and nutritious as conventional potato varieties.

7.0 Phenotypic Performance and Field Observations for X17 and Y9

The purpose of the phenotypic performance and field observation studies was to assess X17 and Y9 phenotypes compared to conventional Ranger Russet and Atlantic varieties, respectively, when grown potato-producing regions of the U.S. Observations throughout the growing season were used to make a thorough assessment of the characteristics listed in Table 7-1 and Table 7-2. The list of tuber evaluation characteristics differ between X17 and Y9 because characteristics for fry and chip varieties are different.

Table 7-1. Characteristics Evaluated for X17

Phenotypic Performance	Tuber Evaluation	Environmental Interactions
Early Emergence	Total Yield	Insect Stressors
Final Emergence	US#2 Yield	Disease Stressors
Stems Per Plant	Tubers Per Plant	Abiotic Stressors
Plant Vigor	Tuber Grading	Arthropod Abundance
Plant Height	Specific Gravity	
Vine Desiccation	High Sugar	
	Sugar Ends	
	Fry Color	

Table 7-2. Characteristics Evaluated for Y9

Phenotypic Performance	Tuber Evaluation	Environmental Interaction
Early Emergence	Total Yield	Insect Stressors
Final Emergence	US#1 Yield	Disease Stressors
Stems Per Plant	Tubers Per Plant	Abiotic Stressors
Plant Vigor	Tuber Grading	Arthropod Abundance
Plant Height	Specific Gravity	
Vine Desiccation	Total Internal Defects	

The assessments, described in detail below, demonstrate that X17 and Y9 are agronomically and phenotypically comparable to their respective parental varieties and other conventional potatoes. Introducing the pSIM1278 and pSIM1678 inserts into X17 and Y9 did not result in unintended effects associated with weediness or pest-like characteristics. The phenotypic comparability of X17 and Y9 with conventional controls supports the lack of somaclonal variation in the events.

7.1 Field Trial Details

Field trial years and locations are shown for X17 studies in Table 7-3 and for Y9 studies in Table 7-4. The agronomic practices, including soil preparation, fertilizer application, irrigation, and pesticide-based control methods, were location-specific and typical for potato. Cultivation practices were recommended by regional potato extension specialists and agronomists.

Trials for X17 in 2013 and 2014 were located in the same county, but not the same location, in different fields or in different places on the farm due to crop rotation requirements (Table 7-3). Field conditions such as environment, field history, soil type, pest presence, and drainage differ from year to year, and each county and year combination was considered a unique site.

While every effort was made to follow consistent study protocols, differences in planted material occurred based on typical seed propagation practices for potatoes. In 2013, small X17 minitubers (G0) were used as the planting material, and in 2014, larger X17 seed pieces (FG1) were used (Table 7-3). Commercial propagation of potato seed also uses minitubers from plantlets in the first year, followed by field-grown seed in the second year. Even with differences in seed, it is appropriate to combine results because in each year the test and control seed were of the same type. Comparison by year was not part of the experimental design.

Table 7-3. X17 Field Trial Locations

Year	Site State	Site County	Rows x Tubers/Row	Material Planted	Plant Date, Harvest Date
2013	ID	Canyon	2x20	Minitubers G0	4/15/13, 9/19/13
		Minidoka	6x20		4/23/13, 9/19/13
	WA	Grant	6x20		4/16/13, 9/11/13
		Adams	2x20		4/18/13, 10/10/13
	WI	Adams	2x20		5/9/13, 9/26/13
2014	ID	Jerome	4x20	FG1	4/29/14, 10/10/14
		Minidoka	4x20		4/30/14, 9/18/14
	ND	Grand Forks	4x20		5/29/14, 9/25/14
	WA	Franklin	4x20		4/22/14, 10/1/14
		Grant	4x20		4/23/14, 9/10/14

Note: Additional varieties including other events, controls, and references were included in the experimental design at some sites.

At all sites, a randomized complete block design with four replications was used. Within each block, each potato variety was planted in plots arranged in random order. In 2013, plots contained two or six rows. In 2014, plots contained four rows. The number of rows per plot was adjusted depending on the number of tuber samples required.

The experimental unit is the plot. A plot is planted with a specified number of seed tubers and contains only one treatment (potato variety). Plots were 2, 4, or 6 rows wide and 20 feet long. Typical seed spacing for potatoes was one tuber per foot of row. Therefore, 80 seed tubers would be planted to create a plot 4 rows wide and 20 feet long. The seed pieces were placed by hand or machine to a depth of 2-4 inches. Additional method details are found in Appendix D.

Table 7-4. Y9 Field Trial Locations

Year	Site State	Site County	Rows x Tubers/Row	Material Planted	Planting Date, Harvest Date
2014	ID	Jerome	4x20	FG1	4-29-2014, 10-10-2014
		Minidoka			4-30-2014, 9-18-2014
	PA	Berks			5-21-2014, 10-16-2014
	MI	Montcalm			5-13-2014, 9-23-2014
	ND	Grand Forks			5-29-2014, 9-25-2014
	WA	Franklin			4-22-2014, 10-01-2014
		Grant			4-23-2014, 9-10-2014

Note: Additional varieties including other events, controls, and references were included in the experimental design at some sites.

7.2 X17 and Y9 Phenotypic and Tuber Assessment Results

All the observed means were within the CVR and no meaningful differences were found, although some statistical differences were observed, between X17 or Y9 and their respective controls. Summaries of the phenotypic and tuber characteristics (yield and grading) are shown in Table 7-5 and Table 7-6 for X17 and Y9, respectively. Explanations of the scoring systems can be found in Appendix D.

No statistical differences were detected between X17 and the Ranger Russet control for total yield, US #2 yield, tubers per plant, tuber grading, sugar ends, fry color, or total internal defects. Specific gravity was higher for X17 compared to the control but within the CVR. Sugar levels were lower in X17 compared to the control, but within the CVR. Fry color 00 scoring was greater for X17 compared to the control, but within the CVR. None of these changes would indicate greater environmental impact of X17 compared to conventional potatoes.

No differences were detected between Y9 and the Atlantic control for total yield, US #1 yield, tubers per plant, tuber grading, and total internal defects. Specific gravity was higher for Y9 compared to the control, but within the CVR. This change would not indicate greater environmental impact of Y9 compared to conventional potatoes.

Overall, the results demonstrate there are no meaningful differences between X17, Y9, and their respective controls. The data support the conclusion that X17 and Y9 are unlikely to have increased plant pest potential compared to conventional varieties.

Table 7-5. Phenotypic, Yield, and Grading Characteristics of X17

Characteristic	Variety	N	Mean	P-Value ¹	SD	CVR Min ²	CVR Max ²
Phenotypic Performance							
Early Emergence (%)	X17	40	50.6	0.1754	23.5	0.0	100.0
	Ranger Ctrl	40	61.7		21.4		
Final Emergence (%)	X17	40	89.7	0.4499	11.2	10.6	100.0
	Ranger Ctrl	40	94.2		7.5		
Stems Per Plant (#)	X17	40	2.6	0.6239	1.4	1.0	6.0
	Ranger Ctrl	40	2.5		1.5		
Plant Vigor (1-5 Scale) ³	X17	40	3.5	0.9550	0.9	1.3	5.0
	Ranger Ctrl	40	3.5		1.0		
Plant Height (cm)	X17	40	57.9	0.8712	16.0	16.4	108.7
	Ranger Ctrl	40	58.5		16.6		
Vine Desiccation (%)	X17	40	21.1	0.5728	20.3	0.0	100.0
	Ranger Ctrl	40	24.9		21.1		
Tuber Evaluation							
Total Yield (cwt/a)	X17	40	562.7	0.9484	207.8	89.2	1410.6
	Ranger Ctrl	40	564.3		221.8		
US#2 Yield (cwt/a)	X17	40	452.8	0.4995	174.6	118.9	693.5
	Ranger Ctrl	40	477.4		178.2		
Tubers Per Plant (#)	X17	40	7.1	0.3805	2.1	3.1	19.5
	Ranger Ctrl	40	6.2		1.9		
Tubers 4-6 oz. (%)	X17	40	19.5	0.2254	7.6	4.6	41.1
	Ranger Ctrl	40	16.7		7.1		
Tubers 6-10 oz. (%)	X17	40	25.4	0.2607	9.2	14.0	41.2
	Ranger Ctrl	40	28.6		9.2		
Tubers 10-14 oz. (%)	X17	40	14.1	0.1052	9.7	1.0	33.2
	Ranger Ctrl	40	17.2		9.8		
Tubers >14 oz. (%)	X17	40	13.6	0.7151	14.6	0.0	51.5
	Ranger Ctrl	40	15.1		13.4		
Specific Gravity	X17	40	1.090	0.0286	0.008	0.835	1.171
	Ranger Ctrl	40	1.086		0.011		
High Sugar (%)	X17	19	0.0	0.0334	0.0	0.0	84.8
	Ranger Ctrl	20	9.3		19.5		
Sugar Ends (%)	X17	39	1.6	0.1351	2.9	0.0	52.6
	Ranger Ctrl	40	7.1		11.1		

Table 7-5. Phenotypic, Yield, and Grading Characteristics of X17 (continued)

Characteristic	Variety	N	Mean	P-Value ¹	SD	CVR Min ²	CVR Max ²
Fry Color 00 (%)	X17	20	4.5	<u>0.0135</u>	3.7	0.0	4.8
	Ranger Ctrl	20	1.7		2.1		
Fry Color 0 (%)	X17	39	56.6	0.1966	42.7	0.0	100.0
	Ranger Ctrl	40	47.8		38.5		
Fry Color 1 (%)	X17	39	0.0	0.1408	0.0	0.0	29.7
	Ranger Ctrl	40	3.4		8.8		
Fry Color 2 (%)	X17	39	0.1	0.3416	0.8	0.0	28.8
	Ranger Ctrl	40	3.4		8.5		
Fry Color 3 (%)	X17	39	0.0	0.1498	0.0	0.0	23.1
	Ranger Ctrl	40	1.2		3.9		
Fry Color 4 (%)	X17	39	0.0	0.1348	0.0	0.0	79.7
	Ranger Ctrl	40	3.4		13.1		
Total Internal Defects (%)	X17	40	0.8	0.9104	1.9	0.0	93.8
	Ranger Ctrl	40	1.0		2.1		

¹ P-values indicating significant differences with controls are underlined and in bold.

² The range of mean values of conventional varieties.

Table 7-6. Phenotypic, Yield, and Grading Characteristics of Y9

Characteristic	Variety	N	Mean	P-Value ¹	SD	CVR Min ²	CVR Max ²
Phenotypic Performance							
Early Emergence (%)	Atlantic Ctrl	28	72.1	0.3276	22.7	0	100
	Y9	28	67.2		20.5		
Final Emergence (%)	Atlantic Ctrl	28	96.0	0.4245	10.9	10.6	100
	Y9	28	93.8		10.2		
Stems Per Plant (#)	Atlantic Ctrl	28	3.3	0.9439	0.5	1	6
	Y9	28	3.3		0.7		
Plant Vigor (1-5 Scale)	Atlantic Ctrl	28	4.1	0.8785	0.9	1.3	5
	Y9	28	4.1		1.1		
Plant Height (cm)	Atlantic Ctrl	28	59.5	0.8858	15.6	16.4	108.7
	Y9	28	59.2		16.5		
Vine Desiccation (%)	Atlantic Ctrl	28	42.5	0.1516	28.7	0	100
	Y9	28	50.5		25.4		
Tuber Evaluation							
Total Yield (cwt/a)	Atlantic Ctrl	28	566.5	0.393	201.3	89.2	1410.6
	Y9	28	535.7		198.0		
US#1 Yield (cwt/a)	Atlantic Ctrl	28	512.5	0.1676	202.4	118.9	693.5
	Y9	28	467.5		206.3		
Tubers Per Plant (#)	Atlantic Ctrl	28	11.6	0.7709	4.0	3.1	19.5
	Y9	28	11.8		3.6		
Tuber Grading Size A (%)	Atlantic Ctrl	28	67.9	0.8448	12.3	28	83.3
	Y9	28	67.1		7.9		
Tuber Grading Size B (%)	Atlantic Ctrl	28	8.6	0.0564	8.3	2	70.5
	Y9	28	11.2		8.8		

¹ P-values indicating significant differences with controls are underlined and in bold.

² The range of mean values of conventional varieties.

Table 7-6. Phenotypic, Yield, and Grading Characteristics of Y9 (continued)

Characteristic	Variety	N	Mean	P-Value ¹	SD	CVR Min ²	CVR Max ²
Oversized (%)	Atlantic Ctrl	28	17.8	0.3732	16.0	0	45.7
	Y9	28	14.7		11.3		
Pick-outs (%)	Atlantic Ctrl	28	2.9	0.1471	3.8	0	17.3
	Y9	28	4.9		5.5		
Specific Gravity	Atlantic Ctrl	28	1.089	<u>0.0003</u>	0.0086	0.835	1.171
	Y9	28	1.092		0.0092		
Total Internal Defects (%)	Atlantic Ctrl	28	3.2	0.7891	1.7	0	93.8
	Y9	28	3.4		1.6		

¹P-values indicating significant differences with controls are underlined and in bold.

²The range of mean values of conventional varieties.

7.3 Insect, Disease, and Abiotic Stressor Assessments

Naturally occurring biotic (insect and disease) and abiotic (environmental conditions) stressors were observed and recorded by the principal investigators with expertise in potato cultivation. The stressor observations provided the opportunity to assess X17 and Y9 across a range of stressors in multiple locations and at several time points throughout the growing season. Observations were made of potential environmental interactions. Recorded stressors varied depending on the stressors present or expected to be present at each site. Even if no stressors were present, zeroes were recorded because the stressors were looked for and comparisons can be made between X17, Y9 and the controls. Examples of common potato disease and insect symptoms can be found in Appendix D, Table 17-1.

Stressors were rated at early season, midseason, and late season on a 0 to 3 scale, where:

0 = No symptoms observed;

1 = Slight symptoms were observed, but not interfering with plant development;

2 = Moderate symptoms were present, intermediate between slight and severe; and

3 = Severe symptoms were observed that interfered with plant development.

The insect, disease, and abiotic stressor evaluations for X17, Y9 and the conventional controls are shown in Table 7-7 and Table 7-8. Stressor evaluations were intended to be categorical and were not statistically analyzed. The range of ratings for X17 and Ranger Russet, and Y9 and Atlantic, were compared for each observation. A difference occurred when the ranges of X17 and Y9 did not overlap with the ranges of Ranger Russet and Atlantic, respectively.

No differences were observed between X17 and Y9 and their respective controls for any of the insect, disease, or abiotic stressors assessed. The results support the conclusion that the ecological interactions of X17 and Y9 are the same as conventional potatoes. X17 and Y9 are not expected to impact non-target organisms or differ with respect to insect, disease, or abiotic stressors, other than intended late blight resistance.

Table 7-7. X17 Abiotic and Biotic Stressor Observations

Stressor	Total Observations	Without Differences	With Differences
Insect Stressors			
Aphid	15	15	0
Colorado Potato Beetle	15	15	0
Leaf Hopper	6	6	0
Looper	9	9	0
Disease Stressors			
Black Dot	1	1	0
Black Leg	3	3	0
Early Blight	14	14	0
Gray Mold	1	1	0
Leaf Roll Virus	1	1	0
Potato Virus Y	1	1	0
Rhizoctonia	4	4	0
Stem Rot	3	3	0
Verticillium Wilt	9	9	0
White Mold	6	6	0
Abiotic Stressors			
Cold Stress	2	2	0
Compaction	1	1	0
Drought	6	6	0
Excessive Moisture	2	2	0
Frost	2	2	0
Hail Damage	9	9	0
Heat Stress	9	9	0
Nutrient Imbalance	1	1	0
Sun Scald	3	3	0
Wind Damage	9	9	0

Table 7-8. Y9 Abiotic and Biotic Stressor Observations

Stressor	Total Observations	Without Differences	With Differences
Insect Stressors			
Aphid	19	19	0
Colorado Potato Beetle	21	21	0
Flea Beetle	4	4	0
Leaf Hopper	10	10	0
Looper	9	9	0
Disease Stressors			
Black Dot	2	2	0
Black Leg	4	4	0
Botrytis	2	2	0
Fusarium	1	1	0
Gray Mold	2	2	0
Leaf Roll Virus	3	3	0
Brown Leaf Spot	22	22	0
Potato Virus Y	1	1	0
Rhizoctonia	4	4	0
Sclerotinia	2	2	0
Stem Rot	1	1	0
Verticillium Wilt	9	9	0
White Mold	8	8	0
Abiotic Stressors			
Cold Stress	1	1	0
Compaction	2	2	0
Drought	10	10	0
Excessive Moisture	5	5	0
Frost	3	3	0
Hail Damage	9	9	0
Heat Stress	16	16	0
Nutrient Imbalance	3	3	0
Sun Scald	3	3	0
Wind Damage	10	10	0

7.4 Conclusions for Agronomic Performance and Field Observations

Results of the agronomy trials confirmed that, like W8, X17 and Y9 are phenotypically and agronomically similar to control varieties, Ranger Russet and Atlantic, when grown at locations representing major areas of potato production in the U.S. Observations throughout the growing season demonstrated no meaningful differences in phenotypic and agronomic characteristics, including tuber characteristics and biotic and abiotic stress susceptibility. No phenotypes that would indicate enhanced weediness, survivability, or plant pest potential were noted for X17 or Y9.

8.0 Compositional Assessment for X17 and Y9

As with W8, compositional analysis of X17 and Y9 was conducted to evaluate the levels of key nutrients (proximates, vitamins, amino acids, and minerals) and glycoalkaloids compared to controls, Ranger Russet and Atlantic varieties. In addition, concentrations of free amino acids, sugars, and acrylamide were measured to evaluate lower acrylamide potential and lowered reducing sugars. The U.S. FDA will review the details of the compositional analyses as a component of the food and feed safety assessment of X17 and Y9 potatoes.

Tubers for the compositional assessment were generated from the field studies used for phenotypic testing (see Table 7-3 and Table 7-4). An exception is that X17 tubers from two 2013 sites (Canyon County, ID and Adams County, WA) were not used for compositional analysis. Therefore, X17 composition data comes from eight sites, and Y9 composition data comes from seven sites. All tubers were grown in commercial potato-growing regions of the U.S.

Test (X17 or Y9), control, and reference tubers were assessed for analytes important to potato nutrition, and those related specifically to trait efficacy. Each sample (replication) consisted of six randomly selected, mid-sized tubers with skin. Samples were powdered in an industrial blender with liquid nitrogen and stored at -70 °C until analysis. Analytical testing was conducted by Covance Laboratories, Inc. Method details for compositional and statistical analyses are in Appendix D.

The nutritional assessment evaluated levels of proximates, vitamins, minerals, amino acids, and glycoalkaloids and demonstrated that X17 and Y9 are compositionally equivalent to respective controls. Trait efficacy assessment evaluated free amino acids, reducing sugars, and acrylamide concentrations in fries and chips and demonstrated that, as expected, X17 and Y9 have lower levels of free asparagine, lower levels of reducing sugars, and lower acrylamide potential compared to Ranger Russet and Atlantic varieties, respectively. The same conclusions were reached for W8, the antecedent event, compared to Russet Burbank.

8.1 Compositional Nutrient Analysis

Analyses were conducted to evaluate the nutritional composition of X17 and Y9 and assess the food quality, feed quality, and safety compared to Ranger Russet and Atlantic varieties and other conventional potatoes. The compositional assessments determined the concentrations of:

- Proximates, vitamins, and minerals (Tables 8-1 and 8-2);
- Total amino acids (Tables 8-3 and 8-4); and
- Glycoalkaloids (Tables 8-5 and 8-6).

8.1.1 Proximates, Vitamins, and Minerals

Mean values of proximate, vitamin, and mineral levels in X17 were within the tolerance interval and/or combined literature range. Statistical differences between X17 and the control were seen for crude fiber, vitamin C, and potassium.

Mean values of proximate, vitamin, and mineral levels in Y9 were within the tolerance interval and/or combined literature range. Statistical differences between Y9 and the control were seen for protein, crude fiber, carbohydrates, calories, moisture, and potassium.

In all cases, the mean X17 and Y9 values were within the tolerance interval and/or the combined literature range, demonstrating equivalency to conventional varieties.

Table 8-1. Proximates, Vitamins, and Minerals in X17 and Ranger Russet

Analyte	Variety	Mean	P-value ¹	S.D.	N	Range		Tolerance Interval		Combined Literature Range ²	
						Min	Max	Min	Max	Min	Max
Protein (%)	X17	2.32	0.6602	0.150	32	2.06	2.57	1.49	3.02	0.7	4.6
	Control	2.30		0.188	32	1.93	2.66				
Total Fat (%)	X17	0.151	0.9889	0.0420	32	0.100	0.250	0	0.397	0.02	0.2
	Control	0.150		0.0510	32	0.100	0.320				
Ash (%)	X17	0.961	0.1406	0.166	32	0.735	1.37	0.450	1.42	0.44	1.9
	Control	0.899		0.223	32	0.287	1.27				
Crude Fiber (%)	X17	0.591	<u>0.0242</u>	0.0950	32	0.449	0.820	0.212	0.807	0.17	3.5
	Control	0.533		0.0800	32	0.406	0.690				
Carbohydrates (%)	X17	20.2	0.1210	2.10	32	15.4	24.9	12.4	24.0	13.3	30.53
	Control	19.6		1.94	32	15.9	25.1				
Calories (kcal/100 g)	X17	91.3	0.1402	8.07	32	71.0	109	59.8	106	70	110.2
	Control	89.0		7.44	32	73.8	110				
Moisture (%)	X17	76.6	0.1346	2.02	32	72.0	81.4	72.6	84.3	63.2	86.9
	Control	77.1		1.87	32	71.8	81.0				
Vitamin B3 (mg/100 g)	X17	2.38	0.7212	0.219	32	1.98	2.82	0.721	3.05	0.09	3.1
	Control	2.41		0.184	32	2.07	2.83				
Vitamin B6 (mg/100 g)	X17	0.120	0.3832	0.0100	32	0.108	0.150	0.077	0.157	0.13	0.41
	Control	0.117		0.0120	32	0.104	0.150				
Vitamin C (mg/100 g)	X17	41.0	<u>0.0007</u>	4.73	32	32.0	48.1	11.2	45.7	1	54
	Control	35.8		7.18	32	20.0	47.0				
Copper (mg/100 g)	X17	0.0931	0.1868	0.0540	32	0.0500	0.290	0	0.251	0.0200	0.700
	Control	0.106		0.107	32	0.0500	0.640				
Magnesium (mg/100 g)	X17	23.6	0.9376	1.89	32	20.2	28.1	14.2	28.8	11.2	55.0
	Control	23.6		1.62	32	20.1	27.0				
Potassium (mg/100 g)	X17	463	<u>0.0475</u>	55.0	32	378	583	281	590	350	625
	Control	444		57.5	32	362	550				

¹ P-values indicating significant differences with controls are underlined and in bold.

² Combined literature ranges are from (Horton and Anderson, 1992; Lisinska and Leszczynski, 1989; Rogan et al., 2000; Talburt et al., 1987).

Table 8-2. Proximates, Vitamins, and Minerals in Y9 and Atlantic

Analyte	Variety	Mean	P-value ¹	S.D.	N	Range		Tolerance Interval		Combined Literature Range ²	
						Min	Max	Min	Max	Min	Max
Protein (%)	Y9	2.52	<u>0.0035</u>	0.217	28	2.14	2.88	1.49	3.02	0.7	4.6
	Control	2.42		0.281	28	1.90	2.93				
Total Fat (%)	Y9	0.131	0.5054	0.0480	28	0.100	0.250	0	0.397	0.02	0.2
	Control	0.145		0.0690	28	0.100	0.340				
Ash (%)	Y9	0.905	0.2192	0.192	28	0.464	1.22	0.450	1.42	0.44	1.9
	Control	0.968		0.128	28	0.707	1.22				
Crude Fiber (%)	Y9	0.469	<u>0.0432</u>	0.108	28	0.326	0.690	0.212	0.807	0.17	3.5
	Control	0.408		0.0930	28	0.233	0.620				
Carbohydrates (%)	Y9	20.6	<u>0.0107</u>	2.53	28	16.7	24.7	12.4	24.0	13.3	30.53
	Control	19.7		2.54	28	15.2	23.8				
Calories (kcal/100 g)	Y9	93.3	<u>0.0067</u>	10.2	28	77.6	111	59.8	106	70	110.2
	Control	89.4		10.1	28	73.0	107				
Moisture (%)	Y9	75.9	<u>0.0090</u>	2.59	28	71.4	79.8	72.6	84.3	63.2	86.9
	Control	76.8		2.51	28	72.4	81.0				
Vitamin B3 (mg/100 g)	Y9	1.69	0.408	0.165	28	1.45	2.03	0.721	3.05	0.09	3.1
	Control	1.64		0.216	28	1.34	2.22				
Vitamin B6 (mg/100 g)	Y9	0.118	0.8428	0.0110	28	0.103	0.140	0.077	0.157	0.13	0.41
	Control	0.117		0.0120	28	0.0980	0.140				
Vitamin C (mg/100 g)	Y9	25.5	0.926	4.90	28	16.1	35.1	11.2	45.7	1	54
	Control	25.5		5.99	28	11.9	36.6				
Copper (mg/100 g)	Y9	0.100	0.9053	0.039	28	0.057	0.250	0	0.251	0.0200	0.700
	Control	0.099		0.032	27	0.057	0.210				
Magnesium (mg/100 g)	Y9	20.3	0.6805	0.993	28	18.3	22.6	14.2	28.8	11.2	55.0
	Control	20.2		1.38	28	17.2	22.5				
Potassium (mg/100 g)	Y9	466	<u>0.0461</u>	40.0	28	401	541	281	590	350	625
	Control	453		41.7	28	355	511				

¹ P-values indicating significant differences with controls are underlined and in bold.

² Combined literature ranges are from (Horton and Anderson, 1992; Lisinska and Leszczynski, 1989; Rogan et al., 2000; Talburt et al., 1987).

8.1.2 Total Amino Acids

Levels of amino acids were measured for X17 and Y9 (Table 8-3 and Table 8-4, respectively). Although, differences were observed in amino acid levels in X17 and Y9, such changes would have minimal impact on food and feed safety considering the low levels of protein (about 2% fresh weight) in potatoes.

A significant difference between X17 and Ranger Russet was observed for all amino acids except histidine and tryptophan (Table 8-3). Aspartic acid was expected to be lower and glutamic acid was expected to be higher, in X17 compared to Ranger Russet, because of the down-regulation of the *Asn1* gene. In all cases, mean values were within the tolerance interval and/or the combined literature range. X17 is considered equivalent to conventional potatoes.

A significant difference between Y9 and Atlantic was observed for all amino acids except lysine and methionine (Table 8-4). Aspartic acid was expected to be lower and glutamic acid was expected to be higher in Y9 because of the down-regulation of the *Asn1* gene. Higher amino acid levels in Y9 would be

consistent with observed higher protein. In all cases, mean values were within the tolerance interval and/or the combined literature range. Y9 is considered equivalent to conventional potatoes. The results for X17 and Y9 indicate that they are equivalent to controls based on levels of amino acids.

Table 8-3. Total Amino Acids in X17 and Ranger Russet

Amino Acid	Variety	Mean (mg/100 g)	P-value ¹	S.D.	N	Range		Tolerance Interval		Combined Literature Range ²	
						Min	Max	Min	Max	Min	Max
Alanine	X17	83.3	<u><.0001</u>	6.67	32	76.5	100	41.8	96.1	39.2	95.2
	Control	69.1		5.90	32	60.2	81.8				
Arginine	X17	155	<u><.0001</u>	26.8	32	123	223	36.5	182	70	138
	Control	125		19.2	32	98.5	174				
Aspartic Acid	X17	281	<u><.0001</u>	27.6	32	225	332	229	708	339	738
	Control	509		47.9	32	437	602				
Cystine	X17	26.6	<u>0.0024</u>	3.29	32	21.4	33.6	7.89	39.5	28.6	1,250
	Control	23.3		3.43	32	17.6	30.7				
Glutamic Acid	X17	458	<u><.0001</u>	34.5	32	400	546	184	507	292	604
	Control	319		25.9	32	255	370				
Glycine	X17	70.8	<u><.0001</u>	7.89	32	56.1	89.0	32.7	91.4	50.0	199
	Control	61.5		7.37	32	47.7	76.8				
Histidine	X17	35.4	0.0642	3.28	32	30.3	43.7	19.3	47.3	13.3	46.9
	Control	33.5		3.32	32	28.5	40.3				
Isoleucine	X17	83.8	<u>0.0060</u>	7.82	32	70.6	99.3	46.5	106	52.5	95.3
	Control	78.1		8.04	32	58.3	90.6				
Leucine	X17	137	<u><.0001</u>	14.4	32	108	170	57.4	176	68.5	138
	Control	118		12.9	32	92.1	144				
Lysine	X17	118	<u>0.0003</u>	8.46	32	103	135	61.4	149	68.7	137
	Control	107		7.41	32	88.1	120				
Methionine	X17	42.5	<u>0.0437</u>	3.17	32	37.1	49.8	25.6	52.6	30	50
	Control	40.2		3.59	32	34.1	47.5				
Phenylalanine	X17	97.9	<u>0.0039</u>	8.52	32	82.9	116	53.2	125	55.2	109
	Control	91.2		9.22	32	75.9	109				
Proline	X17	87.4	<u>0.0290</u>	14.8	32	70.4	132	17.9	132	35.5	146
	Control	77.4		17.0	32	58.1	125				
Serine	X17	90.1	<u><.0001</u>	7.06	32	78.6	109	46.3	104	50.0	102
	Control	77.9		7.29	32	65.5	93.0				
Threonine	X17	87.8	<u><.0001</u>	7.55	32	77.2	107	38.3	109	43.6	85.5
	Control	74.9		6.70	32	62.7	89.4				
Tryptophan	X17	24.7	0.3053	3.55	32	19.6	32.3	13.3	31.8	11.4	28.2
	Control	23.4		3.59	32	17.0	30.8				
Tyrosine	X17	87.2	<u><.0001</u>	7.57	32	72.1	104	37.8	106	45.7	94.2
	Control	74.0		5.75	32	63.4	86.1				
Valine	X17	114	<u>0.0021</u>	7.75	32	102	129	71.5	141	75.2	145
	Control	106		9.21	32	86.0	122				

¹ P-values indicating significant differences with controls are underlined and in bold.

² Combined literature ranges are from (Lisinska and Leszczynski, 1989; Rogan et al., 2000; Talley et al., 1984).

Table 8-4. Total Amino Acids in Y9 and Atlantic

Amino Acid	Variety	Mean (mg/100g)	P-value ¹	S.D.	N	Range		Tolerance Interval		Combined Literature Range ²	
						Min	Max	Min	Max	Min	Max
Alanine	Y9	86.8	<.0001	9.51	28	72.9	109	41.8	96.1	39.2	95.2
	Control	74.6		9.33	28	59.4	96.9				
Arginine	Y9	142	<.0001	19.3	28	112	196	36.5	182	70	138
	Control	127		19.5	28	102	174				
Aspartic Acid	Y9	304	<.0001	31.4	28	256	360	229	708	339	738
	Control	499		69.3	28	350	619				
Cystine	Y9	35.3	0.0086	3.02	28	30.7	42.1	7.89	39.5	28.6	1,250
	Control	32.3		3.27	28	28.1	39.1				
Glutamic Acid	Y9	527	<.0001	55.5	28	417	603	184	507	292	604
	Control	375		48.4	28	266	467				
Glycine	Y9	87.0	<.0001	9.51	28	73.3	110	32.7	91.4	50.0	199
	Control	76.4		9.30	28	61.8	96.7				
Histidine	Y9	36.8	0.0458	3.10	28	30.9	43.7	19.3	47.3	13.3	46.9
	Control	34.6		4.65	28	27.3	44.5				
Isoleucine	Y9	92.6	<.0001	9.14	28	80.9	113	46.5	106	52.5	95.3
	Control	83.9		9.91	28	70.0	108				
Leucine	Y9	169	<.0001	19.1	28	142	218	57.4	176	68.5	138
	Control	147		18.8	28	120	190				
Lysine	Y9	130	0.0745	19.1	28	85.6	173	61.4	149	68.7	137
	Control	120		21.2	28	47.3	157				
Methionine	Y9	41.5	0.1298	5.06	28	28.1	52.6	25.6	52.6	30	50
	Control	40.0		4.39	28	32.7	48.7				
Phenylalanine	Y9	111	<.0001	11.7	28	92.4	140	53.2	125	55.2	109
	Control	100.0		12.1	28	82.9	125				
Proline	Y9	109	0.0006	19.7	28	77.5	153	17.9	132	35.5	146
	Control	89.1		11.1	28	59.9	113				
Serine	Y9	98.0	<.0001	10.3	28	81.9	123	46.3	104	50.0	102
	Control	86.8		9.73	28	72.0	108				
Threonine	Y9	102	<.0001	11.5	28	84.9	132	38.3	109	43.6	85.5
	Control	89.0		11.2	28	73.5	115				
Tryptophan	Y9	24.5	0.0217	2.42	28	20.7	29.5	13.3	31.8	11.4	28.2
	Control	23.4		2.88	28	18.7	28.2				
Tyrosine	Y9	95.4	<.0001	10.0	28	80.8	121	37.8	106	45.7	94.2
	Control	82.5		10.3	28	67.8	107				
Valine	Y9	121	<.0001	11.6	28	104	146	71.5	141	75.2	145
	Control	108		12.2	28	90.2	136				

¹ P-values indicating significant differences with controls are underlined and in bold.

² Combined literature ranges are from (Lisinska and Leszczynski, 1989; Rogan et al., 2000; Talley et al., 1984).

8.1.3 Glycoalkaloids

Glycoalkaloids are toxins commonly found in Solanaceous crops, including potato. Ninety-five percent of glycoalkaloids in potato tubers are ether α -solanine or α -chaconine (OECD, 2002). The widely accepted safety limit for total glycoalkaloids in tubers is 20 mg/100 g fresh weight (Smith et al., 1996).

The mean concentration of glycoalkaloids in X17 and Y9 were not statistically different from controls, and were within the generally accepted safety limit (Table 8-5 and Table 8-6).

Table 8-5. Glycoalkaloids in X17 and Ranger Russet

Variety	Mean (mg/100g)	P-value ¹	S.D.	N	Range		Tolerance Interval		Combined Literature Range ²	
					Min	Max	Min	Max	Min	Max
X17	7.38	0.7555	1.79	32	4.66	11.0	0	14.6	3.20	210.4
Control	7.21		2.08	32	4.07	13.8				

¹P-values indicating significant differences with controls are underlined and in bold.

²Combined literature ranges from Kozukue et al., 2008.

Table 8-6. Glycoalkaloids in Y9 and Atlantic

Variety	Mean (mg/100g)	P-value ¹	S.D.	N	Range		Tolerance Interval		Combined Literature Range ²	
					Min	Max	Min	Max	Min	Max
Y9	6.90	0.6276	2.90	28	3.93	14.4	0	14.6	3.20	210.4
Control	7.27	.	4.33	28	4.13	22.8				

¹P-values indicating significant differences with controls are underlined and in bold.

²Combined literature ranges from Kozukue et al., 2008.

8.2 Composition Efficacy Assessment of X17 and Y9

To evaluate trait efficacy, an assessment of free asparagine and lowered reducing sugars, and their impact on low acrylamide potential was carried out:

- Free amino acids (Table 8-7 and 8-8);
- Reducing sugars (Table 8-9 and 8-10); and
- Acrylamide (Table 8-11 and 8-12)

8.2.1 Free Amino Acids

Free amino acid analysis demonstrated that down-regulation of *Asn1* was effective in reducing levels of free asparagine in tubers. X17 and Y9 tubers had statistically lower levels of free asparagine, but statistically higher levels of free glutamine compared to Ranger Russet and Atlantic varieties (Table 8-7 and Table 8-8). The mean concentrations of free asparagine and free glutamine remained within the tolerance interval and/or combined literature range for conventional potatoes. Free asparagine and glutamine levels in X17 and Y9 are within the normal range for potatoes.

Table 8-7. Free Amino Acids in Tubers at Harvest in X17

Variable	Variety	Mean (mg/100 g)	P-value ¹	S.D.	N	Range		Combined Literature Range ²	
						Min	Max	Min	Max
Asparagine	X17	76.0	<u><.0001</u>	14.3	32	56.5	111	31.2	698
	Control	331		43.1	32	264	434		
Aspartic Acid	X17	45.5	0.1065	7.37	32	23.7	54.5	6.4	75.2
	Control	42.4		7.61	32	24.1	55.3		
Glutamic Acid	X17	61.4	<u>0.0329</u>	8.70	32	44.6	75.5	45	74.2
	Control	55.0		8.51	32	32.5	64.7		
Glutamine	X17	207	<u><.0001</u>	28.5	32	158	257	44	539 ³
	Control	121		23.9	32	73.6	176		

¹ P-values indicating significant differences with controls are underlined and in bold.

² Combined literature ranges are from (Davies, 1977; Lisinska and Leszczynski, 1989).

³ For glutamine, the maximum value from the combined literature range was reported as 539 mg/100 g from the mean of four sites (Davies, 1977). A value of 1,824 mg/100 g from a single site was not included because it appeared to be an outlier.

Table 8-8. Free Amino Acids in Tubers at Harvest in Y9

Variable	Variety	Mean (mg/100 g)	P-value ¹	S.D.	N	Range		Combined Literature Range ²	
						Min	Max	Min	Max
Asparagine	Y9	61.9	<u><.0001</u>	16.0	28	37.7	105	31.2	698
	Control	282		58.8	28	169	404		
Aspartic Acid	Y9	39.5	0.0590	6.64	28	21.9	46.1	6.4	75.2
	Control	41.5		6.83	28	26.2	52.8		
Glutamic Acid	Y9	65.0	<u>0.0004</u>	8.85	28	44.6	86.3	45	74.2
	Control	57.8		8.22	28	45.6	72.7		
Glutamine	Y9	238	<u><.0001</u>	40.3	28	148	300	44	539 ³
	Control	132		33.0	28	74.1	192		

¹ P-values indicating significant differences with controls are underlined and in bold.

² Combined literature ranges are from (Davies, 1977; Lisinska and Leszczynski, 1989).

³ For glutamine, the maximum value from the combined literature range was reported as 539 mg/100 g from the mean of four sites (Davies, 1977). A value of 1,824 mg/100 g from a single site was not included because it appeared to be an outlier.

8.2.2 Reducing Sugars

X17 and Y9 contain cassettes designed to down-regulate *R1*, *PhL*, and *VInv*, which contribute to lower levels of reducing sugars fructose and glucose in tubers. Down-regulation of *R1* and *PhL* slow the breakdown of starch into sugars in the amyloplast, and down-regulation of *VInv* slows the breakdown of sucrose into glucose and fructose in the vacuole (Figure 2-4).

As expected, down-regulation of *R1*, *PhL* and *VInv* resulted in significantly lower levels of reducing sugars at harvest and after 180 days storage at typical storage temperatures. Levels of reducing sugars were measured in tubers either at harvest or after 180 days at typical (7.7 °C-10 °C) potato storage temperatures. Additionally, sugar levels were measured in tubers stored at 3.3 °C, an atypical storage temperature for potatoes. For X17 and Y9 tubers, mean levels of reducing sugars (fructose plus glucose) and sucrose were within the combined literature range for both fresh and stored conditions (Table 8-9 to Table 8-12). Sucrose levels in X17 and Y9 were significantly higher than controls as expected. Down-regulation of *VInv* slows the conversion of sucrose into fructose and glucose.

Table 8-9. Sugars in X17 and Ranger Russet Tubers at Harvest and after Storage at 7.7 °C

Timing	Variety	Mean	P-value ¹	S.D.	N	Range		Combined Literature Range ²	
						Min	Max	Min	Max
Fructose and Glucose (mg/100 g)									
Fresh	X17	21.2	<u>0.0196</u>	5.51	32	9.30	32.8	18.0	803
	Control	85.8		43.3	32	31.8	183		
180 Days Post-Harvest ³ 7.7 °C	X17	74.2	<u><.0001</u>	66.2	28	16.4	272	18.0	803
	Control	220		129	28	89.7	594		
Sucrose (mg/100 g)									
Fresh	X17	326	<u>0.0317</u>	88.9	32	235	644	39.7	1,390
	Control	256		63.0	32	209	433		
180 Days Post-Harvest ³ 7.7 °C	X17	298	<u><.0001</u>	65.5	28	209	433	39.7	1,390
	Control	172		47.1	28	102	354		

¹ P-values indicating significant differences with controls are underlined and in bold.

² Literature Ranges from (Amrein et al., 2003; Vivanti et al., 2006).

³ 180 days post-harvest data not collected in Adams County, Wisconsin in 2013.

Table 8-10. Sugars in X17 and Ranger Russet Tubers after Cold Storage at 3.3 °C

Timing	Variety	Mean	P-value ¹	S.D.	N	Min	Max	Combined Literature Range (Min/Max) ²	
Fructose and Glucose (mg/100 g)									
180 Days 3.3 °C	X17	289	<u><.0001</u>	40.2	4	248	344	18.0	803
	Control	889		120	4	755	1,047	18.0	803
Sucrose (mg/100 g)									
180 Days 3.3 °C	X17	901	<u><.0001</u>	117	4	752	1,030	39.7	1,390
	Control	361		91	4	297	495	39.7	1,390

Note: Data collected from Minidoka County, Idaho in 2013.

¹ P-values indicating significant differences with controls are underlined and in bold.

² Literature ranges from (Amrein et al., 2003; Vivanti et al., 2006).

Table 8-11. Sugars in Y9 and Ranger Russet Tubers at Harvest and after Storage at 10 °C

Variable	Variety	Mean	P-value ¹	S.D.	N	Min	Max	Combined Literature Range (Min/Max) ²	
Fructose and Glucose (mg/100 g)									
Fresh	Y9	7.43	<.0001	2.14	28	3.93	12.7	18.0	803
	Control	20.1		9.49	28	7.46	39.4		
180 Days 10 °C	Y9	15.4	0.0394	15.7	28	6.40	58.7	18.0	803
	Control	107		144	28	20.7	533		
Sucrose (mg/100 g)									
Fresh	Y9	169	0.0386	52.6	28	99.6	283	39.7	1,390
	Control	150		38.1	28	96.3	225		
180 Days 10 °C	Y9	256	0.2533	207	28	127	839	39.7	1,390
	Control	192		65.0	28	101	369		

¹ P-values indicating significant differences with controls are underlined and in bold.

² Literature ranges from (Amrein et al., 2003; Vivanti et al., 2006).

Table 8-12. Sugars in Y9 and Atlantic Tubers after Storage at 3.3 °C

Timing	Variety	Mean	P-value ¹	S.D.	N	Min	Max	Combined Literature Range (Min/Max) ²	
Fructose and Glucose (mg/100 g)									
180 Days 3.3 °C	Y9	11.8	<u>0.0017</u>	3.68	4	8.91	16.9	18.0	803
	Control	35.7		7.47	4	25.6	42.4	18.0	803
Sucrose (mg/100 g)									
180 Days 3.3 °C	Y9	132	0.1307	2.06	4	130	134	39.7	1,390
	Control	162		40.5	4	134	222	39.7	1,390

Note: Data collected from Grant County, Washington in 2014.

¹ P-values indicating significant differences with controls are underlined and in bold.

² Literature ranges from (Amrein et al., 2003; Vivanti et al., 2006)

8.2.3 Acrylamide

Asparagine, together with fructose and glucose, contributes to levels of acrylamide formed during processing of potato products (fries and chips) at high temperatures. Lowering the levels of these reactants in tubers can decrease the levels of acrylamide in potato food products. Free asparagine levels were lower in X17 and Y9 tubers compared to controls, as were levels of the reducing sugars fructose and glucose (see above).

To determine the effect of lower asparagine and sugar levels on acrylamide levels in X17 and Y9, acrylamide was measured in fries and chips made from fresh or 180 day stored (7.7 °C-10 °C) tubers. Also, acrylamide levels were measured in products made from tubers stored at 3.3 °C. The Ranger Russet variety is traditionally made into fries, therefore acrylamide levels in X17 were measured in fries. The Atlantic variety is used for making chip, therefore acrylamide levels in Y9 were measured in chips.

At the time of harvest, fries made with X17 tubers contained 86% less acrylamide than fries made with Ranger Russet (Table 8-13). When potatoes were stored for 180 days at 7.7 °C, acrylamide concentrations in X17 were 84% lower than the control. When potatoes were stored for 180 days at 3.3 °C, acrylamide concentrations in X17 were 93% lower than the control (Table 8-14). Acrylamide concentrations in X17 fries were statistically lower than Ranger Russet at the time of harvest and after 180 days storage at both temperatures.

At the time of harvest, chips made with Y9 tubers contained 85% less acrylamide than chips made with Atlantic (Table 8-15). When potatoes were stored for 180 days at 10 °C, acrylamide concentrations in Y9 were 89% lower than the control. When potatoes were stored for 180 days at 3.3 °C, acrylamide concentrations in Y9 were 97% lower than the control (Table 8-16). Acrylamide concentrations in Y9 chips were statistically lower than Atlantic at the fresh time point and after 180 days storage at both temperatures.

The significantly lower acrylamide levels after storage were expected from down-regulation of the *Asn1*, *R1*, *PhL*, and *Vlnv* genes, which causes low free asparagine and reducing sugar levels. Similar reductions in reducing sugars and acrylamide have been reported (Zhu et al., 2014).

Table 8-13. Acrylamide in Fries from X17 and Ranger Russet at Harvest and after Storage at 7.7 °C

Timing	Variety	Mean (ppb)	P-value ¹	S.D.	N	Percent Reduction	Range	
							Min	Max
Fresh	X17	67.4	<u><.0001</u>	29.9	32	86.1	25.7	113
	Control	485		77.0	32		366	650
180 ² Days 7.7 °C	X17	97.6	<u><.0001</u>	35.1	28	84.1	57.9	189
	Control	614		199	28		291	1,030

¹ P-values indicating significant differences with controls are underlined and in bold.

² 180 days post-harvest data not collected in Adams County, Wisconsin in 2013.

Table 8-14. Acrylamide in Fries from X17 and Ranger Russet Stored after Storage at 3.3 °C

Timing	Variety	Mean (ppb)	P-value ¹	S.D.	N	Percent Reduction	Range	
							Min	Max
180 Days Stored at 3.3 °C	X17	170	<u><.0001</u>	7.41	4	93.3	164	180
	Control	2,538		86.6	4		2,460	2,660

Note: Data collected from Minidoka County, Idaho in 2013.

¹ P-values indicating significant differences with controls are underlined and in bold.

Table 8-15. Acrylamide in Chips from Y9 and Atlantic at Harvest and after Storage at 10 °C

Timing	Variety	Mean (ppb)	P-Value ¹	S.D.	N	Percent Reduction	Range	
							Min	Max
Fresh	Y9	161	<u><.0001</u>	51.546	28	85.1	112	311
	Control	1,087		499.519	27		397	2,620
180 Days 10 °C	Y9	175	<u><.0001</u>	48.657	28	89.0	115	266
	Control	1,591		768.366	28		669	3,450

¹ P-values indicating significant differences with controls are underlined and in bold.

Table 8-16. Acrylamide in Chips from Y9 and Atlantic after Storage at 3.3 °C

Timing	Variety	Mean (ppb)	P-Value ¹	S. D.	N	Percent Reduction	Range	
							Min	Max
180 Days 3.3 °C	Y9	541	<u><.0001</u>	175	4	96.8	402	783
	Control	17,100		1,930	4		15,400	19,700

Note: Data collected from Grant County, Washington in 2014.

¹ P-values indicating significant differences with controls are underlined and in bold.

8.3 Compositional Assessment Conclusions

Like W8, a thorough compositional assessment was conducted for X17 and Y9 and results compared to conventional control varieties. The types of analyses conducted were:

- Compositional nutritional assessment, on analytes important to potato nutrition; and
- Compositional efficacy assessment, on specific analytes related to the introduced traits.

The nutritional assessment evaluated levels of proximates, vitamins, minerals, amino acids, and glycoalkaloids, and demonstrated that X17 and Y9 are compositionally equivalent to Ranger Russet and Atlantic, respectively, and are as safe and nutritious for food and feed as conventional potatoes that have a long history of safe consumption.

The efficacy assessment evaluated levels of free amino acids and reducing sugars, and levels of acrylamide in X17 fries and Y9 chips, and demonstrated that X17 and Y9 have lower levels of free asparagine, reducing sugars, and acrylamide potential compared to Ranger Russet and Atlantic, respectively.

9.0 Environmental Safety Assessment for X17 and Y9

Like W8, the environmental safety of X17 and Y9 is supported by extensive testing. Data from phenotypic performance, trait efficacy, genetic characterization, and compositional assessments was collected and analyzed to determine potential environmental risks associated with X17 and Y9. The following five criteria were considered:

- Potential to become a weed of agriculture or to be invasive of natural habitats;
- Potential for gene flow to sexually compatible plants;
- Potential to become a plant pest;
- Potential impact on non-target species including humans; and
- Potential impact on biodiversity.

Conclusions from a previous Environmental Assessment of the W8 event are applicable to X17 and Y9. X17 and Y9 are no more likely to impact the environment than W8. The traits in X17 and Y9 are intended to enhance late blight resistance and tuber quality of potatoes. Planting, cultivation, management, harvesting, and volunteer management are not expected to change, with the exception that, similar to W8, the cultivation of X17 and Y9 may reduce the amount of fungicide needed to control late blight.

10.0 Stewardship of X17 and Y9 Potatoes

Simplot is committed to the responsible introduction and stewardship of biotech potatoes, including the W8, X17, and Y9 varieties. The Simplot Stewardship Program for Innate® potatoes is based on industry best practices for managing the development, production, sale, distribution and utilization of seed improved using biotechnology.

Simplot Plant Sciences is a member of Excellence Through Stewardship® (ETS) (BIO, 2007). ETS is an industry-coordinated program that provides guidance for stewardship over the entire lifecycle of a biotech product, from early testing through commercial introduction and discontinuation, when appropriate. In 2015, Simplot Plant Sciences completed an ETS Global Stewardship Audit verifying that appropriate stewardship programs and comprehensive quality management systems are in place to manage both regulated materials and deregulated products.

10.1 Stewardship for Commercial Products

After regulatory authorizations, Innate® potatoes will be managed by Simplot and its licensees in accordance with the Innate® Stewardship Program. This commercial stewardship program has been designed to direct Innate® seed and harvested potatoes to Simplot-authorized growers, packers, processors, and marketers who agree to abide by crop stewardship requirements. Innate® seed multiplication will be controlled by Simplot. Seed multiplication will be contracted by Simplot with selected licensees who agree to transfer Innate® seed under the direction of Simplot to its licensed growers. The Simplot requirement for stewardship will help to direct Innate® potatoes in the marketplace and facilitate separation between Innate® and non-biotech potatoes.

10.2 Regulatory Clearances in Foreign Markets and Plan for U.S. Commercialization

To help maintain trade channels of conventional potatoes between the U.S. and other nations, international regulatory approvals on Simplot's Innate® commercial events will be sought from key trading partner countries. Simplot has conducted a U.S. trade and market assessment that will be used to guide the regulatory and commercialization strategies for Innate® potatoes, including X17 and Y9.

11.0 Summary of Environmental Assessment Considerations

USDA recently completed a thorough environmental safety assessment of the W8 event in 14-093-01p in July 2015. X17 and Y9 were generated using the same genetic material and transformation method as W8, have the same traits and gene functions, have been thoroughly characterized molecularly, and are phenotypically and compositionally comparable to conventional potatoes. X17 and Y9 present no new or different environmental issues from those previously considered for W8. There are no additional environmental issues arising from the Ranger Russet or Atlantic varieties that are different from the Russet Burbank variety previously assessed. Conclusions from the environmental safety assessment of W8 are compared to the environmental assessment considerations for X17 and Y9 in Table 11-1.

Table 11-1. Summary of Environmental Assessment Considerations for X17 and Y9

Attribute/Measure	Antecedent Event W8 ¹	X17 and Y9
Meets purpose, need, and objectives	Yes	Yes
Unlikely to pose a plant health risk	Satisfied – risk assessment	Will be satisfied with USDA risk assessment.
Acreage and areas of potato production	Total acreage dedicated to potato is unlikely to change, but adoption of Simplot's biotech potato may reduce acreage dedicated to conventional potatoes.	Same
Management Practices		
Agronomic practices	Agronomic practices will remain the same as used currently.	Same
Pesticide use	Pesticides are currently used to control insects, nematodes, fungi, and weeds.	Like W8, X17 and Y9 could enable reduced fungicide use as part of an overall IPM program.
Potato seed production	Potato seed is primarily supplied by seed potatoes.	Same
Organic potato production	Organic potato growers use practices and standards for production, cultivation, and product handling and processing to ensure that their products are not pollinated or comingled with conventional or GE crops.	Same
Environment		
Water resources	The primary cause of agricultural non-point source pollution is increased sedimentation from soil erosion, which can introduce sediments, fertilizers, and pesticides to nearby lakes and streams. Agronomic practices such as crop nutrient management, pest management, and conservation buffers help protect water quality from agricultural runoff. Water usage for irrigation would be expected to continue to increase.	Same
Soil quality	Agronomic practices such as crop type, tillage, and pest management can affect soil quality. Growers will adopt management practices to address their specific needs in producing potatoes. Erosion potential may continue to increase.	Same

Table 11-1. Summary of Environmental Assessment Considerations for X17 and Y9 (continued)

Attribute/Measure	Antecedent Event W8¹	X17 and Y9
Air quality	Agricultural activities such as burning, tilling, harvesting, spraying pesticides, fertilizing, and emissions from farm equipment can directly affect air quality. Aerial application of herbicides may impact air quality from drift, diffusion, and volatilization of the chemicals, as well as motor vehicle emissions from airplanes or helicopters.	Same
Climate change	Agriculture-related activities are recognized as both direct sources of greenhouse gases (GHGs) (e.g. exhaust from motorized equipment) and indirect sources (e.g. agriculture-related soil disturbances, fertilizer production.	Same
Animal communities	Animals consuming tubers from deregulated events may be exposed to increased levels of glutamine, but this is not expected to be detrimental.	Same
Plant communities	In the unlikely event of hybridization of the deregulated varieties with conventional potatoes, resulting progeny may contain lowered polyphenol oxidase levels. However, this is not expected to be detrimental. The deregulated events are no weedier than conventional potatoes.	Same
Gene flow	Traits in the deregulated events are not expected to increase weediness in potato.	Same
Soil microorganisms	Abundance and diversity of soil microorganisms in and around potato fields is not expected to change.	Same
Biological diversity	The biological diversity in potato fields is lower than in the surrounding habitats.	Same
Human and Animal Health		
Risk to human health	Glycoalkaloid and patatin exposure would continue. For humans consuming high-temperature cooked potatoes, acrylamide levels could be reduced by up 84 to 97% (based upon Simplot data for X17 and Y9).	Similar. Data in this petition demonstrate acrylamide levels in X17 and Y9 could be reduced by up to ~84-97%.
Risk to animal feed	Glycoalkaloids would continue to pose a risk to livestock if potato stems and foliage are fed to them, which is not likely.	Same
Socioeconomic		
Domestic economic environment	Because of potential benefits (lower acrylamide) and potential reduced wastage (lower black-spot) the deregulated potatoes may comprise a larger share of the domestic potato market, and may result in increased revenues.	Same
Trade economic environment	The foreign trade impacts associated with a determination of nonregulated status of the events are similar to the no action alternative. Import of each specific trait requires separate application and approval by the importing company. If the deregulated traits are approved by importing countries, it may make up a larger percentage of potato import markets.	Same

¹Source USDA, 2014.

12.0 Conclusion: Extension of Nonregulated Status for X17 and Y9

As with W8, Simplot's new Ranger Russet and Atlantic potatoes have late blight resistance, reduced black spot, lowered reducing sugars and free asparagine contributing to low acrylamide potential. Considering that Ranger Russet and Atlantic varieties, like other potatoes, are difficult to breed, biotechnology applications are ideally suited for simultaneously incorporating multiple traits. The propagation of commercial potatoes through cloning mitigates concerns surrounding seed dispersal, survival outside of cultivation, and outcrossing, that could contribute to increased plant pest potential. Multi-year field trials evaluating phenotypic performance and insect and disease interactions demonstrate that X17 and Y9 pose no significant risk of persistence in the environment as a result of weediness or increased plant pest potential.

The data presented demonstrates that introduction of X17 and Y9 potatoes will have a similar environmental impact as W8 and conventional potatoes, and poses no increased risk to the environment. The introduction and cultivation of these potatoes is not expected to cause any adverse environmental or biological impacts, or detrimental effects on plant health.

Simplot seeks an extension of the deregulation of the W8 event in 14-093-01p and requests nonregulated status for X17 and Y9 based on the weight of evidence demonstrating that these potatoes are unlikely to pose a plant pest risk. We respectfully submit that X17 and Y9, and their progeny, should not be classified as "regulated articles" as defined under 7 CFR Part 340.

13.0 References

- Amrein, T.M., Bachmann, S., Noti, A., Biedermann, M., Barbosa, M.F., Biedermann-Brem, S., Grob, K., Keiser, A., Realini, P., Escher, F., et al. (2003). Potential of Acrylamide Formation, Sugars, and Free Asparagine in Potatoes: A Comparison of Cultivars and Farming Systems. *Journal of Agricultural and Food Chemistry* 51, 5556–5560.
- Bamberg, J., and Rio, A. (2011). Use of Native Potatoes for Research and Breeding. 2010–2011.
- Bamberg, J., Del Rio, A., Huaman, Z., Vega, S., Martin, M., Salas, A., Pavék, J., Kiru, S., Fernandez, C., and Spooner, D. (2003). A Decade of Collecting and Research on Wild Potatoes of the Southwest USA. *American Journal of Potato Research* 80, 159–172.
- BIO (2007). Product Launch Stewardship Policy. Biotechnology Industry Organization 1–2.
- Bushey, D.F., Bannon, G.A., Delaney, B.F., Graser, G., Hefford, M., Jiang, X., Lee, T.C., Madduri, K.M., Pariza, M., Privalle, L.S., et al. (2014). Characteristics and Safety Assessment of Intractable Proteins in Genetically Modified Crops. *Regulatory Toxicology and Pharmacology* 69, 154–170.
- Daayf, F., and Platt, H.W.B. (2003). US-8 and US-11 Genotypes of *Phytophthora infestans* from Potato and Tomato Respond Differently to Commercial Fungicides. *American Journal of Potato Research* 80, 329–334.
- Davies, A.M.C. (1977). The Free Amino Acids of Tubers of Potato Varieties Grown in England and Ireland. *Potato Research* 20, 9–21.
- Deahl, K.L., Inglis, D.A., and DeMuth, S.P. (1993). Testing for Resistance to Metalaxyl in *Phytophthora infestans* Isolates from Northwestern Washington. *American Potato Journal* 70, 779–795.
- Eck, C. (2013). Final Environmental Assessment. J.R. Simplot Company Petition (13-022-01p) for Determination of Non-Regulated Status for Innate™ Potatoes with Low Acrylamide Potential and Reduced Black Spot Bruise : Events E12 and E24 (Russet Burbank)... USDA-APHIS 24, 1–113.
- Edner, C., Li, J., Albrecht, T., Mahlow, S., Hejazi, M., Hussain, H., Kaplan, F., Guy, C., Smith, S.M., Steup, M., et al. (2007). Glucan, Water Dikinase Activity Stimulates Breakdown of Starch Granules by Plastidial Beta-Amylases. *Plant Physiology* 145, 17–28.
- FDA (2013). Food and Drug Administration. Guidance for Industry: Acrylamide in Foods. 1–37.
- Foster, S.J., Park, T.-H., Pel, M., Brigneti, G., Śliwka, J., Jagger, L., van der Vossen, E., and Jones, J.D.G. (2009). *Rpi-vnt1.1*, a *Tm-2²* Homolog from *Solanum venturii*, Confers Resistance to Potato Late Blight. *Molecular Plant-Microbe Interactions* 22, 589–600.
- Fry, W.E., Birch, P.R.J., Judelson, H.S., Grünwald, N.J., Danies, G., Everts, K.L., Gevens, A.J., Gugino, B.K., Johnson, D.A., Johnson, S.B., et al. (2015). Five Reasons to Consider *Phytophthora infestans* a Re-Emerging Pathogen. *Phytopathology* 1–46.

Garbarino, J.E., and Belknap, W.R. (1994). Isolation of a Ubiquitin-Ribosomal Protein Gene (*ubi3*) from Potato and Expression of Its Promoter in Transgenic Plants. *Plant Molecular Biology* 24, 119–127.

Hanes, C.S. (1940). The Reversible Formation of Starch from Glucose-1-Phosphate Catalysed by Potato Phosphorylase. *Proceedings of the Royal Society of London* 129, 174–208.

Hijmans, R.J., and Spooner, D.M. (2001). Geographic Distribution of Wild Potato Species. *American Journal of Botany* 88, 2101–2112.

Horton, D.E., and Anderson, J.L. (1992). Potato Production in the Context of the World and Farm Economy. In *The Potato Crop*, Harris, P., ed. (Chapman & Hall), 794–815.

Jupe, F., Pritchard, L., Etherington, G.J., MacKenzie, K., Cock, P.J.A., Wright, F., Sharma, S.K., Bolser, D., Bryan, G.J., Jones, J.D.G., et al. (2012). Identification and Localisation of the NB-LRR Gene Family within the Potato Genome. *BMC Genomics* 13, 75.

Kamrani, M., Kohnehrouz, B.B., and Gholizadeh, A. (2011). Cisgenic Inhibition of the Potato Cold Induced Phosphorylase L Gene Expression and Decrease in Sugar Contents. *African Journal of Biotechnology* 10, 10076–10082.

Kessel, G.J., Vossen, J., Cooke, D.E.L., Hansen, J.G., Hutten, R.C.B., Lotz, L.A.P., Schepers, H.T.A.M., and Haverkort, A.J. (2014). Towards a next Level IPM Approach for Potato Late Blight Management. *North American Late Blight Symposium Abstract*.
<https://www.usablight.org/sites/default/files/upload/AbstractBooklet.pdf>.

Kozukue, N., Yoon, K.-S., Byun, G.-I., Misoo, S., Levin, C.E., and Friedman, M. (2008). Distribution of Glycoalkaloids in Potato Tubers of 59 Accessions of Two Wild and Five Cultivated *Solanum* Species. *Journal of Agricultural and Food Chemistry* 56, 11920–11928.

Layne, J., Hystad, S., and Habig, J. (2015a). Characterization of the Insertion Site in Ranger Russet X17. Report 15-04-SPS-MOL.

Layne, J., Hystad, S., and Habig, J. (2015b). Characterization of the Insertion Sites in Atlantic Y9. Study Report 15-12-SPS-MOL.

Leipe, D.D., Koonin, E.V., and Aravind, L. (2004). STAND, a Class of P-Loop NTPases Including Animal and Plant Regulators of Programmed Cell Death: Multiple, Complex Domain Architectures, Unusual Phyletic Patterns, and Evolution by Horizontal Gene Transfer. *Journal of Molecular Biology* 343, 1–28.

Lisinska, G., and Leszczynski, W. (1989). Potato Tubers as a Raw Material for Processing and Nutrition. In *Potato Science and Technology*, (Elsevier Applied Science), 11–128.

Lorberth, R., Ritte, G., Willmitzer, L., and Kossmann, J. (1998). Inhibition of a Starch-Granule-bound Protein Leads to Modified Starch and Repression of Cold Sweetening. *Nature Biotechnology* 16, 473–477.

Love, S.L. (1994). News & Reviews: Ecological Risk of Growing Transgenic Potatoes in the United States and Canada. *Idaho Agricultural Experiment Station* 647–658.

- Malone, J.G., Mittova, V., Ratcliffe, R.G., and Kruger, N.J. (2006). The Response of Carbohydrate Metabolism in Potato Tubers to Low Temperature. *Plant & Cell Physiology* 47, 1309–1322.
- Moffett, P., Farnham, G., Peart, J., and Baulcombe, D.C. (2002). Interaction between Domains of a Plant NBS-LRR Protein in Disease Resistance-Related Cell Death. *The EMBO Journal* 21, 4511–4519.
- Morel, J.-B., and Dangl, J.L. (1997). The Hypersensitive Response and the Induction of Cell Death in Plants. *Cell Death and Differentiation* 4, 671–683.
- O'Malley, R.C., Alonso, J.M., Kim, C.J., Leisse, T.J., and Ecker, J.R. (2007). An Adapter Ligation-Mediated PCR Method for High-Throughput Mapping of T-DNA Inserts in the Arabidopsis Genome. *Nature Protocols* 2, 2910–2917.
- OECD (1997). Organisation for Economic Co-Operation and Development. Consensus Document on the Biology of *Solanum tuberosum* Subsp. *tuberosum* (potato). <http://www.oecd.org/science/biotrack/46815598.pdf>.
- OECD (2002). Organization for Economic Co-Operation and Development. Consensus Document on Compositional Considerations for New Varieties of Potatoes: Key Food and Feed Nutrients, Anti-Nutrients and Toxicants.
- PAA (2015a). The Potato Association of America Atlantic *Solanum tuberosum*. 6, 1–3.
- PAA (2015b). The Potato Association of America. Ranger Russet *Solanum Tuberosum*. 1–3.
- Pallais, N., Mulcahy, D., Fong, N., Falcon, R., and Schmiediche, P. (1988). The Relationship Between Potato Pollen and True Seed: Effects of High Temperature and Pollen Size. In *Sexual Reproduction in Higher Plants: Proceedings of the Tenth International Symposium on the Sexual Reproduction in Higher Plants*, 30 May - 4 June 1988 University of Siena, Siena, Italy, Cresti, M., Gori, P., and Pacini, E., eds. 285–290.
- Pel, M.A. (2010). Mapping, Isolation and Characterization of Genes Responsible for Late Blight Resistance in Potato. Wageningen University.
- Plaisted, R.L. (1980). Potato. In *Hybridization of Crop Plants*, (American Society of Agronomy-Crop Science Society of America), 483–494.
- Rairdan, G.J., Collier, S.M., Sacco, M.A., Baldwin, T.T., Boettrich, T., and Moffett, P. (2008). The Coiled-Coil and Nucleotide Binding Domains of the Potato Rx Disease Resistance Protein Function in Pathogen Recognition and Signaling. *The Plant Cell* 20, 739–751.
- Ritte, G., Lorbeith, R., and Steup, M. (2000). Reversible Binding of the Starch-Related R1 Protein to the Surface of Transitory Starch Granules. *Plant Journal* 21, 387–391.
- Ritte, G., Heydenreich, M., Mahlow, S., Haebel, S., Kötting, O., and Steup, M. (2006). Phosphorylation of C6- and C3-Positions of Glucosyl Residues in Starch Is Catalysed by Distinct Dikinases. *FEBS Letters* 580, 4872–4876.

Rogan, G.J., Bookout, J.T., Duncan, D.R., Fuchs, R.L., Lavrik, P.B., Love, S.L., Mueth, M., Olson, T., Owens, E.D., Raymond, P.J., et al. (2000). Compositional Analysis of Tubers from Insect and Virus Resistant Potato Plants. *Journal of Agricultural and Food Chemistry* 48, 5936–5945.

Shepherd, L.V.T., Bradshaw, J.E., Dale, M.F.B., McNicol, J.W., Pont, S.D.A., Mottram, D.S., and Davies, H.V. (2010). Variation in Acrylamide Producing Potential in Potato: Segregation of the Trait in a Breeding Population. *Food Chemistry* 123, 568–573.

Śliwka, J., Świętek, M., Tomczyńska, I., Stefańczyk, E., Chmielarz, M., and Zimnoch-Guzowska, E. (2013). Influence of Genetic Background and Plant Age on Expression of the Potato Late Blight Resistance Gene *Rpi-phu1* during Incompatible Interactions with *Phytophthora infestans*. *Plant Pathology* 62, 1072–1080.

Smith, D.B., Roddick, J.G., and Jones, J.L. (1996). Potato Glycoalkaloids: Some Unanswered Questions. *Trends in Food Science & Technology* 7, 126–131.

Sowokinos, J.R. (2001). Biochemical and Molecular Control of Cold-Induced Sweetening in Potatoes. *American Journal of Potato Research* 78, 221–236.

Spoel, S.H., and Dong, X. (2012). How Do Plants Achieve Immunity? Defence without Specialized Immune Cells. *Nature Reviews. Immunology* 12, 89–100.

Takken, F.L.W., and Goverse, A. (2012). How to Build a Pathogen Detector: Structural Basis of NB-LRR Function. *Current Opinion in Plant Biology* 15, 375–384.

Talbert, W.F., Schwimmer, S., and Burr, H.K. (1987). Structure and Chemical Composition of the Potato Tuber. In *Potato Processing*, Talbert, W.F., and Smith, O., eds. (Van Nostrand Reinhold Company), 11–46.

Talley, E.A., Toma, R.B., and Orr, P.H. (1984). Amino Acid Composition of Freshly Harvested and Stored Potatoes. *American Potato Journal* 61, 267–279.

USDA (1969). United States Department of Agriculture. Grading Manual for Frozen French Fried Potatoes.

USDA (1997). United States Department of Agriculture. United States Standards for Grades of Potatoes for Processing.

VanHaaren, M.J.J., Sedee, N.J.A., de Boer, H.A., Schilperoort, R.A., and Hooykaas, P.J.J. (1989). Mutational Analysis of the Conserved Domains of a T-Region Border Repeat of *Agrobacterium tumefaciens*. *Plant Molecular Biology* 13, 523–531.

Vardeman, S.B. (1992). What about the Other Intervals? *The American Statistician* 46, 193–197.

Vivanti, V., Finotti, E., and Friedman, M. (2006). Level of Acrylamide Precursors Asparagine, Fructose, Glucose, and Sucrose in Potatoes Sold at Retail in Italy in the United States. *Journal of Food Science* 71, C81–C85.

Webb, R.E., Wilson, D.R., Shumaker, J.R., Graves, B., Henninger, M.R., Watts, J., Frank, J.A., and Murphy, H.J. (1978). Atlantic: A New Potato Variety with High Solids, Good Processing Quality, and Resistance to Pests. *American Potato Journal* 55, 141–145.

Woodell, L., Olsen, N., Brandt, T.L., and Kleinkopf, G.E. (1991). Vine Kill and Long-Term Storage of Ranger Russet Potatoes. 3–6.

Ye, J., Shakya, R., Shrestha, P., and Rommens, C.M. (2010). Tuber-Specific Silencing of the Acid Invertase Gene Substantially Lowers the Acrylamide-Forming Potential of Potato. *Journal of Agricultural and Food Chemistry* 58, 12162–12167.

Zhu, X., Richael, C., Chamberlain, P., Busse, J.S., Bussan, A.J., Jiang, J., and Bethke, P.C. (2014). Vacuolar Invertase Gene Silencing in Potato (*Solanum tuberosum* L.) Improves Processing Quality by Decreasing the Frequency of Sugar-End Defects. *PLoS ONE* 9, e93381.

Zrenner, R., Schöler, K., and Sonnewald, U. (1996). Soluble Acid Invertase Determines the Hexose-to-Sucrose Ratio in Cold-Stored Potato Tubers. *Planta* 198, 246–252.

14.0 Appendix A: X17 and Y9 USDA Notifications

Since 2012, field trials of X17 and Y9 have been conducted several states in the continental U.S. (Tables 14-1 and 14-2). Both tables show plantings through October 31, 2015.

Table 14-1. X17 USDA Release Notifications and Planted Acreage Details

Year of Planting	Notification Number	Valid Date	State	Number of Counties Planted	Acreage (Whole Plot)
2012	12-066-102n	4/2/2013	ID	1	2.3
2013	13-072-112n	4/2/2014	WA	2	3.394
			ID	1	0.88
			PA	1	2
	13-088-107n	4/15/2014	ND	1	0.11
	13-079-108n	4/16/2014	MI	2	3
	13-079-106n	4/8/2014	ID	1	0.5
	13-079-107n	4/10/2014	ID	1	0.5
	13-112-108n	5/13/2014	OR	1	0.17
	13-079-102n	4/10/2014	WI	1	0.95
	13-258-101n	10/1/2014	WA	1	0.63
			PA	1	2.4
			ID	1	2
	13-098-106n	4/29/2014	NE	1	82.44
2014	14-066-105n	3/20/2015	ND	1	0.51
			WA	2	0.78
			MI	1	0.04
			PA	1	0.5
			ID	2	1.9
	14-066-106n	3/19/2015	WA	1	0.185
			ND	2	1.4
	14-110-101n	5/7/2014	ID	1	1.12
	14-105-155n	5/1/2015	NE	1	3.8
	14-084-101n	4/15/2015	MI	1	0.88
			ND	1	0.141
2015	15-060-101n	4/3/2016	ID	3	9.14
			NE	1	126.7
			ND	1	0.58
			WA	3	0.837
	15-157-101n	4/3/2016	ID	1	19.1
	15-051-107n	4/1/2016	ID	1	0.06
	15-064-105n	3/30/2016	MI	1	0.68
			ND	1	1.73

Table 14-2. Y9 USDA Release Notifications and Planted Acreage Details

Year of Planting	Notification Number	Valid Date	State	Number of Counties Planted	Acreage (Whole Plot)
2012	12-066-102n	4/2/2013	ID	1	2.3
2013	13-072-112n	4/2/2014	PA	1	2
	13-070-109n	4/1/2016	WA	1	0.25
	13-088-107n	4/15/2014	ND	1	0.11
	13-079-108n	4/16/2014	MI	1	2.5
	13-079-107n	4/10/2014	ID	1	0.5
			ME	1	0.27
			OR	1	0.28
	13-098-106n	4/29/2014	NE	1	82.44
	13-112-108n	5/13/2014	OR	1	0.17
	13-087-101n	4/8/2014	TX	1	0.5
	13-258-101n	10/1/2014	WA	1	0.63
			PA	1	0.24
			ID	1	2
	13-079-106n	4/8/2014	ID	1	0.22
2014	14-066-105n	3/20/2015	ND	1	0.51
			WA	2	0.78
			PA	2	0.77
			ID	2	1.9
	14-066-106n	3/19/2015	MI	3	3.32
			WA	1	0.185
			NY	1	2.33
	14-105-155n	5/1/2015	NE	1	4.15
2015	15-060-101n	4/3/2016	ND	1	126.7
			NY	1	1.26
			WI	2	9.41
			MI	2	12.03
	15-030-101n	2/13/2016	NC	1	0.13
	15-064-105n	3/30/2016	ND	1	1.73
			MI	1	0.68
	15-077-104n	4/6/2016	ID	1	4.8

15.0 Appendix B: Molecular Methods and Materials

The following methods were used to generate the molecular data presented for X17 and Y9.

Plant Material. Plants were grown in 2-gallon pots with Sunshine mix-1 soil (Sun Gro® Horticulture, Agawam, MA). Temperature (18-27 °C) and light (16-h photoperiod at 1500 $\mu\text{mol}/\text{m}^2/\text{s}$) were held constant. Leaf tissue samples were flash frozen in liquid nitrogen, ground to fine powder, and stored at -80 °C.

DNA Isolation. DNA was extracted by mixing tissue powder in 0.1 M Tris-HCl (pH 8.0) extraction buffer containing 0.35 M sorbitol, 0.05 M EDTA, followed by centrifugation at 3,000 x g for 15 min at room temperature (RT). The pellet was suspended in 2 mL extraction buffer containing 200 μg RNase A and mixed with 2 mL of 0.2 M Tris-HCl (pH 7.5) lysis buffer containing 20 mg/mL Hexadecyl Trimethyl Ammonium Bromide (CTAB) and 800 μL of 5% sarcosyl. After incubation for 20 min at 65 °C, DNA was extracted three times with an equal volume of chloroform:isoamyl alcohol (24:1), mixing, and centrifugation at 3000 x g for 5 min at RT. DNA was precipitated with isopropyl alcohol and centrifuged for 5 min at RT. The pellet was washed in 70% ethanol and dried. Samples were suspended in Tris/EDTA buffer (TE) and DNA concentrations were measured using a Qubit Fluorometer and DNA quantitation kit (Invitrogen™, Thermo Fisher Scientific, Waltham, MA). DNA quality was confirmed by agarose gel electrophoresis in Tris/Acetate/EDTA (TAE) buffer for 30 min at 80 V.

DNA Restriction Digestion and Electrophoresis. DNA was digested overnight at 37 °C with 50 units of the indicated restriction enzyme (Invitrogen™). After digestion, the DNA was precipitated using ethanol followed by a 70% ethanol wash. The dried pellet was suspended in TE buffer. Loading dye (40% sucrose and 0.35% Orange G (Sigma, St. Louis, MO)) was added and samples were separated by agarose gel (0.7%) electrophoresis in TAE buffer for 20 h at 35 V.

Membrane Preparation and Transfer. Gels were imaged using an Alphamager HP instrument (ProteinSimple, San Jose, CA). After imaging, the DNA in the gels was depurinated in 0.25 N HCl by washing twice for 10 min each, denatured in 0.5 M NaOH/1.5 M NaCl by washing twice for 15 min each, and neutralized in 0.5 M Tris-HCl (pH 7.5) with 1.5 M NaCl by washing twice for 15 min. Gels were equilibrated with 10X Saline Sodium Citrate (SSC) buffer for 10 min and DNA was transferred to a nylon membrane (Roche, Indianapolis, IN) by capillary transfer in 10X SSC buffer for 16-18 h.


Probe Labelling. Probes were DIG labeled using PCR. A typical reaction (50 μL) contained 5 μL HotMaster™ Taq Buffer (Thermo Fisher), 0.4-1 μM forward primer, 0.4-1 μM reverse primer, 5 μL DIG-labeled dNTP (Roche), 5-30 ng template, and 0.5-0.75 μL HotMaster™ Taq polymerase. PCR conditions were specific to the probe. The size and purity of the labeled probe was confirmed by agarose gel electrophoresis. As expected, the labeled probe migrated slower than the unlabeled control.

Hybridization. Prior to use, hybridization solution was heated to 68 °C for 10 min. Membranes were incubated in 40 mL warm DIG Easy Hybridization solution (Roche) at 42 °C for 1-4 h with rotation at 20-25 rpm. The hybridization solution was replaced with 40 mL warm hybridization solution containing 25-50 μL of the DIG-labeled probe and incubated for 3-16 h at 42 °C.

Detection. Blots were washed twice with solution I (2X SSC/0.1% SDS) for 10 min at RT with rotation at 25-30 rpm. Blots were washed twice with solution II (0.5X SSC/ 0.1% SDS) for 20 min at 60 °C with rotation at 25-30 rpm. A final wash step was carried out in solution III (0.1X SSC/ 0.1% SDS) for 20 min at

65 °C. Blots were rinsed with 2X SSC to remove SDS. The membrane was rinsed with 100 mL 1X DIG Washing Solution (Roche) for 2 min at RT and then blocked with 1X Blocking solution (Roche) for 30 min to 3 hours at RT with constant shaking. A 1:10,000 dilution of anti-DIG-alkaline phosphate conjugate was added and blots incubated for 30 min at RT with constant shaking. Membranes were washed twice (15 min each) with 1X DIG Washing Solution and equilibrated in 1X detection buffer. A 1:100 dilution of CDP-Star was added. After 5 min the membrane was wrapped in plastic and developed at exposure times ranging from 1 to 25 min using an Amersham™ Imager 600 instrument (GE Healthcare Life Sciences, Pittsburgh, PA).

Southern Blot Presentation. Southern blots are presented with explanatory tables identifying bands and band sizes. Internal bands are sequences within the insert and have predictable sizes. Junction bands extend from restriction enzyme (RE) sites in the insert to sites in the genomic DNA. Junction bands are expected to vary in size and are not always predictable. However, a minimal size can be estimated from distances between restriction sites within the insert and those identified during analysis of the flanking genomic sequences. The estimated junction band sizes were confirmed or modified based on migration during electrophoresis. Junction bands were used to confirm the number of integration sites. There are never more than two junction bands per insert for a particular RE digest and a probe. The T-DNA is derived from potato DNA sequence. Southern blot probes targeting the insert will detect endogenous bands that are common in size and intensity between control and event samples. These bands are not labeled to simplify presentation.

Band Size Determination. Two phenomena were observed that impeded accurate determination of band sizes of potato genomic DNA. First, is a tendency that the bands above ~3 kb to migrate faster than similarly-sized molecular weight markers within the same gel. The discrepancy between band and marker migration makes it difficult to accurately determine sizes for unknown bands, but also raises questions about the sizes of expected bands. The observed migration appears to be due to residual polysaccharides in potato genomic DNA samples. The molecular weight markers run faster when mixed with potato DNA samples, however, spiking the markers with genomic DNA to counter migration variability complicates ladder interpretation from hybridization of the probes to the endogenous DNA. In some cases, the DNA isolated from potato has an altered migration pattern compared to construct or marker DNA. The second is a tendency for bands to smile during electrophoresis. Size measurements taken from the top of these bands have proven to be the most reliable and reproducible so all sizes reported here used this technique (see line marking top of band in following example). 

RNA Isolation and Northern Blot. RNA was extracted from tuber and root tissues using Plant RNA reagent (Invitrogen™, Thermo Fisher Scientific, Waltham, MA). Trizol reagent (Invitrogen™) was used to extract RNA from leaf, flower, and stem tissues. The concentration of isolated RNA was measured using a Qubit 2.0 fluorometer (Invitrogen™) and RNA quality was confirmed by electrophoresis on 1% agarose gels in 200 mM MOPS buffer containing 50 mM NaOAc and 20 mM EDTA (pH 7.0) for 30-60 min at 90 volts. RNA was denatured by heating at 65 °C for 10 min followed by a 5 min incubation on ice. RNA samples were electrophoresed on 1% agarose gels containing 0.1-0.25 µg/mL ethidium bromide and 2% formaldehyde. Gels were run at 80-85 volts for 2-3 h and imaged using an Alphamager HP instrument (ProteinSimple, San Jose, CA). The gels were washed twice in 10X Saline Sodium Citrate (SSC) for 15 min to remove formaldehyde. RNA was transferred to a nylon membrane (Roche, Indianapolis, IN) by capillary transfer in 10X SSC buffer for 16-18 h and stabilized by UV cross-linking (UVP, Upland, CA). Transferred membranes were stored at 4 °C until probed.

Adapter ligation-mediated PCR. Junction fragments were amplified by PCR using digested DNA ligated with adapter primers AP1 and AP2 as described (O'Malley et al., 2007). Briefly, 200 ng genomic DNA was digested for 3-5 hours with a restriction enzyme for which an adapter had been designed (EcoRI, HindIII, BamHI, AseI/NdeI.). The digested DNA was ligated with its respective oligonucleotide adapter in a reaction with 1X T4 Ligation Buffer, 1.5 units T4 DNA Ligase, 64ng digest DNA fragments, 0.3 mM ATP, and the adapter to a final concentration of 0.1 mM. The ligation reaction was used as template for the primary PCR, carried out with a DNA insert-specific primer and AP1 with Hot Master Taq polymerase (Fisher BioReagents) under the following amplification conditions: 1 cycle of 3 min at 95 °C followed by 30 cycles of 30 sec at 94 °C, 30 sec at 60 °C, 4min at 68 °C, and finishing with 10 min at 68 °C. A 1 µl aliquot of the primary PCR product was used for secondary reactions (1 cycle of 3 min at 95 °C; 35 cycles of 30 sec at 94 °C, 30 sec at 62 °C, 2.5 min at 68 °C; 1 cycle of 10 min at 68 °C) with a nested DNA insert-specific primer and AP2. Products of the secondary PCR were run on 1% agarose in TAE buffer. Unique bands were gel-extracted using a Qiagen QIAquick Gel Extraction kit, cloned into pGEM-T Easy vector (Promega, Madison WI), and sequenced. Primers spanning the junction between DNA insert and chromosomal flanking DNA were designed and used to confirm sequences in genomic DNA.

16.0 Appendix C: VNT1 Expression Methods and Materials

Plant Material. Tuber and leaf tissues from field-grown X17 and Y9 plants (three biological replicates labeled -1, -2, and -3, each a separate plant per site) were collected in the state of Idaho (Table 16-1 and Table 16-2). All samples were flash frozen in liquid nitrogen, ground to powder, and stored at -80 °C.

Table 16-1. X17 Plant Material Collection Locations

Line	Tissue	Study Number	Generation of Seed Used	Location	Date
Ranger Russet-1	Leaf	15CT-IDRUPE-01	G2	Idaho	7/28/2015
Ranger Russet-2	Leaf	15CT-IDRUPE-01	G2	Idaho	7/28/2015
Ranger Russet-3	Leaf	15CT-IDRUPE-01	G2	Idaho	7/28/2015
X17-1	Leaf	15CT-IDRUPE-01	G2	Idaho	7/28/2015
X17-2	Leaf	15CT-IDRUPE-01	G2	Idaho	7/28/2015
X17-3	Leaf	15CT-IDRUPE-01	G2	Idaho	7/28/2015
Ranger Russet-1	Tuber	15CT-IDRUPE-01	G2	Idaho	7/28/2015
Ranger Russet-2	Tuber	15CT-IDRUPE-01	G2	Idaho	7/28/2015
Ranger Russet-3	Tuber	15CT-IDRUPE-01	G2	Idaho	7/28/2015
X17-1	Tuber	15CT-IDRUPE-01	G2	Idaho	7/28/2015
X17-2	Tuber	15CT-IDRUPE-01	G2	Idaho	7/28/2015
X17-3	Tuber	15CT-IDRUPE-01	G2	Idaho	7/28/2015

Table 16-2. Y9 Plant Material Collection Locations

Line	Tissue	Study Number	Generation of Seed Used	Location	Date
Atlantic-1	Tuber	14-01-SPS-ENV	G2	Idaho	5/28/2015
Atlantic-2	Tuber	14-01-SPS-ENV	G2	Washington	5/28/2015
Atlantic-3	Tuber	14-01-SPS-ENV	G2	Washington	5/28/2015
Y9-1	Tuber	14-01-SPS-ENV	G2	Washington	5/28/2015
Y9-2	Tuber	14-01-SPS-ENV	G2	Idaho	5/28/2015
Y9-3	Tuber	14-01-SPS-ENV	G2	Washington	5/28/2015
Atlantic-1	Leaf	15-03-SPS-EXP	G2	Idaho	5/28/2015
Atlantic-2	Leaf	15-03-SPS-EXP	G2	Idaho	5/28/2015
Atlantic-3	Leaf	15-03-SPS-EXP	G2	Idaho	5/28/2015
Y9-1	Leaf	15-03-SPS-EXP	G2	Idaho	5/28/2015
Y9-2	Leaf	15-03-SPS-EXP	G2	Idaho	5/28/2015
Y9-3	Leaf	15-03-SPS-EXP	G2	Idaho	5/28/2015

Protein Extraction. Proteins were extracted in 50 mM Tris-HCl (pH 7.5) buffer containing 2.5 mM EDTA, 150 mM NaCl, 10% glycerol, 0.1% IGEPAL, 1 mM DTT, and 1 mM PMSF added to 150-250 mg of tissue powder and incubated at room temperature (RT) with frequent mixing for 10 min. The sample was centrifuged at 20,000 x g for 20 min at 4 °C. The supernatant was collected and centrifuged again. The total protein concentration was measured by Bradford assay (Thermo).

VNT1 Expression in *Nicotiana benthamiana* (NB). Infiltration was performed as described by Moffett, 2011. *Agrobacterium tumefaciens* strain AGL1 transformed with a VNT1 expression vector was used for infiltration. *A. tumefaciens* cultures were incubated at 28 °C with kanamycin (50 µg/mL) and carbenicillin

(100 µg/mL) until the O.D.₆₀₀ reached 0.2 (1:10 dilution). Cells were harvested and suspended in 10 mM Tris HCl (pH 7.5) buffer containing 10 mM MgCl₂. Cultures were diluted (O.D.₆₀₀ = 0.25) and injected at 2-6 different sites on the underside of NB leaves using a syringe. Leaves were harvested 2-3 days post-infiltration, ground in liquid nitrogen, and stored at -80 °C. Proteins were extracted from powdered leaf tissue, and VNT1 was enriched by ion-exchange chromatography.

***N. benthamiana* (NB) VNT1 Quantification.** A purified VNT1-LRR domain enabled estimation of the amount of full-length VNT1 in enriched NB extracts (NB VNT1) by comparative western blot. The VNT1-LRR domain was quantified by Bradford assay, and increasing amounts of VNT1-LRR and NB VNT1 were run on the same SDS-PAGE gel. VNT1 was detected by western blot, and band intensities were fit to a regression line (slope = 17.233, Y-intercept = 0, and R² = 0.9504). Using the regression line, the NB VNT1 amount in 0.561 µl was calculated to be 97 picograms (pg).

Western Blot. Proteins were denatured in 4x Laemlli Buffer (BioRad) for 10 min at 85 °C, separated on 7.5% TGX™ Mini-PROTEAN® gels (BioRad), and transferred to PVDF membranes using a wet tank transfer system in 25 mM Tris-HCl (pH 8.3) buffer, 192 mM glycine, and 20% methanol (transfer buffer). The gels were soaked in transfer buffer for 15 min. Membranes were soaked in methanol for 10 min and then in transfer buffer for 10 min. The transfer apparatus was assembled according to manufacturer's instructions and run at 150 V for 1 h or at 60 V overnight. The membrane was placed in 1X PBS with 0.1% Tween-20 and 5% non-fat milk added (blocking buffer) for 1 h at RT. Three 5 min washes in transfer buffer + 0.1% Tween-20 (wash buffer) were performed before addition of primary antibody. VNT1 antibody (generated using a VNT1-specific peptide, FHSSSKLPFGVWESKILC) was used at a 1:1000 (v/v) dilution. The membrane was incubated with primary antibody for 30 min and washed three times for 10 min, each in wash buffer. The secondary antibody (anti-rabbit-IgG-peroxidase; Sigma-Aldrich) was added at a dilution of 1:20,000 (v/v). The membrane was incubated for 30 min and washed four times (10 minutes each): once in wash buffer, once in 0.2% Tween-20 / 1X PBS, once in 0.1% NP40 in 1X PBS, and wash buffer. SuperSignal® West Femto Maximum Substrate (Thermo Scientific) was added and after 10 min, blots were imaged with a Bio-Rad Chemi-Doc™ XRS+ system and quantified using Image Lab™ software (Bio-Rad).

Limit of Quantitation (LOQ) of VNT1 in Potato. The LOQ, in parts per billion (ppb), for VNT1 was calculated based on the detectable amount of NB VNT1 (97 pg) spiked into 20 µg of potato protein. The amount of total potato protein was calculated, as the product of the tissue extract concentration (mg-tissue (fresh weight)/volume of extraction buffer (e.g. a sample of 196 mg/500 µL=0.392 mg/µL)) and the volume equal to 20 µg of protein (8.3 µL, based on a protein concentration of 2.4 mg/mL measured by Bradford assay), to be 0.0032 g. The detectable amount of NB VNT1 was 0.097 ng/0.0032 g or 30 ppb. An estimate of LOQ was determined by comparing the western blot signal from 97 pg of NB VNT1 to the background signal in "blank" RR samples (not containing VNT1). Mean LOQ values of 40 ± 7 ppb and 65 ± 24 ppb for tuber and leaf were calculated from RR tuber and leaf protein extracts (n=3), respectively. The rounded values of 40 ppb in tuber and 70 ppb in leaf represent the LOQs in RR tissues.

Densitometry. NIH image J was used to perform densitometric analysis of western blot band intensities (<http://www.yorku.ca/yisheng/Internal/Protocols/ImageJ.pdf>). A rectangle around the NB VNT1 spike band was duplicated and used to capture the pixel density (255, assuming a white background, minus raw density values) in the area of VNT1 migration and a corresponding background region in each lane. Background-normalized pixel densities were calculated for each sample as the "VNT1" density (around the area of VNT1 migration) minus the background density. A density value relative to the amount of

protein loaded on the gel was calculated by dividing normalized pixel densities by the fresh weight (mg) of tissue.

RNA Isolation. RNA was extracted from tubers and leaf tissue using Plant RNA or Trizol reagents (Invitrogen™, Carlsbad, California). DNA was removed by DNaseI (Qiagen) treatment and the RNA cleaned with phenol:chloroform:isoamyl alcohol (25:24:1 (v/v), Sigma-Aldrich). The aqueous phase was transferred to a new tube with a 0.1 volume of 3 M sodium acetate (pH 5.2) and 2 volumes 95% ethanol. After centrifugation, the pellet was washed in 70% ethanol. RNA concentration was measured using a Qubit 2.0 fluorometer (Invitrogen™).

cDNA Synthesis. cDNA was synthesized from total RNA using an iScript Reverse Transcription kit (Bio Rad). Reactions were incubated for 5 min at 25 °C, 30 min at 42 °C, and 5 min at 85 °C.

RT-qPCR. Endogenous reference genes (*Elongation Factor 1 α* and *α -Tubulin*) were used to normalize the qPCR results (Table 16-3). Reactions contained 10 ng of cDNA added to 2X SSO Advanced SYBR Green Supermix (Bio Rad) and 0.2 μ M primers. Cycling parameters are shown in Table 16-4. Negative control samples (without reverse transcriptase or template) were included to ensure absence of contaminating DNA in the reaction. The level of *Rpi-vnt1* mRNA was calculated from raw quantitation cycle (Cq) values after PCR amplification of *Rpi-vnt1* using gene-specific primers. Analyses were performed on three biological replicates with three technical replicates each. Standard curves were used to measure the efficiency of the PCR reactions. The specificity of the qPCR reaction was demonstrated by melt curve analysis (Figure 16-1 and Figure 16-4).

Table 16-3. Primers Used for qPCR

mRNA	Primers (5'-3')	Size (bp)
<i>Elongation Factor 1α</i>	GTTGGTGTATCAAGAGT	154
	CATAGCAAGTTCTCGTAA	
<i>α-Tubulin</i>	AATTTGTCGACTGGTGTCTT	151
	GTCAATGCGAGAGAAGACT	
<i>Rpi-vnt1</i>	AGAGACCTGGATATATTTTCATAGCTCT	289
	CGCTCTAGGCACAGGGCTCAATGCTGT	

Table 16-4. Cycling Parameters

Reference Gene Cycling Parameters		
1.	98 °C for 2 m	35 cycles
2. (Denaturing)	98 °C for 5 s	
3. (Annealing)	50 °C for 15 s	
4. (Elongation)	56 °C for 60 s	
Rpi-vnt1 Cycling Parameters		
1.	98 °C for 30 s	35 cycles
2. (Denaturing)	98 °C for 10 s	
3. (Annealing)	55 °C for 15 s	
4. (Elongation)	60 °C for 30 s	
Melt Curve		
1.	95 °C for 10 s	
2.	65-145 °C increased in 0.5 °C increments every 5 s	

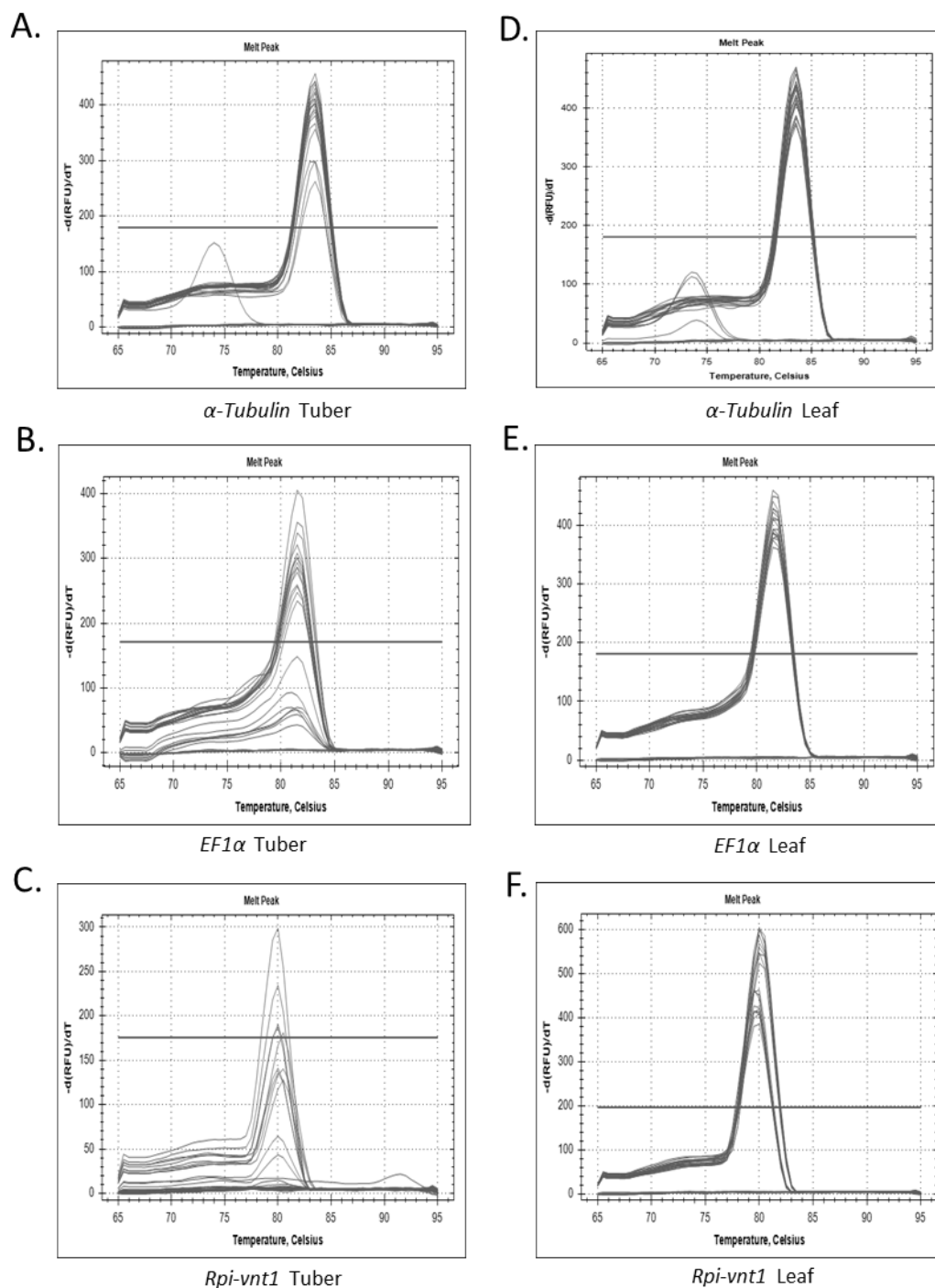


Figure 16-1. Melt Curve Analysis of the *Rpi-vnt1* Amplicon in X17

Graphs are melt curve results from amplification of target genes in tuber and leaf tissues. Single peaks observed in each case show specificity of the PCR reactions. Tuber and leaf tissue analysis was performed on three biological replicates in triplicate.

VNT1 Protein Expression. Protein extracts from X17 and RR plants were assayed for VNT1. The full-length VNT1 protein is about 75 kDa. The VNT1 protein was not detected in X17 tuber or leaf tissue protein extracts by Coomassie staining of SDS-PAGE gels (Figure 16-2).

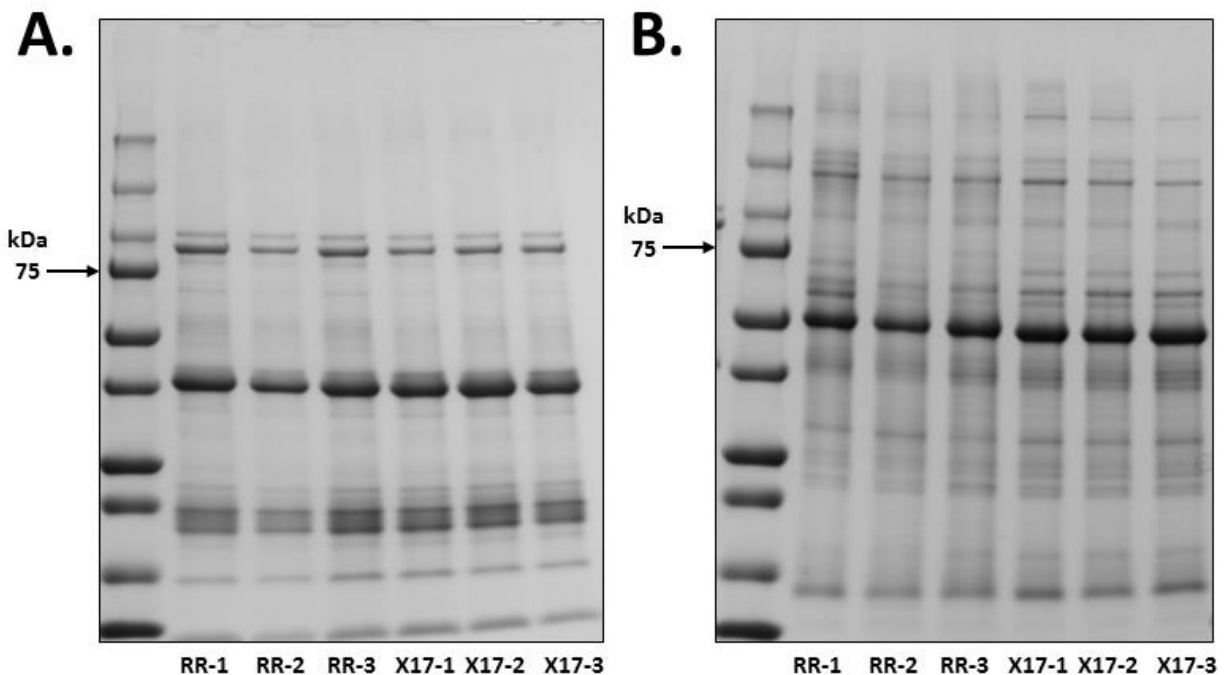


Figure 16-2. Coomassie Stained SDS-PAGE Gel of Ranger Russet and X17 Tissue Protein Extracts
Whole protein extracts (20 µg) from tubers (A) and leaf tissue (B) were separated by SDS-PAGE and stained with Coomassie. The VNT1 protein, expected to migrate at 75 kDa, was not observed in X17 tuber or leaf tissues.

An immunoblot assay for detecting VNT1, using a VNT1 polyclonal antibody, was used to analyze X17 leaf and tuber tissue. The limit of detection of the VNT1 antibody used in this assay was 9 pg. LOQs of 30 and 60 ppb in Russet Burbank (RB) tuber and leaf samples, respectively, were established by serial dilution of full-length VNT1 expressed and enriched from *N. benthamiana* (NB VNT1) spiked into RB tissues. Similar limits were established in field-grown RR plants (Figures 16-3E and 16-3F). The NB VNT1 was observed by western blot when isolated or when spiked into RR tuber.

A high number of VNT1 homologs in potato made development of a specific antibody challenging (Figures 16-3A and 16-3B). Thus, despite the high sensitivity of the antibody, cross-reactivity was high in leaf and tuber samples. The presence of signal in RR, which lacks *Rpi-vnt1*, demonstrates the high level of non-specific background even at the expected VNT1 region on the gel. Some level of background signal (and/or bands) was observed in RR and X17 samples (Figures 16-3C and 16-3D).

Densitometric analysis was used to compare the background levels between X17 and RR samples at the expected region of VNT1 migration. The region was determined from the NB VNT1 control band. The calculated mean signal intensities of RR and X17 tuber samples were 11 ± 2 and 8 ± 2 , respectively. The values were not significantly different between RR and X17 (Student's t-test, $p=0.21$). The calculated mean signal intensities of RR and X17 leaf samples were 10 ± 5 and 12 ± 3 , respectively. These values were also not significantly different between RR and X17 (Student's t-test, $p=0.58$) indicating that the

observed background in X17 tissues was not due to the presence of VNT1, but most likely non-specific cross-reactivity. VNT1 levels were not detectable above background, and the concentration of VNT1 in X17 tissues is below the LOQ. Due to antibody cross-reactivity causing variation in background levels, a conservative estimate of < 100 ppb was established for VNT1 in X17 tuber and leaf tissue.

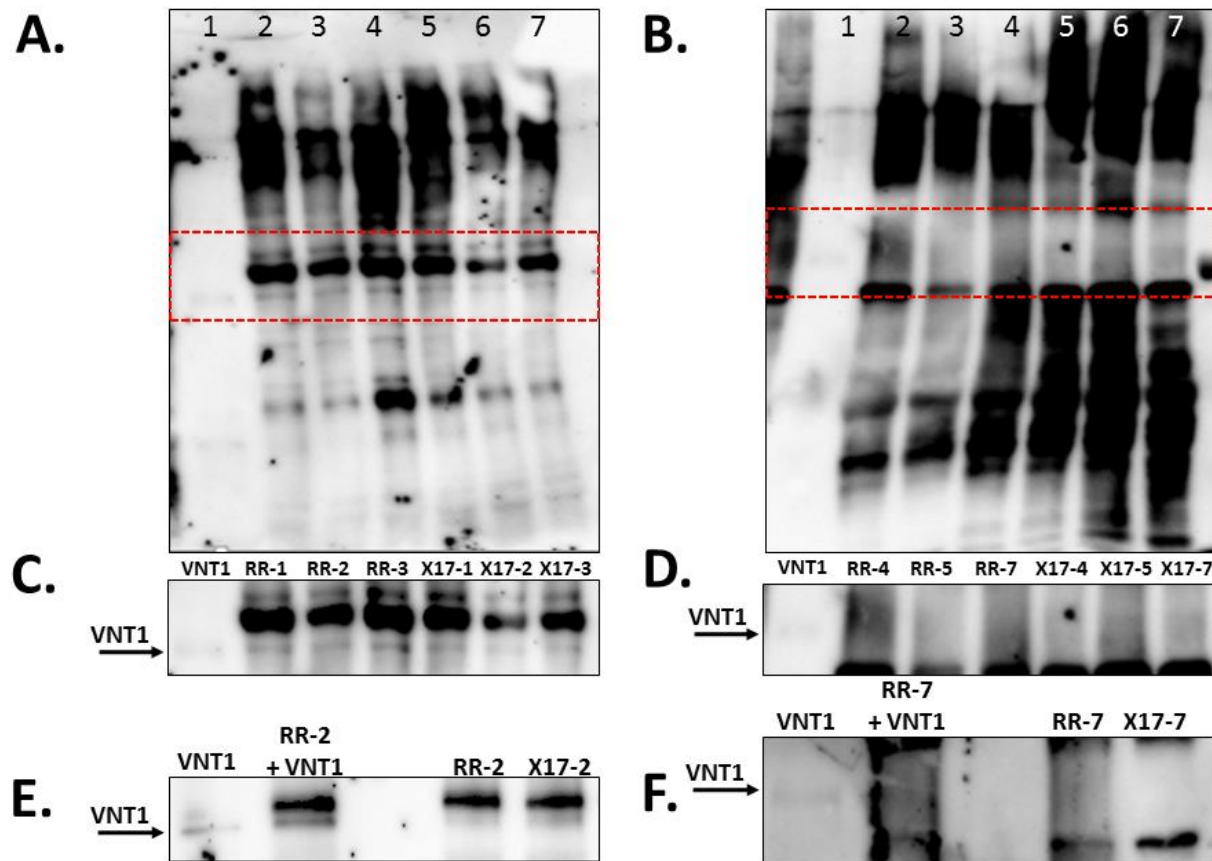


Figure 16-3. VNT1 Limit of Quantitation in X17

Total protein extracts from tubers (A, C, E) and leaf tissue (B, D, F) samples were separated by SDS-PAGE and transferred to PVDF membranes for immunodetection. **A-B**, images show western blot (whole gel) of tuber (A) and leaf (B) protein extracts. Lane 1, NB-VNT1 (97 pg); Lanes 2-4, RR; Lanes 5-12, X17. Red boxes indicate regions shown in **C-D**, focusing on the area of VNT1 migration. Three biological replicates were analyzed. **E-F**, NB VNT1 alone and spiked into RR samples at the limit of quantitation for tuber (40 ppb) and leaf (70 ppb). Unspiked RR and X17 samples are shown for comparison.

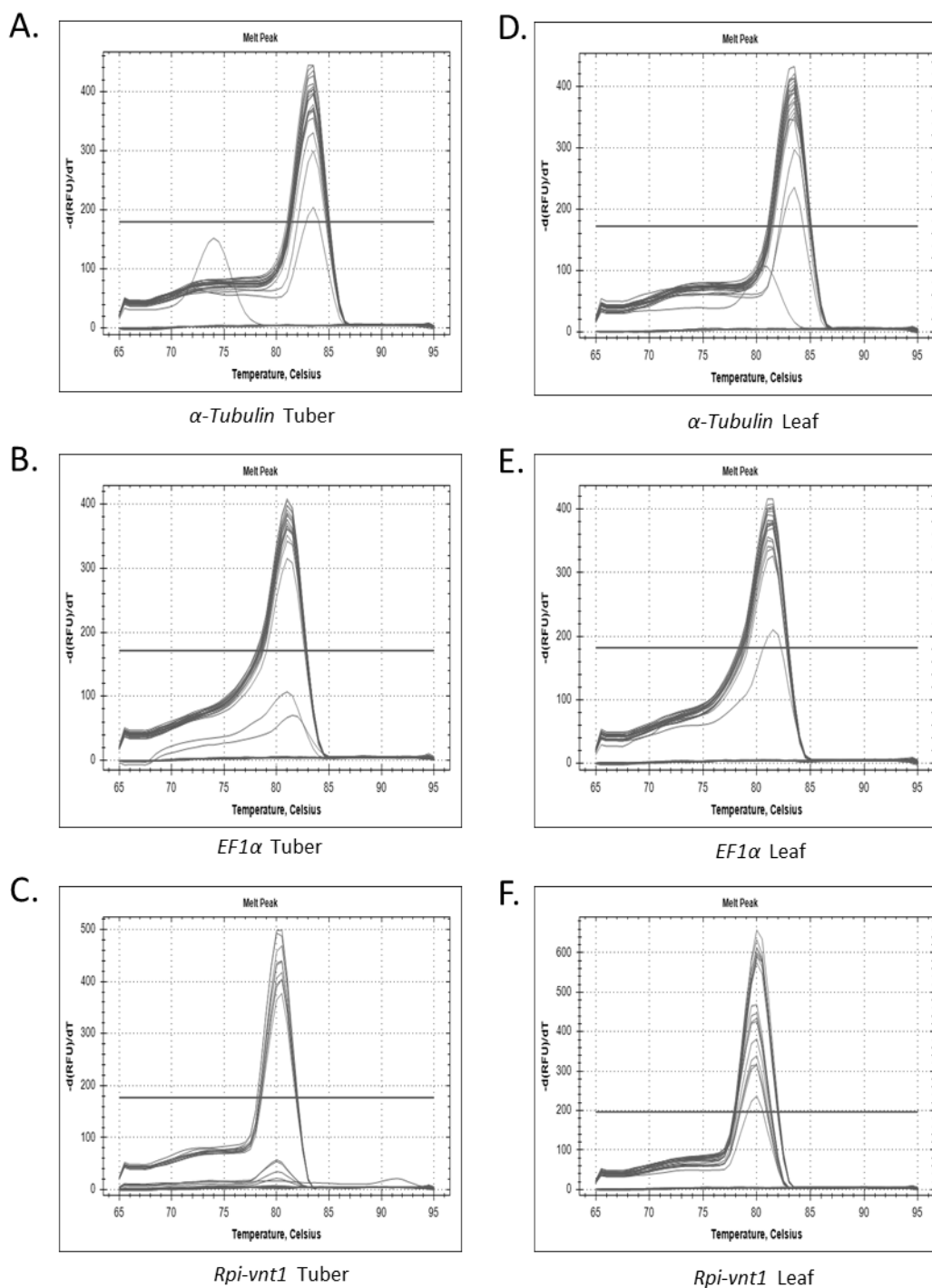


Figure 16-4. Melt Curve Analysis of the *Rpi-vnt1* Amplicon in Y9

Graphs are melt curve results from amplification of target genes in tuber and leaf tissues. Single peaks observed in each case show specificity of the PCR reactions. Tuber and leaf tissue analyses were performed on three biological replicates in triplicate.

Protein extracts from Y9 and Atlantic plants were assayed for VNT1. The full-length VNT1 protein is about 75 kDa. The VNT1 protein was not detected in Y9 tuber or leaf tissue protein extracts by Coomassie staining of SDS-PAGE gels (Figure 16-5).

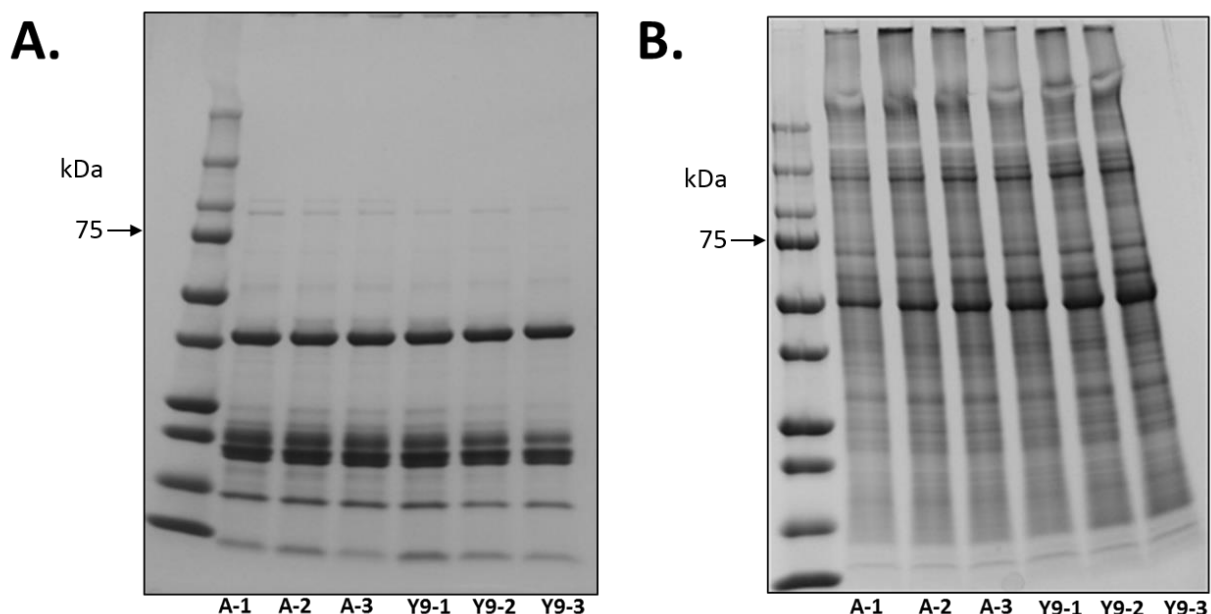


Figure 16-5. Coomassie Stained SDS-PAGE Gel of Atlantic and Y9 Tissue Protein Extracts

Whole protein extracts (20 µg) from tubers (A) and leaf tissue (B) were separated by SDS-PAGE and stained with Coomassie. The VNT1 protein, expected to migrate at 75 kDa, was not observed in Y9 tuber or leaf tissues.

An immunoblot assay for detecting VNT1, using a VNT1 polyclonal antibody, was used to analyze Y9 leaf and tuber tissue. The limit of detection of the VNT1 antibody used in this assay was 9 pg. LOQs of 30 and 60 ppb in Russet Burbank (RB) tuber and leaf samples, respectively, were established by serial dilution of full-length VNT1 expressed and enriched from *N. benthamiana* (NB VNT1) spiked into RB tissues. Similar limits were established in field-grown Atlantic plants (Figures 16-6E and 16-6F). The NB VNT1 was observed by western blot when isolated or when spiked into Atlantic tuber.

A high number of VNT1 homologs in potato made development of a specific antibody challenging (Figures 16-6A and 16-6B). Thus, despite the high sensitivity of the antibody, cross-reactivity was high in leaf and tuber samples. The presence of signal in Atlantic, which lacks *Rpi-vnt1*, demonstrates the high level of non-specific background even at the expected VNT1 region on the gel. Some level of background signal (and/or bands) was observed in Atlantic and Y9 samples (Figures 16-6C and 16-6D).

Densitometric analysis was used to compare the background levels between Y9 and Atlantic samples at the expected region of VNT1 migration. The region was determined from the NB VNT1 control band. The calculated mean signal intensities of Atlantic and Y9 tuber samples were 9 ± 5 and 10 ± 5 , respectively. The values were not significantly different between Atlantic and Y9 (Student's t-test, $p = 0.81$). The calculated mean signal intensities of Atlantic and Y9 leaf samples were 4 ± 3 and 5 ± 2 , respectively. These values were also not significantly different between Atlantic and Y9 (Student's t-test, $p = 0.57$) indicating that the observed background in W8 tissues was not due to the presence of VNT1, but most

likely non-specific cross-reactivity. VNT1 levels were not detectable above background, and the concentration of VNT1 in Y9 tissues is below the LOQ. Due to antibody cross-reactivity causing variation in background levels, a conservative estimate of < 100 ppb was established for VNT1 in Y9 tuber and leaf tissue.

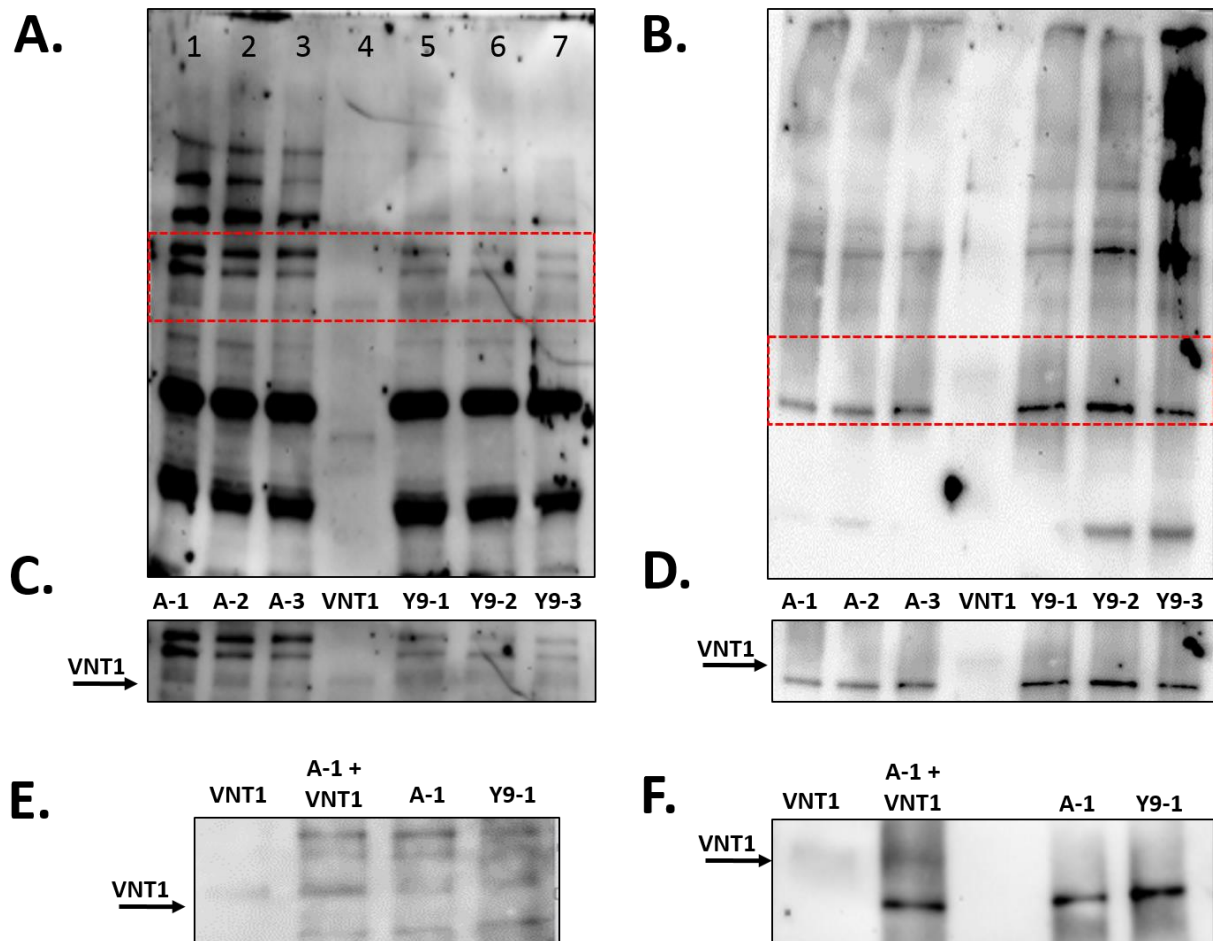


Figure 16-6. VNT1 Limit of Quantitation in Y9

Total protein extracts from tubers (A, C, E) and leaf tissue (B, D, F) samples were separated by SDS-PAGE and transferred to PVDF membranes for immunodetection. **A-B**, images show western blot (whole gel) of tuber (A) and leaf (B) protein extracts. Lane 4, NB-VNT1 (97 pg); Lanes 2-4, Atlantic; Lanes 5-7, Y9. Red boxes indicate regions shown in **C-D**, focusing on the area of VNT1 migration. Three biological replicates were analyzed. **E-F**, NB VNT1 alone and spiked into Atlantic samples at the limit of quantitation for tuber (60 ppb) and leaf (60 ppb). Unspiked Atlantic and Y9 samples are shown for comparison.

The VNT1 protein was not detectable above background in X17 or Y9 tuber and leaf tissues, and background levels between WT and events did not differ significantly. These results indicate that the level of VNT1 is below the limit of quantitation. However, due to variation in the observed background, a conservative estimate for the levels of VNT1 in X17 and Y9 tissues was established to be less than 100 ppb.

17.0 Appendix D: Comparative Assessment Methods and Materials

Statistical Analysis. All attributes were analyzed using SAS 9.3 (SAS Institute, Cary, NC) by combining data from multiple years and locations using the following linear mixed model:

$$Y_{ijkl} = \alpha_i + \beta_j + \gamma_{k(j)} + (\alpha\beta)_{ijl} + \varepsilon_{ijkl}$$

α = mean of treatment (fixed)

β = effect of site (random)

γ = rep[site] (random)

ε = residual random error

Where α_i denotes the mean of the i^{th} treatment (fixed effect), β_j denotes the effect of the j^{th} site (random effect), $\gamma_{k(j)}$ denotes the random rep effect (within site), $(\alpha\beta)_{ijl}$ denotes the interaction between the i^{th} treatment and random j^{th} site effect, and ε_{ijkl} denotes the residual random error.

Means from the statistical analysis output are least square means. Least square means are the same as means when no data are missing. When data are missing, least square means are a statistical estimate of the mean based on available data. A significant difference was established with a p-value ≤ 0.05 . The tolerance intervals were calculated, with 95% confidence, using 99% of the values contained in the population (Vardeman, 1992). The tolerance interval represents measurements from conventional varieties, controls, and reference varieties from all sites in the study (Table 17-2). Every effort was made to generate p-values to aid in the interpretation of the data. Some departures from the assumptions of normality and equal variances were allowed since the results were always interpreted in the context of variation observed in the conventional varieties.

Phenotypic Methods for X17 and Y9. For X17 and Y9, early emergence and final emergence were evaluated by determining the percentage of plants that emerged (visible at the soil surface) out of the 40 seed pieces planted in the middle two rows of each plot. In the case of two-row plots, “middle two rows” refers to both rows. Early emergence was evaluated at approximately 50% emergence in order to assess emergence rates between potato varieties. Final emergence was evaluated during the early season approximately 45 days after planting when emergence was complete.

Each seed piece can produce multiple stems. Stems per plant were evaluated by counting the number of stems of 10 plants in the middle two rows of each plot. Evaluation was made during the early season.

At approximately mid-season (early bloom stage), plant vigor was visually assessed in the middle two rows of each plot using the following 1 to 5 comparative scale. Evaluation of plant vigor was based on the principal investigators’ experience with the potato varieties being grown in that environment.

- 1 = Severely less than the varietal average
- 2 = Noticeably less than varietal average
- 3 = Plants are similar to the varietal average
- 4 = Slightly more than varietal average
- 5 = Obviously more than the varietal average

At approximately mid-season, plant height was measured in centimeters for 10 plants per plot from the middle two rows in each plot. Measurements were made from the soil surface to the top of the uppermost leaf.

At approximately late season (crop senescence stage), natural vine desiccation was assessed by visually estimating the percent of vines desiccated in the middle two rows of each plot prior to chemical or mechanical vine desiccation.

Tuber Evaluation. Total yield was determined after harvest by weighing all tubers from a single row of each plot and converting to CWT/acre. For X17, US#2 yield was determined by subtracting the weight of tubers failing to meet the US#2 standard (undersize and unusable tubers) prior to conversion. For Y9, US#1 yield was determined by subtracting the weight of tubers failing to meet the US#1 standard prior to conversion. The average number of tubers per plant was determined by counting the total number of tubers in each yield sample and dividing by the total number of plants in the sample row. After harvest, all tubers from one row of each plot were transported to a facility equipped to conduct grading.

For X17, the grading methods employed were identical to those used to grade commercial potatoes intended for the production of fries. Tuber grading size profiles were determined by weighing tubers from the sample sorted by size. The size categories included 4-6 oz., 6-10 oz., 10-14 oz., and >14 oz. The percentage of tubers in each size category was reported. Potatoes greater than six ounces produce optimal fries and allow the processor to meet most customer specifications at the highest potential recovery.

For Y9, the grading methods employed were identical to those used to grade commercial potatoes intended for the production of chips (USDA, 1997). Tuber grading size profiles were determined by weighing tubers from the sample sorted by size. The size categories included: 2-3.25 inches in diameter (A); <2 inches in diameter (B); >3.25 inches in diameter (oversized); and unmarketable tubers based on physiological defects (pick-outs).

For both X17 and Y9, specific gravity was determined by using a weight in air/weight in water measurement. Sub-samples of the tubers used to determine yield were first weighed in air and then weighed submerged under water at room temperature. From the two measurements, specific gravity was calculated using the following formula: $\text{specific gravity} = \text{weight in air} / (\text{weight in air} - \text{weight in water})$.

For X17, fried potato strips were prepared by cutting several (10-20) tubers into approximately 3/8 inch strips. The center strip was selected from each tuber and fried in cooking oil for three minutes at 375 °F. The color of the fried strips were compared to a USDA Munsell color chart. High sugar is the percentage of tubers with fry strips which, when compared with the Munsell Color Chart for fries, has on the darkest side a predominate color of a number 3 or darker. Sugar ends is the percentage of tubers with fry strips which has an end ¼ inch long or longer on the darkest side of the strip for the full width of the strip, testing number 3 or darker color (USDA, 1969).

X17 and Y9 tubers were checked for internal defects which included hollow heart, vascular necrosis, brown center, internal discoloration, insect, internal brown spot, nematode, and other internal defects. Total internal defects represent the percentage of tubers affected by any internal defect.

Environmental Interactions. Observational data on environmental interactions such as plant-insect, plant-disease, and plant-environment interactions are useful to assess adverse impacts. Each plot was evaluated at approximately early season, mid-season, and late season for the presence of naturally occurring insects, diseases, and abiotic stressors using the following 0 to 3 categorical rating scale:

0 = No symptoms present;

1 = Slight symptoms observed;

2 = Moderate symptoms observed; and

3 = Severe symptoms observed.

During each point in time, three insect stressors, three disease stressors, and three abiotic stressors were selected by the Principal Investigator at each site based on stressors observed or expected to be present. Therefore, the same stressors were not necessarily evaluated at every site or point in time. An observation is defined as looking for a specific insect, disease, or abiotic stressor during a point in time and evaluating the extent of damage caused by that stressor. Even if no stressors were present, zeroes were recorded because the stressors were looked for and comparisons can be made between the test material and the conventional control.

Examples of common potato insect and disease symptoms can be found in Table 17-1.

Table 17-1. Common Potato Insect and Disease Symptoms

Insect or Disease Agent	Symptom
<i>Empoasca fabae</i> (Potato Leafhopper)	Leaf feeding damage
<i>Epitrix species</i> (Flea Beetle)	Shot-holes in leaves
<i>Leptinotarsa decemlineata</i> (Colorado Potato Beetle)	Defoliation
<i>Limonius californicus</i> (Wireworm)	Bored holes in tubers and shoots
<i>Ostrinia nubilalis</i> (European Corn Borer)	Severe vine wilting above point of injury
<i>Bactericera (Paratrioza) cockerelli</i> (Potato Psyllid)	Yellows
<i>Phthorimaea operculella</i> (Tuberworm)	Foliar and tuber damage
Various aphid spp.	Leaf suckling damage
Aster Yellows MLO	Purple top disease
Potato Leafroll Virus	Rolling of leaves and net necrosis
Potato Spindle Tuber Viroid	Potato spindle tuber disease
Potato Virus A,M, X, Y	Mosaic symptoms
Tobacco Rattle Virus	Stem mottling
<i>Erwinia carotovora</i>	Blackleg, aerial stem rot and tuber soft rot
<i>Corynebacterium sepeidonicum</i>	Bacterial ring rot
<i>Ralstonia solanacearum</i>	Brown rot
<i>Phytophthora infestans</i>	Late blight
<i>Phytophthora erythroseptica</i>	Pink rot
<i>Verticillium</i> spp.	Early dying
<i>Sclerotinia sclerotiorum</i>	Sclerotinia stalk rot
<i>Rhizoctonia solani</i>	Causes cankers
<i>Streptomyces scabies</i>	Scab
<i>Fusarium</i> spp.	Dry rot
<i>Pythium ultimum</i>	Water rot, shell rot, <i>Pythium</i> leak
<i>Alternaria solani</i>	Early blight
<i>Botrytis cinerea</i>	Gray mold

Note: All stressors shown here were not necessarily observed at all sites or observation timings. This table is meant to give the reader an example list of insects and diseases that may impact potatoes.

Composition Methods for X17 and Y9. Field trials were conducted for phenotypic and agronomic assessment and to provide tuber samples for compositional analysis. During 2013 and 2014, X17 and its parental control were grown at a total of eight locations in potato growing regions of the U.S. (Table 7-3; note: Canyon County, ID and Adams County, WA sites were not used for compositional analysis). During 2014, Y9 and its parental control were grown at seven locations (Table 7-4). At 12 sites during 2013 and 2014, additional reference varieties were grown and used to establish a value range for conventional potatoes. A list of all reference varieties is shown in Table 17-2, giving details of the specific reference varieties used at specific sites. Not every test, control, or reference variety was grown at every site or year. The clonal cycle or type of seed planted was not expected to impact composition or trait efficacy. Within each field trial site, the test and control materials were of the same type.

The field trials were established in a randomized complete block design. There were four replicates at each site. Within each replicate, each potato variety was planted in plots arranged in random order. In

2013 each plot contained two or six rows and in 2014 each plot contained four rows. The number of rows per plot was adjusted to meet tuber sample needs.

Selection of Control and Reference Varieties. To ensure appropriate evaluations of X17 and Y9, proper selection of control varieties was important. For X17 and Y9 the most relevant comparators are the parental varieties, Ranger Russet and Atlantic, respectively. The difference between the events and parental controls are the two successive transformations of X17 and Y9 with pSIM1278 and pSIM1678.

Conventional potato varieties, with a history of safe use for food and feed, were used as reference varieties. These varieties are commonly used in the chip, fry, dehydrated or fresh markets. Included reference varieties, used to establish a range of values common to conventional potatoes, were: Atlantic, Bintje, Golden Sunburst, Lamoka, Nicolet, Red Thumb, Ranger Russet, Russet Burbank, Russet Norkotah, and TX278.

The tolerance interval and the combined range of values for each analyte available from the published literature were used to interpret the composition results. In interpreting significant differences, emphasis was placed on the analyte means; means that fell within the tolerance interval and/or combined literature range for the analyte were considered to be within the normal variability of commercial potato varieties.

Table 17-2. Reference Variety Sites and Sample Size

Variety	2013 Sites	2014 Sites	N Per Attribute
Atlantic ¹	None	ID-Jerome, ID-Minidoka, MI-Montcalm, ND-Grand Forks, PA-Berks, WA-Franklin, WA-Grant	27-28 (one missing copper value)
Bintje	ID-Jerome, ID-Minidoka, ID-Canyon, MN-Sherburne, ND-Grand Forks, WA-Adams, WA Grant, WI-Adams	None	32
Golden Sunburst	ID-Jerome, ID-Minidoka, ID-Canyon, MN-Sherburne, ND-Grand Forks, WA-Adams, WA Grant, WI-Adams	None	32
Lamoka	None	ID-Jerome, MI-Montcalm	8
Nicolet	ID-Jerome, ID-Minidoka, ID-Canyon, MN-Sherburne, ND-Grand Forks, WA-Adams, WA Grant, WI-Adams	ID-Jerome, MI-Montcalm	40
Ranger Russet ¹	ID-Minidoka, WA Grant, WI-Adams	ID-Jerome, ID-Minidoka, ND-Grand Forks, WA-Franklin, WA-Grant	32
Red Thumb	WI-Adams	None	4
Russet Burbank	ID-Jerome, ID-Minidoka, ID-Canyon, MN-Sherburne, ND-Grand Forks, WA-Adams, WA Grant, WI-Adams	None	32
Russet Norkotah	None	ID-Minidoka, PA-Berks	8
TX 278	ID-Jerome, ID-Minidoka, ID-Canyon, MN-Sherburne, ND-Grand Forks, WA-Adams, WA Grant	ID-Minidoka, PA-Berks	36

¹ Ranger Russet and Atlantic are both controls and conventional potato varieties, have a history of safe use as food and feed, and were included in the tolerance intervals. Including Ranger Russet and Atlantic in the tolerance interval did not impact the statistical analysis, since it was calculated separately from the statistical comparisons.